INFORMATION TO USERS

This manuscript has been reproduced from the microfilm master. UMI films the text directly from the original or copy submitted. Thus, some thesis and dissertation copies are in typewriter face, while others may be from any type of computer printer.

The quality of this reproduction is dependent upon the quality of the copy submitted. Broken or indistinct print, colored or poor quality illustrations and photographs, print bleedthrough, substandard margins, and improper alignment can adversely affect reproduction.

In the unlikely event that the author did not send UMI a complete manuscript and there are missing pages, these will be noted. Also, if unauthorized copyright material had to be removed, a note will indicate the deletion.

Oversize materials (e.g., maps, drawings, charts) are reproduced by sectioning the original, beginning at the upper left-hand corner and continuing from left to right in equal sections with small overlaps. Each original is also photographed in one exposure and is included in reduced form at the back of the book.

Photographs included in the original manuscript have been reproduced xerographically in this copy. Higher quality 6" x 9" black and white photographic prints are available for any photographs or illustrations appearing in this copy for an additional charge. Contact UMI directly to order.

UMI

A Bell & Howell Information Company
300 North Zeeb Road, Ann Arbor MI 48106-1346 USA
313/761-4700 800/521-0600

Université d'Ottawa • University of Ottawa

Seismic Retrofit of Low-Rise Masonry and Concrete Walls by Steel Strips

by

MUSTAFA TAGHDI

A thesis submitted to
the Faculty of Graduate Studies and Research
in partial fulfilment of the requirements
for the degree of
DOCTORATE OF PHILOSOPHY

in Civil Engineering*

Department of Civil Engineering
University of Ottawa
Ottawa, Canada
February 1998

*The Ph. D. Program in Civil Engineering
is a joint program with Carleton University,
administered by the Ottawa-Carleton
Institute for Civil Engineering

Abstract

A large number of low-rise non-ductile masonry (unreinforced and partially reinforced) and reinforced concrete shear walls were built before seismic provisions have been introduced in modern building codes. During seismic evaluation of existing buildings, such walls are frequently found to be in need of seismic retrofit. This research investigates the in-plane cyclic inelastic behaviour of such low-rise walls, as well as that of comparable walls retrofitted using steel strips.

Four concrete block masonry and two reinforced concrete walls of large scale were subjected to combined constant gravity load and incrementally increasing lateral deformation reversals. All the walls had an aspect ratio of 1.0 and a height of 1800 mm. Masonry walls had a thickness of 190 mm, and concrete walls 100 mm. They were designed to simulate walls built using provisions in effect decades ago, before the enactment of earthquake-resistant design provisions. The first pair of masonry walls were unreinforced (URM), and the second pair were partially reinforced masonry (PRM). Three #15 reinforcing bars, one in each exterior cell and one in the central cell, were used in the vertical direction of the PRM walls. One truss type bed joint reinforcement, No. 8 gauge, was placed in mortar joints every two courses. Each concrete wall was reinforced using 3 pairs of 9.5 mm reinforcing bars, uniformly distributed along the length, in both directions. One wall from each pair was retrofitted using a steel strip system.

The steel strip system consists of diagonal (220x3.81 mm) and vertical (80x3.81) strips attached to the walls using through-thickness bolts. Stiff steel angles and anchor bolts were used to connect the steel strips to the foundation and the top loading beam. The unretrofitted walls had a relatively low shear strength. However, the URM wall exhibited a very stable rocking response at an in-plane load of 61 kN. The PRM wall exhibited a non-ductile shear failure at a maximum load of 120 kN. The reinforced concrete wall showed flexural failure at 171 kN with buckling of the end re-bars. The ultimate strength of the retrofitted URM, PRM and R/C walls were respectively 7, 3.8 and 2.9 times

that of the unretrofitted walls. These tests show that the steel-strip system is most effective to significantly increase the in-plane strength and ductility of low-rise unreinforced and partially reinforced masonry walls, and lightly reinforced concrete walls. The tests also demonstrated that the desirable in-plane rocking behaviour, observed in unreinforced brick masonry walls by other researchers, can also develop in concrete block walls.

In the analytical part of this research, a truss model was developed for analysis of retrofitted low-rise walls. This model consists of an indeterminate truss having five members each representing part of the retrofitted wall. A step-by-step calculation procedure was used to find strength and deformation of each wall. The results of this analytical model were in good agreement with experimental results reported in this study. Based on this model a displacement based design procedure is proposed as a simple design procedure that may be used for retrofitting existing non-ductile low-rise walls. This design procedure proved to be easy and effective.

To my wife, Iman Aburawi

Acknowledgment

The author great appreciation and sincere thanks go to his thesis supervisors Dr. Michel Bruneau and Dr. Murat Saatcioglu for their guidance, advice, encouragement and financial support throughout this research project.

I would like to thank the technical staff of the Civil Engineering Department, specially Mr. Mongi Grira, for their assistance in constructing the wall specimens and testing them.

Special thanks are due to Tom Watson senior field engineer of Canadian Portland Cement Association, Ontario region, Ron Sakares, from Ontario Region Masonry Contractors Association and Peter Punkari of George and Asmussen Limited for donation of material and labor for the construction of the masonry walls.

My appreciation and thanks are due to Mr. Adel Taghdi, Mr. Adel Gherari, Mr. Omar Ahmed Mr. Mohammed Ammar and Mr. S. Elmuradi for their valuable help during this research.

Thanks are also extended to fellow graduate students for their help during constructing the wall specimens.

Finally, I wish to thank my parents for their support and prayer. Many thanks to my wife and my children for their encouragement, patience, support and continuous prayer.

Table of Contents

List of Tables

List of Figures

Notations

A_d	Area of diagonal steel strip used to retrofit walls
A_v	Area of vertical steel strip used to retrofit walls
A_s	Area of reinforcing steel
A_{si}	Cross-sectional area of i^{th} vertical reinforcement
b	Width of the wall
d	depth of the wall
d_v	distance between the vertical steel strips tied to a wall
E_c	Modulus of elasticity of concrete
E_s	Modulus of elasticity of steel
f_c'	Concrete compressive strength
f_m'	Masonry compressive strength
f_y	Yield strength of reinforcement
f_{yp}	Yield strength of steel strips
V_c	Wall shear cracking capacity (concrete)
V_m	Wall shear cracking capacity (masonry)
V_u	Ultimate in-plane load
V_{uo}	Ultimate in-plane load of unretrofitted wall
θ	Inclination of the diagonal steel strips

Chapter 1

Introduction and Review of Literature

1.1 Introduction

Many existing buildings in Canada would suffer damage or even collapse in the event of a severe earthquake. The deficient seismic strength and/or ductility of many older existing buildings is a very critical problem in most of eastern and western Canada, particularly since the first earthquake-resistant design requirements only appeared in the National Building Code of Canada (NBCC) in 1953. Moreover, the scope of the NBCC has always been limited to new constructions or existing buildings subjected to major changes in occupancy, and has never addressed the potential danger created by existing buildings that may be incapable of withstanding a strong earthquake.

Concrete and masonry walls are two of the most common lateral resistance structural systems used in these buildings. The Canadian Institute of Steel Construction (CISC) estimates that over 90 percent of all existing buildings, three-stories or taller, rely on shear-walls to resist wind and earthquake loads. Single-story buildings are also very common in Canada (for schools, shopping canters, hospitals, ..etc.) and many of them rely on walls to resist both vertical and lateral loads. Because of the high risk

of earthquake damage to older unreinforced or lightly reinforced shear walls and the potential for a great loss of life in these important community buildings, the non-ductile concrete and masonry walls have been the subject of extensive research in recent years.

Typically, these older reinforced concrete or masonry shear walls exhibit an insufficient in-plane shear strength, flexural strength and/or ductility to behave satisfactorily during earthquakes. These deficiencies can be corrected by one of the following techniques:

- Increasing the effectiveness of the existing walls using external coatings on the inside or outside face of the walls, as illustrated in Fig. 1.1.
- Filling existing windows or doors, with reinforced concrete or masonry, as shown in Fig. 1.2.
- Constructing new shear walls or new steel braced frames, inside or outside on the boundary of the building, or building new external walls as shown in Fig.1.3.

While the above upgrading techniques are effective, they require a great deal of preparation work, and usually result in an increase in the mass of the structure. As a result of this additional mass, higher inertia forces will develop, potentially making the foundation critical with a need for foundation upgrade. Also, for some of these techniques, the ongoing building functions will be seriously disrupted by the construction activities, and new exterior elements may affect the architectural aesthetics of the building. Hence, an alternative method of retrofitting is worth considering. The retrofit method proposed here consists of adding steel strips to reinforce the existing non-ductile walls. At an early stage of this research project, a retrofit strategy was developed to cover entire walls with steel plates on both sides using tied anchor bolts. However, the resulting capacity of the fully plated walls were found to be up to 8 to 10 times the original wall capacity, even when using very thin steel plates. While this would likely ensure seismic survival by limiting response to linear range, this was significantly beyond the aimed improvement and cost in material and hence might be prohibitive. Therefore, in the retrofit concept studied here, diagonal and vertical strips of steel are attached on both sides of lightly reinforced concrete and masonry walls. The use of steel strips to retrofit lessens the improvement in capacity to approximately 3 to 5 times the original capacity, and limits the amount of new steel to about 35 % of the wall surface area. The objective of this research project is to develop and experimentally validate this retrofit strategy to ensure a predominantly

ductile performance by promoting flexural yielding prior to shear failure. To qualitatively and quantitatively assess the adequacy of the proposed retrofit procedure, the behaviour of retrofitted low-rise walls will be compared with results obtained from tests conducted on non-retrofitted walls. The expected increase in strength and ductility of the upgraded shear wall makes it a suitable retrofit strategy for buildings in high risk seismic zones. This type of strengthening strategy has the following advantages:

- Retrofitting can be conducted with minimal disruption to occupants.
- Minimal architectural impact, as alterations on the existing walls do not result in loss of rentable floor space or changes to exterior appearance of the building, as would be the case if new interior or exterior shear walls were added instead.
- The minimal increase in wall thickness due to the steel plates makes this a preferred alternative for existing walls close to mechanical equipment, such as an elevator cores.

1.2 Review of Literature

Numerous tests have been conducted around the world to examine the behaviour of columns, beams and slabs strengthened by the addition of steel plates. Generally these tests showed that this method of strengthening is an effective and convenient method to improve member strength and ductility. However, only a limited amount of this research is relevant to walls. Moreover, most of that previous research was conducted mainly to improve the flexural behaviour of reinforced concrete elements and few studies were carried to improve shear behaviour. Likewise, very few of these studies were done in the perspective of seismic retrofitting. In most experimental studies reported, the structural elements tested were subjected only to monotonic loading. Finally, while steel plates have been added to retrofit walls in few existing buildings, there is no evidence of any experimental work done on this subject.

A summary of the available literature on flexural retrofitting and shear retrofitting of reinforced concrete elements is presented in this section. The results from experimental studies on low-rise walls reinforced diagonally with steel bars are also summarized as they indirectly relate to the subject of this proposed research. Indeed, some analogy is possible between those diagonal shear reinforced bars installed in new walls and the diagonal steel strips used here to retrofit existing weak walls.

1.2.1 Flexural Retrofitting of Reinforced Concrete Elements Using Steel Plates

Retrofitting of reinforced concrete members using externally bonded and or bolted steel plates is a strategy that has been used in different parts of the world since 1964 (Mckenna et al. 1994). In this strategy, steel plates or strips are added to reinforced concrete members at their extreme tension fibre. Fig. 1.4 shows an example of how a simply supported beam can be retrofitted using this method. Mckenna pointed out that this method has been used quite successfully for the last 25 years on many types of structures to correct a wide range of structural problems. Yet it has not been frequently attempted in North America. He also summarized results from more than ten experimental research projects along with some examples of practical applications. These reported tests, mostly conducted in England, investigated the structural performance and ductility of reinforced concrete members acting compositely with externally bonded steel plates, and subjected to various loading conditions (e.g. central point load, third point loads. etc.). The effect of variation in glue thickness, plate thickness, and plate configuration (e.g. single plates compared to plates lapped at joints, double plates..etc) was also studied. Mckenna concluded that, in general:

1. The retrofitting of reinforced concrete beams using steel plates has been proven in the field to control flexural crack widths and deflections, and to increase the load carrying capacity of members subjected to either service or ultimate load conditions.
2. Use of steel plates with width-to-thickness ratio in excess of 50 results in a sudden and brittle failure, caused by horizontal cracking, near one of the supports of the plated concrete member.
3. Full composite action can develop when a steel plate is bonded to a reinforced concrete member using an epoxy resin adhesive provided that the glue thickness exceeds 1.5 mm.
4. The last two limits must be satisfied to guarantee a ductile flexural failure.

In order to suppress the above undesirable sudden failure modes, Jones et al.(1988) tested a series of seven rectangular reinforced concrete beams retrofitted by the use of epoxy-bonded steel plates. They used two different types of anchorage; namely side steel plates and bolts. They concluded that:

1. Plate separation was due to high local interface bond stresses and peeling forces at the ends of the plates.
2. Fully composite action between the concrete and steel plate was achieved, hence, the capacity of the retrofitted beams could be predicted by current design procedures.

1.2.2 Shear Retrofitting of Reinforced Concrete Elements Using Steel Plates

The use of external steel plates to retrofit structural members having shear problems has been recognized during the past two decades as an adequate remedial measure. In this scheme, steel plates or strips are added to reinforced concrete (R/C) members on their web sides, along the shear regions as shown in Fig. 1.5. A number of experimental attempts have been made to validate this method. A brief summary of three investigations is presented in the following paragraphs.

A series of full-scale coupling beams were tested by Kent et al. (1994) in an effort to improve the response of existing reinforced concrete coupling beams in moderate seismic zones. These coupling beams were designed with a shear strength deficiency to represent old R/C coupling beams. They were then retrofitted by attaching steel plates on their webs. In this study, a number of different techniques for connecting the plates to the coupling beams were examined. In the first retrofitted coupling beam the steel plate was attached using only epoxy. The steel plates in the other two specimens were connected with both epoxy and bolts. The behaviour of these retrofitted specimens under reversed cyclic loading was compared with a control specimen. These tests showed that strength, stiffness, ductility and energy dissipation capacity of R/C coupling beams can be improved significantly by employing this kind of retrofitting. The improvement level depends on the type of connections and the extended length of the plate over the length of the beam. Each retrofitted beam could reach or exceed its original flexural capacity.

Vanek (1986) tested nine beams designed to fail in shear. Three of them were tested to determine their strength for comparison with retrofitted beams. The other six beams were strengthened in shear using steel strips glued on externally where additional stirrups would be desirable. In three of these six beams the bond between the steel strip and the concrete was increased by dowels. Testing revealed a 46 percent and 52 percent increase in strength of the beams retrofitted using glued and glued plus dowelled steel strips respectively. The dowels used to transfer stresses between the concrete surface and the steel strip provided only a small increase in strength of beams. However, these dowels could not act as an effective confinement reinforcement since the anchorage length of the dowels used was short and they did not extend through the cross section of the beams.

Taghdi (1989) tested twenty six beams to investigate the shear performance and effectiveness of

strengthened R/C beams using steel plates bonded to their sides by means of epoxy or epoxy and bolts. In these tests, the load capacities of strengthened beams were found to be 50 % higher than the original load capacity when epoxy was used in the strengthening process. An increase of 79 % in strength was achieved when bolts were used with epoxy in the strengthening process. In this case the bolts increased the strength by 29 % and they worked as confinement reinforcement since the bolts were running through the width of the beams.

1.2.3 Seismic Retrofitting of Reinforced Concrete Columns Using Steel Plates "Steel Jacketing"

Steel jacketing is a well known retrofit technique for reinforced concrete columns. It is widely used in practice. It was initially introduced for circular columns. This procedure involves covering the area of the column to be retrofitted by a circular steel shell in the case of circular columns and an elliptical shell for rectangular columns. It is recommended to use an elliptical jacket consisting of two half cylinder steel plates with a radius larger than the column radius to cover the area to be retrofitted. The steel plates are welded together at the site to form a complete steel pipe. The gap between the steel jacket and the concrete is filled with pure cement grout. Bearing of the steel jacket on the foundation of the retrofitted column must be avoided by providing a space of about 50 mm to prevent an increase in foundation moments and shears during an earthquake. The steel jacket effectively act as continuous hoop reinforcement in that it laterally confines the concrete, preventing it from expanding in the compression zone under high strains. Also, it confines the lap splice in the tension zone of the column in flexure when the tensile strength of the concrete is not sufficient to transfer stresses between reinforcement bars (Priestley and Calvi 1996).

1.2.4 Walls Reinforced With Steel Plates

Experimental study

Makino et al. (1965) carried out tests on seven RC walls. Three of them were reinforced with an internal steel plate in addition to the ordinary reinforcement. The steel plate was stiffened by vertical ribs to prevent local buckling and was connected to the surrounding steel frame by rivetted splice plates. Experimental data showed that the concrete panel and steel plate cooperate well and that the shear wall in-plane load capacity can be obtained by summing up those of the steel plate and concrete. This kind of shear wall is much more ductile than an ordinary reinforced concrete shear wall.

Composite steel concrete sandwich panels have been proposed (Adams; 1987 and Matsuishi; 1980) as a cost effective structural system for the exterior walls of offshore oil and gas production structures located in Arctic waters. The composite system consisted of two continuous steel plates enclosing a concrete core to which they were intermittently fastened by some mechanical means. Research focussed on the static and cyclic lateral out-of-plane load capacity of composite panels rather than in-plane load capacity of this type of structure.

Case study

Sharpe et al.(1984) used externally bonded steel plates to strengthen elevated shaft walls. Steel plates were applied on only one side of the walls. Combination of epoxy and bolts were used to bond the plates to the concrete. Steel plates of 12.5 mm and 16.0 mm thickness were applied to walls 200 mm and 250 mm thick. In absence of experimental data to support this retrofit solution Sharpe's design was based on engineering judgement.

1.2.5 Seismic Retrofitting of Unreinforced Masonry Walls by Steel Bracing

Durgesh et al. (1994) tested one unreinforced masonry (URM) wall with openings representative of a typical building and strengthened it with steel bracing in accordance with the current *Uniform Code for Building Conservation* (UCBC 1991). The test specimen was a 2340 mm long and 1680 mm high half-scale model, in which a two-wythe 216 mm thick wall represented the four-wythe 432 mm thick wall of the prototype. Four piers, approximately 530 mm wide and 1000 mm high, were created in this wall by three 76 mm wide openings. The wall was expected to fail by rocking as indicated by the UCBC general procedure. Braces were designed in accordance with UCBC (1991) to resist all lateral seismic design forces. Tubes of size 63x38x4.8 mm were used as braces. Pin-ended vertical steel members were provided at both ends of the wall and they resisted only overturning moments. This idealized end condition for the steel vertical members was used to simplify the determination of the lateral force resisted by the wall. The braces were connected to top and bottom gussets by welding. There was no connection between the brace and the wall. The specimen was subjected to symmetric cycles of increasing amplitude in predetermined steps. Testing revealed that braces mostly behaved independently of the wall throughout the loading. The failure mode of the wall did not change in spite of the retrofit, and the masonry piers behaved in a rocking mode during the entire loading history. However, the rocking shear capacity of the piers was dramatically increased by the hold-down forces due to the vertical steel members of the bracing system. Eventually, the connection of the brace to

the foundation unexpectedly failed, forming an undesirable failure mode.

1.2.6 Seismic Behaviour of Walls Diagonally Reinforced With Internal Steel Bars

The use of diagonal ordinary reinforcement in shear walls, coupling beams and columns is not new. Many researchers have investigated these types of construction (e.g. Paulay (1974), Barney et al. (1980), Paulay et al. (1982), Ogata et al. (1984), Wakabayashi (1986) and Chang-Sik (1993)). The earliest reference found on this topic related to walls is the work done by Paulay et al. (1982). In their study, they tested four reinforced concrete shear walls. Two of these walls were diagonally reinforced to reduce excessive sliding shear displacement under cyclic reversed loading, particularly at construction joints. The four walls were identical in every aspect, except that the last two were reinforced diagonally. The amount of diagonal reinforcement was made equivalent to the vertical and horizontal reinforcement in the first two walls, so that flexural and shear capacity was approximately the same. It was assumed that the force in the diagonal steel may be resolved to vertical and horizontal components. These two components were assumed to increase both the flexural and shear capacity of the walls. It was found that the shear walls with diagonal reinforcement showed better shear strength, ductility and energy-dissipation capacity when compared with the ordinary reinforced walls.

Diagonal reinforcing bars were also used to retrofit tall walls by adding them to the walls near their base. Fiorato et al. (1983) presented a summary of experimental data for new and repaired reinforced concrete shear walls. Three walls, with an aspect ratio of slightly less than 2.4, were investigated in two stages. In the first stage, the three walls were tested and severely damaged at their lower web portions. In the second stage, the webs in each wall were replaced. Three different approaches were used to replace the damaged web concrete in the test specimens. In one wall, the damaged web was replaced at its original thickness with new concrete. In another wall, the web thickness was increased as part of the repair. In the last wall, supplementary reinforcement was added to the web prior to replacement of the web concrete at original thickness. The supplementary reinforcement was diagonally placed inside the lower web portion of the wall. Re-testing showed that strengths of the repaired walls were approximately equivalent to those of the original walls. The wall that was repaired with diagonal reinforcement had an 18 % higher strength than that of the original wall, whereas the compressive strength of concrete in the web of the repaired specimen was considerably

lower than that of the original specimen.

1.3 *Findings From Previous Research*

The literature review done on this project has shown that very little knowledge exists on the retrofitting of shear walls using external steel plates. Nevertheless, some useful observations may be drawn from the literature review on related topics. Diagonal reinforcement was found to considerably improve the seismic response of walls, and this suggests that external diagonal steel plates are expected to do the same if proper anchorage to the wall is ensured. Whenever steel plates are used to retrofit an element, it is preferable to fix these steel plates using both anchorage bolts running across the element and high-strength epoxy. A minimum epoxy thickness of 1.5 mm is recommended to overcome the problem of steel plate separation due to shearing stresses in the epoxy layer. Clearly, experimental data is required to develop a good understanding of how URM, PRM and RC walls, strengthened by diagonal steel strips will behave under severe cyclic loading.

1.4 *Research Objectives*

The objective is this research project is to develop a simple retrofit concept to upgrade existing non-ductile low-rise concrete and masonry shear walls to a performance level that will satisfy modern seismic design codes. The retrofit concept considered in this research consisted of adding diagonal and vertical steel strips tied to the walls using through-thickness bolts. These steel strips were connected to the foundation using stiff steel angles and anchorage bolts. This method appeared to be an efficient upgrading technique worth investigating. The principal objectives of this experimental investigation are:

- To quantify the improvement in seismic resistance of non-ductile low-rise masonry and concrete shear walls provided by the proposed retrofit technique, and determine whether the resulting cyclic ultimate behaviour is adequate.
- To acquire the supporting data necessary to develop simple retrofit design recommendations for low-rise masonry and concrete shear walls, to provide satisfactory seismic performance.

These objectives were achieved by designing, constructing and testing six large scale wall specimens. The first three were unretrofitted walls of masonry, partially reinforced masonry and reinforced

concrete. The last three were identical walls retrofitted using the proposed diagonal steel strip system. Each specimen tested was subjected to quasi-static reversed cycles of in-plane loads. Based on results obtained, and study of the resulting behaviour, a simple design procedure to retrofit low-rise shear walls was formulated. This thesis provides the details of this research work.

1.5 Organization

The objectives and the scope of the proposed research project and the proposed method were described in Section 1.4. The overall behaviour of a retrofitted shear wall cannot be anticipated without clarifying the characteristic behaviour of each of its constituent part. Such knowledge is prerequisite to the determination of the lateral load capacity of retrofitted walls. Chapter 2 reviews the characteristics, behaviours, and failure modes of low-rise walls and steel strips under reversed cyclic loading. Chapter 3 describes the design of the specimens and the expected behaviour of the retrofitted walls. The details of test specimens and testing procedure are also described in Chapter 3. Chapter 4 reports the behaviour observed during the test and the experimental results. Chapter 5 compares the observed behaviour and results between the retrofitted and unretrofitted walls. Models of behaviour are proposed and verified in Chapter 6 along with displacement-based retrofitting design procedure. Chapter 7 presents a summary of research findings and conclusions.

Chapter 2

Low-Rise Walls and Steel Strip System

2.1 General

The overall behaviour of a retrofitted shear-wall cannot be anticipated without clarifying the characteristic behaviour of each constituent part. Such knowledge is prerequisite to the determination of the lateral load capacity of retrofitted walls. This chapter reviews the characteristics, behaviour, and failure modes of low-rise walls and steel strips, respectively under reversed cyclic lateral loading.

2.2 Low-Rise Shear Walls

A shear-wall, bearing or non-bearing, is a wall that resists horizontal forces applied in the plane of the wall. It acts either as a cantilever wall, or a wall in double curvature if adequate fixity exists at the top, relying on flexural and shear strength to resist these horizontal loads. A low-rise wall is a wall with an aspect ratio (i.e., with a ratio of height to horizontal length) of less than two. The cross-sectional depth of this type of wall gives it an extremely high moment of inertia, and therefore, a great stiffness against horizontal deflection. Most walls have rectangular cross-sections in plan; some have

transverse "flange elements". Masonry walls may be constructed of concrete blocks or bricks. This study will be limited to low-rise walls, without opening, built from unreinforced masonry, partially reinforced masonry, and reinforced concrete.

2.3 *Characteristics of Existing Non-Ductile Low-Rise Shear Walls*

2.3.1 Unreinforced Masonry Walls

An unreinforced masonry (URM) bearing wall is a wall that provides vertical support for floor or roof gravity loads in excess of 15 Newtons per linear metre of wall (NEHRP 1992). A URM wall is built by laying a large number of masonry units on a bed of mortar in successive courses, one above the other. Since no reinforcement is provided in this type of construction and no formwork is needed, they are very easy to build. Being unreinforced, on the other hand, is a disadvantage because reinforcement plays a major role in resisting tensile stresses. As a consequence, the use of URM walls is limited to conditions that do not produce tensile stresses normal to the bed joints at working stress. Currently, design codes do not allow new structures in moderate to severe seismic zones to be constructed of unreinforced masonry because such walls must rely on the tensile strength of masonry units and mortar to resist horizontal loads, a condition that is considered non-ductile. Unfortunately, many existing walls have been built using unreinforced masonry before this code requirement was enacted.

2.3.2 Existing Non-Ductile Partially Reinforced Masonry Walls

A partially reinforced masonry wall, also called lightly reinforced, may be defined as a wall made of masonry units reinforced horizontally and vertically. These walls are either; (i) Bearing walls with less then 0.2 percent steel; (ii) Bearing walls with steel reinforcing bars in either vertical or horizontal direction spaced at more than 1200 mm; (iii) Non-bearing walls with less then 0.05 percent steel reinforcement. For concrete block walls, vertical reinforcement is placed in the hollow cells of the blocks, and only the cells where reinforcement is present are grouted. With reinforcement being placed at a large spacing, the grouted cells along each steel bar link to create a kind of reinforced concrete column, and the wall can be thought of as a series of columns with unreinforced masonry infills (and some horizontal reinforcement) in between. While reinforcing bars are the only type used as vertical reinforcement, joint reinforcement (i.e., horizontal reinforcement) can consist of light steel

wires in a ladder or truss configuration placed in the mortar between courses as an alternative to standard reinforcing bars. This study considers only partially reinforced walls having joint reinforcement. The main advantages of partially grouted walls compared to fully grouted walls is that less material (grout) is needed. Their main disadvantage is their lesser cross-sectional area, and thus lower shear, axial, and flexural strength.

2.3.3 Existing Non-Ductile Reinforced Concrete Walls

A reinforced concrete shear wall is a concrete wall reinforced in both vertical and horizontal directions. The minimum vertical and horizontal reinforcement ratio (area of steel to the gross concrete area) is 0.15 % and 0.2 %, respectively. Spacing between the vertical and horizontal reinforcement is limited to 3 times the wall thickness or 500 mm, whichever is smaller. Usually vertical reinforcement is distributed uniformly over the full length of the wall. Current codes recommend the increase of flexural reinforcement near the ends of walls to provide boundary elements and thereby increase their flexural strength and ductility. Reinforcement, in each direction, is usually placed in two layers parallel to the faces of the wall.

Many reinforced concrete walls have been designed and constructed with only the minimum required reinforcement. By today's standards, although these walls are somewhat ductile, they are not considered ductile in the perspective of seismic resistance.

2.4 Parameters Affecting the Strength of Low-Rise Walls

It is clear from many investigations of low-rise shear walls that the behaviour of these walls is affected by different parameters. A review of the influence of these parameters is helpful in providing an understanding of the behaviour and failure modes involved. The following discussion will focus on important parameters relevant to this study.

2.4.1 Wall Aspect Ratio

Walls with aspect ratios of less than two, when subjected to large shear force reversals may exhibit non-ductile behaviour. The flexural capacity of these walls cannot be attained, and diagonal tension, compression or sliding-shear failures develop prematurely. These modes of shear failure may be

brittle. Therefore, inelastic deformability and hence dissipation of earthquake induced seismic energy is reduced. Thus, the aspect ratio of a shear wall is a major parameter that dictates its behaviour.

2.4.2 Type of Loading

Reversed cyclic loading applied to low-rise shear walls produces criss-crossing of diagonal shear cracks created by lateral load reversals. These intersecting diagonal cracks reduce the capacity of diagonal compressive struts that form a major part of the mechanism of shear resistance. Moreover, cyclic loading may cause shear walls to slide along their construction joints. This sliding does not occur in monotonically loaded walls. Therefore, while monotonic force-deformation relationships may be taken as representative of the envelopes of hysteresis loops in flexure dominant members, the same may not be true at later stages of loading for low-rise walls where cyclic loading effects often result in strength degradation (Doostdar 1994).

2.4.3 Axial Loading

Generally, axial compression tends to increase the strength of walls. Also, in presence of axial compressive stress, the inclination of diagonal shear cracks tends to be greater than 45° (as would be predicted by Mohr circle). Concrete low-rise shear walls normally carry only relatively small gravity loads and consequently benefit little from these gravity loads. Higher axial compression results in increased shear capacity, as well as increased flexural capacity except for compression-controlled failures (Drysdale et al.1994).

2.4.4 Construction Joints

A construction joint is the weakest point in a low-rise shear wall subjected to inelastic load reversals. Due to the interaction of flexure and shear, sliding along the construction joint may take place before the wall reaches its capacity. The interface along the construction joint is destroyed by this sliding, accentuating the problem. This will severely lower the strength of the wall, and result in a poor energy dissipation mechanism. Walls with low aspect ratios are more likely to develop sliding shear along their construction joints.

2.4.5 Vertical Reinforcement

In addition to its usual role in providing flexural resistance, vertical reinforcement plays a significant

role on shear strength. Indeed, vertical reinforcement is highly effective in resisting shear because diagonal cracks cannot open unless they deform the vertical bars crossing this path. The contribution of vertical web reinforcement in controlling inclined cracks becomes more efficient as the wall aspect ratio decreases. Also, if vertical reinforcement is uniformly distributed along the wall width, spacing and distribution of cracks can be controlled. Flexural capacity of low-rise walls can be achieved only when the shear capacity is relatively large.

2.4.6 Horizontal Reinforcement

Horizontal reinforcement contributes to shear strength and is effective in inhibiting the opening of shear cracks. Walls exhibit better ductility and energy-dissipation capacity when horizontal bars are well distributed over their heights.

2.4.7 Diagonal Reinforcement

The use of diagonal reinforcement in reinforced concrete shear walls is a relatively new idea. When diagonal bars are used in shear walls and adequate ties are provided to enable the compression struts to sustain yield loads without buckling, satisfactory performance can be expected. Diagonal reinforcement may contribute to the flexural and shear strengths of walls, and are useful to prevent sliding shear. The effectiveness of diagonal reinforcement in resisting sliding shear increases with decreasing bar inclination, and spacing of the diagonal steel bars intersecting the construction joint. If diagonal bars are made to intersect at the base and mid-width of the wall, their contribution to flexural resistance will diminish and their entire strength may be used to resist sliding shear (Paulay et al. 1992).

2.4.8 Boundary Elements

Current building codes require boundary elements and confinement of the ends of reinforced concrete shear walls. These boundary elements are provided to delay buckling of the vertical bars, and to facilitate confinement of the compression zone when it is needed. A boundary element usually consists of four bars or more, tied with closely spaced stirrups. Walls built before seismic provisions were introduced into building codes usually do not have boundary elements.

2.5 *Seismic Behaviour of Unreinforced Masonry Walls*

The capability of unreinforced masonry walls to resist lateral loads is limited by the strength of both masonry units and bed joint mortar. As mentioned in Section 2.1, axial loads affect the behaviour of low-rise walls.

At low loads, two failure modes are possible for the wall aspect-ratio considered here: (i) when earthquake forces act in the plane of the wall, sliding may take place along bed joints (see Fig. 2.1), or, (ii) a horizontal crack may develop along the base and the wall may rock, i.e. overturn around its toe. Localized cracks will appear at the comprised corner due to the overturning moment. These cracks increase until complete toe crushing occurs. This toe crushing does not affect the overall stability of the building when deformations are small, which is usually the case for non-slender walls. Fig. 2.2 illustrates typical ultimate behaviour of a wall rocking when subjected to lateral in-plane forces combined with low vertical loads.

Above a certain level of axial load, lateral sliding is suppressed, and diagonal cracks form within the masonry blocks due to an increase in bed joint friction. Under seismic loading, cracks will occur in directions parallel to principal tensile stresses. These in-plane shear cracks are commonly expressed by double-diagonal (X) shear cracking as presented in Fig. 2.3. Such unreinforced walls are generally incapable of withstanding severe repeated load reversals, suffering from low energy-dissipation capacity and severe strength degradation characteristics. In a severe earthquake, these plain masonry structural members may suffer extensive damage, leaving the building without an adequate lateral load-resisting system.

2.6 *Seismic Behaviour of Reinforced Concrete and Masonry Walls*

Although, reinforced concrete walls are usually labelled as "reinforced" without any reference to their amount of reinforcement, walls with low percentage of steel do exist. However, reinforced *masonry* walls are generally classified in accordance to their amount of reinforcement.

Only a few number of investigations (Ghanem 1993) have been performed on the in-plane behaviour

of partially reinforced concrete masonry walls. It is believed that code provisions for partially reinforced masonry walls are based on the observation of past practice and on available limited test data of reinforced masonry shear walls (Ghanem 1993; Schaltz 1994). The postulated mechanism of shear resistance in reinforced concrete masonry walls is generally similar to that encountered in reinforced concrete shear walls. However, concrete masonry shear walls are made of concrete hollow blocks, and this results in far more complex shear resistance mechanisms. While concrete is a homogeneous material in which the initiation of cracks is basically controlled by the tensile strength of concrete, crack initiation in concrete masonry is usually triggered along the bed and head joints due to the low tensile strength of these joints. However, regardless of these differences, overall behaviour is similar between the two materials because of the affinity of the shear resistance mechanism supplied by the aggregate interlock in cracked concrete members and an equivalent action in concrete masonry (Englekirk and Hart 1984).

2.7 Ductility and Energy Dissipation in Low-Rise Walls

Ductility is defined as the ratio of a specific deformation at any instant to that at the beginning of yield. Ductility in structural walls can be exhibited only if the constituent material itself is ductile. Although concrete and masonry can carry considerable compressive stresses, their performance in tension is weak. Therefore, detailing of this kind of a composite structure becomes extremely important to achieve ductile behaviour.

Yielding of vertical reinforcing bars at the base of a laterally loaded cantilever wall is a major source of energy dissipation. A reinforced shear wall will dissipate a satisfactory amount of energy if the following failure modes are prevented: *diagonal tension or diagonal compression caused by shear, sliding shear along construction joints, buckling of slender walls or of the compression reinforcement, and shear or bond failure along lapped splices or anchorages*. Hysteretic response curves for shear walls governed by shear are pinched, with significant stiffness degradation occurring in subsequent deformation to the same displacement (Fig. 2.4). To ensure that shear will not inhibit the desired ductile behaviour of a wall and that the shear effects will not significantly reduce the hysteretic energy dissipation capability of the wall during seismic response, shear must not be allowed to control strength. Therefore, an estimate must be made for the maximum shear force that might

need to be sustained by a shear wall during extreme seismic response, and design should be modified to ensure that energy dissipation can be restricted primarily to flexural yielding. (Priestley 1990).

2.8 Failure Modes in Reinforced Shear Walls

Shear walls with a small aspect ratio are likely to behave inelastically when subjected to severe lateral in-plane load reversals, provided that their foundations will not overturn or uplift. Low-rise reinforced walls can fail in diagonal tension, diagonal compression and shear sliding.

Diagonal tension is characterized by the initiation of diagonal hairline cracks, when the principal tensile stresses exceed the tensile strength of concrete (or masonry) under increasing horizontal displacements. If the horizontal reinforcement is insufficient to adequately transfer the tensile stresses across the diagonal cracks, these initial diagonal cracks will trigger shear failure. Under high reversal loading, these cracks will widen and a major diagonal crack pair will develop, leading to a dramatic and irrecoverable shear failure. This type of failure represents an unfavourable ultimate behaviour mode of shear walls and is classified as brittle shear-failure (Fig. 2.5).

By increasing the amount of shear reinforcement, the diagonal tension failure will be eliminated and the average shear stress in the wall section will increase to higher values. This will produce very high compressive stresses in diagonal struts. Under such severe compressive stresses concrete may crush. In the case of reversed cyclic loading, the compression strength of concrete will be reduced, and diagonal compression failure may occur earlier. Diagonal compression failure is responsible for extreme degradation of strength and stiffness (Fig. 2.6).

For walls heavily reinforced in the horizontal direction with relatively small amounts of vertical reinforcement, the diagonal cracks are eliminated. However, initial horizontal cracks at the base of the walls can extend throughout the cross-section. Due to the reversal of loading, grinding of the concrete (or masonry) material occurs, gradually leading to crushing at the bottom of the wall. This crushing forms a continuous weak plane near the base. The remaining part of the wall is undamaged, as schematically illustrated in Fig.2.7. This sliding failure is responsible for a considerable reduction in energy dissipation and ductility. The possibility of failure in any of these modes reduces with an

increase in axial load. However, if the axial load is increased beyond a certain limit, the accompanied reduction in ductility may offset the increase in strength.

2.9 Overview of Proposed Retrofit

It is intended to preclude the above types of failures that are typically observed in low-rise shear walls and to make the walls behave in a ductile manner. To achieve this favourable behaviour, diagonal bracing and vertical steel strips of plates will be used to cover the areas where principal stresses develop. The diagonal steel strips will extend between the corners of the wall. One of these strips will cover the diagonal tension field. It will strengthen diagonal tension resistance and will prevent diagonal tension failure. The other diagonal steel strip will cover the diagonal compression field. This element will improve diagonal compressive resistance in two ways. Firstly, significant portion of the diagonal stress at high level of loading will be transferred to the steel plate. Secondly, the diagonal segment of concrete or masonry between the steel strips will be confined from both sides of the wall, resulting in a higher compressive strength. Finally, the wall will be secured against sliding using very stiff steel angles and high strength anchors.

2.10 Behaviour of a Steel Strip Under Reversed Axial Loading

The overall behaviour of the retrofitted walls studied here will be strongly influenced by the cyclic behaviour of steel strips. That behaviour is essentially the axial hysteretic behaviour of a steel member reviewed below.

A hysteresis loop for a straight steel strip under a reversed axial loading is shown in Fig. 2.8. Each portion of the curve represents a different deflected shape and loading condition of a steel strip. It begins with a compressive load being applied to the steel strip and associated axial deformations. Portion OA in Fig.2.8 represents this initial elastic stage. The corresponding deflected shape is illustrated at the right top corner of the same figure. At point A, yielding may develop at the centre of the steel strip. Subsequently, an increase in axial deformation equal to the length of plateau AB may occur. This increase in axial deformation is caused by lateral deflection of the steel strip. At this point the steel strip reaches its maximum load in compression. A plastic hinge will form at point B

at the centre of the steel strip, and the plate will be forced to plastically deform due to instability effects. At this stage of loading, the compression force will be small because equilibrium can be maintained only if the compression force decreases. This phenomena is represented by curve BC in Fig. 2.8. If the compression reverses at any point along curve BC to a subsequent tension, the deformation will decrease and the steel strip will start to behave elastically. Residual rotation will remain prior to the reversal as a consequence to this plastification. During this elastic recovery the load will decrease to zero, followed by an increase in tension. The elastic recovery is exhibited by portion CD in Fig. 2.8. Point D represents the end of elastic recovery and the return of plastification at the centre of the steel strip. The behaviour of the steel strip from point D to point E is characterized by hinge action under tension. The load will increase to the yield strength. During this process the steel strip will restore straightness. The response of the steel strip between stage E and stage F involves yielding under constant yield load. Unloading to zero will be considered the end of the first hysteresis loop. The shape of the hysteresis loop changes mainly with the slenderness ratio (KL/r). For large KL/r ratio the hysteresis loop is thinner and energy-dissipation capacity is smaller. This ratio synthesizes the influence of the steel strip length, flexural stiffness and its end conditions.

In this study, the diagonal steel strips are expected to remain in their linear elastic range of behaviour when subjected to compression. This is achieved by limiting their slenderness ratio and axial stress under applied loads. However, the vertical steel strips, forming part of the retrofitting should undergo inelastic buckling during testing.

Chapter 3

Experimental Program

3.1 Introduction

This chapter outlines details of: 1) Design of unretrofitted and retrofitted walls 2) Expected behaviour of retrofitted walls 3) Wall configurations 4) Fabrication of walls 5) Retrofitting details 6) Material tests and 7) Testing procedure.

This research program sought to study the behaviour of retrofitted existing non-ductile, low-rise shear walls and to compare their ultimate cyclic behaviour with that of identical but unretrofitted ones. To reach the objectives of this experimental study, wall specimens with geometry shown in Fig. 3.1 were selected.

3.2 Design of Retrofitted and Unretrofitted Walls

This section offers a detailed description of all factors believed to affect the design of the walls, the design procedure, design details, expected overall behaviour of the retrofitted walls and expected

behaviour of steel strips used for retrofitting. Assumptions used in the calculation of the predicted ultimate lateral load resistance for all unretrofitted and retrofitted walls are described below as well.

3.2.1 Factors Affecting the Design of Walls

Because axial loads carried by shear walls in reinforced concrete buildings are small, and for simplicity in testing, axial loads were neglected in many tests of walls by other researchers, including eight walls tested at the University of Ottawa (Saatcioglu, Wasieewicz and Pillette 1998; Doostdar and Saatcioglu 1998). However, in this test program, axial loads were applied to all specimens in addition to the lateral loads, to create more realistic load conditions, and because this research study includes masonry walls whose ultimate behaviour is considerably affected by the presence of gravity loads. For example, the rocking capacity of URM walls depends directly on the magnitude of the applied axial load. If bearing loads are not applied on such a masonry wall, its lateral capacity is theoretically zero (if the self weight of the wall is neglected). Identical axial loads were applied to all specimens of this research study. This simulated identical tributary floor areas, and made it convenient to compare the results between specimens. A realistic axial load of 100 kN was chosen to simulate service gravity loads that typically act on a single-story building. Current code provisions for masonry concrete blocks do not permit compression service stresses greater than 22.5 % of $\sqrt{f_m'}$. The above load of 100 kN does not produce a stress in excess of the permissible limit.

Walls with aspect ratios of less than 1.0 have flexural strength higher than their shear strength because of their long lever arms between the resultant of compressive and tensile stresses. These walls fail in shear in a non-ductile manner as described previously. The proposed retrofitting system aimed to improve the performance of walls by increasing shear strength above their flexural strength, to promote flexural failure, and by increasing ductility and energy dissipation capability. All specimens were chosen with an aspect ratio of 1.0 to ensure that most of the unretrofitted walls would exhibit shear-induced damage. Other factors that had an impact on the selection of wall geometry and aspect ratio in this research project were the capacity of the actuators and limitation in the reaction frame.

The unretrofitted wall specimens were designed to resist low in-plane lateral forces and were detailed to represent existing non-ductile shear walls, i.e., walls built before the provisions for seismic design of walls were introduced in building codes. The strength of reinforcing steel bars, concrete, mortar

and concrete blocks used to build the six walls were chosen to reflect the past practice as much as possible. As expected, this choice was affected by availability of materials, as will be seen later. Furthermore, the steel strips were selected to be of mild steel with relatively low strength and high elongation prior to failure to ensure significant yielding of the steel before any crushing of masonry and concrete. The stress-strain relationships of masonry, concrete, and steel, shown in Figures 3.2 and 3.3, respectively, were used for strength predictions of the unretrofitted and retrofitted walls.

3.2.2 Unretrofitted Walls

The rocking strength of URM wall specimen was calculated using simple statics, where the stability of URM wall is provided by the axial load. This rocking can develop only because the shear strength of the wall calculated based on CSA S304 clause 11.5.3 is not reached at a lower lateral load level.

Flexural strength of the PRM wall specimen (layout of reinforcement shown in Fig. 3.4) was evaluated using the conventional theory of flexure. Shear strength for the same wall was determined based on CSA S304 clause 11.5.3.

The flexural strength of the RC wall specimen (layout of reinforcement shown in Fig. 3.5) was calculated using the same procedure used to estimate the PRM wall capacity. However, shear strength was computed based on a recommended simplified approach developed at the University of Ottawa (Doostdar 1994).

Details of the calculations used in designing the specimens are presented in appendix A.

3.2.3 Retrofitted Walls

For a single-story building located in Vancouver or Quebec City, the ratio of the base shear force calculated based on the NBCC 1995 to the corresponding value based on NBCC 1957 is in the range of 4 to 6 depending on its period, importance, and soil conditions. This implies that to retrofit a building located in one of these seismic zones to meet the current seismic requirements, its lateral-load resistance must be increased by the same ratio or more. The seismic retrofit solution was therefore designed to provide this level of increased strength in addition to ductile behaviour. Diagonal steel strips of 220x3.81 mm dimensions were chosen to satisfy this criteria. These steel

strips were connected to the top beam and the footing using stiff steel angles on each side of the wall.

To ensure an optimum ductile performance of the retrofitted wall, it is necessary to preclude severe inelastic buckling of the diagonal steel strips. When a steel member develops nonlinear buckling during cyclic loading, it can lose a large percentage of its original strength and its ability to dissipate energy reduces. Furthermore, in this case, buckling of the steel strips can produce undesirable stress redistributions that could lead to a premature wall failure. To ensure that the diagonal steel strips do not buckle prior to the attainment of large ductility and drifts, their slenderness ratio was chosen such that stresses at the maximum applied load were kept below their buckling values.

Vertical steel strips were placed near the ends of each wall to resist tensile and compressive flexural stresses. Although old existing reinforced concrete and reinforced masonry walls have vertical reinforcement, this reinforcement is much less than considered necessary nowadays to produce ductile walls, and is often placed at the ends of the walls without the lateral ties necessary to resist buckling of the bars (NEHRP 1992). As for URM walls, they have no steel reinforcement. Buckling of the vertical strips was expected at higher level of loading under repeated cycles of inelastic deformations. To limit excessive yielding due to inelastic buckling, and maintain the energy dissipation capacity of the steel strips, anchor bolts used to connect the steel strips to the wall were spaced at 100 mm and 150 mm, staggered for vertical and diagonal steel strips, respectively. This respected the CSA-S16.1-M94 limit of $L/r \leq 1900/\sqrt{f_y}$ for ductile bracing members, while respecting geometrical constraints to keep anchor bolts outside of the masonry bed joints. Under the above restriction, the vertical steel strips were expected to perform well in terms of strength, deformability and energy dissipation.

The flexural capacity of each retrofitted wall specimen was evaluated assuming full composite behaviour between the walls and steel strips. Shear strength of these retrofitted walls was found by adding the contribution of the steel strips to the original capacities based on a model for control of shear failure by diagonal tension in low-rise shear walls reinforced diagonally (Paulay et. al 1990). Details of calculation are presented in Appendix A.

Summary of the predicted capacities for each of the six wall specimens along with reinforcement ratio and schematics of the walls is shown in Fig. 3.6. This figure indicates that the predicted strengths of

the retrofitted walls were 140% to 600% higher than those of the unretrofitted walls. Although the strength improvements may seem high, they are representative of strengthening expected to bring existing walls in compliance with current codes, as indicated earlier.

3.3 Expected Ultimate Behaviour of Retrofitted Walls

The proposed upgrading method was expected to result in a large shear strength resistance, a large ductility capacity, and a large energy-dissipation capacity, with an eventual strength and stiffness degradation and failure by flexure. At higher loads, the retrofitted shear walls were expected to develop a truss behaviour where the diagonal steel strips along with the confined concrete or masonry act as bracing members, one in tension and the other in compression, as can be seen in Fig. 3.7. These diagonal strips were not expected to buckle prior to the development of large inelastic deformations, because of the lateral support that would be provided by the anchor bolts. The vertical compression member in that truss mechanism (i.e. the concrete or masonry acting with steel reinforcement, or the steel strips alone in the case of URM wall) was anticipated to deteriorate near the mid-height of the wall after a relatively large number of load cycles, by crushing of the concrete. At the same time, on the other side of the wall, the vertical tension member would undergo excessive yielding and might reach strain hardening.

With this type of retrofit, the dramatic and irrecoverable loss of strength caused by the non-ductile shear failure would be prevented and the retrofitted walls would exhibit ductile flexural response. The most likely modes of failure for each type of retrofitted walls were schematically drawn and are presented in Figs. 3.8, 3.9 and 3.10, respectively.

3.4 Test Specimens

The wall specimens are described in the following sections. Wall configuration and geometry are described along with reinforcement details, fabrication procedure, material tests and top and bottom beams.

3.4.1 Wall Configuration

This work is part of an ongoing research project at the University of Ottawa on the behaviour of low-rise shear walls. Eight reinforced concrete walls were previously tested under simulated seismic loading (Saatcioglu, Wasieewicz and Pillette 1998; Doostdar and Saatcioglu 1998). Six additional large scale walls with rectangular cross sections were constructed and tested in the current phase of the study. These specimens were labelled as Wall9, Wall9R, Wall10, Wall10R, Wall11 and Wall 11R following the notation for the previously tested 8 low-rise walls. The first and the second pairs of wall specimens were made of concrete masonry and the third pair of wall specimens were made of reinforced concrete. Letter R in specimen labels indicate retrofitting.

3.4.1.1 Masonry Wall Specimens

Four concrete block wall specimens were prepared using standard blocks with 200 mm nominal size. These concrete blocks satisfy the CSA standard A165-1-M1988 specifications for compressive strength of the concrete block. Head and bed joints with an approximate thickness of 10 mm were used to provide effective masonry unit dimensions of 200x400mm. All masonry walls were face-shell beaded using type O mortar which represents the practice of that of existing walls built in the 1950's and 1960's. The cells containing reinforcement were filled with the same mortar. Each wall consisted of a total of nine courses, providing a nominal height of 1800 mm, as illustrated in Fig. 3.1.

Three #15 (16.4 mm diameter) deformed reinforcing bars, providing a total of 600 mm^2 of steel area, were used to reinforce each partially reinforced masonry (PRM) wall. This resulted in one bar in each exterior cell and the third bar in the central cell. The vertical reinforcement ratio, based on gross area of horizontal section, was 0.17 %. The bars extended above and below the 1800 mm height of the masonry wall to ensure sufficient anchorage. Details of vertical reinforcement as well as the cells filled with mortar are shown in Fig. 3.4. Joint reinforcement, usually used to ensure some continuity in a masonry wall and to resist shrinkage cracking, was used in PRM walls. One truss type bed joint reinforcement was placed in mortar joint every two courses. Each truss reinforcement consisted of steel wires 4.11 mm in diameter (No. 8 gauge) interconnected by welded cross wires. The total horizontal reinforcement area was 106 mm^2, resulting in total reinforcement ratio of 0.13 %. Horizontal reinforcement was continuous over the length of the wall. The ends were anchored to the vertical reinforcement. The horizontal reinforcement details are shown in Fig. 3.4.

3.4.1.2 *Concrete Wall Specimens*

Two identical walls with 100 mm thickness were built from concrete, representing the construction practice of 1950's and 1960's. The two concrete walls were reinforced using 3 pairs of 9.5 mm hot-rolled deformed reinforcing bars (# 3 Imperial bar size), uniformly distributed along the length, providing a total area of 426 mm^2. This resulted in a vertical reinforcement ratio of 0.24 %. Equal area of reinforcement was provided as horizontal steel. Details of vertical and horizontal reinforcement are shown in Fig. 3.5.

Two coupons of the same reinforcing bars were tested before installing them to check their strength. The result of tests revealed 642 MPa as yield strength. It must be pointed out that 9.5 mm deformed reinforcement was not available in industry, since this is an older size # 3 bar that was used prior to metrication. An effort was made to obtain this size reinforcement with the strength level used in 1950's and 1960's. However, higher strength steel of the required size was found and used instead.

3.4.1.3 *Footing and Top Beam*

A stiff reinforced concrete footing was cast to provide full fixity at the base. The footing had an "I" shape to accommodate the bolt locations in the laboratory strong floor. To achieve full foundation fixity, they were over-designed, both in terms of strength and stiffness. Each footing was provided with four 3 in (76.2 mm) diameter holes. These holes were located to match with the holes in the strong floor. High-strength bolts with 2 3/4" (69.85 mm) diameter were used to fix the foundation to the strong floor. Four hooks with adequate anchorage length were cast in footings for handling and lifting the specimens. Also, a stiff reinforced concrete top beam was built at the top of each wall specimen. Its function was to transfer in-plane shear and vertical compressive stresses uniformly to the wall.

3.5 *Fabrication of Wall Specimens*

The reinforcement cage for footings and the reinforced concrete wall specimen were prepared first. They were placed in wooden forms for concrete casting, as shown in Fig. 3.11. Vertical and horizontal reinforcement were then assembled and anchored to the footing. The footing concrete was

cast first with the wall reinforcement in position. The construction joint between the footing and the wall panel was prepared by roughening the surface with a brush. The top beam reinforcement was then placed in its designated position with the help of a wooden form. This is illustrated in Fig 3.12. Wooden struts and threaded rods were used to stiffen the formwork against lateral concrete pressure. Forms were removed two days after casting concrete. Fig. 3.13 shows a concrete wall specimen after wooden forms have been removed.

Masonry walls, both reinforced and unreinforced were built by a licensed mason. Each footing were constructed as it was described for reinforced concrete specimens. The first mortar joint above the footing was fully mortared. The bottom course of blocks was laid on that mortar bed. For the partially reinforced masonry wall, the vertical reinforcement was accurately located prior to the casting of the footing. The first bed joint reinforcement was placed in the second bed joint mortar above the first course of masonry. The rest of the joint reinforcement was placed at every two courses as described earlier.

A URM wall under construction is shown in Fig. 3.15a. Figs. 3.14 and 3.15b display a PRM wall during construction. Cells with vertical reinforcement were filled with mortar after each course was laid. The top beam formwork was then placed and supported by a wooden frame, and the beam reinforcement was placed in its position. Three pairs of 400 mm long #15 (16 mm diameter) reinforcing bars were used as dowel bars to ensure proper connection of the top beam to the unreinforced masonry panel. Two of these pairs were placed in the external cells and the third pair in the central cell of the masonry blocks in the top course. Fig. 3.16 shows the masonry walls after construction.

3.6 Retrofitting Details

3.6.1 Steel Strips Details

Companion wall specimens were upgraded by adding two 220x3.81 mm diagonal steel strips on both sides as shown in Fig. 3.17. The diagonal steel strips were 9 gage (3.81 mm) thick. The strip width was chosen to ensure yielding of steel in tension prior to fracturing at bolt locations. The specified

yield strength of diagonal steel strips was 227 MPa.

Different procedures available for connecting steel strips to concrete are discussed in Chapter 1. These include epoxy, anchor bolts and through-wall bolts. Usually each procedure is appropriate for a specific ductility demand. Through-wall anchor bolts were selected in this application in view of the expected ductility range. Structural steel bolts of A325-3/8 in (9.5mm) and A325-5/8 in (15.9 mm) were used to fasten vertical and diagonal steel strips to the walls, respectively. The anchor bolts were expected to brace the steel strips and confine the in-between concrete or masonry. The spacing between these bolts was decided with due considerations given to post buckling behaviour. The bolts locations were selected to avoid interference with vertical and horizontal reinforcement. A nut and a washer were used to fasten the strips from each side of the wall, at each bolt location. The steel strips were also connected to concrete footing and top beam, using eight 150x100x16 mm angles having 300 mm length each.

The bolt diameter was selected such that the bolts remained elastic throughout the test. The steel strips were welded together at the centre of the wall, where they overlapped, and to the steel angles at the top and bottom. The steel angles were connected to concrete using 400 mm long high-strength anchor bolts. In addition to the above diagonal steel strips, two 80x3.81 mm vertical steel strips were added on each side of the walls as boundary elements, as shown in Fig. 3.17.

3.6.2 Installation of steel strip system

The nuts of the anchor bolts were not strongly torque when installing the steel strip system to the masonry walls. Tries had been done on stand-alone half blocks before the installation of steel strips to the masonry walls to establish the critical level of tightening to avoid local damages to hollow masonry. That torque was not measured; rather the technician developed a feel for what was acceptable. It is recommended that such trials be conducted before any installation to similarly train the construction crew. The above recommendation does not apply to reinforced concrete walls. In fact a high torque applied to anchor bolts may be desirable as it would result in higher confinement of the concrete between the steel strips.

3.6.3 Connections Between the Steel Strip System and Foundation

Steel angles and anchor bolts were used to connect steel strips to the foundation and top loading beam. They were over-designed to suit current as well as future research needs. A continuous rectangular washer plate, with three holes, was inserted between the nuts and the steel angle to prevent yielding of the angles. Details of this connection are shown in Fig. 3.18. Cement mortar bearing pads of 10 to 20 mm thick were used to distribute the load over the bearing area under all angles of retrofitted walls.

Once the steel strips were tied to the walls using through-thickness bolts, and the eight steel angles and rectangular washers were installed and secured by nuts, all joints between the diagonal steel strips, vertical steel strips and steel angles were welded. Full penetration groove welds were used between the steel strips. All edges of the steel strips were beveled prior to welding. The joints between diagonal steel strips and steel angles were welded last. Calculations showed that plug welds should be used in addition to fillet welds to ensure satisfactory transfer of stress from diagonal strips to angles. A certified welder executed all the above welds using gas metal arc welding (GMAW) and an electrode equivalent to EXX480.

3.7 Material Properties

Standard cylinders of 150x300 mm were cast from each batch of concrete and tested to determine their compressive strength, tensile strength and the stress-strain relationship of concrete. Prism Standard compression tests were performed for concrete block masonry. The height-to-thickness (h/t) ratio of the masonry prism was equal to 1. Sufficient tests were conducted to characterize filled and voided masonry prisms. The average compressive strength was 12.5 MPa for ungrouted masonry prisms and 8.1 MPa for grouted masonry prisms.

Tension coupon tests for vertical and horizontal reinforcing bars as well as steel strips were conducted. Stress-strain relationships of concrete, reinforcing bars and steel strips are presented in Figs. 3.19, 3.20 and 3.21, respectively. These tests indicate the following material properties:

- Concrete compressive strength : 29 MPa.

- Yield strength of reinforcing steel bar (imperial # 3) : 480 MPa.
- Yield strength of reinforcing steel bar (#15) : 400 MPa.
- Yield strength of vertical steel strips for Wall 10R and Wall 11R: 248 MPa.
- Yield strength of all steel strips except vertical strips used for Wall 10R and Wall 11R: 227 MPa.

3.8 Test Procedure

The specimens were allowed to cure for more than 20 days. Then, they were painted with whitewash to facilitate observation of crack patterns during testing. In addition, black lines were drawn on the painted surface to indicate reinforcement locations. The test setup and test procedure are described in the following sections.

3.8.1 Test Setup

Figure 3.22 illustrates the test setup. It consists of three 1000 kN capacity MTS actuators, two of which are positioned vertically to apply axial compression, and the third one positioned horizontally and supported by a frame to apply horizontal deformation reversals. The MTS actuators were controlled by an electro-hydraulic servo controlled system. The vertical actuators applied constant axial compression in the force controlled mode. The horizontal MTS actuator was used in the deformation controlled mode. The supporting frame consists of pairs of 457 mm deep channel sections secured to the laboratory strong floor and a pair of A-frames attached on top. Wall specimens are post-tensioned to the laboratory floor and have full base fixity. The lateral load is transferred through a stiff concrete beam, simulating a floor diaphragm. The setup allows walls to be tested as cantilever elements.

3.8.2 Assembling the Loading System

Fig. 3. 23 illustrates vertical and horizontal loading assembly. The vertical actuators were connected to the floor using square steel plates. Each plate had 2 ¾ in (69.8 mm) threaded hole near its centre and matching threaded bolt. Each actuator was attached to the steel plate using four 1½ in (38.1 mm) high strength bolts. The actuators were connected to a loading-beam-steel-spacer assembly at the other ends, which is secured to the specimens.

A 2 in (50.8 mm) thick steel plate was used to attach the horizontal actuator to the top concrete beam. The plate was slightly larger than the cross section of the top-beam to accommodate four horizontal anchor holes used to tie four 40 mm steel loading rods, connected to another plate of the same size at the other end of the concrete beam. The near end plate was secured to the horizontal actuator using high strength steel bolts. This arrangement of steel plates, one at each end of the concrete beam, allowed load reversals by pulling and pushing on the top beam.

3.8.3 Safety Measures and Lateral Support System

Two steel frames were placed on either side of wall specimens during testing , as a safety measure, to prevent out-of-plane instability of walls. They were built of hollow steel sections and were supported by the laboratory strong floor. Thick angles clamped to the frames were intended to guide the wall if necessary. A gap was left between the specimen and the guiding angles at the beginning of each test. The above frames are shown in Fig. 3.24.

3.8.4 Loading History

Each specimen was subjected to horizontal displacement reversals while also subjected to constant axial compression. The horizontal displacements followed a loading history that consisted of elastic and inelastic stages. At first, each wall was cycled elastically three times at a displacement level corresponding to 50 % of its computed original ultimate load capacity. Subsequently, the wall was cycled three times at each of the incrementally increasing inelastic displacement amplitude until failure. The displacements were expressed in terms of story drift, defined as top displacement divided by wall height. Specimens were deemed to have "failed" when the strength decay exceeded half of the peak strength. Fig. 3.25 shows the load history followed for each wall.

Note that loading histories were not the same for the seven sets of walls. Each wall specimens were subjected to slightly different displacement histories as a result of their particular behaviour characteristics, and ductility.

3.8.5 Instrumentation and Data Acquisition System

The specimens were well instrumented for displacement, rotation and strain measurements. Electrical resistance strain gauges (ERSG) were used to measure strains in reinforcing bars and steel strips.

Two types of electrical strain gauges were used. Electrical strain gauge type EA-06-125BT-120 with a gauge factor of 2.055 and maximum strain of 0.5% was used for horizontal masonry wall joint trusses. Electrical strain gauges type EP-08-250BG-120 with a gauge factor of 2.055 and maximum strain of 20% were used for the remaining reinforcement and for steel strips.

ERSG were placed on all vertical and horizontal reinforcing bars in Wall 10 and Wall 11, as illustrated in Figs. 3.26 and 3.27. Vertical and horizontal reinforcement in Wall 10R and Wall 11R were instrumented in the same way as Wall 10 and Wall 11. Strain gauges were also installed on south-side steel strips of Wall 9R, Wall 10R, and Wall 11R. Three strain gauges were installed on each vertical steel strip located at the north-west end of Wall 9R and Wall 10R. An additional eight strain gauges were installed on the north side of wall 11R. The locations of strain gauges installed on the north side of Wall 9R, Wall 10R and Wall 11R are shown in Fig. 3.28.

Displacements were measured by two types of instrument. These include, three Temposonic Maquotostrictive transducers with ±250 mm stroke capacity, and four linear variable displacement transducers (LVDT's) with ±25 mm stroke capacity. Figure 3.29 illustrates the locations of LVDTs. The displacement measurements were taken with respect to the foundation of wall to exclude any effect of sliding or uplift of the foundation on the laboratory strong floor. Three light steel frames, made of slotted angles, were erected on the footing to support instrumentation. The applied vertical and horizontal loads were recorded by load cells inside the actuators.

Two data acquisition systems were used to record forces and deformations. Namely, an MTS controller system linked to a micro computer, and a low speed Scimetric 200 data-acquisition system with 64 independent channels, linked to another micro computer.

Chapter 4

Observed Behaviour and Test Results

4.1 General

In this chapter, results and observed behaviour of seven tested walls are presented. Cracking loads, yield loads, ultimate loads, crack patterns, and failure modes are identified. Lateral load at top of wall versus horizontal displacements, cracking loads, yield loads, ultimate loads, crack patterns, and failure modes are presented. Interpretation, analysis and discussion of the recorded data follow in Chapter 5.

Each corner of the specimen was marked with a cardinal abbreviation (NE for north-east, SE for south-east, NW for north-west and SW for south-west) to facilitate descriptions of the observed behaviour. In general, three cycles were performed at each drift level. Each cycle began by subjecting the specimen to westward displacements (actuator was pushing the specimen) which are considered positive displacements for the remainder of this discussion. The second half of each cycle consisted of eastward displacements (pulling the specimen) which are considered negative displacements. The lateral loads follow the same sign convention as the displacements.

All wall specimens had an aspect ratio of 1.0. They were subjected to a constant vertical stress equivalent to 100 kN which simulated the gravity load likely to be applied to such structural members. Note that the lateral load applied to each wall specimen during testing was amplified by the vertical load imposed by the vertical actuator on the wall specimen due to $P\Delta$ effect. However, the vertical load was small and $P\Delta$ effect was ignored.

4.2 Observed Behaviour

Seven tests were conducted on the previously described six wall specimens. Wall 11 was repaired and retested as described in Section 4.2.4. The observed behaviour during each test is described, in the following paragraphs as illustrated by photographs depicting damage in specimens at different stages of loading.

4.2.1 Wall 9 (Unreinforced Masonry Wall)

This wall was subjected to the displacement history shown in Fig 3.25. The hysteretic lateral load-displacement relationship for Wall 9 is presented in Fig. 4.1. The photos in Figures 4.2, through 4.6 taken at various drift levels during testing, illustrate the type and extent of damage that Wall 9 experienced. Calculations done prior to testing predicted that the wall would rock on its base at a lateral load of 46 kN, i.e. much less than the load of 89 kN that would be required to produce shear cracking.

During the first two elastic cycles, the wall reached a load of 47 kN and did not develop any cracks. In the third cycle, cracks started to occur above the first row of blocks near the wall base, at 57 kN and -51 kN in each direction respectively. This is illustrated in Figs. 4.2a and 4.2b. At these loads, the horizontal displacements were 0.64 mm and -0.36 mm, respectively. At about twice these drifts, the cracks extended horizontally to the middle of the wall where they moved down one block. Loads of 60 kN and -57 kN were applied when a drift of 0.1% was reached in each direction. At this level the cracks at the ends of the wall opened up about 2.0 mm and 2.5 mm for westward and eastward loading, respectively. From that point onward, the wall was cycled between progressively increasing target drifts.

At drifts of ±0.2% (first cycle), the wall reached its peak lateral load resistance of 64 kN and -57 kN. Cracks (3.0 mm to 4.0 mm wide respectively) suddenly opened between the second and the third rows of blocks at the west end. A few shear cracks also developed through the blocks on the first row at the east and west lower ends of the wall, as can be seen in Figs.4.2c and 4.2d. During the second cycle at this drift level, lateral load resistance suddenly dropped from 60 kN and -57 kN to 52 kN and -48 kN respectively. Inspection of the specimen revealed vertical and diagonal cracks in a few blocks near the west end. At the east end, cracks propagated horizontally towards the joint between the second and third rows of blocks (Fig. 4.3a and 4.3b). A horizontal crack also developed along the bed joint between the third and the fourth rows for a length of half a block (Fig. 4.3c). Evidence of initial crushing (Fig. 4.3b) of the lower west corner block was observed at the end of this cycle. During the first half of third cycle, more crushing developed at the base corner on the west side, and a vertical crack went up to the fourth row of the edge block, on the east side of the wall. During the second half of that cycle, the wall slipped by approximately 3.5 mm eastward, sliding on top of the second row of blocks. This slippage was not recovered when the load was reversed.

Crushing at the west end extended only half a block when the wall was pushed to the first cycle of 0.3% drift (Fig. 4.3d). A huge vertical crack (7 mm wide) opened on the east side, together with another 7 mm wide vertical crack between blocks near the middle of the wall. No new cracks were observed when the specimen was pulled toward east, but clear evidence of rocking on top of the second layer of blocks was visible. A few new minor cracks due to the progression of compression crushing were observed during the second and third cycles at 0.3% drift. Fig 4.3c shows the east end of Wall 9 at the end of the third cycle of 0.3% drift.

A major drop in strength (from -54 kN to -42 kN) was observed during the second cycle of 0.4% drift as new cracks formed on the east side. At this stage of testing, the wall was clearly rocking when loaded toward east, and sliding when loaded toward west. This is shown by the wide vertical cracks in Figs. 4.4a and 4.4c, and the wide horizontal cracks in Figs. 4.4b and 4.4d, at the east and west ends, respectively. The wall was then loaded in both directions to 0.8% drift. The blocks at lower corners of the wall suffered severe crushing damage (Fig. 4.5d), leading to significant strength degradation. The overall wall behaviour also changed from sliding westward and rocking eastward to rocking in both directions, as shown in Figs. 4.5 and 4.6.

Crushing damage became more severe at higher levels of lateral drift. A portion of a block fell off as a result of this crushing. Extensive strength deterioration was suffered when drift reached 2.0%. Strength decreased to 55% of the maximum experimental value, and testing was stopped. The failure of this wall was categorized as toe crushing failure due to excessive rocking. Fig. 4.6 illustrates different views of Wall 9 at the end of the test (2.0% drift).

4.2.2 Wall 10 (Partially Reinforced Masonry Wall)

This wall was subjected to the displacement history shown in Fig 3.25. Calculations done prior to testing predicted that the wall would reach its ultimate (shear strength) at a lateral load of 120 kN. This wall was subjected to fewer cycles compared to other walls because of a rapid degradation of strength at the end of the test. The maximum drift applied during this test was 0.8%. The recorded lateral load-displacement hysteresis loops of Wall 10 are shown in Fig. 4.7. Figures 4.8, through 4.11 illustrate the behaviour as well as type and extent of damage at various drift levels during testing.

Cracking of this wall initiated at lateral loads of 68 kN and -50 kN for loading in westward and eastward directions, respectively. The wall was cycled three times at a drift level corresponding to these loads. Many small cracks developed in horizontal and vertical mortar joints during the third cycle, forming a diagonal stair-step pattern as shown in Figs. 4.8b and 4.8c. A horizontal crack was formed along the mortar joint at the base.

The first crack outside mortar joints (i.e. in a masonry block) formed at the end of the first cycle of 0.2% drift. It occurred through the second block in the fourth row on the east side of the wall as, shown in Fig. 4.9a. The maximum strength of the wall was reached at this drift, for applied lateral loads of 119 kN and -120 kN. A diagonal crack in the east-end blocks, near the base formed during the second cycle (Fig. 4.9b). Similarly, a small diagonal crack formed in the second block of the second row, at the west end of the wall, during the first half of the third cycle (Fig. 4.8d).

Once the drift reached 0.4% in the westward direction, a diagonal crack opened near the base (see Figs. 4.9c and 4.9d), and the strength of the wall dropped by 23%. Some sliding started to develop on top of the third layer of blocks. This behaviour was detected due to the presence of a visible offset at the east end of the wall. Some vertical and horizontal cracks in the middle of the wall also formed

and opened sufficiently wide to let light through the wall. In the reversed direction, the strength dropped but only about 8.3 %. The loss of strength continued in the second and third cycles as the existing cracks extended and new cracks formed. By the end of the cycles at 0.4% drift, cracks had spread over the entire wall (Fig 4.10). There was also evidence that the grouted cells at both ends of the wall were splitting away from the centre part of the wall. A vertical crack formed at each end, extending from top to bottom. This is visible in Figs. 4.10b and 4.10c. These cracks split the joints between the grouted cell and the remaining wall. This splitting was similar to what is frequently observed during tests of infill frames, with the grouted cells in this case playing the role of reinforced concrete columns.

The wall strength at 0.6 % drift decreased to 45% of the maximum value reached during the test. Inspection of the wall revealed that diagonal crushing was beginning to occur at the top of east and west end half blocks at the third level. This is illustrated in Fig. 4.10d. The width of all vertical cracks was measured as there was some sliding accumulating over all layers. These measurements showed that the wall had widened. Upon further cycling at 0.6% drift, both bottom end blocks crushed along with the mortar inside the cells, exposing buckling of west end reinforcing bars (Fig. 4.11a and Fig. 4.11b, respectively). The end corner masonry blocks and some middle blocks exhibited severe crushing when the wall reached 0.8% drift. This is shown in Figs. 4.11c and 4.11d. This crushing lead to a dramatic strength decay. The test ended after the third cycle at this drift level.

4.2.3 Wall 11 (Reinforced Concrete Wall)

Wall 11was subjected to the displacement history shown in Fig 3.25. Calculations showed that the lateral load required to reach the wall flexural strength would be 155 kN. This was less than the load of 210 kN required to produce shear cracking. The lateral load-displacement response of Wall 11 is given in Fig. 4.12. A series of photographs were taken during the test to illustrate the observed damage and behaviour at various drift levels. Figs. 4.13 and 4.14 illustrate the extent of damage observed during testing.

The first crack occurred at the base of the wall, along the construction joint. The applied force and corresponding drift were 84 kN and 0.05%, respectively. This crack propagated horizontally to a length of 1680 mm during cycles at 0.1% drift, corresponding to a lateral load of 138 kN. Vertical

cracks were observed on the east and west faces (i.e. narrow faces) of the wall after two cycles, suggesting that the vertical reinforcement was buckling at these locations. The concrete cover started to spall off on the east face during the third cycle, exposing the buckled bar at the SE corner (Fig. 4.13a). The crack at the base widened and lengthened to cover the entire wall base during the first cycle at 0.2% drift. The corresponding loads recorded during this cycle were 125 kN and -148 kN in each direction. Vertical splitting cracks were observed on the west face of the wall indicating that the vertical reinforcement was starting to buckle. The SW corner bar buckled during the second cycle in the westward direction, and the cover spalled off almost completely.

The wall behaviour did not change during cycles at 0.3% drift, except that the cracks became wider and some crushing was observed near the base. The vertical bars at the east end also buckled, showing more spalling than that observed earlier at 0.1% drift, exposing more of extreme bars. The crack at the base opened wider at this stage of loading. No new cracks appeared during the cycles at drifts of 0.5 to 1.5%. The wall started rocking in both directions with no sign of sliding. The wall damage concentrated mostly to the base due to this rocking behaviour. The horizontal crack progressed slightly upward near the corners, as shown in Fig. 4.15. This behaviour could be explained by lesser resistance provided in regions where the bars were buckled, compared to lower regions where pieces of concrete remained attached to the base due to the anchorage of reinforcement.

The concrete cover at the centre of the wall near the base spalled off at 1.5% drift, exposing the middle reinforcement. The middle bar on the north side of the wall ruptured during the first cycle at 2.0% drift at a lateral load of 171 kN, as illustarted in Fig. 4.14d. The other middle bar ruptured when the wall was subjected to the same drift in the reverse direction. At this stage of loading, the strength dropped considerably and testing was discontinued. Fig. 4.14 shows different views of Wall 11 at 2% drift.

4.2.4 Wall 11RP (Repaired Reinforced Concrete Wall)

Wall 11 was damaged along the construction joint to a degree such that there was no continuity left between the wall panel and its foundation. Damage at the ends was also localized where the reinforcement buckled. However, the rest of the wall above the construction joint did not experience any damage or even cracking. A decision was made to repair and retest this wall, as representative

of a wall damaged by a severe earthquake. The objective of the repair strategy was solely to restore the flexural capacity to a level not less than that corresponding to diagonal tension capacity. This was done by connecting two pairs of vertical steel strips to the ends of the damaged specimen. The design of these steel strips and the details of their connection to the wall and its foundation is described in the following paragraphs.

4.2.4.1 Design of Vertical Steel Strips and their Connections

The vertical steel strips used to repair and strengthen Wall 11 were sized to raise the flexural strength of the wall above its shear strength. This would also provide an opportunity to compare the behaviour of the repaired wall with vertical steel strips only, with that retrofitted using the full steel strip system. The predicted shear strength of the virgin wall was 207 kN. Steel strips of 160 mm by 4.8 mm ensured that a lateral load of at least 300 kN would be resisted before flexural failure could develop in the repaired wall. A staggered through-thickness bolt arrangement was selected to tie the vertical strips to the wall panel, as shown in Fig. 4.16. This arrangement was designed to ensure the yielding of gross steel section prior to fracturing net steel section at bolt location. The bolt spacing was chosen to avoid elastic buckling of strips.

Eight 154x154x15.9 steel angles were selected to connect vertical steel strips to the foundation and top beam. These angles were 250 mm long. The joints between the vertical strips and the steel angles were welded. Three 19 mm steel anchor bolts were used to connect each steel angle to the foundation and top beam. The anchor bolts were designed to resist reaction forces transmitted through the steel angles. An anchorage length of 250 mm was found to be adequate for this purpose. The details of the repairs made to Wall 11RP are shown in Fig. 4.16.

4.2.4.2 Repairing Procedure for Wall 11RP

Repairing started by cutting the buckled end reinforcement. The wall ends were then repaired using cement mortar, mostly for aesthetic reasons. Steel strips with pre-drilled holes were held in place on the wall using large clamps. Fourteen 16 mm diameter holes were drilled through the wall at each end using the steel strips as templates. Through-thickness bolts were then used to tie the steel strips. Subsequently, twenty-four holes of 20 mm diameter were drilled in the foundation and top beam to a depth of 300 mm. Wedge anchors were inserted in these holes to connect the steel angles. Epoxy

adhesive was used to increase the bond and to eliminate slippage of the anchors. Finally, all the connections between the vertical strips and the steel angles were welded by a certified welder.

4.2.4.3 *Instrumentation of Wall 11RP*

Twelve strain gages were used to record the distribution of strains in the vertical steel strips, in addition to the LVDT's used, as in all other walls. Three strain gages were glued on each vertical steel strip, one at mid-height and one at each end, as shown in Fig. 4.17. The strain gages on reinforcing bars were disconnected since it was believed that they were damaged during the test of Wall 11.

4.2.4.4 *Observed Behaviour of Wall 11RP*

Wall 11RP was first subjected to the same displacement history as Wall 11. Nevertheless, additional cycles were applied on Wall 11RP because it was capable of resisting higher drifts, i.e. while the maximum drift of Wall 11 was 2%, this repaired wall (Wall 11RP) was tested to a drift of 3%. The displacement history for this specimen is shown in Fig. 4.18, while the resulting hysteretic relationship is presented in Fig. 4.19. The experiment damage at various drift levels is shown in Fig. 4.20 through 4.25.

Testing started by subjecting the wall to three cycles at 0.1% lateral drift. Although the wall showed no cracking, rocking of the steel angles was observed when they were pulled up by the steel strips. This rotation of the angles forced the steel-strips to move away from wall surfaces, as seen in Figs.4.20a and 4.20b. The behaviour remained essentially the same during the cycles of 0.5% to 1.0% drift. A vertical crack formed in the east (narrow face of the wall), extending up 300 mm, as depicted in Figs. 4.20a and 4.20c. The corresponding lateral load levels, at this stage of loading, were +202 kN and -244 kN, respectively. The anchors in the foundation experienced about 12 mm of pullout due to significant rocking of steel angles. This was attributed to inadequate bond between the anchors and concrete. An attempt was made to prevent rocking by closing gaps between the angles and the footing, using steel shims. Unfortunately, their beneficial effect was limited. This rocking could have been reduced if cement bearing pads had been used under the steel angles.

The first shear crack was observed at a drift of 1.16% when two diagonal cracks appeared at the east

end. One of the cracks started at about 120 mm below the top beam, and the other at mid-height. They started near the east top corner and propagated towards the bottom west end as shown in Figs. 4.21a and 4.21b. The first crack in the reversal direction appeared approximately at 1.32% drift and followed the same pattern (Fig.4.21c). At around the same level of drift, the steel strips started to show mild plastic-buckling just above the bottom steel angles (Fig.4.21d). The control system shut down and the test stopped when the horizontal actuator was pulling the specimen eastward during cycle 11. A safety mechanism of the controller was triggered automatically when measurements revealed that the specimen was moving excessively sideways due to insufficient lateral support. Indeed the wall had moved sideways towards south at its west end. The lateral support was then reinforced and testing resumed.

The specimen reached its peak lateral load resistance of 260 kN during the first cycle of 2.0% drift. The middle diagonal crack opened wider and propagated horizontally towards the ends as illustrated in Figs. 4.22a, 4.22b and 4.22c. Excessive plastic-buckling of the SW steel strip was observed at this stage of loading. This is shown in Fig. 4.22d. Severe deterioration of concrete was observed near the ends. More pull out of anchors was observed. The outermost anchor at the NE side drastically pulled out by approximately 24 mm. New shear crack appeared during the first half cycle of 2.5% drift, and the existing cracks opened more than 12 mm wide as shown in Fig. 4.23b. A sudden drop in load was observed at 2.3% drift. The cause of this drop was not obvious. However, some damage was observed in the top beam near the east anchor during the second cycle of 2.5% drift. This is shown in Fig.4.23c. The base anchors at the west end pulled out by approximately 34 mm during the third cycle (Fig. 4.24a).

The wall severely twisted at the east end, and moved south during the third cycle at 3.0% drift. This is shown in Figs.4.24b and 4.24c. The maximum lateral load reached during this cycle was 119 kN and -130 kN towards east and west, respectively. This was a drop of more than 50% in lateral load resistance. The test was stopped at this stage of loading. Fig. 4.24d illustrates the damage in Wall 11RP at the end of the test.

4.2.5 Wall 9R (Retrofitted Unreinforced Masonry Wall)

This wall was subjected to the displacement history shown in Fig 3.25. The predicted ultimate lateral

load resistance was 390 kN. The force-displacement hysteretic relationship for Wall 9R is shown in Fig. 4.25. Figs. 4.26 through 4.31 illustrate observed damage at selected stages of loading.

Horizontal cracks in mortar joints between the blocks were visible since the first cycle. The initial crack started at the west end above the second block, and propagated through the entire wall width. The cracking loads were 100 kN and -100 kN in the westward and eastward directions, respectively. Additional hairline cracks developed near the east end, during the first half of the third cycle at 0.1% drift. They occurred along horizontal and the vertical joints throughout the height, as shown in Fig. 4.26a. The vertical steel strips seemed to distribute the cracks rather uniformly along the height of the wall. The same phenomenon was observed along one of the diagonal steel strips, propagating from top west to bottom east corner. These cracks formed a stair-step pattern as depicted in Fig. 4.26c.

A small gap of approximately 4 to 5 mm opened between the steel strips and the wall. This phenomenon was similar to that observed for Wall 11RP, and was caused by movement of the anchor angle at 0.2% drift. New diagonal cracks developed during the second half of the second cycle, propagating from bottom west to top east corner. These cracks were similar to those observed earlier in the reversed direction (Fig. 4.26a). The first through block crack developed in a block located between the vertical steel strip and diagonal steel strip on the SE side, as shown in Fig. 4.26d. Maximum loads achieved at this drift level were 264 kN and -235 kN in respective directions of loading. A vertical crack formed on the east narrow face of the top block at the end of the third cycle. This is shown in Fig. 4.27a, and was interpreted as a sign of the initiation of masonry crushing.

The load dropped from 318 kN to 303 kN just before reaching the target drift level of 0.4%. Inspection of the wall, as shown in Fig. 4.27, revealed that a big horizontal crack had formed at the lower corner of the west side. Also, noticeable crack opening occurred along the entire length of the wall base (Fig. 4.27b). Buckling of vertical steel strips on the SE side was observed, as illustrated in Fig.4.28b, as 0.4% drift was approached. Separation between the steel angles and the wall did not increase beyond the values reported earlier at smaller drifts. A wide diagonal through block crack developed on the west end of the wall when it was loaded to 0.6% drift. Subsequently, a number of horizontal cracks formed on the east side, as shown in Figs. 4.28c and 4.28d. The lower part of the

diagonal steel strip on the SE side started to buckle, as illustrated in Fig. 4.29a. A new diagonal crack with an inclination of 63° with the horizontal also developed near the east end of the wall. This is shown in Figs. 4.28c and 4.28d. The diagonal steel strips on both sides of the wall buckled near the bottom west end during the second cycle of 0.6% drift. This can be seen in Figs. 4.29b and 4.29c. Crushing of masonry at top east and bottom west ends intensified throughout the cycles at 0.6% drift. After the cycles of 0.6% drift, it was decided to increase the drift to 1.0%. However, the wall started to lean noticeably northward when 0.91% drift was reached. It was therefore decided to limit the target drift at this stage to 0.8% to continue testing.

The highest lateral load resistance recorded was -348 kN at the end of the first cycle of 0.8% drift. Excessive buckling of the lower end of the NE vertical strip was observed at this deformation level. This is evident in Fig. 4.30b. The west end of the wall was severely crushed during the second cycle of 0.8% drift, as shown in Fig. 4.30a. Therefore, the wall suffered strength degradation. A 25% drop in lateral load resistance was recorded, while a noticeable clockwise twisting of the wall was observed. This twisting was attributed to unsymmetrical buckling of the steel strips. An attempt was made to reinforce the lateral support frames and the third cycle at 0.8% drift was applied. The wall lost significant portions of its narrow faces by the end of these cycles.

The strength degradation became more rapid as the contribution of masonry to lateral load resistance further decreased at 1.0% drift (Figs. 4.30c). Consequently, the number of loading cycles was reduced to two per target drift level. At the end of the first cycle at 1.0% drift, both vertical strips at the east end buckled simultaneously, in a global mode. Clearly, the vertical steel strips were left without lateral supports after the loss of masonry near the ends (Fig. 4.30d). The wall lost the face shell of all east end blocks when the drift level was increased to 1.25%. This is shown in Fig. 4.31a. The vertical strips further buckled in a global mode as illustrated in Fig. 4.31b. The load resistance dropped to 153 kN and -149 kN in each direction when a drift level of 1.5% was attained. Because the major portions of the masonry wall were destroyed as shown in Figs. 4.31c and 4.31d, the wall started to lose its integrity. The load resistance increased up to 200 kN during the first cycle at 2.0% drift, but dropped subsequently to 114 kN in the following cycle. The test was terminated as it became laterally unstable.

4.2.6 Wall 10R (Retrofitted Partially Reinforced Masonry)

This wall was subjected to the displacement history shown in Fig 3.25. The predicted ultimate lateral load resistance was 539 kN. Wall 10R experienced weld failure at two locations during testing. Therefore, the test had to be stopped to reinforce the failed joints, as described below. The hysteretic force-displacement relationships obtained prior to the weld failure and after repairing the weld, are presented in Figs. 4.32 and 4.33, respectively. The combined hysteretic relationship is shown in Fig. 4.34. Experimentally observed damage at various drift levels is shown in Figs. 4.35 through 4.42.

Initial cracks at 0.1% drift were in the form of hairline cracks, taking place near the SE corner. The corresponding lateral load resistance was 150 kN. Additional hairline cracks formed in mortar joints when the load was reversed. These cracks are illustrated in Figs. 4.35a, 4.35b and 4.35c. Diagonal cracks were observed at the end of 0.1% drift cycles, following a stair-step pattern near the diagonal strips (Fig. 4.35d). The cracks that had developed earlier extended further during 0.2% drift cycles. New vertical and horizontal cracks also formed between the blocks, mostly near the diagonal steel strips. These cracks were mostly visible within the upper half of the wall, as illustrated in Figs. 4.36a, 4.36b and 4.36c. The lateral load resistance reached 212 kN and -231 kN in westward and eastwards directions, respectively. No distress of steel strips was observed at this stage of loading, and the steel angles did not show any visible rotation.

A long diagonal crack formed and propagated through the NW side blocks during the first cycle of 0.4% drift. This is shown in Fig. 4.36d. Some rotation of the base steel angles at the west end was observed when the load was reversed. Also, some cracks opened at the base. Identical rotation and cracking was observed at the east end under load reversal. Pinching of hysteresis curves became noticeable during the third cycle of 0.4% drift. Maximum lateral loads applied during these cycles were 321 kN and -342 kN in the westward and eastward directions, respectively. Through block diagonal cracks appeared on the SE side, during the first cycle at 0.6% drift and a peak lateral load of 397 kN. This is shown in Fig. 4.37a. At the same time, a crack across the base of the wall started to widen. Buckling of diagonal steel strips started near the bottom west end during the end of the first cycle (Fig. 4.37c), and in the opposite direction during the first half of the second cycle (similar to that shown in Fig. 4.37d). The vertical steel strip at the SE bottom corner buckled at the end of the second cycle (Fig. 4.37d). A few new cracks due to crushing were observed on both faces of the wall

during the first cycle at 0.8% drift . At this stage of loading, the lateral load resistance was 417 kN and -460 kN in each direction. During the second cycle, diagonal steel strips on the south side buckled slightly near the mid-height. The east end of the wall started to lose some shell cover at the end of the second cycle.

Evidence of squeezed mortar and crushed masonry was noticed behind the buckled parts of steel strips during the first cycle at 1.0% drift. At the peak of the first cycle, while sustaining a load of 400 kN, some noise was heard, and the west end of the wall started to lean towards north. Then, a big bang was heard and a safety mechanism automatically stopped the test and released pressure from the actuators. The specimen was unloaded at once. Inspection of the specimen revealed no weld fracture and no extraordinary damage. It was decided to resume the test and try loading the specimen again.

During reloading, however, the wall did not reach its expected strength. The drift and maximum load resistance were 1.0% and 270 kN, respectively. A horizontal crack formed under the top layer of blocks indicating sliding of the top part, as illustrated in Fig. 4.38a. Inspection of the specimen revealed that the welded joint connecting the two diagonal steel strips on the north side had fractured. This is shown in Figs. 4.38b, 4.38c and 4.38d. Examination of the failed joint showed inadequate penetration of the weld. The weld extended only a small distance into the groove, contrary to what was specified in the details indicated in Chapter 3. The specimen was then unloaded and the test was stopped.

Testing resumed after re-welding the fractured joint (Fig. 4.39a). The wall started to move sideways when the drift reached 1.2% at a corresponding lateral load of 300 kN. The reinforcing bar on the east side of the wall buckled near the base. It was then decided to load the wall back to -300 kN to find the origin of the hysteresis loops. Measures were also taken to prevent lateral movement in subsequent cycles. The wall was pulled only about 0.7% drift when the NW side weld of the joint connecting the vertical steel strip to the diagonal strip broke near the base. This is shown in Figs. 4.39b and 4.39c. Testing had to stop again. At this point, it was decided to reinforce all welds of the steel strips, including those for Wall 11R, retrofitted reinforced concrete wall that was scheduled for testing next. All welded steel strip joints were reinforced with 60 mm x 25 mm x 7 mm lap-plates,

fillet welded all-around. This can be seen in Figs. 4.40a, 4.40b and 4.40c.

Testing resumed again by loading from a drift of 0.4% to 1.1%. The peak load resistance attained was 302 kN. The wall was cycled twice at this drift level. In the second cycle the west side shell of masonry spalled off due to the buckling of reinforcing bar, similar to that shown in Fig. 4.40c. The lateral load resistance of the wall increased slightly at 1.5% drift. Spalling exposed the bolts used to attach the vertical strips. This indicated that the bolts were useful in providing lateral restraints against the buckling of reinforcing bars. This is shown in Fig. 4.40c. The vertical and diagonal strips continued to buckle and yield as was observed earlier. Severe buckling of SE vertical strip was visible at mid length between the bolts, during the third cycle of this deformation level. The severity of buckling suggested that low-cycle fatigue would eventually lead to the fracture of vertical strips (Fig. 4.40d). It indeed ruptured in the manner expected, as illustrated in Figs. 4.41a and 4.41b, at a drift level of 1.6% (160 kN), during the second cycle at a target drift of 2.0%. As soon as the steel strip ruptured, the wall started to twist clockwise. The wall also sled out-of-plane above the second row of blocks on the west side, as seen in Fig. 4.41d. However, testing was pursued. During the third cycle at 2% drift, a piece of broken block fell off the wall on the NW side. More broken blocks fell off from the same side upon returning to zero load. At this stage, the wall had a large see-through hole on the west side, between the diagonal strip and the vertical strip. This is illustrated in Figs. 4.41c and 4.41d. The vertical steel strip on the NW side ruptured while loading towards 2.5% drift, at 1.5 % drift. This was followed by the vertical strip on the SW side. The lateral load at failure was 90 kN, when the test was terminated. Fig. 4.42 shows the damage in Wall 10R at the end of the test.

4.2.7 Wall 11R (Retrofitted Reinforced Concrete Wall)

Wall 11R was subjected to the displacement history shown in Fig 3.25. The ultimate lateral load resistance was predicted to be 497 kN. The hysteretic force-displacement relationship recorded during testing is presented in Fig. 4.43. Observed behaviour at various drift levels was captured by a series of photos, as illustrated in Figs. 4.44 through 4.52.

Initial flexural cracking was observed at the east end of the wall, at a drift of 0.1% and a corresponding lateral load of 250 kN. The cracking started just above the welded joint connecting the vertical and diagonal steel strips, and extended up to the mid-width of the wall along the

construction joint. A few horizontal cracks crossed the narrow face of the wall, approximately at the location of the through-thickness bolts. This is illustrated in Fig. 4.44b. Horizontal cracks developed in concrete at about mid-height, followed an inclined path after extending to about one quarter of the wall length. The crack pattern under reversed loading was the same when the wall was subjected to an eastward load 238 kN. More cracks appeared at 0.2% drift when the load reached 300 kN in westward direction. A near full-width diagonal crack formed at this stage, as shown in Figs. 4.44c and 4.44d. The diagonal cracks had an approximately 45° inclination, and often originated at bolt locations. The diagonal steel strut remained intact, as shown in Fig. 4.44d. There was no sign of buckling and crushing of concrete.

First yielding of vertical steel strip was detected on the SE side, near the base, when the lateral load (i.e. yield load) was 366 kN. Some of the cracks crossing narrow faces opened up at a drift of 0.5%. This is shown in Figs. 4.45a and 4.45c. Other cracks near the bottom corners extended further, as shown in Figs. 4.45b and 4.45d. First visible buckling of diagonal and vertical steel strips was observed during the second and third cycles at 0.5% drift. Yielding of the vertical strips continued and the diagonal strips also started to yield at a lateral load of 450 kN. Some minor spalling and crushing were observed at the ends of the wall due to the buckling of vertical reinforcing bars. This is shown in Fig. 4.45b.

Both vertical and diagonal steel strips experienced severe buckling on the NW side near the base, during the first cycle at 1.0% drift when the load was 483 kN. Figs. 4.47a and 4.47b illustrate the buckling of steel strips at this stage of loading. Some diagonal cracks opened 2.0 to 3.0 mm wide at the centre of the wall and other new cracks formed as depicted in Fig. 4.46a. Buckling of vertical reinforcing bars on the east side, and buckling of vertical steel strips at mid-height on the SE side, and at the bottom on the NE side, was observed (Figs. 4.46b, 4.46c and 4.46d). The lateral load at this stage of loading was 483 kN. The load resistance increased to 496 kN and -497 kN at a drift of 1.4%. Severe buckling of diagonal and vertical steel strips was observed as illustrated in Figs. 4.47c, 4.47d, 4.48a, 4.48b and 4.48c. Diagonal cracks became wide enough to see through the wall. Nevertheless, the wall maintained its integrity. Buckling of reinforcing bars was more evident at both ends of the wall, as shown in Figs. 4.48a and 4.48c. The wall experienced the same behaviour with more severe buckling of reinforcement. Some new vertical cracks formed at this stage along the vertical steel

strips. No major change in behaviour was observed during the first cycle at 2.0% drift, except for minor strength degradation. However, the vertical steel strips at buckling locations were severely distressed as shown in Figs. 4.49a and 4.49c. At the same time re-bars continued to buckle as depicted in Figs. 4.49c and 4.49d. The NE vertical steel strip ruptured at the top, during the third cycle of 2% drift, at a lateral load of 401 kN. This is shown in Figs. 4.50a and 4.50b. Testing, nonetheless continued with cycles at 2.5% drift. Rupturing of the vertical steel strips occurred at other locations. Severe crushing of the concrete was observed at mid-height of the wall, between the vertical and diagonal steel strips. This is shown in Figs. 4.50c and 4.50d. The steel strip near the SE top corner fractured during the first cycle of 2.5% drift, followed by the steel strip on the NW side, during the second cycle. This is shown in Fig. 4.51b. During the last cycle, the vertical steel strip located on the SW side of the wall fractured near the base, as shown Fig. 4.51d. The test was stopped at this stage when the strength loss was in excess of 50%. Fig. 4.52 shows the damage sustained by Wall11R at the end of the test.

Chapter 5

Discussion and Comparison of Results

5.1 General

The behaviour of each unretrofitted wall specimen tested and that of the repaired wall specimen are discussed in Sections 5.2 and 5.3, respectively. A discussion on the general behaviour of retrofitted wall specimens, including the comparisons of predicted and experimentally measured behaviours follows in Section 5.4. Other sections compare the behaviour of the retrofitted and unretrofitted wall specimens in terms of ultimate capacity, load-deformation characteristics, stiffness, shape of hysteretic curve, energy dissipation and ductility.

5.2 Behaviour of Unretrofitted Walls

5.2.1 Wall 9 (Unreinforced Masonry Wall)

The hysteretic relationship of lateral load versus horizontal displacement of Wall 9 is shown in Fig. 4.1. Drifts shown in this figure are measured relative to the displacement of the beam centerline at the top. The hysteresis loops can be described as fairly stable. Moreover, the wall maintained its

strength until lateral drift of 1.0%.

This wall behaved in combination of rocking and sliding, as evidenced by the unsymmetric hysteresis loops of Fig. 4.1. The sliding developed in one direction, at an ultimate force of 64.5 kN, while the rigid-body rocking (with some small amount of sliding) developed in the other direction, at an ultimate force of -58.5 kN. The wall exhibited relatively large deformations with minor strength decay before failure. Rocking and sliding could develop only as a consequence of cracking along the bed joint. In this test, cracking did extend along the length of the wall, but, the path followed by the crack was unusual. Cracking did not occur at the base, nor at the first bed joint above the base, but in the bed joint above the second course of masonry, as indicated in Fig. 5.1. Another crack of a shorter length also appeared in the third bed joint above the base. After cracking, drift in both directions increased without any significant increase in lateral loading.

On the hindsight, even though calculations prior to testing predicted that rocking would develop at a lateral load of 46 kN, assuming cracking along the base of the wall, cracking above the base joint should not be surprising. Examination of the base joint revealed a fully mortared joint, in compliance with the requirements presented in Section 3.6. Obviously, the tensile resistance of this joint was large enough to force the crack to occur in the above weaker joints, rather than at the base. However, the reason for cracking above the second course of masonry instead of the first is unclear at this time.

The above non-symmetric behaviour until a drift of 0.8% can be best explained by the free-body diagram shown in Fig. 5.2. In this figure the forces consist of; i) variable lateral load applied by the horizontal actuator, V_{u1}, vertical load of 100 kN applied by actuators, weight of the top beam assembly (16 kN), and half of the weight of the horizontal actuator (5 kN). Considering these unsymmetrically applied vertical forces, a different value of the lateral forces required to produce the rocking force, V_u, can be calculated for each direction of horizontal loading. Thus, the horizontal actuator weight may have increased the rocking strength above the sliding strength in one direction of loading. In later stages of testing, as the mortar bed became more damaged and irregular, the friction coefficient along that bed joint may have increased sufficiently to promote more visible rocking in both directions of lateral loading. In addition, the unsymmetrical cracking pattern, probably resulting from the 4 ½ block (unsymmetrical) width of every masonry course, may also have

contributed to the rocking/sliding behaviour in the early stages of loading. Unfortunately, the wall was not instrumented in a way that permits verification of these hypotheses put forward based on observed behaviour.

The lateral load necessary to produce rocking at the crack level can be calculated using the diagram of Fig. 5.1 and the rocking equations suggested by Priestley (Bruneau 1994), assuming uniform compression under rocking of $0.85 f'_m$. Based on the average compressive strength of the tested masonry prisms, the ultimate horizontal force was calculated in both directions using equation 5.1.

$$V_u = \frac{P(0.5l-a)+W_a\,(l-a)}{h} \tag{5.1}$$

where P is the applied axial load, W_a is half the actuator's weight, l is the length of the wall and h is the lever arm of the applied lateral load V_u as shown in Fig. 5.2. Note that a is the depth of the compression block at ultimate and for simplicity $a/2$ can be set equal to the block shell thickness. Note that $W_a\,(l-a)$ is taken equal to zero when calculating V_u in the east direction.

Therefore, the lateral load resistance in the east direction is

$$V_u = 116\frac{(0.5(1.8)-0.034)}{(1.8+0.24-0.4)} = 61.3kN$$

and the lateral load resistance in the west direction is

$$V_u = \frac{116(0.5(1.8)-0.034)+5\;(1.8-0.034)}{(1.8+0.24-0.4)} = 66.6kN$$

These calculated forces are 3.3 % and 4.8 % larger than the experimentally obtained values for lateral loading in the westward and the eastward directions, respectively. Note that while there was no visible rocking in the west direction, in the early stages of loading, the above comparison is valid because sliding requires flexural cracking and some crack opening to develop, which in essence is rocking.

Despite, the low strength of this wall, which indicates a certain strength deficiency, its sliding friction and rocking behaviour noticeably dissipates energy.

5.2.2 Wall 10 (Partially Reinforced Masonry Wall)

Cracks appeared along vertical and horizontal mortar joints, corner to corner of the wall, in a stair-step pattern at about 50% of the wall ultimate strength. The number of diagonal cracks increased with increasing load, and the cracks started to propagate towards the body of the blocks. This lead to the formation of diagonal struts, as the wall developed truss behaviour. At this stage of loading, the wall exhibited its maximum strength. However, because the diagonal struts could not withstand large compressive stresses, the wall rapidly suffered loss of strength and stiffness.

Yielding of vertical reinforcement at the base of the wall was not observed prior to the formation of diagonal struts. The rapid loss of strength in diagonal compression struts also precluded the attainment of flexural strength.

The vertical cracks between grouted masonry cells and elsewhere in the wall suggest that the behaviour changed into that of an infilled frame with the ungrouted cells of the wall playing the role of the infill, and the grouted cells forming the columns of the frame. This mode of behaviour further contributed to the generation of large compressive forces at wall corners where the grouted masonry cells are located, leading to local buckling of vertical reinforcement and crushing and spalling of masonry and mortar. Horizontal reinforcement did not appear to contribute significantly to the overall behaviour of the wall.

Wall 10 exhibited symmetrical hysteretic force displacement relationship with relatively wide loops. This is shown in Fig. 4.7. However, it suffered shear failure, with progressive crushing of masonry diagonal struts, leading to early strength degradation and relatively low energy dissipation. This behaviour is further discussed in Section 5.7.

5.2.3 Wall 11 (Reinforced Concrete Wall)

Wall 11 experienced symmetrical and stable hysteretic behaviour, as shown by its force-displacement relationship in Fig. 4.12. These stable hysteresis loops also clearly show that Wall 11 experienced

rocking behaviour in later stages of testing, making it possible for this wall to maintain its strength up to 2.5 % drift.

After the formation of flexural cracking across the base, a vertical crack appeared in the middle of the narrow face of the wall in compression. This crack also formed at the opposite end of the wall upon load reversal. These cracks indicated elastic buckling of end reinforcement. The extreme bars were effectively laterally unsupported (concrete cover was very small and there were no lateral ties). As the vertical cracking extended up to two thirds of the wall height, buckling of vertical rebars became visible, causing the spalling of cover concrete. As a result, a significant length of these vertical rebars became exposed.

Tensile yielding of these exposed rebars required progressively larger wall rotations, and a wider horizontal crack at the base. The wall progressively developed significantly high rigid-body rotation, and went into the "rocking" mode of behaviour, with reinforcing bars controlling the wall rotation. No additional inelasticity was introduced in the main body of the wall panel above the base. The wall ends severely crushed when the vertical rebars yielded and its strength dropped to 93% of the ultimate capacity. While the strains in the end bars were not large, the rebars in the middle of the wall experienced extensive yielding. The middle bars also developed strain hardening as applied drift increased. The wall resistance did not change significantly beyond this load stage. However, the strength dropped drastically after the middle reinforcement ruptured. Beyond this load stage, the wall was left to rely on pure rocking behaviour to resist the lateral loads, much like the unreinforced masonry wall (Wall 9). Although, the performance of this wall can be considered to be satisfactory, in terms of ductility and energy dissipation, its lateral load resistance could be inadequate to resist earthquakes and may still require a retrofit.

5.3 Behaviour of Repaired Wall (Wall 11RP)

Wall 11RP is Wall 11 repaired using vertical steel strips only. Figure 4.19 shows the lateral force versus top horizontal displacement relationships recorded during the test. Qualitatively, Wall 11RP dissipated more hysteretic energy than Wall 11, with approximately no strength decay up to drifts of 1.5%. Furthermore, its hysteresis loops exhibited early pinching, mostly due to the pullout of its

anchor bolts.

Measurements indicated that the wall experienced significant shear sliding. Slippage of the anchor bars was believed to be the main reason behind this noticeable sliding. On the other hand, axial load applied to the wall did not increase friction resistance sufficiently to prevent sliding under lateral loading. Shear cracks appeared at drifts of 1.5%, starting with two opposite diagonal cracks near the top beam. These cracks first followed a horizontal path, extending from both sides a distance approximately equal to one third of the wall length, then followed a diagonal path and intersected at about one third of the wall height. This pattern indicated that the first shear crack originated from other cracks of flexural origin. The number of diagonal cracks was limited because of the reinforcement characteristics of this wall. It is well known that well distributed reinforcement promotes well distributed smaller size cracks. In this repaired wall, however, only the middle re-bars remained from the original vertical reinforcement, although they were ruptured at the wall base. Therefore, their contribution would be limited to diagonal crack control. Beyond the initial diagonal cracking, the bolt holes in concrete triggered any further diagonal cracks.

The behaviour of this wall emphasized the interaction of shear and flexural in low-rise walls. The capacity of this repaired wall was limited to its shear strength. The experimentally obtained lateral load capacity of the wall was 269 kN, whereas the capacity of the virgin wall (Wall 11) was 171 kN. This indicates that a 52% increase in lateral load capacity was provided by the repair. The shear cracking capacity V_c, calculated using Section 21.6.5.2 of the ACI- 318/318R-305 code is given below:

$$V_c=0.25\sqrt{f_c'}\ bd=0.25\sqrt{31}\ (1620)(100)10^{-3}=226kN$$

This value is 7.2% lower than the value of 244 kN recorded when the first shear crack was observed with naked eye during testing.

5.4 *Behaviour of Retrofitted Walls*

5.4.1 Common Behaviour

In general, all retrofitted wall specimens exhibited superior behaviour when compared with that of unretrofitted wall specimens. The effectiveness of the steel strip retrofit solution was demonstrated in this section for each wall specimen. For Wall 9R, the retrofitted URM wall, cyclic loading of progressively increasing magnitude led to some uniform cracking of the masonry, followed by yielding of the steel strips, and eventually inelastic buckling of the strips. This inelastic buckling led to the crushing of masonry. Better performance was observed in the PRM and R/C retrofitted walls, in which crushing was delayed until after excessive yielding of vertical steel strips and re-bars occurred. In all cases, the behaviour followed that of the indeterminate truss model presented in Section 3.5, reasonably well. Enhanced versions of this model are presented in Chapter 6.

The retrofitted walls eventually tended to slide or rock in all cases as the lateral load gradually increased. However, this sliding or rocking would only appear after cracking of the masonry or concrete, at or near the base, parallel to the direction of applied load. After a horizontal crack had formed above the second row of blocks in Wall 9R and Wall 10R, and at the base in Wall 11R, the unretrofitted walls would have rotated as rigid bodies. However, presence of the steel strip system prevented development of this rigid body rotation. As the vertical and the diagonal strips yielded, cracks spread more evenly over the entire wall. Crack widths were controlled by vertical steel strips.

As the applied deformation cycles were increased, the steel strips between the bolts were subjected to large tension and compression strains. Yielding of the steel strips in tension produced permanent plastic elongations that could not be fully recovered in compression. Accumulated tensile plastic strains eventually triggered a plastic hinge midway between the bolts. The diagonal steel strips yielded shortly after the vertical steel strips, which experienced similar strain characteristics. Because the diagonal strips were wider and had a more favorable anchor bolt configuration, they exhibited only limited buckling.

5.4.2 Behaviour of Masonry and Concrete

The masonry/concrete between the diagonal strips was confined to some degree. This confinement

improved the behaviour of the masonry/concrete in the compression zone. However, when vertical and diagonal steel strips buckled under increased compression, their compressive resistance reduced, progressively transferring the burden to the masonry/concrete struts. This redistribution accelerated the crushing of masonry in the case of Wall 9R (URM), and to a lesser extent the other retrofitted walls. The through-thickness anchor bolts also helped in confining the masonry/concrete. This confinement did not last long in Wall 9R, because of the low masonry strength. However, it was particularly beneficial in concrete compressive zone of Wall 11R, which could reach drifts of 2.5% without a significant strength degradation.

5.4.3 Strength of the Retrofitted Walls

Comparison between the ultimate lateral load resistance of the unretrofitted and retrofitted walls is presented in Table 5.1. This table also compares the retrofitted walls among each other. Wall 10R showed the highest absolute increase in lateral load resistance, whereas Wall 9R showed the lowest increase. However, the absolute increases in all the retrofitted walls are within less than 15% different from each other (355 kN, 456 kN and 499 kN respectively for Wall 9R, Wall 10R and Wall 11R). Note that the difference in increase in load resistance of Wall 10R and Wall 11R is only 2.4%. This implies that the increase in lateral load resistance provided by the addition of steel strips is approximately the same. It is believed that the early crushing of the masonry at the ends of Wall 9R prevented it from developing the same increase in resistance attained by the other retrofitted walls. The horizontal component of diagonal steel strips in tension were also calculated for each retrofitted wall when they were at yield. It was found that they were 15%, 26%, and 25% lower than the increase in lateral load resistance provided by the addition of steel strips for Wall 9R, Wall 10R and Wall 11R, respectively (see Table 5.1).

5.4.4 Wall 10R and Wall 11R

The presence of reinforcement bars in walls 10R and 11R increased their redundancy over Wall 9R, as described in Chapter 6. The anchor bolts used to attach the vertical steel strips to the wall were also helpful in enhancing cyclic inelastic performance of walls as these bolts provided lateral support to re-bars against premature buckling. The anchor bolts used in Wall 11R also delayed premature buckling at higher drift levels by confining the concrete surrounding the end rebars.

The torsional behaviour observed in Wall 10R after the fracture of the weld, described in Chapter 4, was useful in demonstrating why steel strips must be on both sides of the wall. The symmetric arrangement helps avoid eccentric loading that may cause twisting of the retrofitted walls. It also provides additional redundancy to retrofitted walls and superior support against out-of-plane failures of walls, although not tested in this investigation.

5.5 Comparison of Hysteretic Behaviour

Hysteretic curves recorded experimentally are useful indicators for effects of various parameters. They also provide a basis for comparison of retrofitted and unretrofitted wall specimens. They are excellent tools that help understand the behaviour of structural members under simulated seismic loading.

In the experiments reported here, all displacement measurements were taken with respect to the wall foundations, and therefore exclude any possible sliding or uplift of the foundation on the strong laboratory floor. Measurement locations for each deformation component were shown in Fig. 3.31 and discussed in Section 3.9.3. Two horizontal displacements were recorded for Wall 9, namely top horizontal displacement and mid-height horizontal displacement. Load-deformation history, cracking loads, yield loads, ultimate loads, crack patterns, and failure modes are examined in the following sections. Top horizontal and vertical displacements, mid-height horizontal displacement and sliding displacement are also presented in the same sections. Load-strain relationships and strain distributions along steel strips are also included.

5.5.1 Lateral Load versus Horizontal Displacement Relationships

Lateral load versus top horizontal displacement relationships, plotted to the same scale, are presented in Figs. 5.3, 5.4 and 5.5 for each set of retrofitted and unretrofitted walls.

The two hysteretic relationships shown in Fig. 5.3 indicate that the retrofitted URM wall exhibited approximately symmetrical stable hysteretic behaviour with significant increase in ductility, stiffness and dissipation of energy. They also indicate that Wall 9R experienced a lateral load resistance 4.5 times that of Wall 9, up to drifts of 1.0 %. The hysteresis loops of Wall 9R showed noticeable

pinching. This pinching is attributed to bolt slippage prior to the development of composite action at low drift levels, and buckling of steel strips at a drift of 0.4%. Crushing of the masonry at both ends of the wall (i.e. the compression zone), contributed to the pinching of the loops. After 1.0% drift, the hysteresis loops showed 25% strength drop with further pinching due to excessive crushing of masonry and global buckling of vertical steel strips. In spite of this, the hysteretic behaviour of Wall 9R, beyond 1.0% drift, was superior to that of Wall 9 in terms of strength, stiffness, ductility and dissipation of energy.

After the retrofitted URM wall lost its end masonry, the hysteretic behaviour resembled that of a tension-only braced steel frame where the buckled compression members contributed little to lateral resistance. The loss of strength of the retrofitted wall during the first cycle at 1.25% drift was also caused by the loss of masonry blocks at the ends. Although, Wall 9R showed a 25% drop in lateral load resistance, its strength remained much higher than that of Wall 9 during these large drift cycles.

The hysteretic lateral load versus top horizontal displacement relationships of the retrofitted and unretrofitted PRM walls are shown in Fig. 5.4. It is clear that the hysteresis loops of the retrofitted PRM wall demonstrate good strength, stiffness, ductility and overall energy dissipation, compared to those of the unretrofitted PRM wall. When the hysteretic behaviour of Wall 10R is compared with that of Wall 9R, it is observed that Wall 10R exhibited somewhat better lateral load resistance (as discussed earlier), stiffness, ductility and energy dissipation. The presence of rebars and grouted cells in Wall 10R helped delay the global buckling of the steel strips.

Wall 10R showed less than 7.0% drop in its lateral load resistance up to about 1.0% drift, whereas the lateral load resistance of the unretrofitted wall had fallen by more than 50% of wall maximum lateral load resistnce at 0.8% drift. However, once Wall 10R lost the masonry at its ends, the shape of the hysteresis loops became similar to that of Wall 9R. They resembled the hysteresis loops of a tension-only braced frame, in which the buckled compression members contribute little to lateral load resistance. A slight difference was observed because the rebars were still contributing to the overall hysteretic behaviour in Wall 10R at that point.

Fig. 5.5 compares the hysteretic response of Wall 11, Wall 11RP and Wall 11R. Despite the observed

sliding in Wall 11RP, it exhibited a relatively symmetrical and stable hysteretic behaviour with a significant increase in ductility, stiffness and energy dissipation when compared with Wall 11. It also sustained a relatively higher lateral load resistance (57% more than that of Wall 11) up to 1.5% drift. Beyond 1.5% drift, the hysteresis loops show a drop in strength of 16.5% with further pinching due to shear cracking, buckling of steel strips, sliding, and slippage of anchor bolts. The hysteretic behaviour of Wall 11RP, beyond 1.5% drift, was a bit different than that of Wall 11 in terms of strength (16.9% higher), stiffness, ductility, and energy dissipation. A further drop of 18.2% in strength was observed beyond a drift level of 2.0% in Wall 11RP. After this drop, Wall 11RP hysteretic behaviour was relatively similar to that of Wall 11.

The hysteretic behaviour of Wall 11R was superior to that of any other walls tested in the current investigation. The hysteresis loops, shown in Fig. 5.5, indicate high lateral load resistance, stiffness, ductility, and energy dissipation with no strength decay up to 2.0% lateral drift. The lateral load resistance dropped by 25% at a drift of 3.0%. However, the shape of these hysteresis loops still exhibited a lot of of pinching, similar in shape to what is often observed in tension-only braced steel frames.

5.5.2 Lateral Load Versus Top Vertical Displacement Relationships

Vertical displacement was recorded at two locations at the top of each wall, except Wall 9. Recall that an attempt was made to measure displacements due to crack opening for Wall 9 by locating an LVDT at each end of Wall 9 where crack opening due to rocking was expected. But the wall rocked about a different joint and no data was recorded by either LVDT. To replenish this unexpected loss of data, vertical displacements were measured and recorded manually during testing, whenever possible, by measuring the horizontal crack opening at different locations along the length of the wall. Fig. 5.6 shows lateral load versus crack opening for Wall 9 at the end of selected cycles when the applied load was towards east. The same measurement was not recorded in the other direction since the wall exhibited mostly sliding in this direction. Consequently, there was no visible horizontal crack wide enough to measure. Fig. 5.7 through 5.12 show the lateral load-top vertical displacements for Wall 9R, Wall 10, Wall 10R, Wall 11, Wall 11RP and Wall 11R, respectively. Each figure presents vertical top displacements at both ends.

Fig. 5.6 shows that the maximum crack width attained without a major drop in the lateral load resistance of Wall 9 was 12.5 mm. Fig. 5.7 shows that Wall 9R started to move down significantly by as much as 10.0 mm, when drifts of 1.5% were recorded when crushing of masonry started. A similar behaviour was obtained for Wall 10R (Fig. 5.9) starting at 2.0% lateral drift. Walls 10, 11, 11RP, and 11R did not exhibit such downward movement except in the later phases of testing in some cases. However, the amplitude of upward movement in Walls 11 and 11RP confirms the presence of important rocking during the test.

5.5.3 Lateral Load Versus Sliding Shear Displacement Relationships

Sliding shear displacements were observed and recorded for each wall except Wall 9. Recall that an attempt was made to measure sliding shear displacement for Wall 9 by locating an LVDT at the west end of the wall on the base, but the wall base did not experience any noticeable sliding at that location as described in Chapter 4. Only the unretrofitted reinforced concrete wall "Wall 11" and the repaired wall "Wall 11RP" experienced significant slippage at the base. Figs. 5.13a and 5.13b show the lateral load versus sliding shear displacements for Wall 11 and Wall 11RP, respectively. It can be seen that the sliding displacements are 10 % and 25% of total displacement for Wall 11 and Wall 11RP, respectively.

5.5.4 Lateral Load Versus Strains in steel strips and Re-bars

Strains in reinforcing bars and steel strips were recorded during each test of reinforced masonry and concrete specimens. The strain gauge locations, numbering, data acquisition and details are given in Chapter 3. Zeroing of the strain gauge readings in the system was usually done before applying any load. However, reading of the recorded data started before the application of lateral load but only after the application of full gravity load.

Figures 5.14 to 5.16 and 5.18 to 5.22 show typical lateral load-strain diagrams for vertical and diagonal steel strips of the repaired and retrofitted walls. These diagrams were organized so that a comparison can be made between strain behaviours of each individual wall. Additional lateral load-strain diagrams for a number of reinforcing bars are shown in Appendix B. A number of strain gauges installed on reinforcing bars did not function properly. Also, the Seimetric DAS lost some data during testing of wall 10R and Wall 11R, which explains the incompleteness of some curves.

Fig. 5.14a shows lateral load versus strains in the two vertical steel strips located at the east end of Wall 11RP. This figure reveals that steel strips yielded only at the bottom. As can be seen in Fig. 5.14a the maximum strain was 2.3%. Fig 5.15b shows the same strain data at a different scale. Yield strain of these steel strips is 0.2%. Theoretically, the strain hysteresis loops of Gauges 3 and 6 should be the same. However, Gauge 3 exhibited larger tensile and compressive strains than Gauge 6. This unsymmtrical behaviour can be attributed, to some extent, to the twisting of Wall 11RP observed near the end of the test. Fig. 5.16 shows the strain hysteresis loops of the vertical strips on the south side of Wall 9R. The strains recorded by gages 1,2,16 and 19 are concistent with the observed behaviour. The vertical strips significantly yielded and buckled at the bottom. However, gauges at mid-height of the wall (Gauge 2) as well as the top (Gauges 1 and 16) did not show any evidence of buckling or yielding. Strains recorded by Gauge 3 may seem excessive, but are simply the consequence of Gauge 3 being glued on top of a plastic hinge (see Fig. 5.17). Global buckling of the vertical steel strips located at the west end explains the strain hysteresis loops recorded by Gauge 17. After Wall 9R lost its masonry shell at the west end, the vertical steel strips experienced global buckling, as described earlier in Section 4.2.5. This type of buckling made the steel strip on the SW side bent southward. The vertical strip bending created tensile strains on the outer strip surface where Gauge 17 was located, even when the lateral load was positive (i.e. when the actuator was pushing the wall westward - see Fig. 4.31d).

The strain hysteresis loops of the diagonal strips on the south side of Wall 9R are shown in Fig. 5.18. The maximum strain recorded was 0.95%, and occurred at the SE corner near the base (i.e. Gauge 4). Gauge 13 recorded lower tensile strains due to buckling (the maximum tensile strain recorded by this gauge was 0.35%). Other locations (Gauges 7,15 10 and 9) showed moderate yielding. Only limited strain data was recorded for Wall 10R as shown in Fig. 5.19. Data of Gauges 3 and 18 (located at the bottom end of the vertical steel strips of Wall 10R on SE and SW sides, respectively) were not available. The available data showed that these vertical steel strips yielded. A maximum tensile strain of 0.2% was recorded by Gauge 1. Note that the yield strain of these steel strips is 0.18%. Fig. 5.20 shows the strain hysteresis loops of diagonal strips for Wall 10R. The strain hysteresis loops of Gauge 4 recorded strains before the weld failure and after the reinforcement of the weld. The diagonal strip yielded before the weld fracture and Gauge 4 recorded maximum tensile strain of 0.35%. After reinforcing the welds, Gauge 4 recorded maximum strain of 0.52%. The limited

available data plotted in Fig. 5.20 showed that Gauges 14 and 15 did not yield. The steel strip in the other diagonal direction showed a maximum strain of 0.63% recorded by Gauge 12. Gauge 13 recorded strain data before the weld failure, but not after. It likely suffered from the heat generated during reinforcing the welds due to its proximity to that location. However, Gauge 12 worked better than Gauge 13 and recorded strain data after re-welding.

The strain hysteresis loops for the vertical strips of Wall 11R are shown in Fig. 5.21. The maximum tensile strain of 0.65% was recorded by Gauge 2. Fig. 5.21 also shows that both vertical steel strips yielded at the bottom and mid-height.

Gauge 13 located on the diagonal steel strip of Wall 11R recorded a maximum strain of 1.26%. In Fig. 5.22, Gauges 4, 6, 13 and 11 showed stable strain hysteresis loops, which indicated that these steel strips behaved as good energy dissipators.

5.5.5 Stiffness Variation

Variation in wall stiffness with lateral drift is plotted in Fig. 5.23 for each wall. The stiffness at every drift level was calculated using the two peak values of each cycle. Only the first cycle of each drift was considered. The stiffness of each cycle was computed using the peak-to-peak method as shown in Fig. 5.23. The above curves indicated the sensitivity of the stiffness of each specimen with respect to the top horizontal displacement. As can be seen from the three figures presented, stiffnesses of retrofitted walls significantly improved compared to those of their respective unretrofitted counterparts.

5.6 Behaviour of Steel Strips

This section describes analytical studies that were performed to predict the local buckling load for vertical and diagonal steel strips. The analytically predicted behaviour of steel strips that was described in Chapter 3 and the effective length requirement presented in Chapter 4 are compared with the experimental behaviour observed in the repaired reinforced concrete wall specimen, as well in the three retrofitted wall specimens. The impact of buckling behaviour on the overall performance of retrofitted walls is also discussed.

The vertical steel strips used in retrofitted walls showed similar behaviour and behaved mostly as predicted. However, wall type played a major roll in delaying buckling of vertical strips. Wall 9R vertical strips experienced some mild local buckling during earlier drift cycles, as shown in Fig. 4.28b. However, because the lateral support provided by the wall was lost after the crushing of masonry blocks at the ends, the vertical strips buckled in a more global way, as shown in Fig 5.17. As a result, Wall 9R exhibited strength decay as early as 0.8% drift. A better lateral support to vertical steel strips was provided in Wall 10R by the reinforced cells at the ends. Local buckling, shown in Fig. 4.37d, dominated over global buckling, shown in Fig. 5.17. Consequently the wall kept its integrity and was able to sustain higher levels of drift without a significant strength decay. Figures 4.30d and 4.39d show the condition of the ends of Wall 9R and Wall 10R, respectively at 1.0% drift. The behaviour of vertical strips in Wall 11R was similar to that of Wall 10R because of the strong lateral support provided by concrete (see Fig. 4.46b). Note that although local buckling prevented the vertical steel strip from sustaining its plastic capacity up to the desired strain (deformation) capacity, its impact on the overall behaviour is preferred over the global buckling.

The above illustrates the importance of providing adequate lateral support to prevent global buckling of vertical steel strips. For that reason, even though Wall 9R showed a satisfactory behaviour up to 1.5% drift, grouting of the end cells may delay their crushing and help attain higher drifts without any strength deterioration. However, this remains to be verified experimentally.

5.7 Energy Dissipation

The amount of hysteretic energy per cycle dissipated by a specimen at a specific drift level is equal to the area enclosed by a hysteresis loop of the lateral load versus top displacement curves (Figs. 4.1, 4.7, 4.12, 4.19, 4.25, 4.34 and 4.43). The hysteretic energy dissipated during the first cycle of each drift level is presented in Fig. 5.24 as a function of lateral drift, for all the walls. This makes it possible to compare the relative energy dissipation capability of the retrofitted, repaired, and unretrofitted walls.

Fig. 5.24 shows that Wall 11R dissipated the largest amount of energy per cycle, and Wall 10 the smallest amount. Wall 10R dissipated almost the same amount of energy per cycle as Wall 11R.

Although Wall 9 went to higher drifts (2%), Wall 10 could also have been pushed to higher drifts, but the test was stopped when the strength dropped to 50% of the maximum capacity.

Note that inelastic behaviour of the retrofitted walls was dominated by truss action and hysteretic energy was dissipated primarily by yielding of steel strips. In spite of pinching of hysteresis curves the steel strip system in all of the retrofitted walls produced a considerable amount of energy dissipation. Many factors contributed to the above pinching, among them; the nature of the masonry and concrete (brittle), the relative movement of the anchor bolts in drilled holes and the buckling of steel strips during testing.

Because not all walls have the same amount of reinforcement, steel strip sizes, and strength, it is informative to calculate normalized hysteretic energy of the retrofitted walls. This can be done by dividing the previously calculated hysteretic energy by the product of the yield strength and the yield displacement. Fig. 5.25 presents the resulting normalized energy per cycle as a function of drift for the three retrofitted walls. In that perspective, Wall 11R still showed superior energy dissipation capability, but that of Wall 10R became close to that of Wall 9R.

5.8 Crack Patterns of Wall Specimens

Crack patterns for all masonry walls and the retrofitted concrete wall tested here are shown in Figs. 5.26 to 5.31. These crack patterns show the progression of cracking at different drift levels. In the retrofitted walls, it shows the effectiveness of steel strips in distributing the cracks over the entire wall as opposed to cracks concentrating only at certain locations.

Figs. 5.26a and 5.26b show crack opening in Wall 9 up to drifts of 0.4% in eastward and westward directions, respectively. Tables 5.2 and 5.3 list drifts versus crack widths for Wall 9 at selected locations shown in Figs. 5.26a and 5.26b. Recall that this wall was rocking in the east direction and sliding in the west direction, and consequently, the crack pattern did not change with increases in drift. Fig 5.27 shows Wall 9 crack opening when the wall started to rock in both directions for drifts beyond 0.8%. The corresponding crack widths are listed in Tables 5.4 and 5.5. Fig. 5.28 shows crack patterns of Wall 9R for comparison. Only a few bed joint cracks were visible at 0.1% drift, which

indicated that the steel strips were effective in distributing cracks over the entire wall. This good distribution persisted throughout the test. The first through-block crack was observed at a drift level of 0.2%. Clearly, retrofitting URM wall with steel strips changed its cracking pattern and behaviour extensively.

Crack patterns for Wall 10 are shown in Fig. 5.29. Cracks at 0.1% drift were limited to vertical and horizontal mortar joint. Cracks outside the mortar joints (i.e. through masonry blocks) started to develop at 0.2% drift. More diagonal cracks through masonry blocks, and crushing of east end of the masonry wall were visible at 0.4% drift. This is shown in Fig 5.29c. The existing cracks extended further during the cycles of 0.6% drift, and more crushing of masonry was recorded at both sides. The progression of cracking in Wall 10R is shown in Fig. 5.30 for comparison. Wall 10R showed a well distributed cracking pattern, at a drift level of 0.2%, with all the cracks in bed joints. Through-block cracks appeared at drifts beyond 0.2%, as shown Fig. 5.30c.

Fig. 5.31 shows crack patterns for Wall 11R at selected stages of loading. Here, horizontal cracks originated mostly from bolt holes along vertical strips. Most diagonal cracks were extensions of these horizontal cracks.

Note that, when the steel strips were present (Walls 9R, 10R and 11R), the crushing zones moved above the diagonal strips. Whereas, in non-retrofitted walls the cracking started near the base, since masonry/concrete acted as compression struts. Furthermore, most of the cracks in retrofitted walls developed in the zone between the vertical and diagonal steel strips, except for Wall 11R which also suffered considerable cracking over the entire length near the base. This is shown in Figs. 5.28, 5.30 and 5.31.

It may be concluded from the above discussion that:

- The first through masonry crack in Wall 9R developed at a drift of 0.2%, whereas in Wall 10R it developed at a drift of 0.4%. This may be attributed to the presence of horizontal truss reinforcement in four horizontal bed joints of Wall 10R.

- At a drift of 0.1%, cracks were well distributed in Wall 10, whereas very few cracks were observed in Wall 10R.

- The masonry crushing observed near the base of Wall 10 at 0.4% drift was delayed in Wall 10R until after 1.0% drift.

- In all the retrofitted walls, more severe diagonal cracks were observed on the west side than east side.

- Both Walls 10 and 10R had vertical cracks at the ends, indicating separation of grouted cells from the rest of the wall panel.

Chapter 6

Analysis and Design of Retrofitted Walls

6.1 General

The results of the experimental work carried out in this investigation demonstrate that the proposed steel strip system is an effective seismic retrofit strategy. Analyses of these walls will be conducted in this chapter in an effort to explain the mechanism of load resistance in the retrofitted walls. Simple analysis tools, suitable for design office environment will be used and the results will be compared with those obtained from the experimental research.

Three simplified techniques, based on the lower bound theorem of the theory of plasticity, are presented and verified against experimental data. A displacement-based design procedure is proposed subsequently for retrofitting non-ductile low-rise walls. A numerical design example, using this procedure, is also presented.

6.2 Simple Truss Model

A simplified truss model is introduced for the analysis of retrofitted walls to obtain their load-deflection relationship. An indeterminate truss with five members is used to represent each wall, as shown in Fig 6.1. The vertical steel strips and any vertical reinforcing bar that may be present, provide the tension member, labelled "1" in Fig. 6.1. The member in the plane of the floor or roof, or the upper rigid top beam in the case of wall specimens is labelled "2". The vertical strut in compression, at the other end of the wall, is referred to as member "3". The width of this compression strut is assumed to be one tenth of the wall length. The diagonal strips in tension and compression are labelled as member "4" and "5", respectively. Members "1" and "2", as well as "4" and "5" swap places when the horizontal load reverses.

A step-by-step calculation procedure is required to conduct inelastic analysis of the truss model described. This involves a series of elastic analyses. An elastic analysis is performed first, to determine member forces in terms of total applied force V. Since there are three equations of equilibrium available for four unknowns of the truss, the structure is statically indeterminate to the first degree. Hence, one more equation is needed to determine the reactions and member forces. The flexibility method is used to find the horizontal reaction R at the left hand support of the truss shown in Fig. 6.1.

$$R=V\frac{\dfrac{\sin^3\theta}{A_1}+\dfrac{1}{A_5}}{\left(\dfrac{\sin^3\theta}{A_1}+\dfrac{\cos^3\theta}{A_2}+\dfrac{\sin^3\theta}{A_3}+\dfrac{1}{A_4}+\dfrac{1}{A_5}\right)} \tag{6.1}$$

$$F_1 = (V-R)\tan\theta \tag{6.2a}$$

$$F_3 = R \tan\theta \tag{6.2b}$$

$$F_4 = \frac{R}{\cos\theta} \tag{6.2c}$$

$$F_5 = \frac{V-R}{\cos\theta} \tag{6.2d}$$

Where; F_1, F_3, F_4 and F_5 are forces in members 1, 3 , 4 and 5; A_1, A_2, A_3, A_4 and A_5 are the areas of truss members; and the angle θ is as described in Fig. 6.1. The subscripts used in these notations refer to member number.

Equating each member force to its yield capacity and solving for V gives four values of V. The smallest value is the elastic capacity, V_{yl}, of the truss. Usually, the compression capacity of members 3 and 4 are large enough to promote yielding of tension members 1 and 5 first. A number of factors dictate which tension member yields first. These factors include, type of material used in the wall (concrete or masonry), yield strength of steel strip, reinforcement layout in the wall, lateral restraint provided to longitudinal reinforcing bars, by bolts used to attach the vertical strips and the amount of steel added to the wall in each direction. Note that, the stiffness and the capacity of each member has to be reduced gradually in the step-by-step approach to account for degradation due to cracking and possible buckling of reinforcing bars.

The deflection at first yield, Δ_{yl}, is:

$$\Delta_{yl} = \frac{V_{yl}\, L}{E\left(\left(A_2 + A_4\cos^2\theta\right) - \sin^2\theta\cos^2\theta \dfrac{A_4^2}{A_1 + \sin^2\theta A_4} - A_2^2 \dfrac{A_3 + \sin^2\theta A_5}{A_3A_2 + A_3A_5\cos^2\theta + \sin^2\theta A_2A_5}\right)} \tag{6.3}$$

When the lateral load is increased beyond the above elastic limit the truss develops contained plastic flow. The first tension member undergoes plastic deformations while the second tension member remains elastic. If the yield strength of steel strips is different than the yield strength of reinforcing bars, an elastic analysis must again be performed for the new statically indeterminate truss, discounting those members that have already yielded. The reactions, member forces, capacity V_{y2} and corresponding deflection Δ_{y2} of the new statically indeterminate truss would be calculated as described above. The total load capacity at this stage is equal to the sum of V_{y1} and V_{y2}, and the total deflection is equal to the sum of Δ_{y1} and Δ_{y2}. At this level of loading, either one or both of the vertical tension elements, i.e., the steel strip and/or reinforcing bars, as well as the diagonal tension member have yielded. Depending on the yield pattern, the model reduces to either one of the statically determinate trusses shown in Fig. 6.1b. Finally, when the horizontal load increases to reach the elastic limit, V_{y3}, of either of these simple trusses, then the plastic collapse mechanism is reached. The load capacity, V_{y3}, and its corresponding elastic deflection, Δ_{y3}, can be found using simple statics. The ultimate strength of the retrofitted wall at the plastic collapse mechanism is given by the sum of V_{y1}, V_{y2} and V_{y3}. The deflection corresponding to the ultimate capacity is given by the sum of Δ_{y1}, Δ_{y2} and Δ_{y3}. The resulting load-deflection envelope for a retrofitted wall can be constructed using these values.

Major advantages of the truss analysis are its relative simplicity and the ability to describe inelastic behaviour and failure mechanism. Yet, this model can be improved by introducing more members, as described in the next section.

Note that the gravity loads were not considered in the above truss model. If the steel strips are placed as retrofitting elements after the gravity loads have been applied, as would be the case in a seismic retrofit, the compressive strength of concrete or masonry in the truss model can be reduced by an amount corresponding to the gravity-induced stresses. If the gravity loads are applied after the strips are installed, as was the case in this experimental program, both the existing concrete wall and the new steel strips will resist the entire gravity load together. A correction can be made in the above procedure. However, for the low amount of axial force considered here, this effect is negligible.

6.3 Improved Truss Model

The truss model described in the previous section can be improved by introducing additional members to the truss model. This will generate a truss model that is more representative of the behaviour observed during tests, as discussed in Chapter 5. These additional members consist of a tension member that would represent the middle reinforcing bars and a compression member that would represent the compression strut coupled to the new tension member. The addition of this pair of members give the improved truss, shown in Fig. 6.2. This improved truss model can be used to conduct the same analysis described earlier. The only difference is that the redundancy of the model will increase. This requires a greater computational effort. However, it is still relatively easy and suitable for hand calculations. It also has the advantage of better describing the behaviour of walls and offers more information about the inelastic deformability of retrofitted wall.

Fig. 6.3 describes the behaviour of a retrofitted reinforced concrete wall having a middle pair of bars. The stages at which each member of the model develops tension yielding, can be obtained by successive elastic analyses, as done previously. The results produce force displacement data pairs that can be plotted on the force-displacement relationship. Therefore, analysis of a model with more tension members will result in more data points to define the force-displacement relationship. It must be pointed out that in the case of retrofitted unreinforced wall, there are no reinforcement bars, and the improved truss model reduces to the original simple truss model described in Section 6.2.

Fig. 6.3 summarizes the yielding sequence of each tension member of a retrofitted wall in both the simplified truss model and the improved truss model. Note that the yielding sequence varies depending on the yielding strength, size and location of the existing reinforcement and the lateral support provided by the through-thickness bolts.

The above procedure is based on the assumption that reinforcing bars and the steel strips are detailed to prevent premature buckling at the ends of the wall, as these effects may alter the sequence of yielding. For example, buckling of the steel strip may prevent the wall from sustaining its plastic capacity up to the desired strain "deformation" capacity.

6.4 Lower Bound Method

The strength of the retrofitted low-rise walls may be estimated using the lower bound theorem from the theory of plasticity. This theorem is based on the following assumptions:

i) The material behaviour must be elastic-ideal-plastic, or rigid-ideal-plastic.
ii) Equilibrium is formulated in the undeformed geometry of the structure.

The lower bound theorem states that, "*Every load computed on the basis of a stable and statically admissible system is not higher than the true ultimate load of the system*". Consider the equilibrium of the stable free body diagram shown in Fig. 6.4, and assume that yielding takes place in all tension members, i.e the diagonal steel strips and all vertical steel elements. The summation of moments due to the internal and external forces around a point (Point O in this case) gives one equation with one unknown. Solving this equation give a lower bound value for the ultimate horizontal lateral load capacity of a retrofitted wall, V_u:

$$V_u = \frac{A_v f_{yp} d_v + \left(A_d f_{yp} d_v \sin\theta + 0.5Pd_v + \Sigma A_{si} f_y d_i \right)}{H} \tag{6.4}$$

Where A_v is the area of the vertical steel strips in tension; A_d is the area of the diagonal steel strips in tension, A_{si} is the area of i^{th} vertical pair of reinforcing bars; f_{yp} and f_y are the yield strength of steel strips and re-bars, respectively. d_v is the distance between the vertical steel strips. All other values are geometrical dimensions indicated in Fig. 6.4.

Note that the increase in lateral load resistance, ΔV, is:

$$\Delta V = V_u - V_{uo} \tag{6.5}$$

where V_{uo} is the original (unretrofitted) capacity of the wall and if ΔV conservatively taken to be equal to the horizontal component of the force in diagonal steel strips:

$$V_u - V_{uo} = A_d f_{yp} \cos\theta \tag{6.6}$$

then:

$$A_d = \frac{V_u - V_{uo}}{f_{yp} d_v} \tag{6.7}$$

substituting Eq. 6.7 into Eq. 6.5 gives:

$$A_v = \frac{V_u H - (V_u - V_{uo}) \tan\theta \; d_v - 0.5 P d_v - \Sigma A_{si} f_y d_i}{f_{yp} d_v} \tag{6.8}$$

The above two equations may be used for preliminary retrofit design of non-ductile low-rise walls as described in Section 6.8.

6.5 Validation of the Proposed Techniques

Force-displacement relationships from the simplified truss models described in this chapter have been compared with experimentally obtained envelopes of the lateral force-horizontal displacement relationships of three retrofitted walls. These results are presented in Figs. 6.5, 6.6 and 6.7 for Wall 9R, Wall 10R and Wall 11R, respectively. The models provide good correlations with test data and can be considered as effective analytical tools. The improved truss model provides additional data in the high inelastic deformation range.

6.6 Effects of Vertical and Diagonal Strut widths on the Accuracy of Truss Models

The width of the compression struts used in previous truss models were found by taking the strut width equal to the steel strip width for diagonal elements, and to one tenth of the length of the wall for the vertical elements. This is within the range of values recommended by other researchers in studies of other types of structures. For example, Drysdale et al. (1994) recommended, based on studies by others, diagonal strut widths equal to one-tenth to one-third of the diagonal length of the wall for truss models used in analysis of infilled frames. The New Zealand Code specifies a width

equal to one quarter of the infill length. Paulay (1992) proposed a width equal to one-quarter of the diagonal length for design of infilled frames. However, given that the force distribution in indeterminate trusses depends on the relative stiffness of members, one may question the significance of different widths. The effect of strut width was investigated by considering a range of widths for vertical struts, and employing a truss model for all the retrofitted walls of this study. In all cases, the area of steel was not a parameter.

Figs. 6.8a, 6.8b and 6.9 show force-displacement relationships obtained for different vertical strut widths for Wall 9R, Wall 10R and Wall 11R. The variation is insignificant, and any one strut width can be used without affecting the results significantly. Using one tenth of the length of the wall for the vertical compressive strut seems reasonable.

6.7 A Displacement-Based Design Approach for Retrofitting Non-Ductile Low-Rise Walls

Seismic displacement requirements in the inelastic range must be satisfied to ensure superior performance of a retrofitted wall during a strong earthquake. Design of a retrofitting system, in this case the steel strip system, based on strength demands alone is not sufficient.

The proposed design approach presented here checks the wall displacement capacity for a given steel strip system capacity. The procedure involves the following steps:

Step 1 Determine the lateral seismic forces using a design code, such as the NBCC.

Step 2 Use Eqs. 6.7 and 6.8 to find the size of the vertical and diagonal steel strips needed to resist this force.

Step 3 Use the step-by-step procedure outlined earlier to compute the load-deflection relationship.

Step 4 Check the ultimate displacement (δ_u) calculated using the step-by-step procedure against the

maximum displacement (δ_{max}) expected during design earthquake (i.e. the displacement demand). If $\delta_u \geq \delta_{max}$, then the wall has sufficient ductility. If not, the design must be modified. Note that the displacement demand is not expected to exceed the ultimate displacement, and if exceeded there is a need for farther research to determine how to modify the design.

Step 5 Find the required spacing of the through-thickness bolts based on the post-buckling requirement discussed in Chapter 3.

Step 6 Design the connections of the steel strip system to foundation and roof.

The above approach is conservative because the maximum deflection calculated in *step 3* does not correspond to the ultimate drift capacity. This is the short-coming of the model. The procedure does penalize unreinforced masonry walls. Fig. 6.5 provides the comparison of analytical results with those obtained experimentally for Wall 9R.

6.8 Retrofit Design Recommendations

The following design recommendations can be made based on the findings of current research. They are limited to low-rise concrete masonry blocks and reinforced concrete walls.

- Avoid crushing of vertical and diagonal compression struts at low drift levels. This may be achieved by using a steel strip system that has sufficiently low strength to allow yielding of vertical tension elements (steel strips and/or reinforcing bars) before either the yielding or crushing of diagonal elements. The behaviour described can be obtained in different ways, depending on the amount and yield strength of reinforcing bars that may be present.

- To avoid out-of-plane movement and to increase wall redundancy, it is highly recommended that the steel strips are placed on both sides of the wall.

- The CSA-S16.1-M94 limits specified for ductile bracing members (see Chapter 3) must be

used to determine the spacing of the through-thickness bolts in attaching the steel strips to the wall, to ensure overall ductile behaviour.

- Through-thickness bolts are more effective if they can be placed between the end cover and the reinforcing bars in reinforced concrete/masonry walls to provide lateral support against bar buckling at the ends.

- The anchor bolts used to attach the steel strip system to the masonry walls must not be fastened (torque) to a level that could damage the masonry.

6.9 Sample Design of Steel Strip System

A sample design of the steel strip system developed in this research program is presented in this section. The design problem involves the single-storey building shown in Fig. 6.10. The wall is to be retrofitted using the steel-strip-system, as shown in Fig. 6.11. The building is 38.4 m x 48 m in plan, and has 4.8 m clear height. It is enclosed by four reinforced concrete end walls in each direction. The length of each wall is 4.8 m. A 300 mm thick reinforced (0.25%) concrete slab was used at the roof, for parking. The walls are 100 mm thick, each. The concrete compressive strength is 25 MPa and reinforcement Grade is 400 MPa. The building is assumed to be in seismic Zone 5 of the NBCC for both seismic accelerations and seismic velocities.

The equivalent static seismic base shear, V, in the East-West direction must be determined first. This requires the computation of weight, W. The weight of the roof is computed as:

$$W_1 = (0.3)(24.0)(48.0)(38.4) = 13271\ kN$$

The weight of the upper half of each wall is;

$$W_2 = (0.1)(24.0)(0.5)(4.8)(4.8)(8) = 221\ kN$$

The weight due to *25%* of the snow load is;

$$W_3 = (0.25)(48.0)(38.4)(2.0) = 922\ kN$$

The total weight is;

$$W = W_1 + W_2 + W_3 = 14414\ kN$$

For seismic velocity-related Zone 5, the peak ground velocity, v, is taken as 0.3. The period of the building is estimated as $T=0.09h_n/\sqrt{Ds}$, where h_n is the height to the roof level and D_s is taken as the length of the building in the East-West direction, giving:

$$T=\frac{0.09(4.95)}{\sqrt{38.4}}=0.072\ s$$

If $Z_a = Z_b$, the seismic response factor, S, is equal to 3.0. The importance factor, I, and the foundation factor, F, are both taken equal to 1. The selection of the force modification factor, R, requires an explanation because this type of walls is not included in *Force Modification Factors* table of the NBCC. Observations and results of this experimental study show that walls retrofitted by means of steel-strips are ductile structural members with hysteresis curves representative of an element between a ductile braced frame ($R= 3.0$) and a wall with nominal ductility ($R=2$). Therefore, an average value of $R = 2.5$ was chosen. This gives a minimum lateral seismic force of;

$$V= (0.3)(3)(1.0)(1.0)(14414)(0.6)/2.5=3113\ kN$$

The seismic base shear tributary to each wall;

$$V_u = V/4 = 778\ kN$$

Knowing that the original (unretrofitted) capacity, V_{uo}, is 300 kN (using Doostdar's program) and using Eqs. 6.7 and 6.8, derived in Section 6.4, A_d and A_v can be calculated as:

$$A_d=\frac{(778-300)10^3}{(225)\ \cos 46}=3058\ mm^2$$

$$A_v=\frac{((778)(4.65)-(778-300)(4.4)\ \tan 46-535)10^6}{(225)(4.4)10^3}=914 mm^2$$

Note that the contribution of the vertical load was considered in finding the original capacity of the wall and should not be included in Eq. 6.8.

From these preliminary sizes of diagonal and vertical steel strips, the force-displacement relationship of the retrofitted wall can be found by using a truss model. The displacement capacity is then compared with the displacement demand. If the available displacement capacity is found to be less than the demand, steel strip areas in both vertical and horizontal directions have to be revised until the required displacement capacity is achieved.

Fig. 6.11 shows the resulting force-displacement curves using two versions of improved truss models. In the first model, the reinforcing bars were lumped at three locations, as shown in Fig. 6.10. In the second model, each reinforcing bar was left at its actual position. Clearly, the second version better describes the behaviour and gives more information about the inelastic deformation capability of this retrofitted wall.

Chapter 7

Summary and Conclusions

7.1 Summary

Many existing masonry and concrete low-rise shear walls, built before the 1960's, were not designed to resist earthquakes. As a result, their seismic behaviour may not be adequate, and may need to be retrofitted. A new retrofitting procedure has been developed in the current research project. The retrofitting strategy includes a steel strip system, designed to raise both strength and ductility to a level compatible with today's standards. Four large-scale concrete block masonry and two reinforced concrete shear walls were designed, constructed and tested under combined gravity load and in-plane deformation reversals. Masonry walls had a thickness of 190 mm, whereas the concrete walls had a 100 mm wall thickness. All walls had an aspect ratio of 1.0 and a height of 1800 mm. They were designed to simulate the detailing used prior to the introduction of seismic design provisions into building codes.

The first pair of masonry walls investigated were unreinforced masonry (URM). The second pair were partially reinforced masonry (PRM). Three #15 (16.5 mm diameter) reinforcing bars, one in each

exterior cell and one in the central cell, were used in the vertical direction of the PRM walls. A truss type bed joint reinforcement, No. 8 gauge, was placed in mortar joints, every two courses. The concrete wall was lightly reinforced, as well. Three pairs of 9.5 mm reinforcing bars, one at each end and one at the centre, were used in the vertical direction of reinforced concrete wall. They were reinforced with the same amount of steel in the horizontal direction. One wall from each pair was retrofitted using the proposed steel-strip system.

The steel strip system consisted of diagonal (220x3.81 mm cross-section) and vertical (80x3.81 mm cross-section) strips, attached to the walls using through-thickness bolts. Stiff steel angles and anchor bolts were used to connect the steel strips to the foundation and top beam.

Analyses of walls were conducted using truss models of various sophistication. A lower bound plasticity approach was also used to determine wall capacity. A step-by-step procedure was developed to establish inelastic force-displacement relationship of low-rise walls. The results computed using these analytical techniques were compared with those recorded experimentally. The comparisons showed good agreement. Hence, a design procedure was developed based on the analytical approach.

7.2 Conclusions

Experiments conducted in this study show that the steel strip system, proposed to retrofit low-rise masonry and concrete walls, is most effective in significantly increasing the in-plane strength, ductility and energy-dissipation capacity. For the particular wall specimens considered, the addition of steel strips increased the lateral load resistance of each wall by approximately 300 kN, making the retrofitted walls 4.5, 2.8 and 1.9 times stronger than the unreinforced masonry, partially reinforced masonry, and reinforced concrete wall specimens, respectively. The details and connections used to ensure continuity between the steel strip system and foundation, as well as the strip system and top beam, also enhanced the sliding friction resistance.

Various techniques were used to predict the strength and ductility of the retrofitted walls. The ultimate shear strength of the retrofitted wall can be simply obtained by equilibrium on the basis of

lower-bound method. A simplified truss model approach, described in this thesis, gives analytical results that are in good agreement with experimental results. The global lateral force-displacement behaviour of all retrofitted low-rise walls can also be captured with a reasonable degree of accuracy using the modified truss models described in this thesis. The steps involved in this analysis procedure also correctly describe the yielding sequence of steel components of the retrofitted walls. Finally, a displacement based design procedure is proposed as a simple design tool that engineers may use to retrofit existing non-ductile low-rise walls.

It should be noted that, although no out-of-plane tests were conducted within the scope of this work, the author believes that it is preferable to use the proposed strip system on both sides of the wall, to develop a greater out-of-plane strength, and minimize out-of-plane displacements. Furthermore, comparing the behaviour of the end reinforcing bars in retrofitted PRM wall and those in retrofitted R/C wall, it is shown that anchor bolts can be placed such as to provide lateral supports to the end reinforcing bars of the existing walls, helping to eliminate their premature buckling. It should also be noted that retrofitting existing walls by only vertical steel strips is not as effective as using the entire strip system, since their ultimate strength can be limited by the less ductile shear failure.

Tests of non-retrofitted walls provided valuable observations, in addition to providing data for comparison with retrofitted walls. In particular, the stable in-plane rocking mode of failure, experimentally observed in unreinforced brick masonry walls by other researchers, could be developed in concrete block walls. Tests also suggest that partially reinforced masonry walls tend to behave in a manner similar to infill frames. Finally, buckling of the end reinforcing bars at rather low drifts provided further evidence in support of code requirements for boundary elements.

References

Adams, P.F., and Zimmerman T.J.E. (1987), "Design and Behaviour of Composite Ice-Resisting Walls", C-FER special publication, No. 1, October , pp. 23-40.

Amrhein, J. (1992), Reinforced Masonry Engineering Handbook, 5th Ed., Masonry Institute of America, Los Angeles.

Bruneau, M. (1994), "State-of-the-Art Report on the Seismic Performance of Unreinforced Masonry Buildings". *ASCE Journal of Structural Engineering*, 120(1): 230-251.

Bruneau, M. (1990), "Preliminary Report of Structure Damage from the Loma Prieta Earthquake of 1989 and Pertinence to Canadian Structural Engineering Practice", *Canadian Journal of Civil Engineering*, Vol. 17, No. 1, 198-208.

Canadian Standards Association (1984), CSA Standard S 304-1984, "Masonry Design for Buildings," CSA, Rexdale, Ontario.

Canadian Institute of Steel Construction (1991), "Handbook of Steel Construction", Fifth edition, Markham, Ontario

Doostdar, H.M. and Saatcioglu, M. "Inelastic Shear Behavior of Reinforced Concrete Walls", Research Report No. OCEERC 98-23, Department of Civil Engineering, University of Ottawa, Ottawa, Canada, 1998.

Doostdar, H. (1994), "Behaviour and Design of Earthquake Resistant Low-Rise Shear Walls" *Thesis presented to the Dept. of Civ. Engrg.*, Univ. of Ottawa, in partial fulfilment of the requirements for the degree of Doctor of Philosophy, Ottawa.

Drysdale, R. G., Hamid, A. A., and Baker, L. R.(1994), "Masonry Structures, Behaviour and

Design", Prentice-Hall, Inc., Englewood Cliffs, NJ.

Durgesh C. Rui, Subhash C. Goel, and William, T. Holmes (1994), "Seismic Strengthening of URM Buildings with Steel Bracing", Fifth U.S. National Conference on Earthquake Engineering, July 10-14, Chicago, Illinois, pp. 697-705.

Englekirk, R, Hart, G. and Concrete Masonry Association of California and Nevada (1984), Earthquake Design of Concrete Masonry Buildings, Vol. 2, Strength Design of One-to-Four Story Buildings, Prentice-Hill, Inc., Englewood Cliffs, NJ.

FEMA. (1992), NEHRP Handbook of Techniques for Seismic Rehabilitation of Existing Buildings. National Earthquake Hazards Reduction Program, Federal Emergency Management Agency, Building Seismic Safety Council, Washington, D.C.

Fiorato, A.E., Oesterle,R.G, and Corley, W.G. (1983) "Behaviour of Earthquake Resistant Structural Walls Before and After Repair", ACI Journal, Detroit, pp. 403-413.

Ghanem, G. M., Esswy, A. and Hamid, A.A. (1992) "Effect of Steel Distribution on the Behaviour of Partially Reinforced Masonry Shear Walls", Proceedings of Sixth Canadian Masonry Symposium, Saskatoon, Saskatchewan.

Jones, R., Swamy, R.N., and Charif, A. (1988), "Plate Separation and Anchorage of Reinforced Concrete Beams Strengthened by Epoxy-Bonded Steel Plates" *The Structural Engineer*, V. 66, No. 5, March, pp. 85-94.

Lunoe, R.R., and Willis, G.A. (1957), "Application of Steel Strap Reinforcement to Girders of Rigid Frames, Special AMC Warehouses", *ACI Journal*, Proc. V. 57, January , pp. 669-678.

Makino, M., Ozaki, M., and Hirsosawa, M. (1965), "Bearing Walls of Steel Framed R/C with Steel Plates", (In Japanese), Report of the Building Research Institute, No. 46, October , pp. 99-130.

Matsuishi, M., Nishimaki, K., Iwata, S., and Suhara, T.(1980), "On the Strength of Composite Steel-Concrete Structure of a Sandwich System", (4th Report). Hitachi Zosen Technical Review, V. 40, December.

McKenna, J.K., and Erki, M.A. 1994. Strengthening of Reinforced Concrete Flexural Members Using Externally Applied Steel Plates and Fibre Composite Sheets a Survey. Canadian Journal of Civil Engineering, 21(1): 16-24.

National Building Code of Canada (NBCC) Associated Committee on National Building Code, National Research Council Canada, Ottawa, Ontario, Canada, 1995.

National Building Code of Canada (NBCC) Associated Committee on National Building Code, National Research Council Canada, Ottawa, Ontario, Canada, 1970.

National Building Code of Canada (NBCC) Associated Committee on National Building Code, National Research Council Canada, Ottawa, Ontario, Canada, 1957.

National Building Code of Canada (NBCC) Associated Committee on National Building Code, National Research Council Canada, Ottawa, Ontario, Canada, 1942.

Park, R., and Pauley, T.(1975) , Reinforced Concrete Structures, John Wiley, NY.

Pauley, T, and Priestley M.J.N. (1992), Seismic Design of Reinforced Concrete and Masonry Buildings, John Wiley & Sons, NY.

Priestley M.J.N, and Calvi G.M. (1996), Seismic Design of Retrofit of Bridges, John Wiley & Sons, NY.

Richard C., and Hognestad, E. (1957) ,"Laboratory Investigation of Rigid Frame Failure", *ACI Journal*, January, Proc. V. 53, pp. 637-668.

Roeder, C.W.(1984), "Composite and Mixed Construction", Proc. of the U.S./Japan joint seminar, American Society of Civil Engineers, July .

Saatcioglu, M., Pilette, C., Z.F. Wasiewicz, and S. Wiradinata. "Tests of Low-Rise Concrete Shear Walls under Lateral Load Reversals", Research Report No. OCEERC 98-22, Department of Civil Engineering, University of Ottawa, Ottawa, Canada, 1998.

Schultz, A. E. (1994), "NIST Research Program on the Seismic Resistance of Partially-Grouted Masonry Shear Walls", NISTIR 5481, National Institute of Standards and Technology, Gaithersburg, MD.

Sharpe, R., and Ugrte, E. (1988), "Seismic Strengthening of PALO ALTO Civic Centre", Proc. of Ninth World Conference on Earthquake Engineering, August , V. vii, pp. 445-450.

Shing, P. B., Schuller, M., Hoskere, V. S., and Carter, E.(1990), "Flexural and Shear Response of Reinforced Masonry Walls", *ACI structural Journal*, Vol. 87, No. 6, Nov.-Dec., pp 646-656.

Sveinsson, B., McNiven, H and Sucuoglu, H.(1985), "Cyclic Loading Tests of Masonry Single Piers Vol. 4-Additional Test With Height to Width Ratio of 1", EERC Report No.UCB/EERC-85/15, University of California, Berkeley, California.

Swamy, R.N., Jones, R., and Bloxham, J.W.(1987), "Structural Behaviour of Reinforced Concrete Beams Strengthened by Epoxy-Bonded Steel Plates", *The Structural Engineer*, V. 65 A, No. 2, February, pp. 59-68.

Swamy, R.N., Jones, R., and Charif, A. (1989), "The Effect of External Plate Reinforcement on the Strengthening of Structurally Damaged R/C Beams", *The Structural Engineer*, V. 67, No. 3, February, pp. 45-56.

Taghdi, M.(1989) "Shear Strengthening of Existing R/C Beams", M.Sc. Thesis, Ar-Rayha Al-Khadra University, Tripoli, Libya,.

Thurston, S. and Hutchinson (1982), "Reinforced Masonry Shear Wall Cyclic Load Tests in Contra flexure," *Bulletin of the New Zealand Society for Earthquake Engineering,* Vol. 15, No.1, March .

Vanek, T. (1986), "Shear Strengthening of Old Concrete Beams", Batim Int. Building Research Practice, V. 14 No. 5 September-October , pp. 311-316.

Wakabayashi, M. (1986), "Design of Earthquake-Resistant Buildings", McGraw-Hill Book Company, NY.

Woodward, K., and Rankin, F (1985a), "Influence of Aspect Ratio on Shear Resistance of Concrete Block Masonry Walls" NBSIR 84-2993, National Bureau of Standards, Gaithersburg, MD.

Woodward, K., and Rankin, F (1984a), "Influence of Vertical Compressive Stress on Shear Resistance of Concrete Block Masonry Walls" NBSIR 84-2929, National Bureau of Standards, Gaithersburg, MD.

Woodward, K., and Rankin, F (1985b), " Shear Resistance of Concrete Block Masonry Walls" Proceedings of Third North American Masonry Conference,

Yoshimura, K., Kikuchi, K., and Iguchi, K.(1988), "A proposal of Seismic Shear Strengthening Method for R/C Short Columns in Existing Building Structures", Proc. of Ninth World Conference on Earthquake Engineering, Tokyo-Kyoto, Japan, V. vii, August , pp. 327-332.

Table 5.1 Strength increase in retrofitted walls

Wall Label	V_u, kN (unretrofitted)	V_{ur}, kN (retrofitted)	ΔV_u, kN (increase)	$\Delta V_u / V_u$, % (increase)	V_d*, kN
9R	64.5	355	290.5	450	243
10R	120	456	336	280	243
11R	171	499	328	192	243

* Horizontal component of the yield strength of diagonal steel strips in tension.

Table 5.2 Wall 9 (eastward) Crack widths measured with a ruler (estimated error ±0.5 mm)*

Drift, % / Location	Crack width, mm					
	①	②	③	④	⑤	⑥
0.2 (1st. cycle)	3.0	4.0	-	-	3.5	-
0.2 (3rd cycle)	3.0	3.5	-	-	5.0	-
0.3	10	7.0	4.5	1.5	9.5	6.5
0.4	12.0	9.0	5.0	3.0	9.5	10.0
0.4(3rd cycle)	9.0	6.5	3.5	0.0	13.0	14.5

* See Figure 5.26 for crack locations.

Table 5.3 Wall 9 (westward) Crack widths measured with a ruler (estimated error ±0.5 mm)*

Drift, % / Location	Crack width, mm					
	①	②	③	④	⑤	⑥
0.3(1st cycle)	4.5	-	-	5.5	-	-
0.3(3rd cycle)	4.0	9.5	5.0	6.5	-	-
0.4(1st cycle)	-	11.0	8.0	7.0	-	-
0.4(3rd cycle)	11.5	-	-	12.0	-	-

* See Figure 5.26 for crack locations.

Table 5.4 Wall 9 (eastward) crack widths measured with a ruler (estimated error ±0.5 mm)*.

Drift, % / Location	Crack width, mm				
	①	②	③	④	⑤
0.8 (1st. cycle)	17.0	10.0	5.0	0.5	13.5
0.9 (1st. cycle)	-	11.5	-	-	-
1.2(1st. Cycle)	-	12	5.0	-	-
1.5 (1st. cycle)	-	15.0	6.0	-	-
2.0(1st. cycle)	-	22.0	8.0	-	-

* See Figure 5.27 for crack locations.

Table 5.5 Wall 9 (westward) Crack widths measured with a ruler (estimated error ±0.5 mm)*.

Drift, % / Location	Crack width, mm		
	①	②	③
0.8(1st cycle)	27.0	6.0	24.0
0.9(3rd cycle)	32.0	9.0	37.0
1.2(1st cycle)	41.0	15.5	8.0
1.5(3rd cycle)	48	21.0	41.0
2.0(3rd cycle)	55.0	26.0	43.0

* See Figure 5.27 for crack locations.

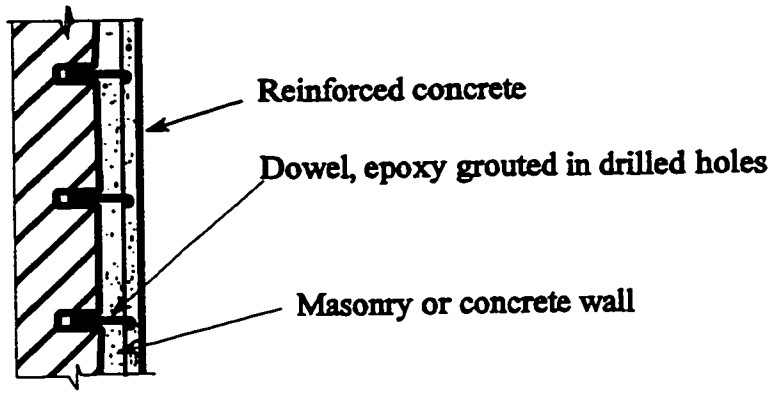

Figure 1.1 External Coating of a Wall (NEHRP 1992)

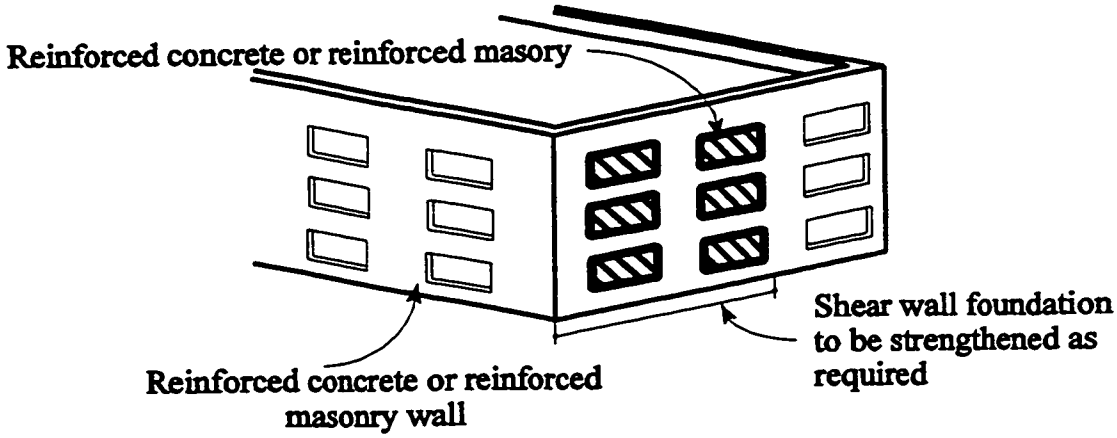

Figure 1.2 Filling Windows or Doors, with Reinfored Concrete or Masonry (NEHRP 1992)

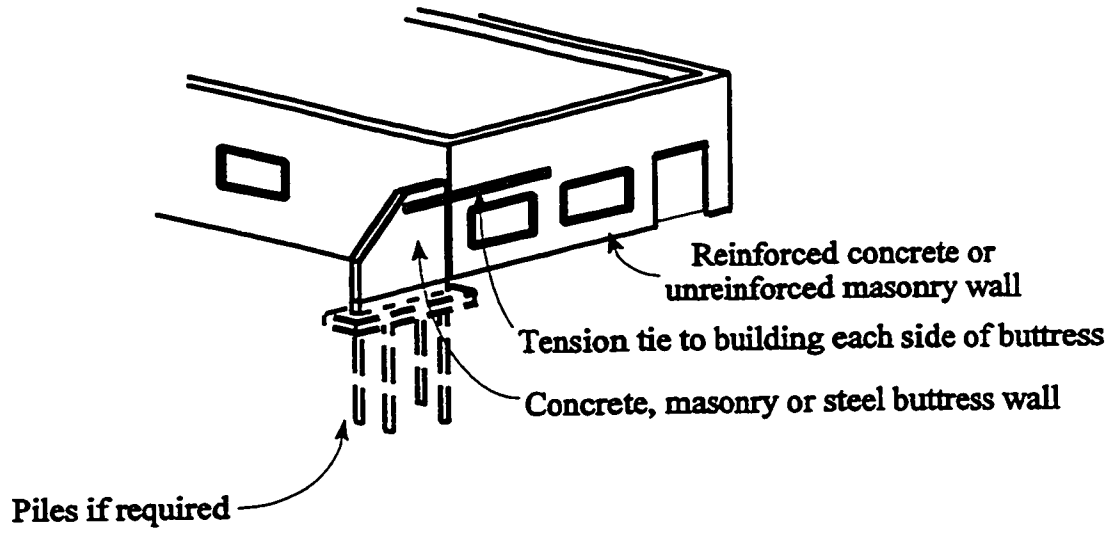

Figure 1.3 New External R/C Wall (NEHRP 1992)

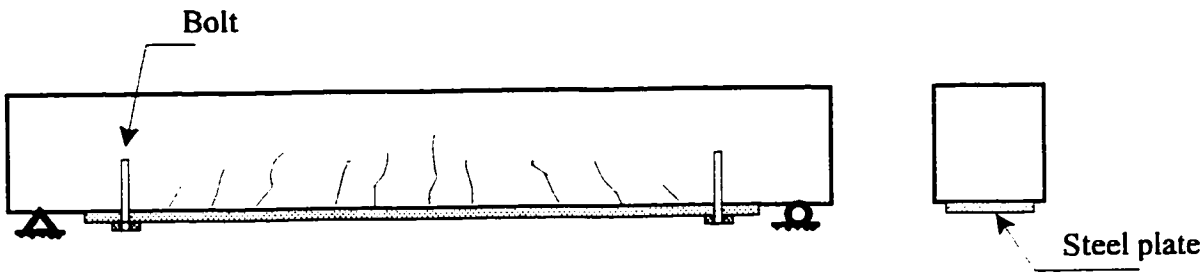

Figure 1.4 Flexural strengthening detail of R/C typical beam, with anchored plate

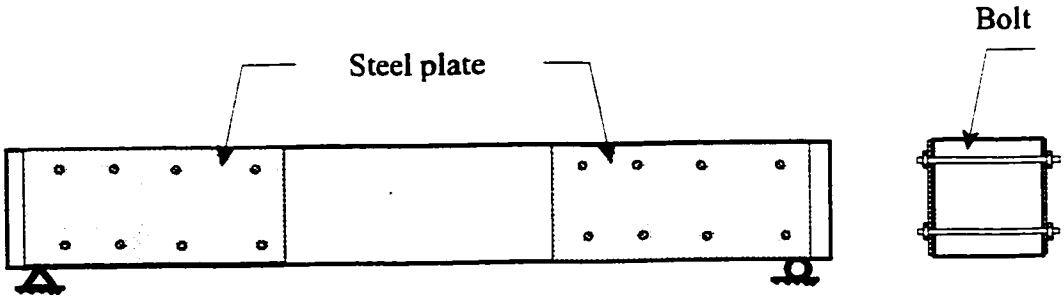

Figure 1.5 Shear strengthening detail of R/C typical beam, with anchored plate

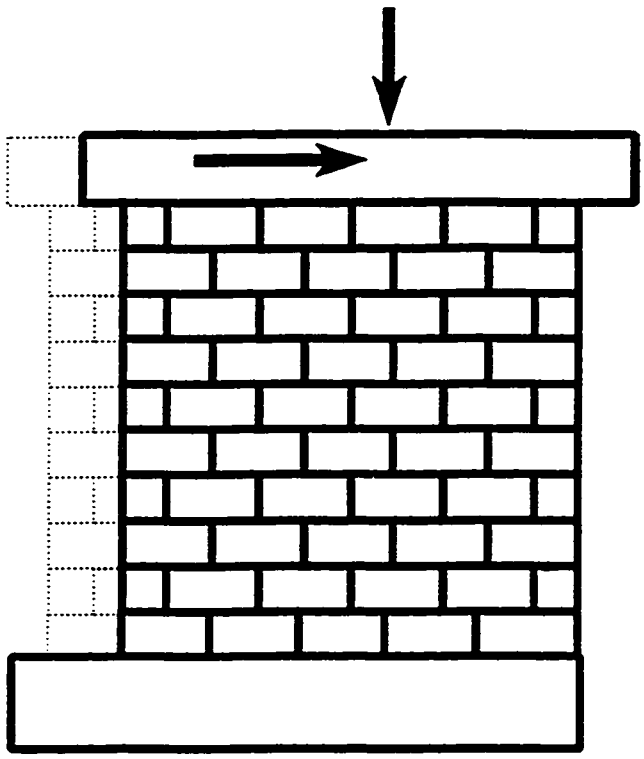

Figure 2.1 Sliding shear failure in low-rise masonry walls

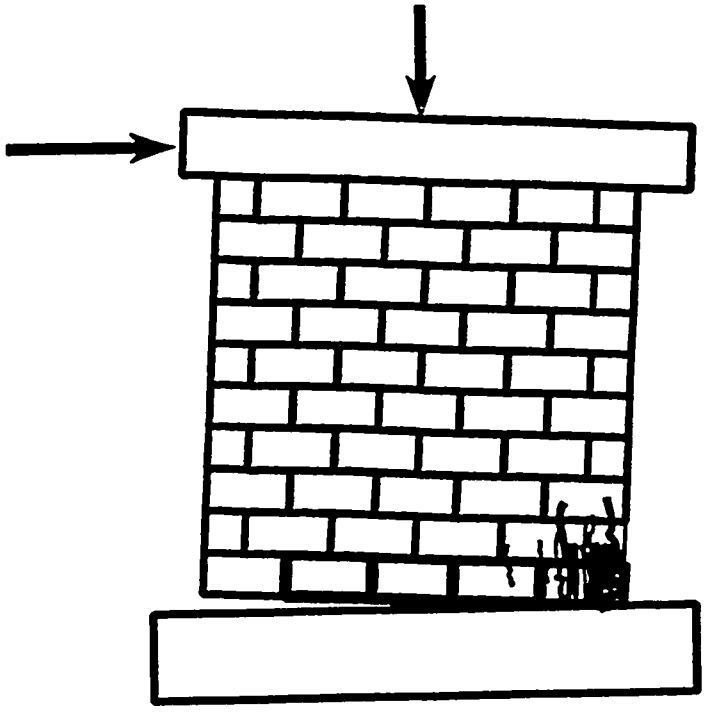

Figure 2.2 Toe crushing (rocking) failure in low-rise masonry walls

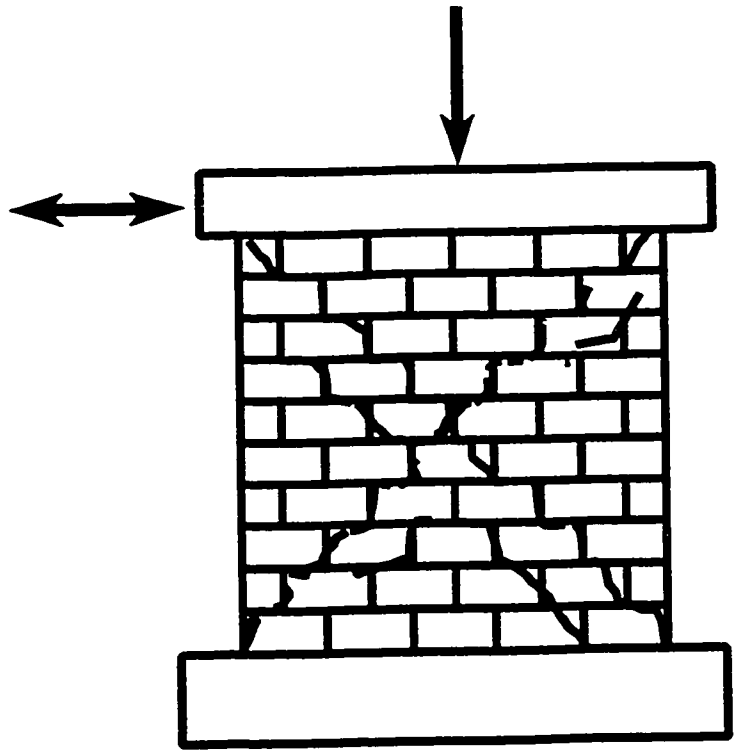

Figure 2.3 Diagonal tension filure in low-rise masonry walls

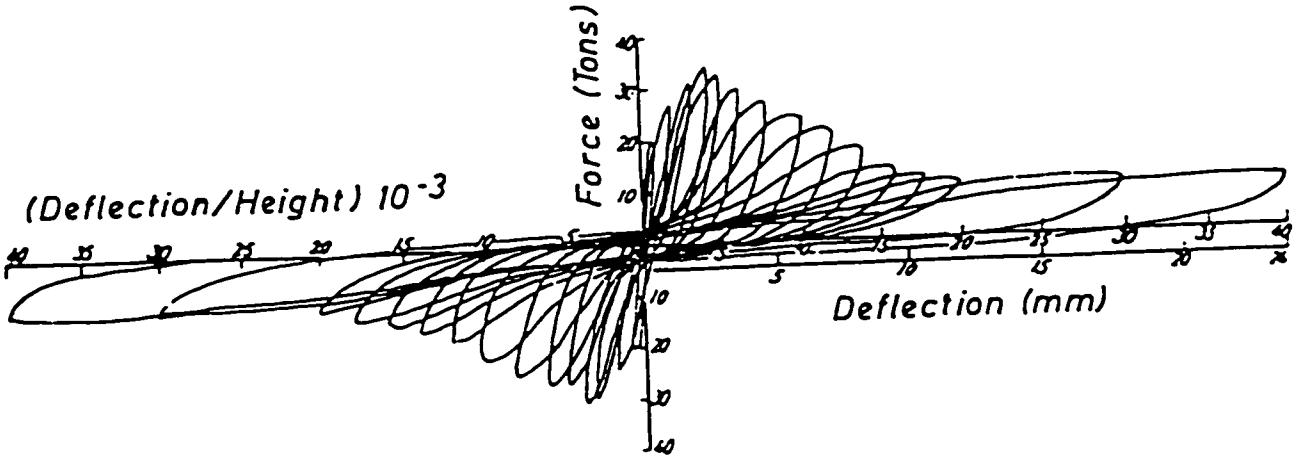

Figure 2.4 Hysteretic response of a structural wall controlled by shear strength (Paulay 1990)

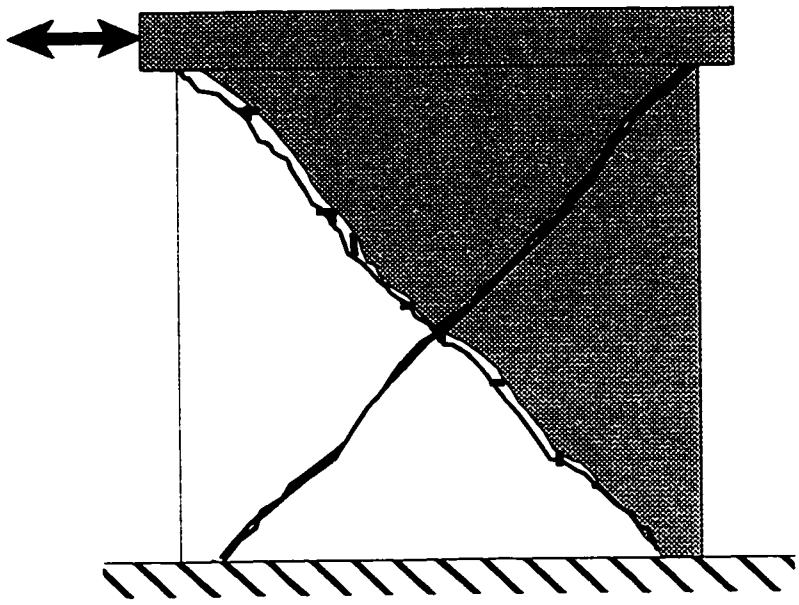

Figure 2.5 Diagonal tension failure mode in low-rise R/C walls

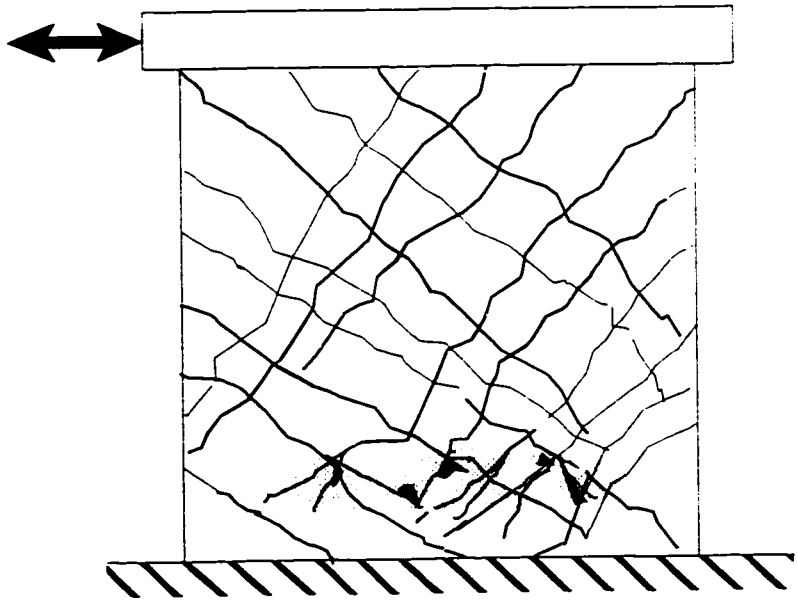

Figure 2.6 Diagonal compression failure mode in low-rise R/C walls

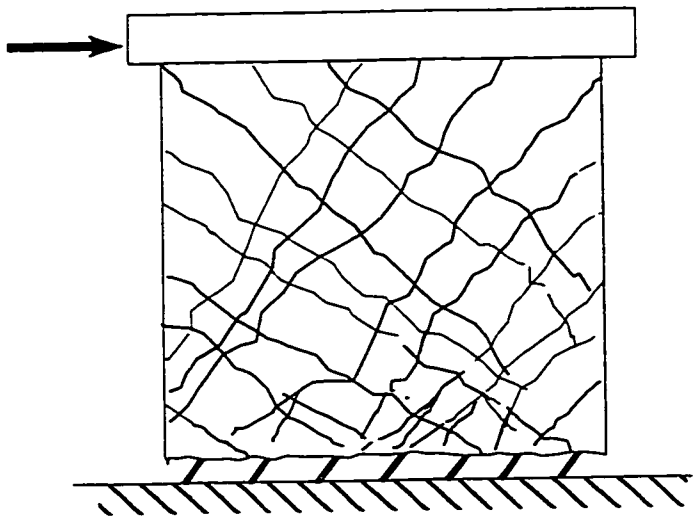

Figure 2.7 Sliding shear failure mode in low-rise R/C walls

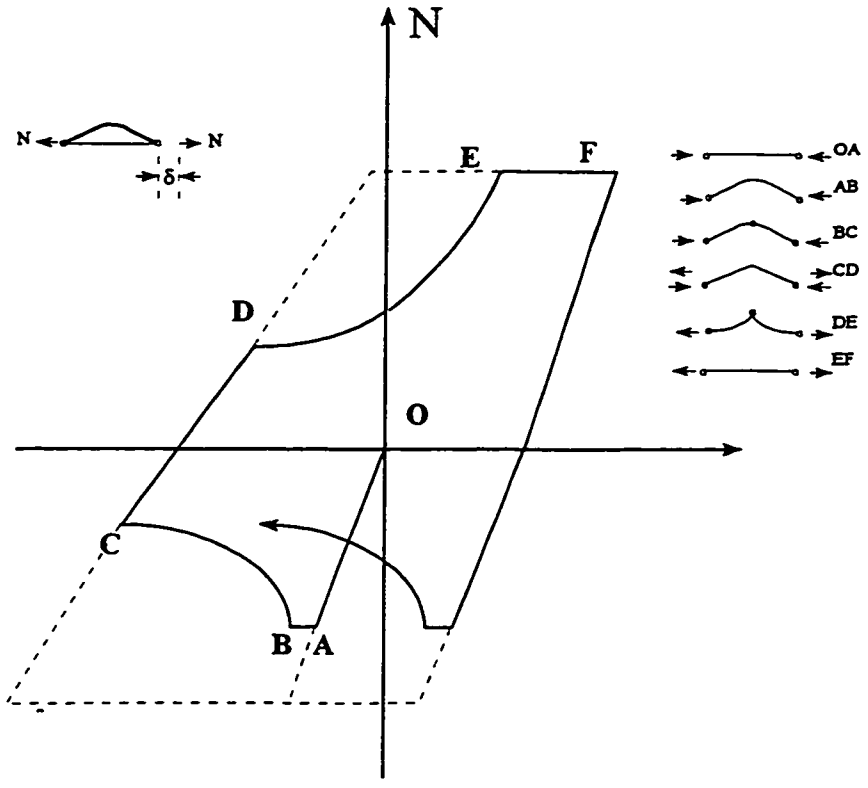

Figure 2.8 Hystersis loop for an initial straight steel strip (Wakabayashi 1986)

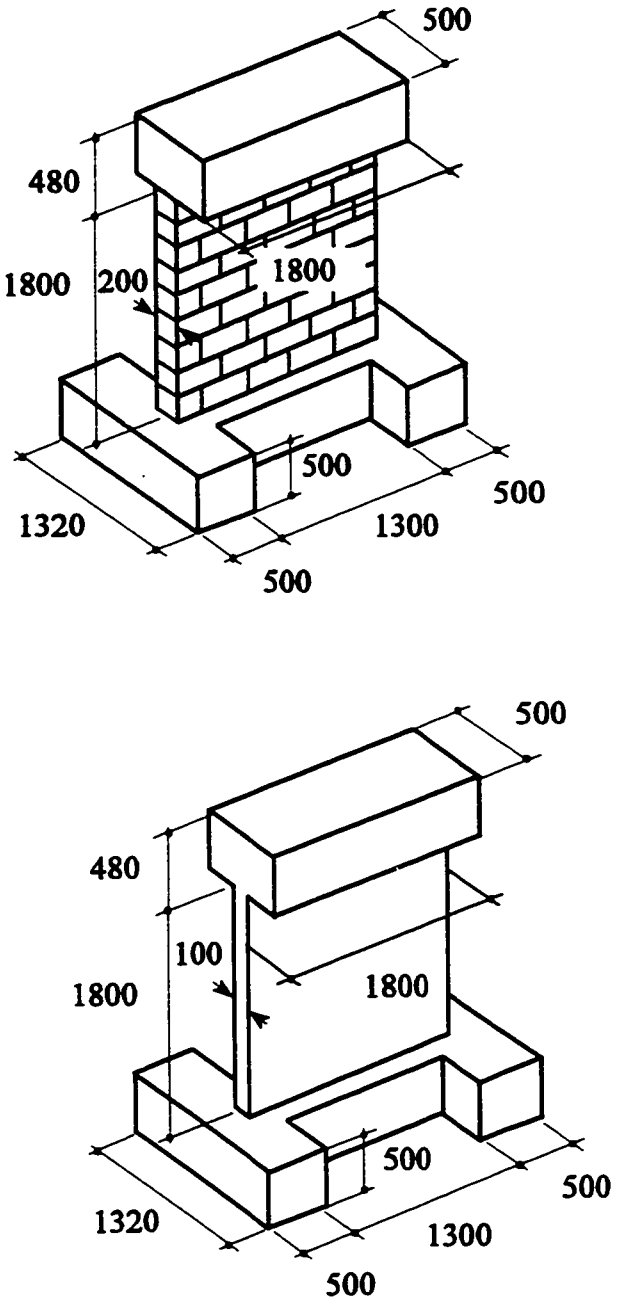

Figure 3.1 Top: Layout of masonry wall specimen
Bottom: Layout of concrete wall specimen

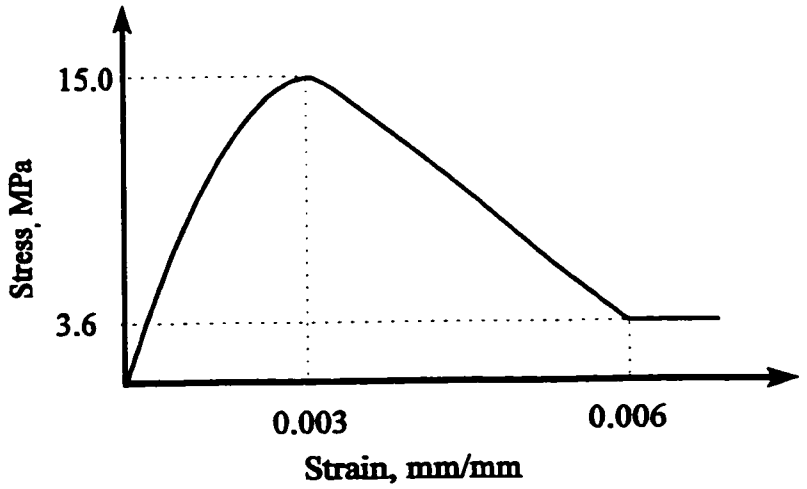

Stress-strain for grouted and ungrouted masonry concrete

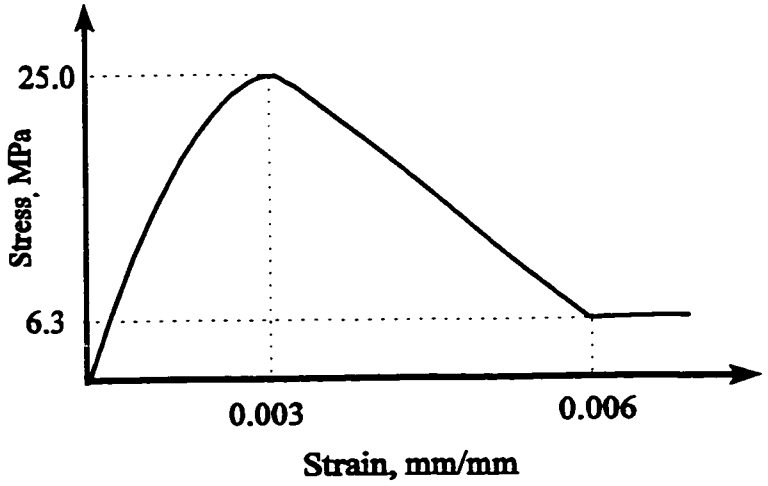

Stress-strain for concrete

Figure 3.2 Stress-strain for concrete and masonry used in strength prediction

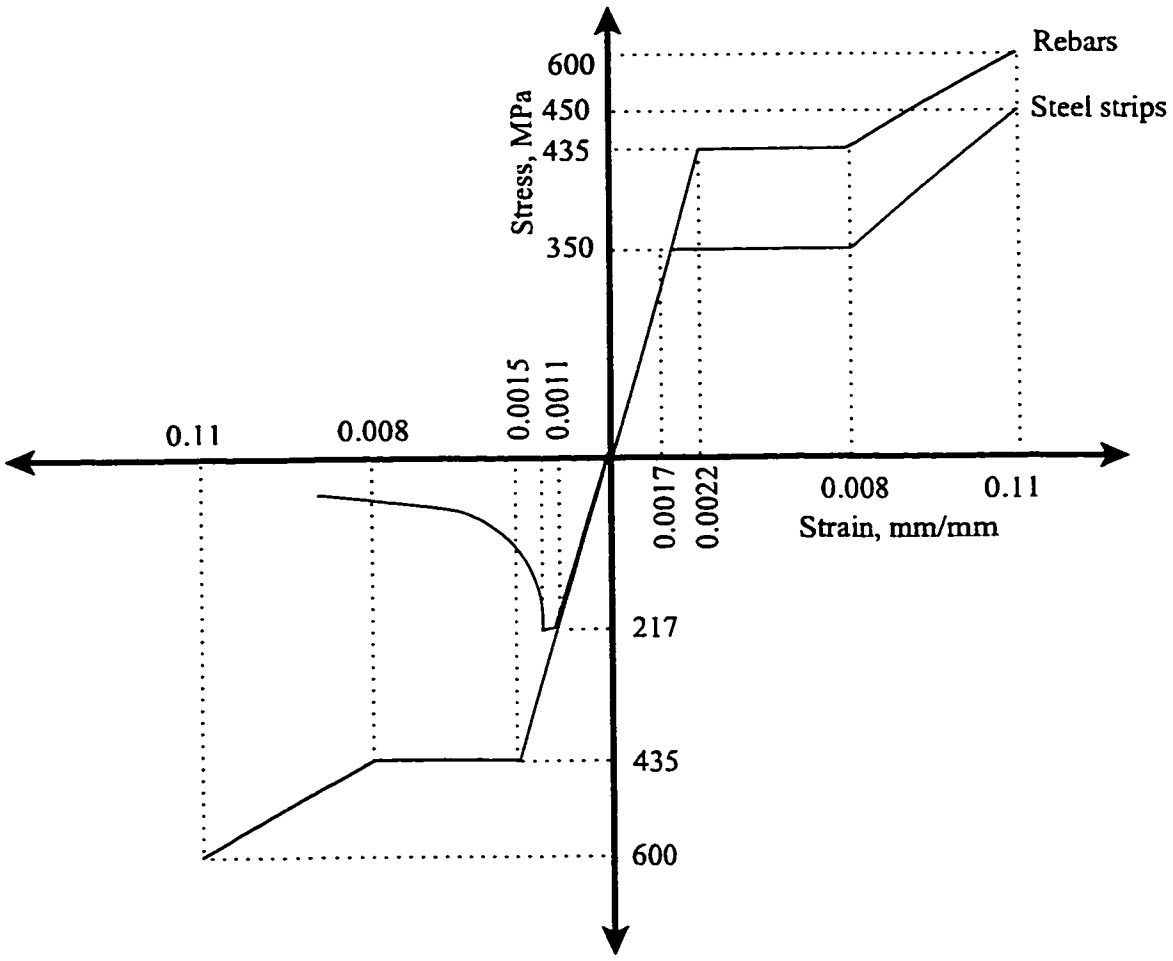

Figure 3.3 Stress-strain relationship for steel used in strength prediction

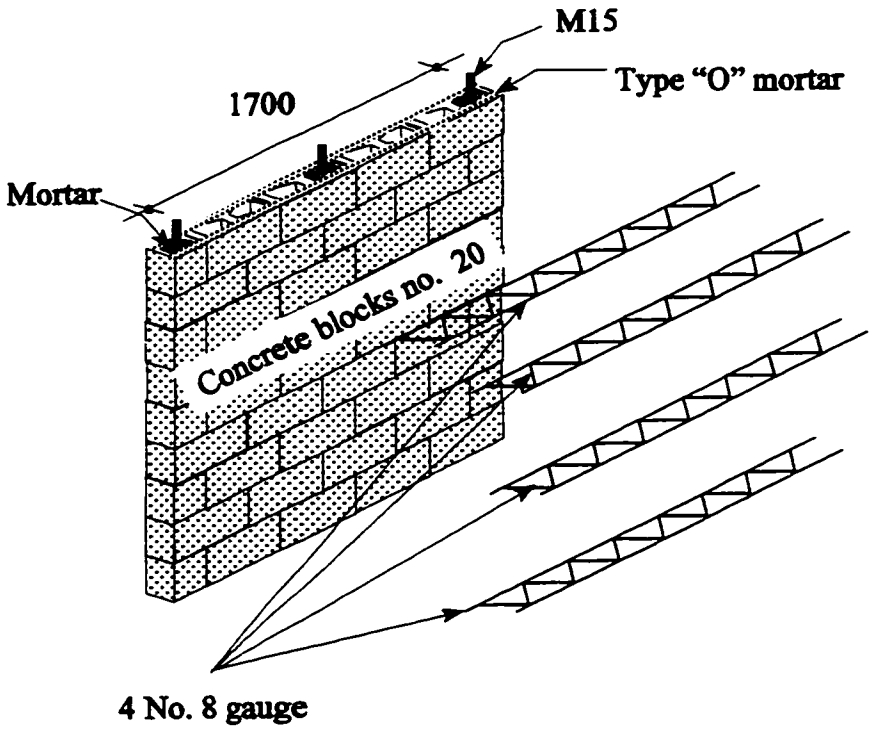

Figure 3.4 Details of reinforcement of Wall 10 (PRM)

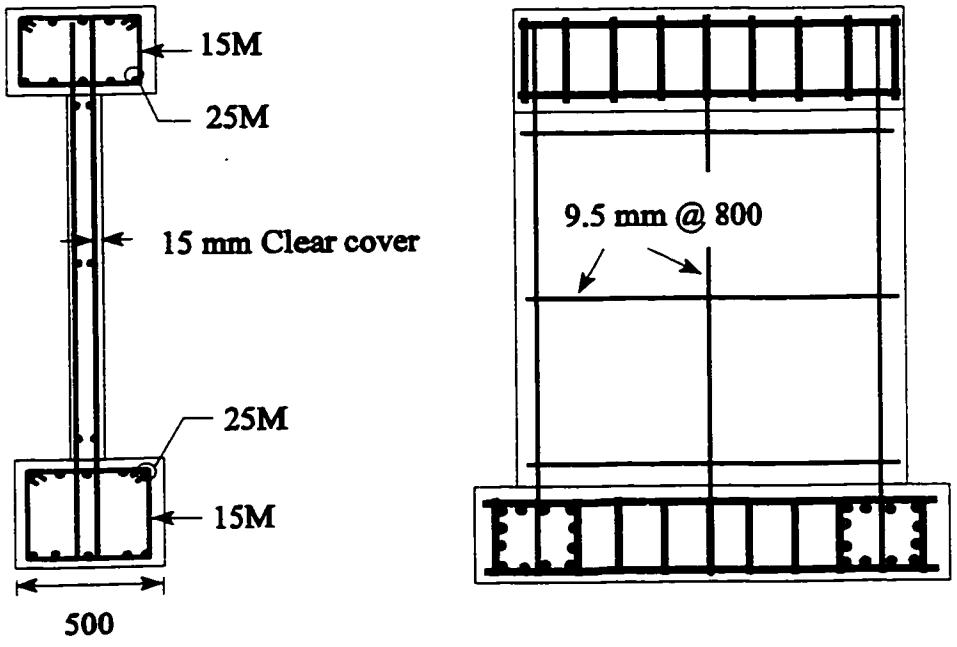

Figure 3.5 Details of reinforcement of Wall 11 (RC)

Wall Type	ρ_v	ρ_h		
URM	N/A	N/A	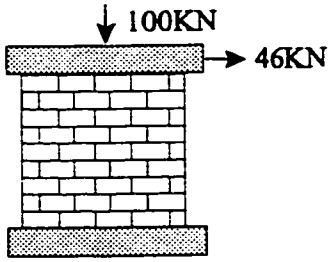	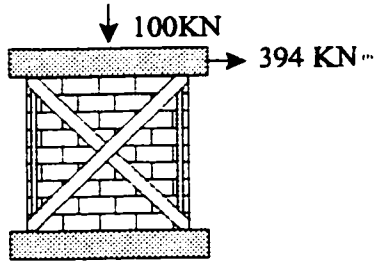
PRM	0.17%	0.13%	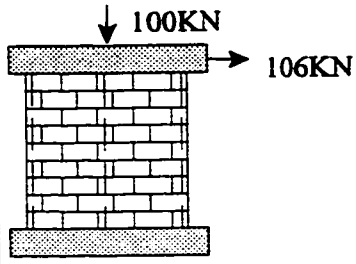	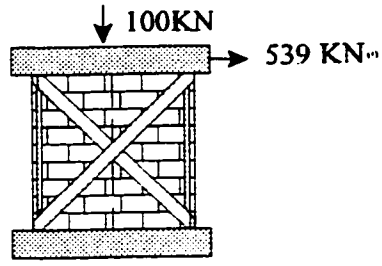
RC	0.24%	0.24%	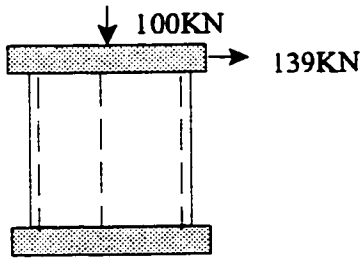	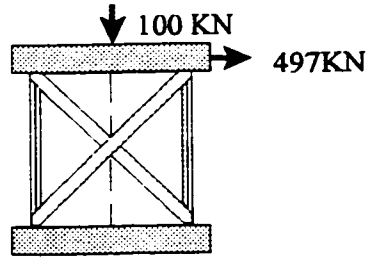

(1) Flexural failure, 100 mm above the base
(2) Flexural failure, at wall mid height

Figure 3.6 Predicted capacities for wall specimens

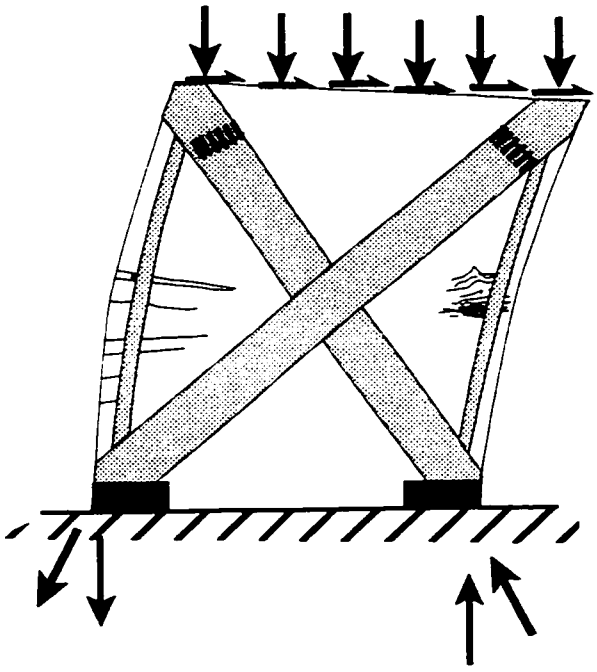

Figure 3.7 Shear transfer in retrofitted wall

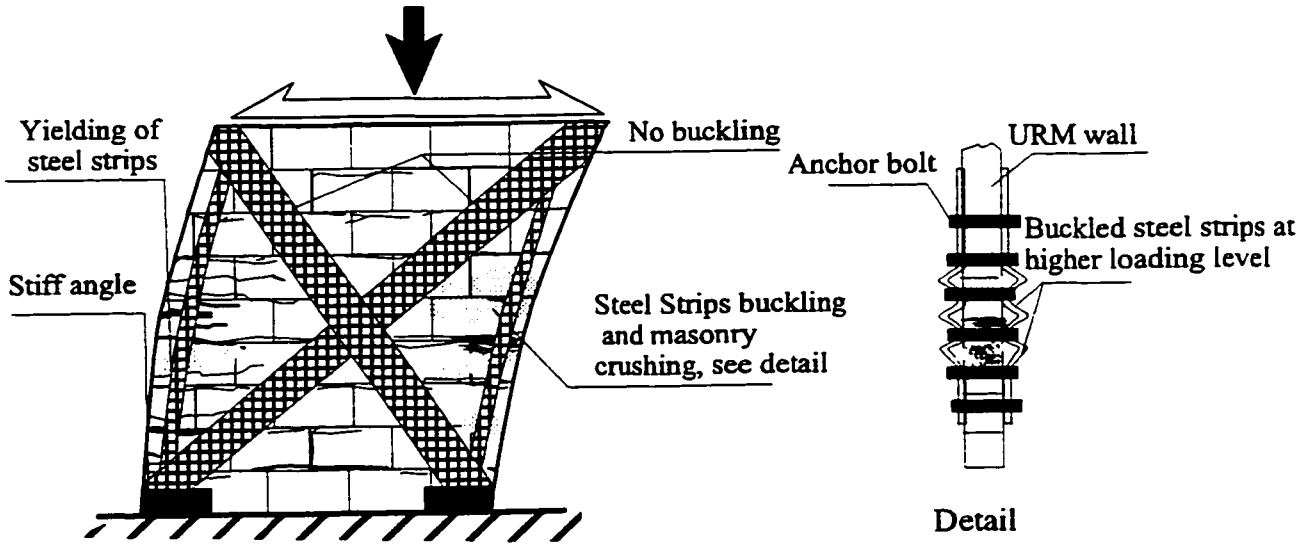

Figure 3.8 Expected mode of failure (URM wall)

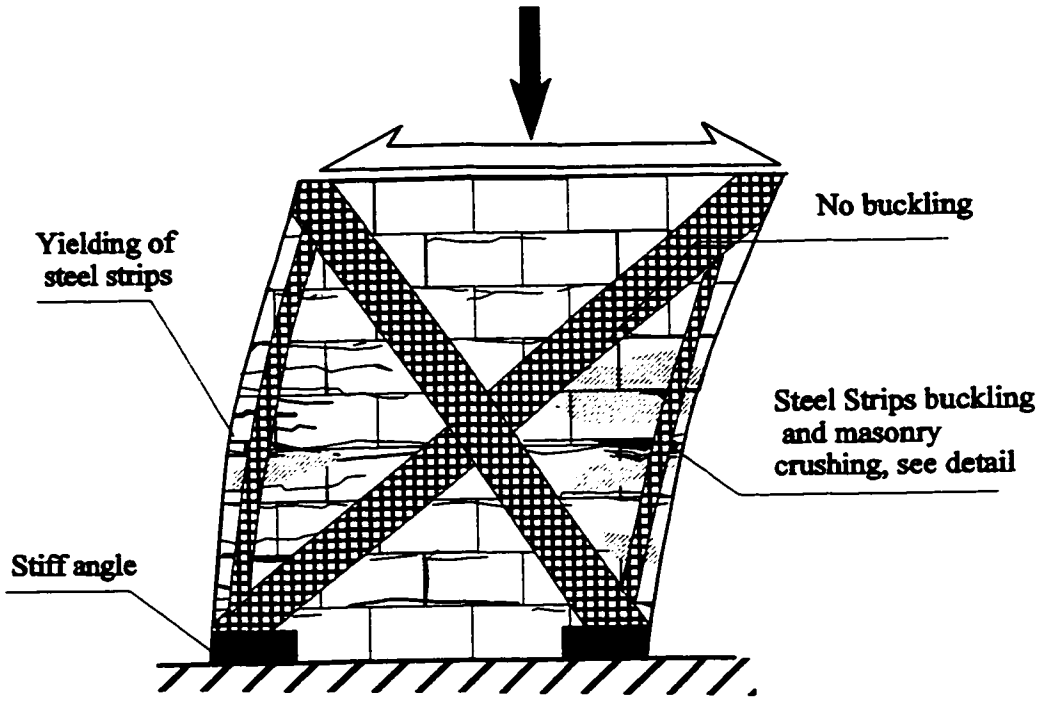

Figure 3.9 Expected mode of failure (PRM wall)

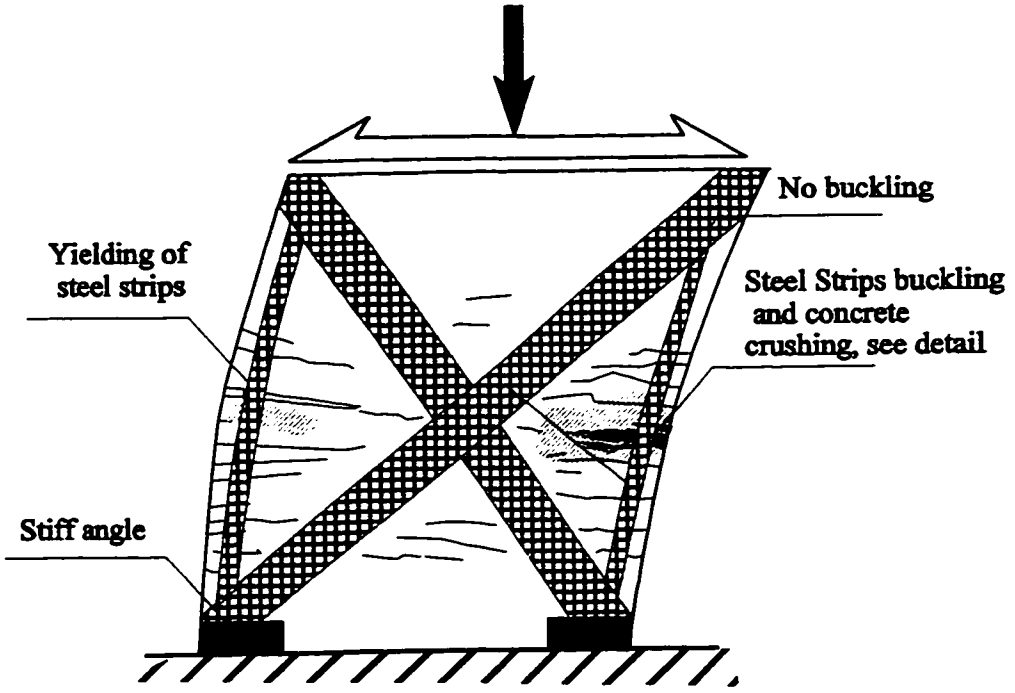

Figure 3.10 Expected mode of failure (RC wall)

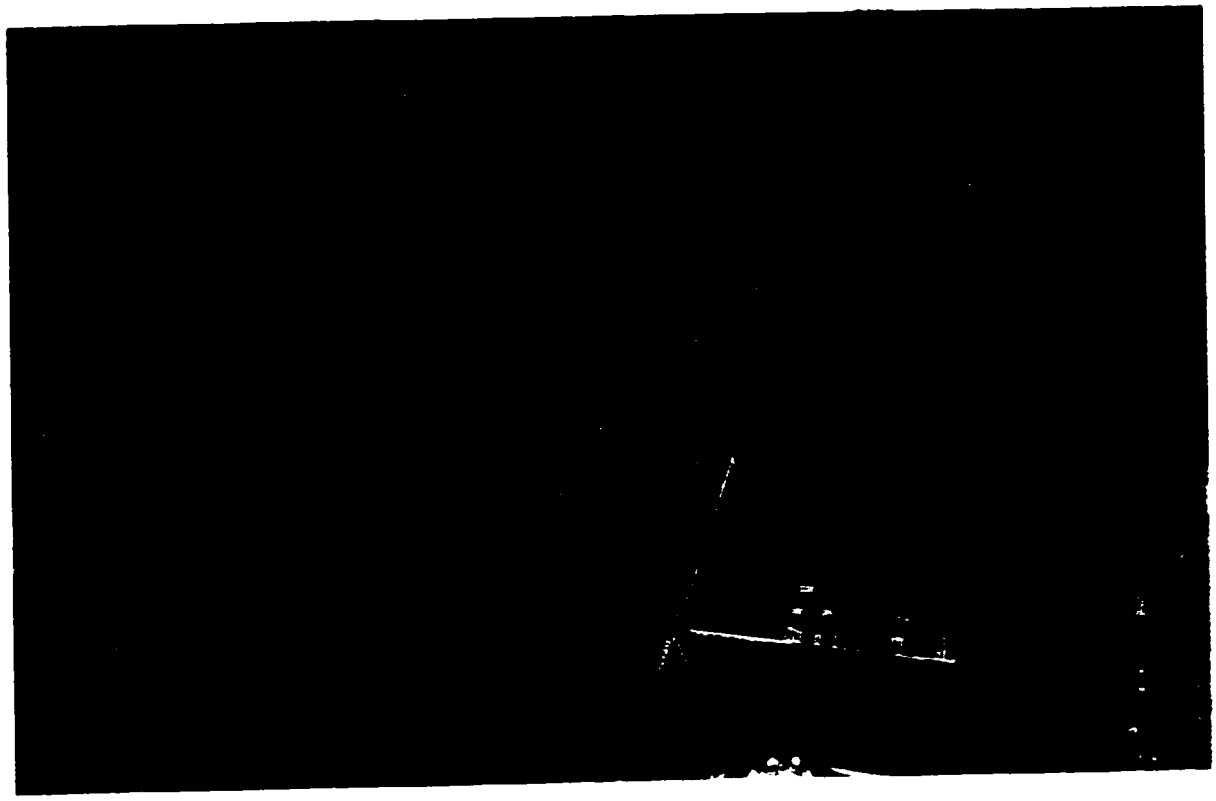

Figure 3.11 Footing and wall reinforcement in wooden form before casting

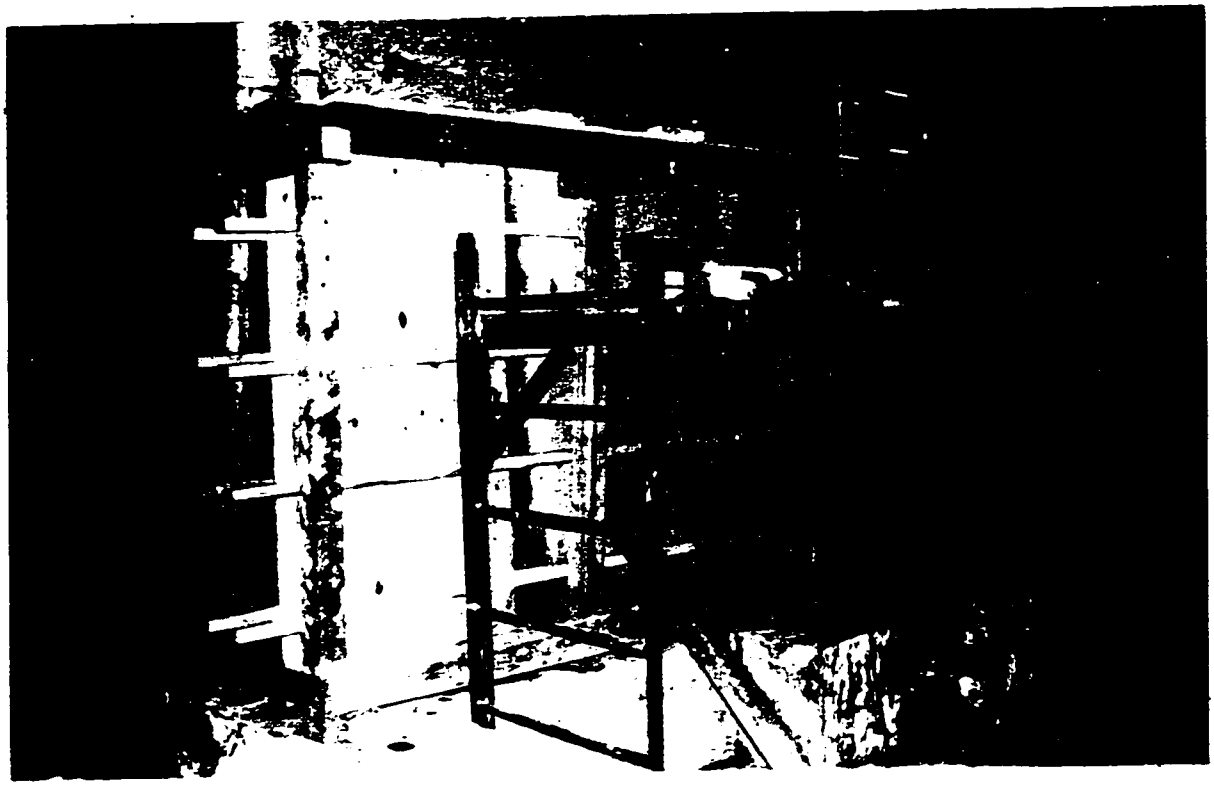

Figure 3.12 Wooden form for RC walls before casting

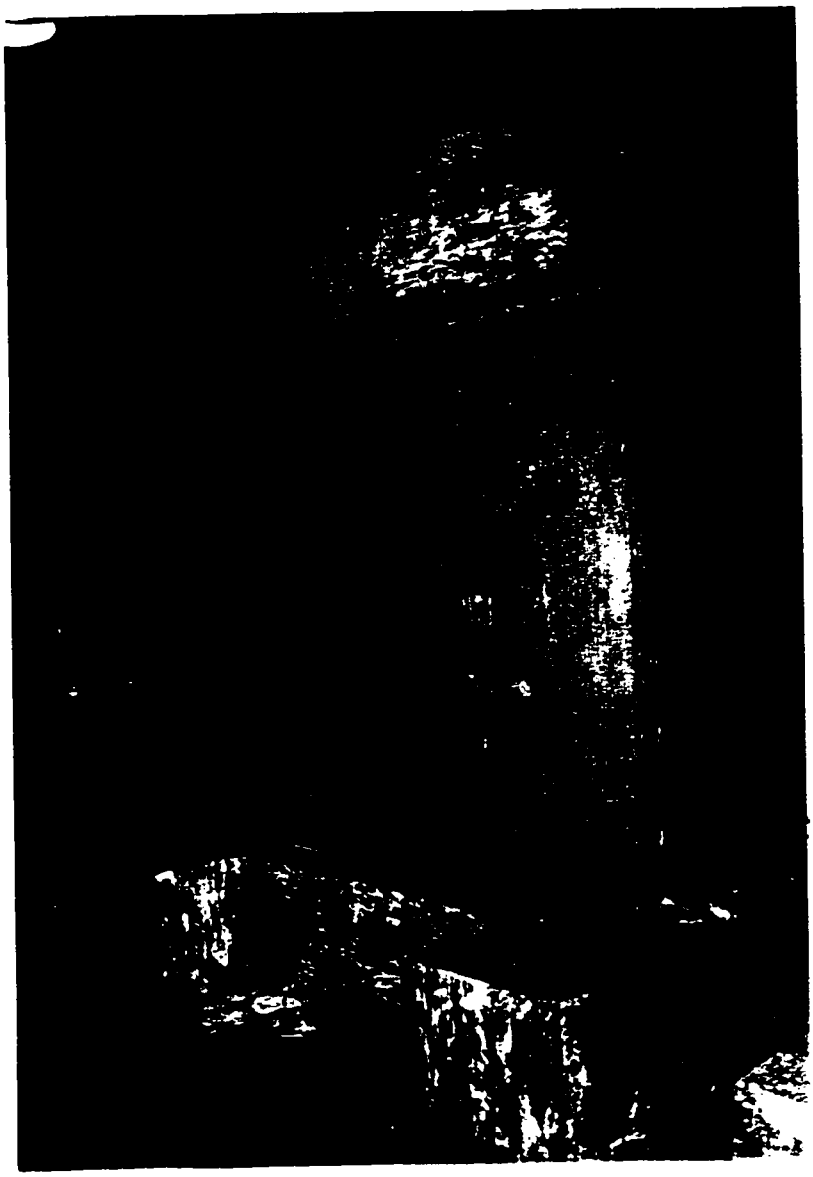

Figure 3.13 Reinforced concrete wall after construction

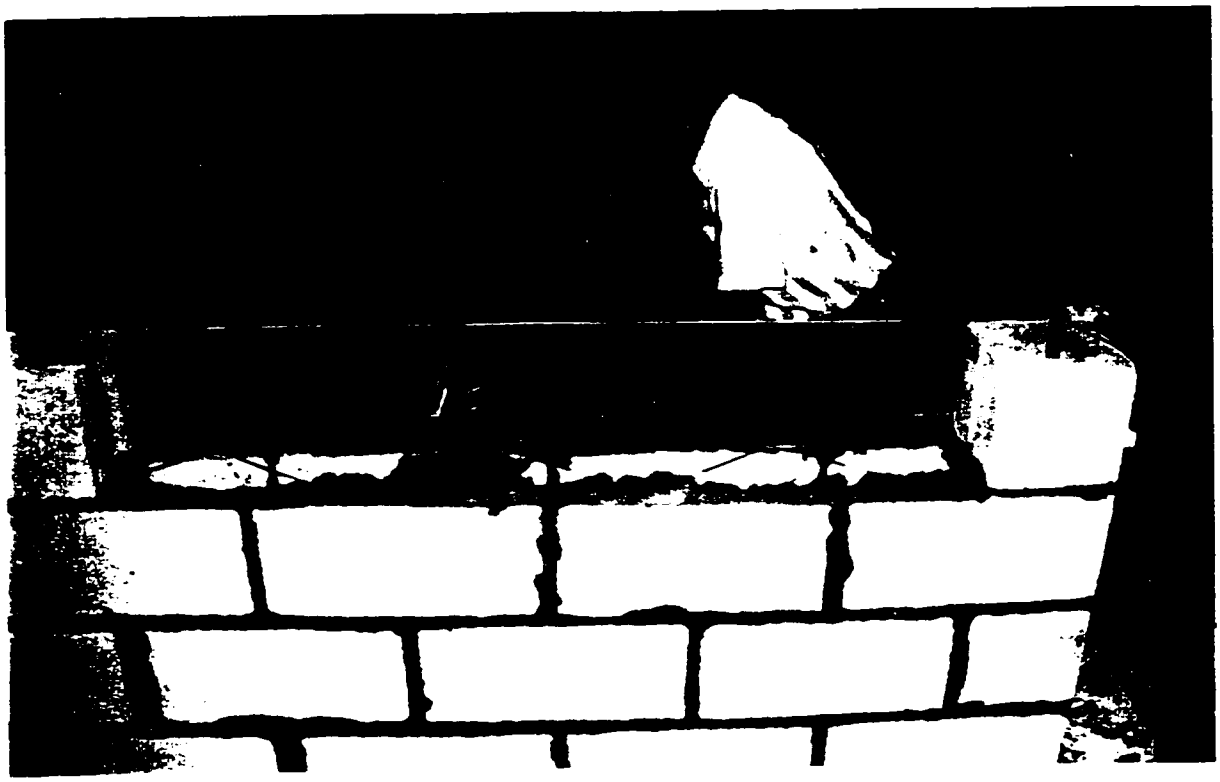

Figure 3.14 Partially reinforced masonry (PRM) wall under construction

Figure 3.15b PRM wall under construction

Figure 3.15a URM wall under construction

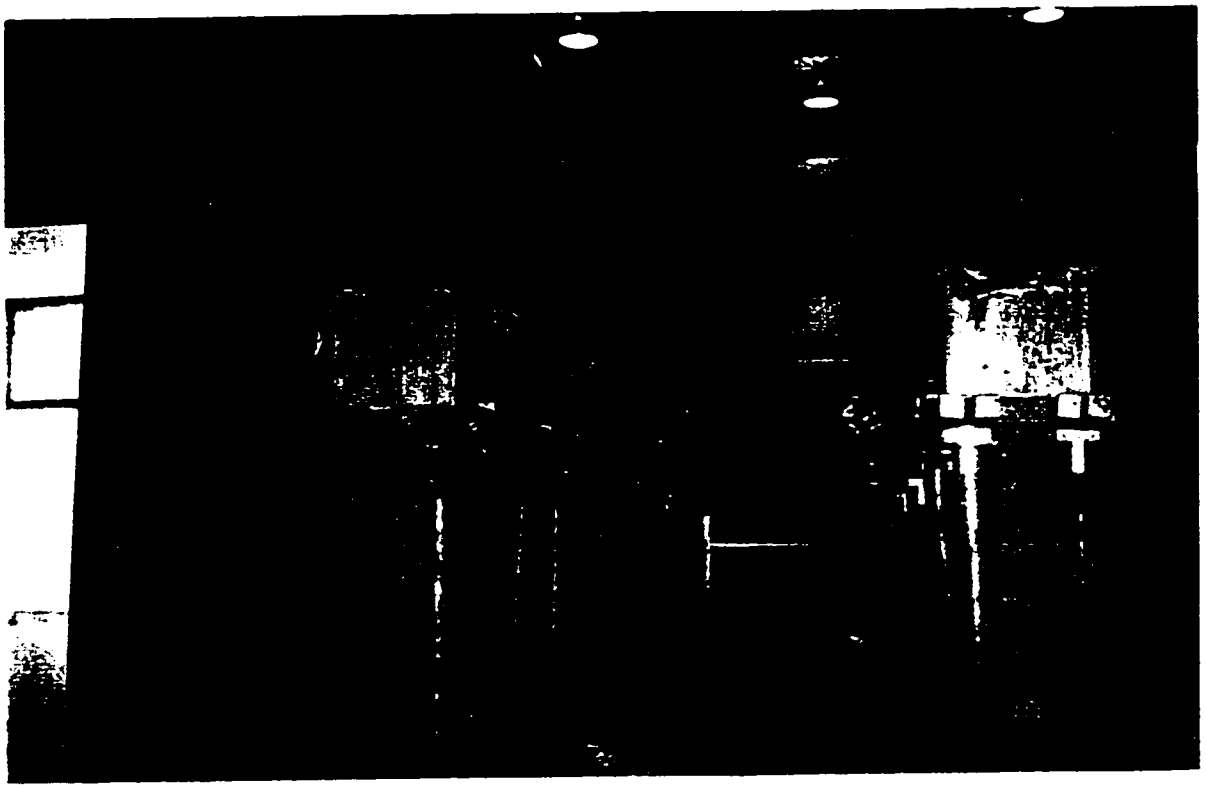

Figure 3.16 Masonry walls after construction of the top-beams

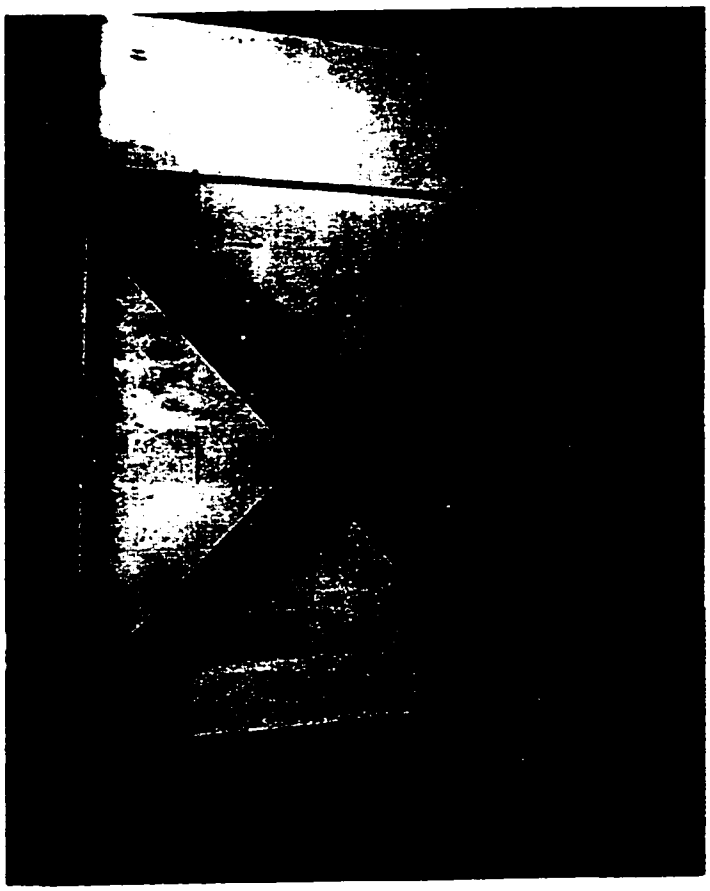

Figure 3.17 Steel strip system tied to URM wall

Figure 3.18 Details of steel strip conection to steel angle

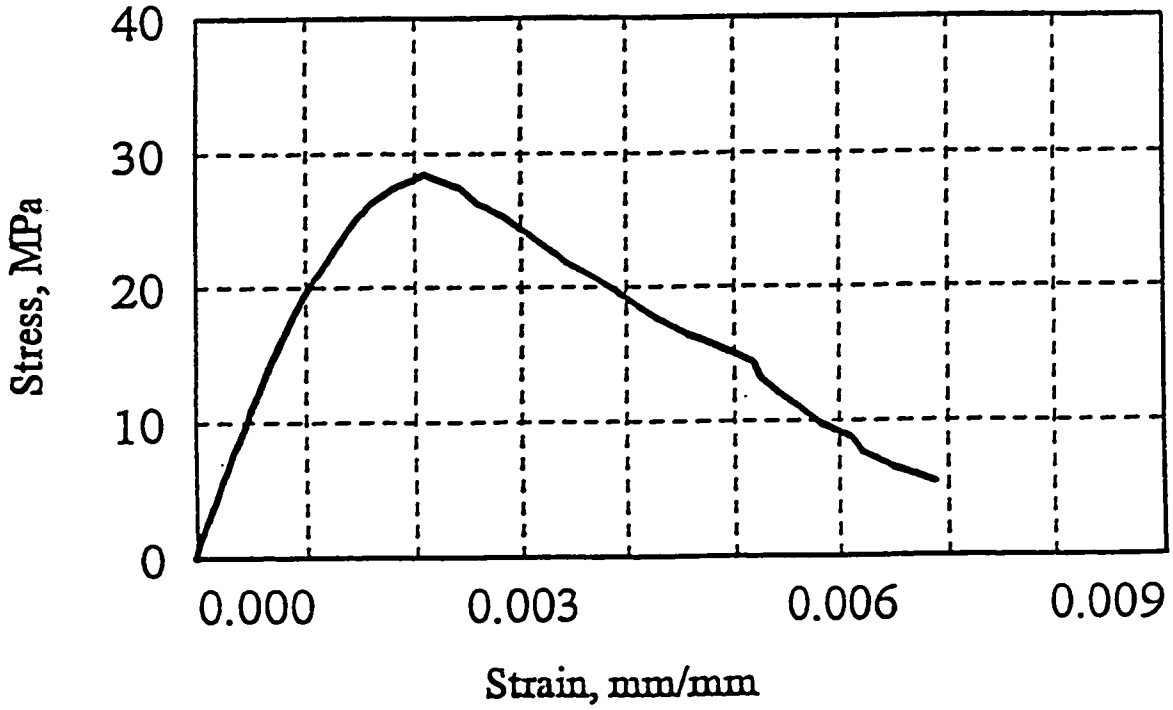

Figure 3.19 Concrete stress-strain relationship

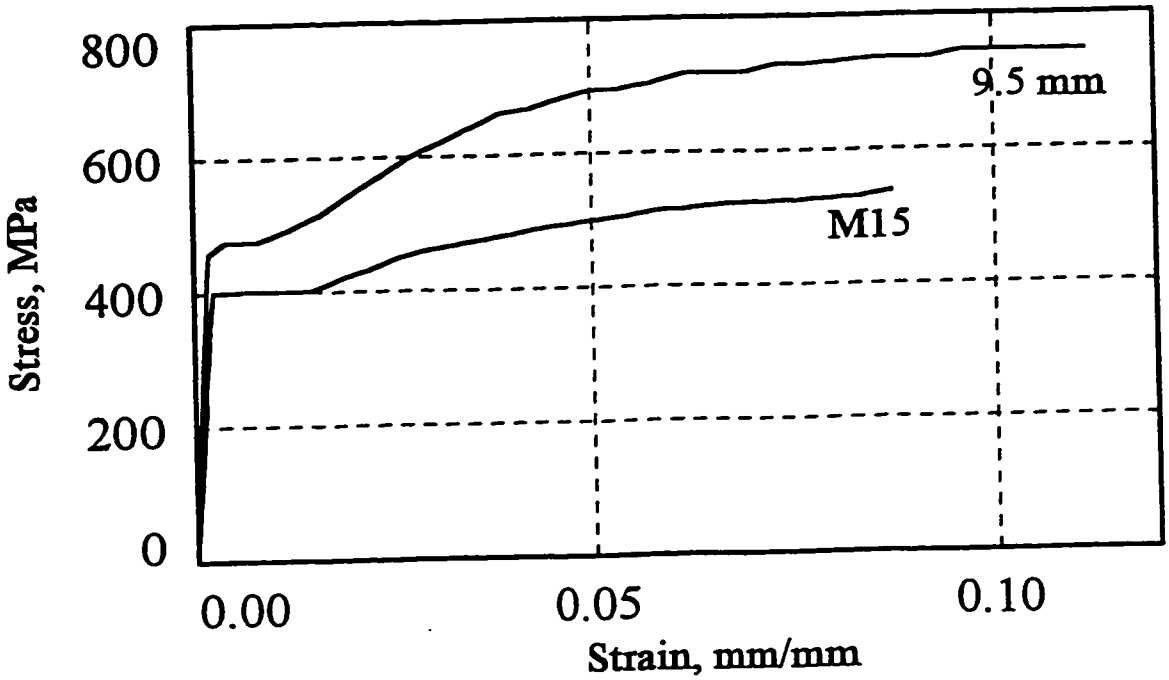

Figure 3.20 Reinforcing steel stress-strain relationship

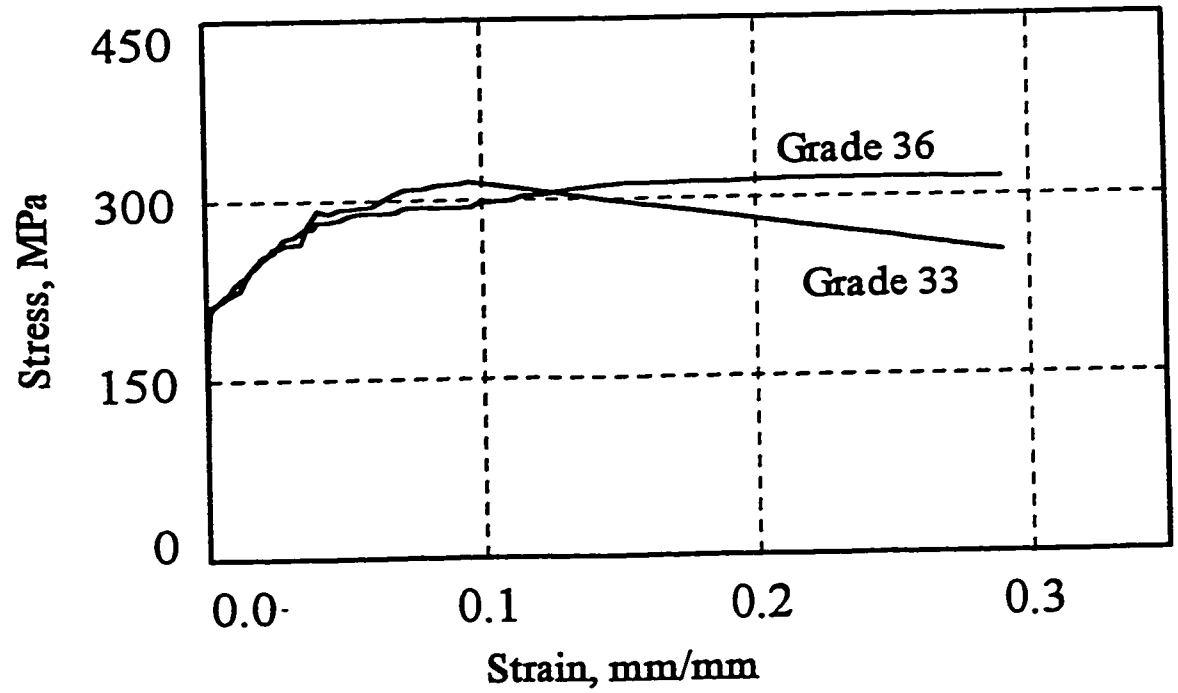

Figure 3.21 Steel strips stress-strain relationship

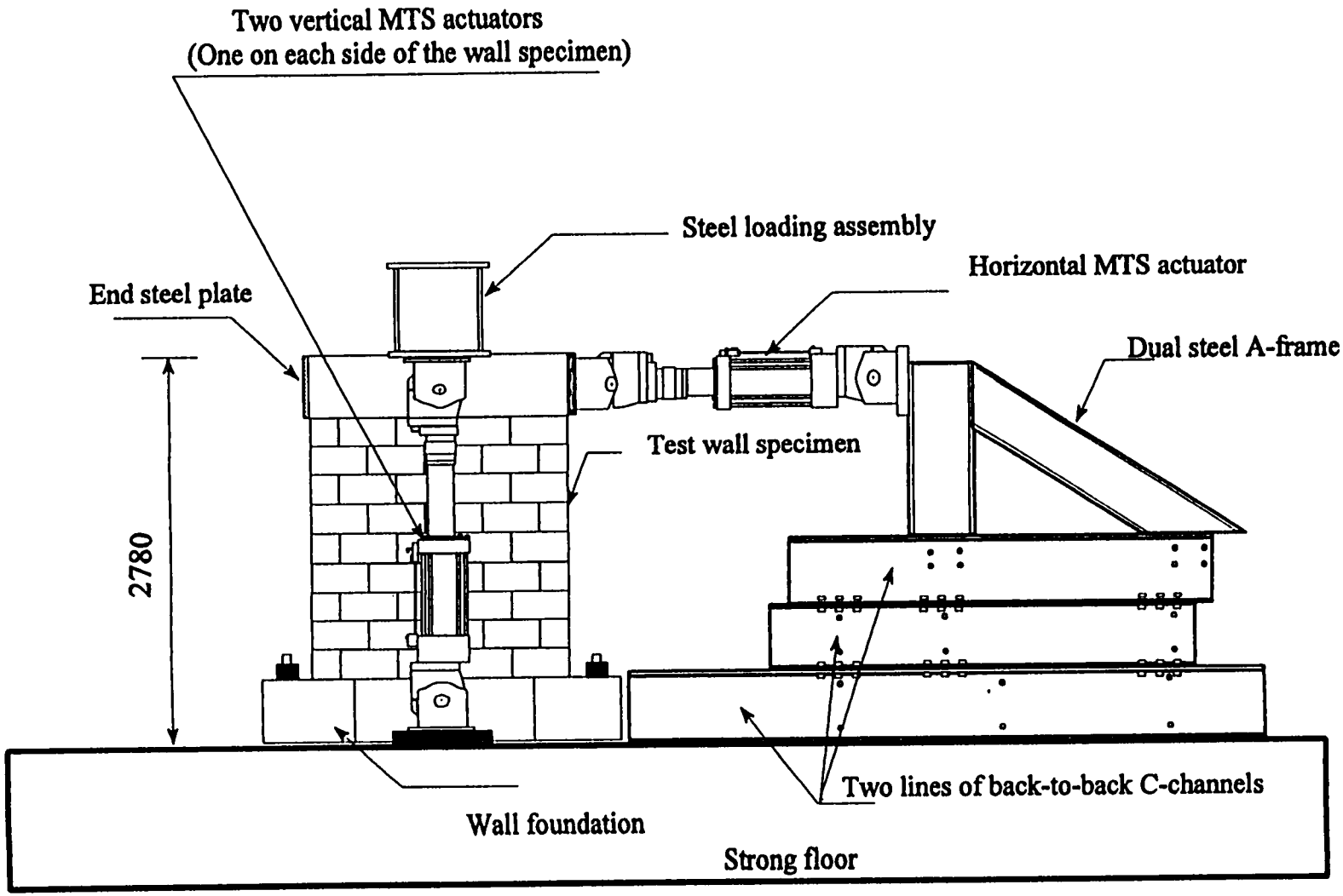

Figure 3.22 Test setup

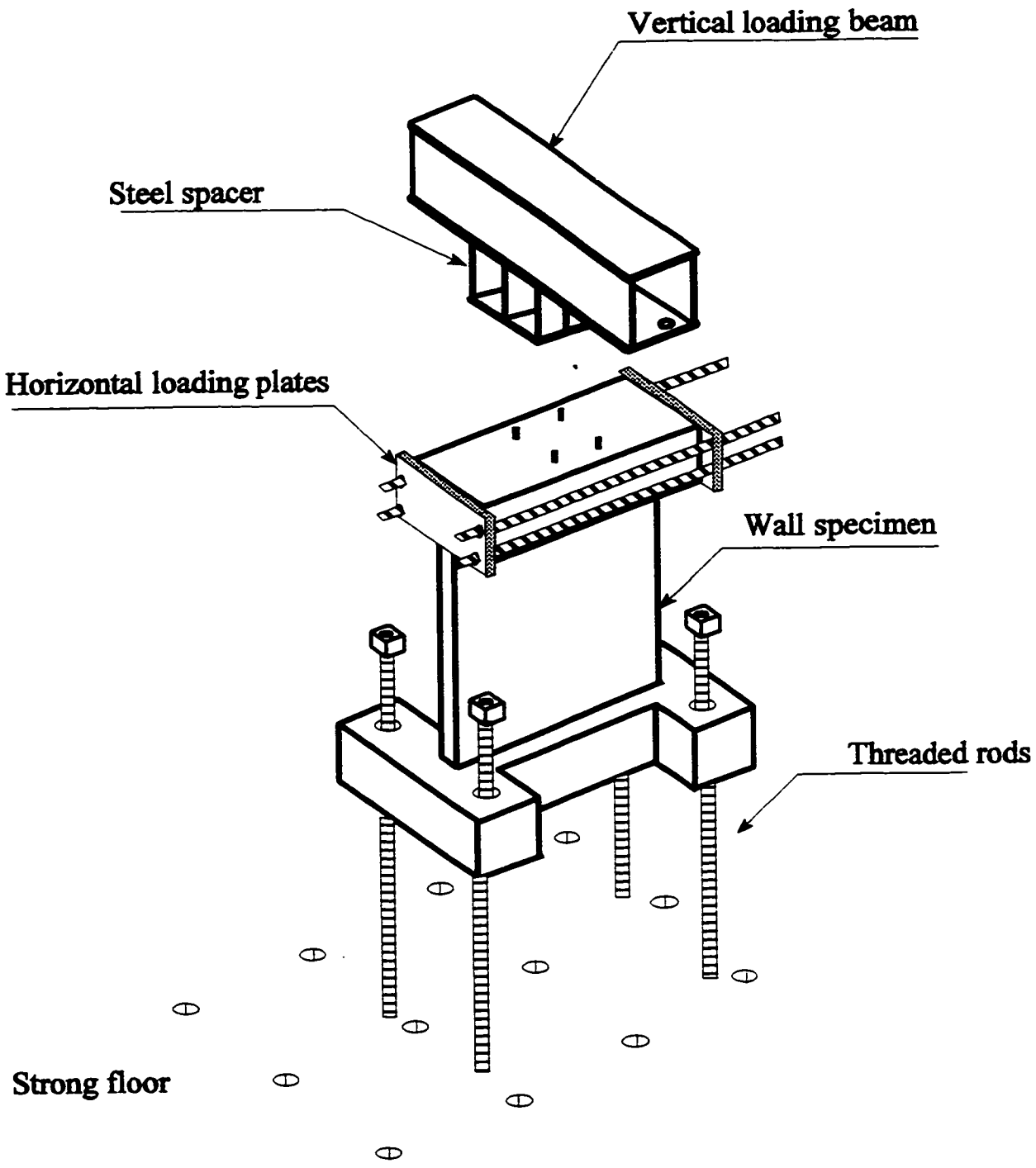

Figure 3.23 Vertical and horizontal loading assembly

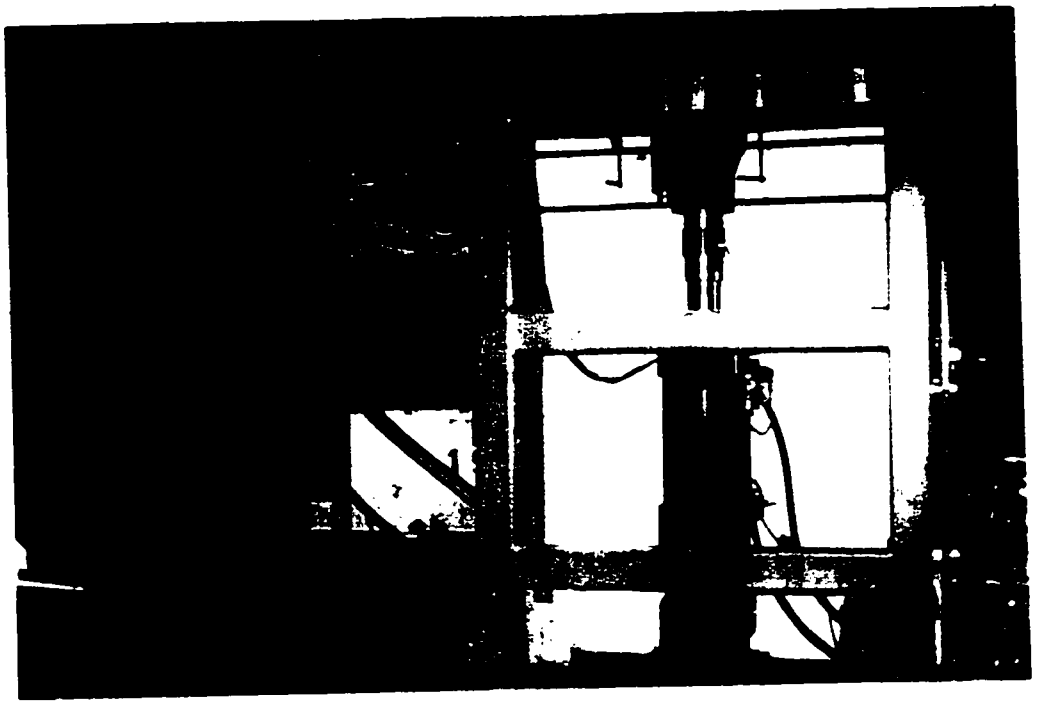

Figure 3.24 Test setup and lateral support frame

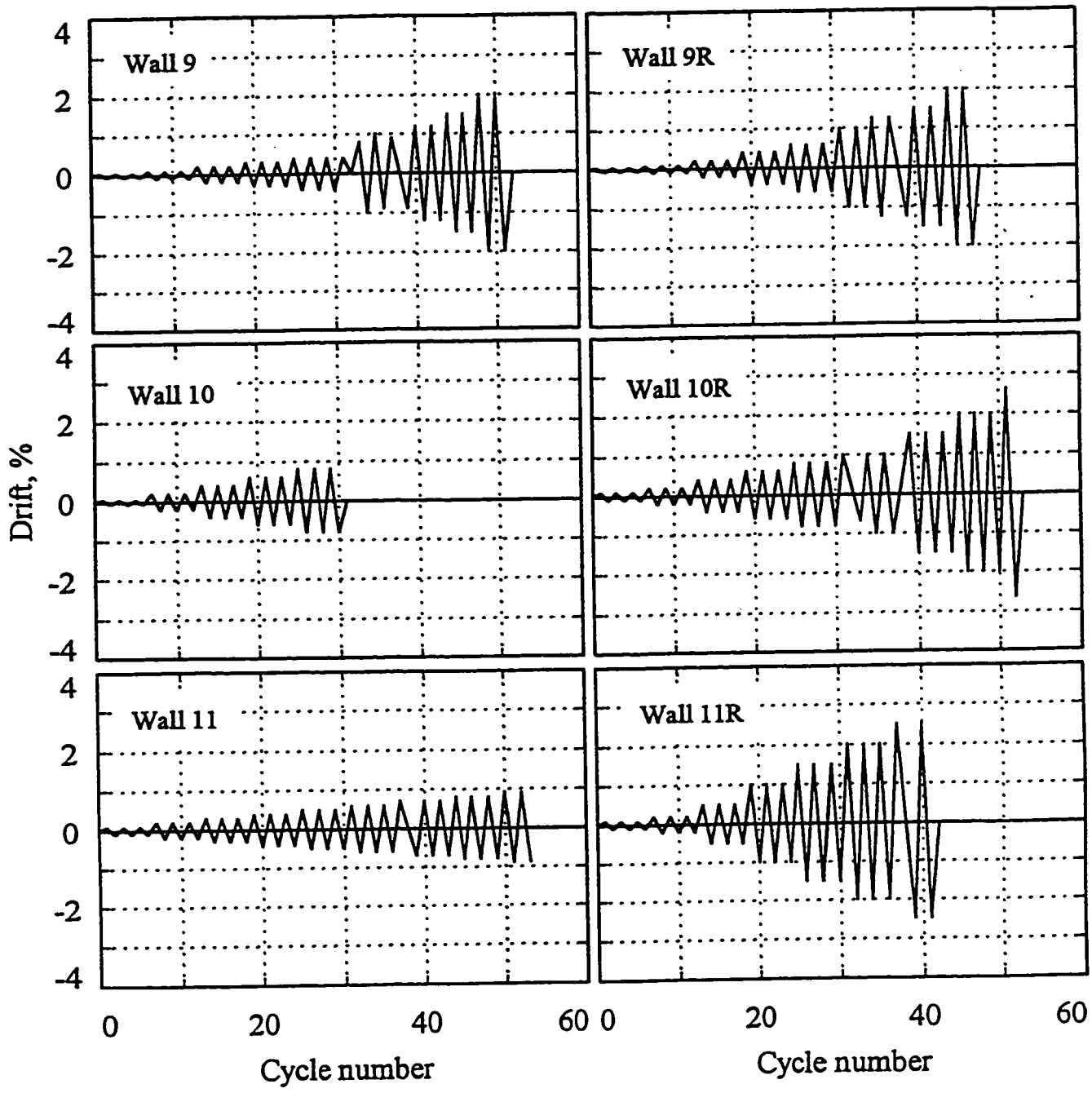

Figure 3.25 Load history for unretrofitted and retrofitted walls

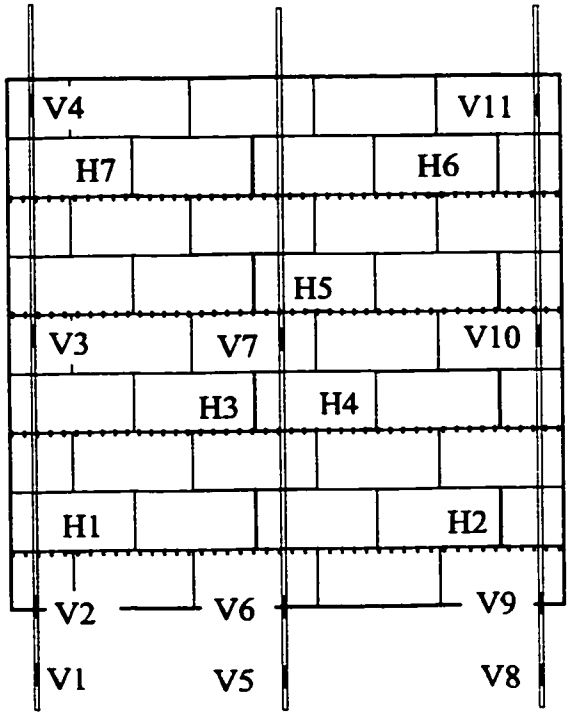

Figure 3.26 Strain gauge locations on masonry wall reinforcement

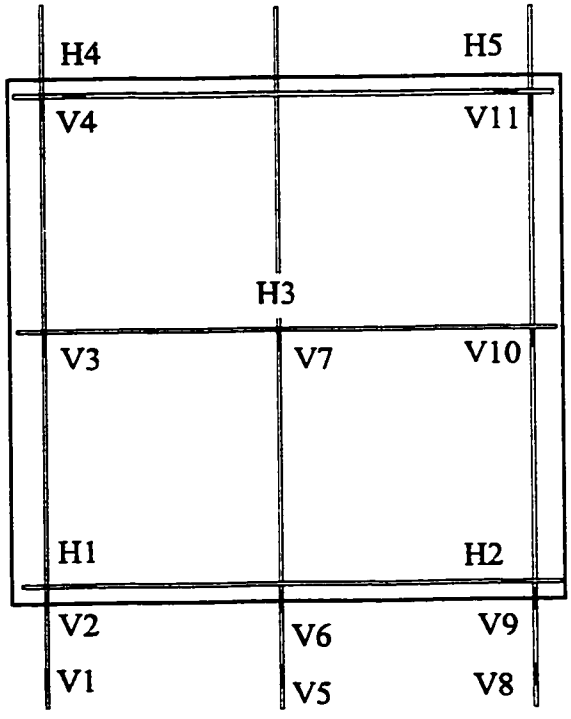

Figure 3.27 Strain gauge locations on concrete wall reinforcement

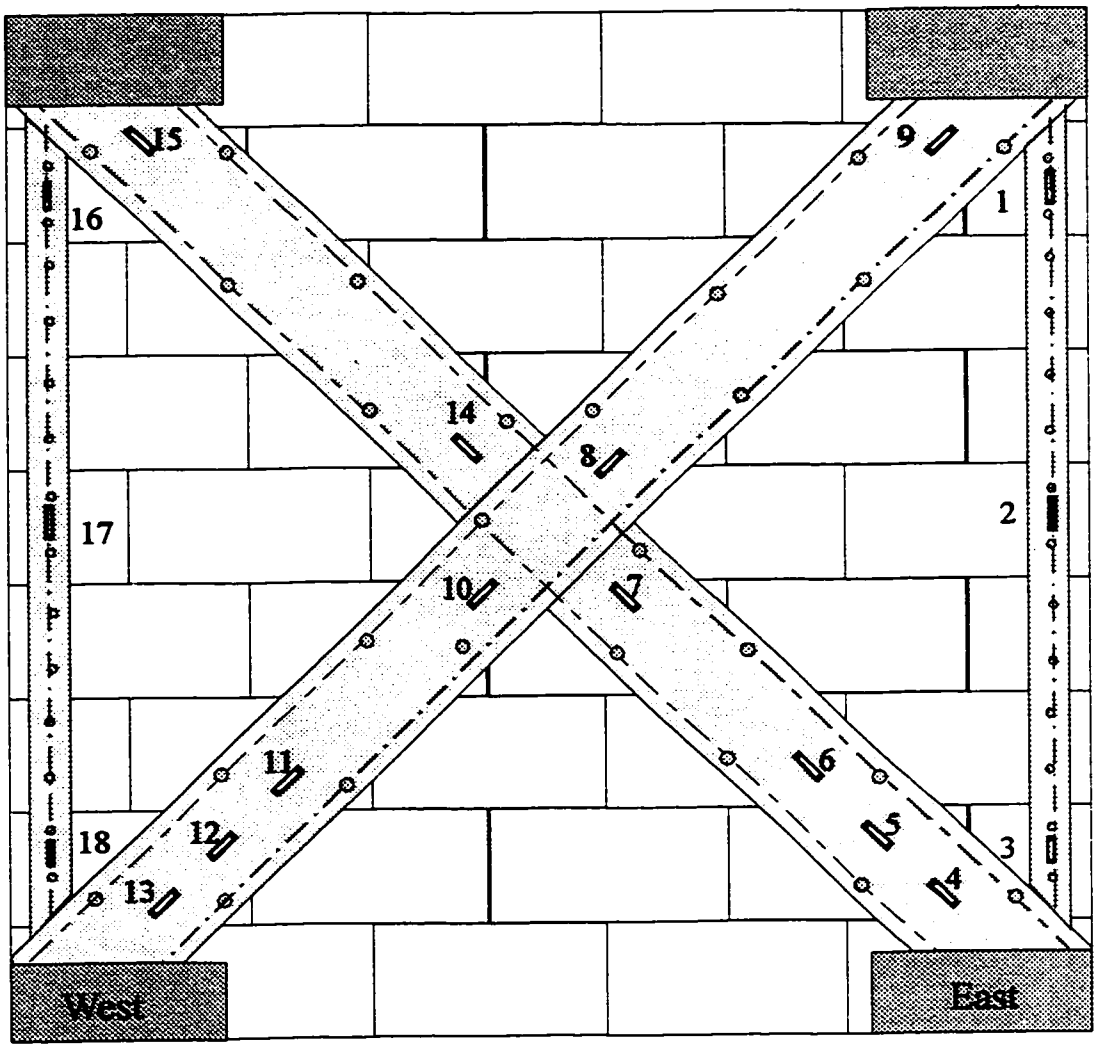

Figure 3.28 Strain gauge locations on steel strips

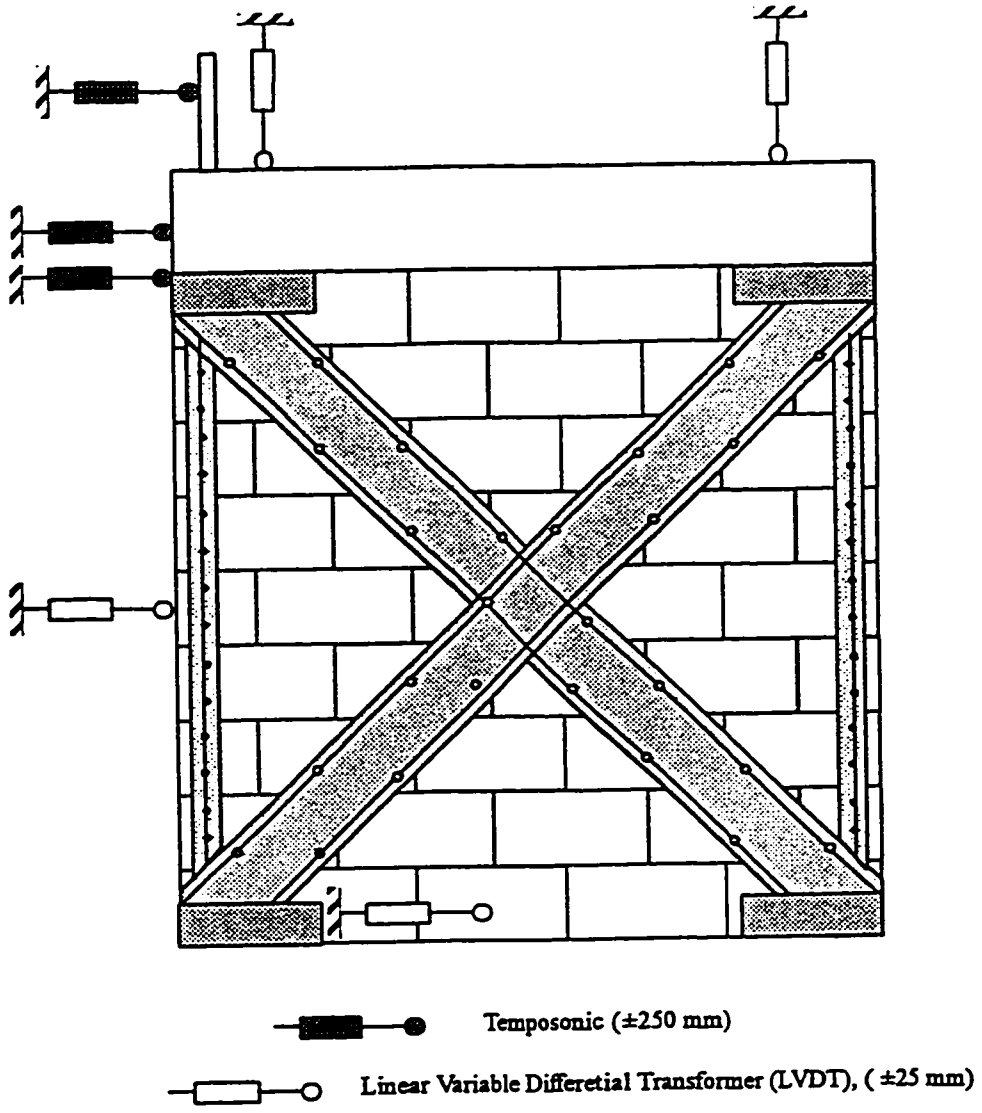

Figure 3.29 Displacement transducer locations

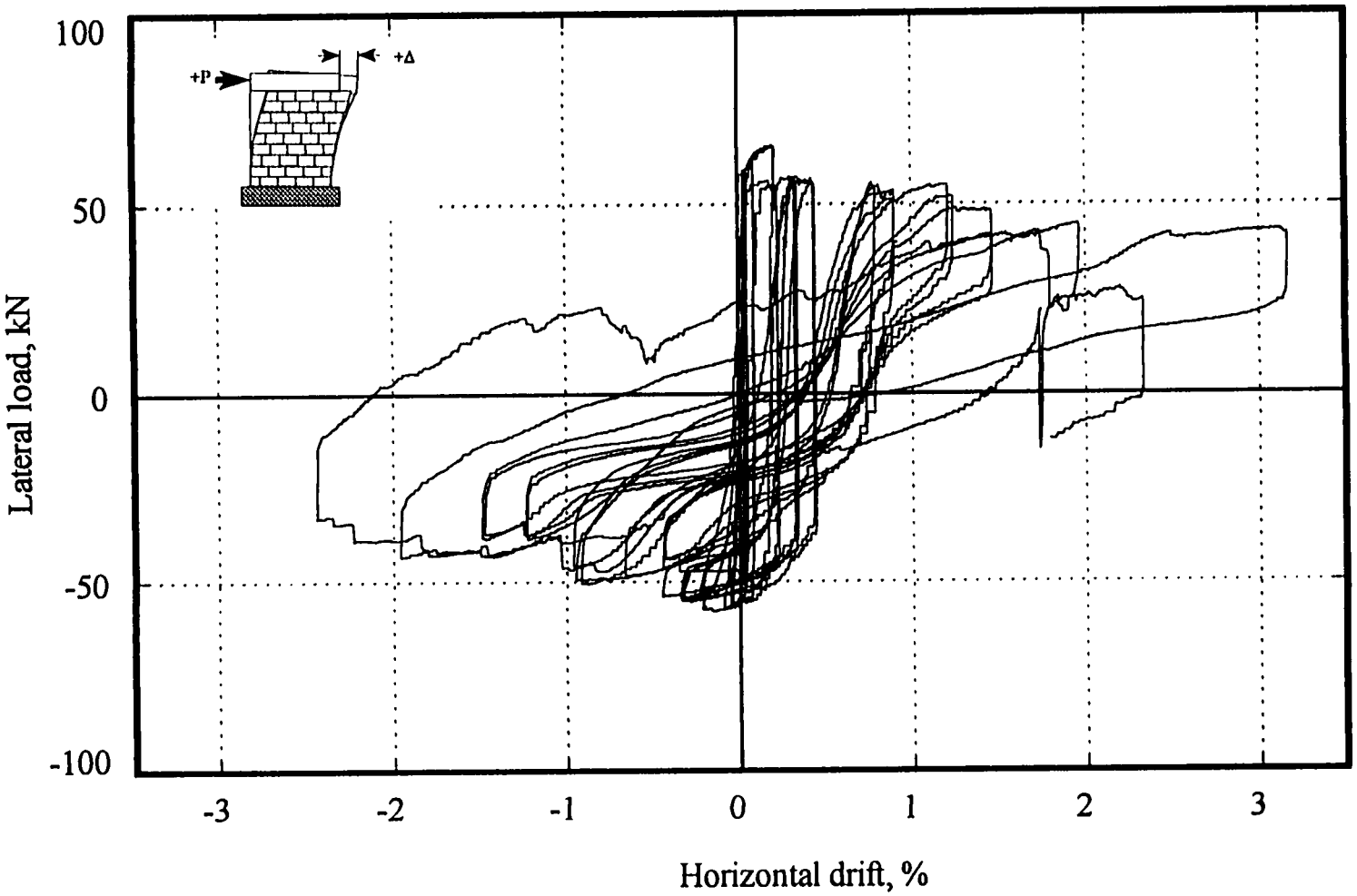

Figure 4.1 Hysteretic lateral load-displacement of Wall 9

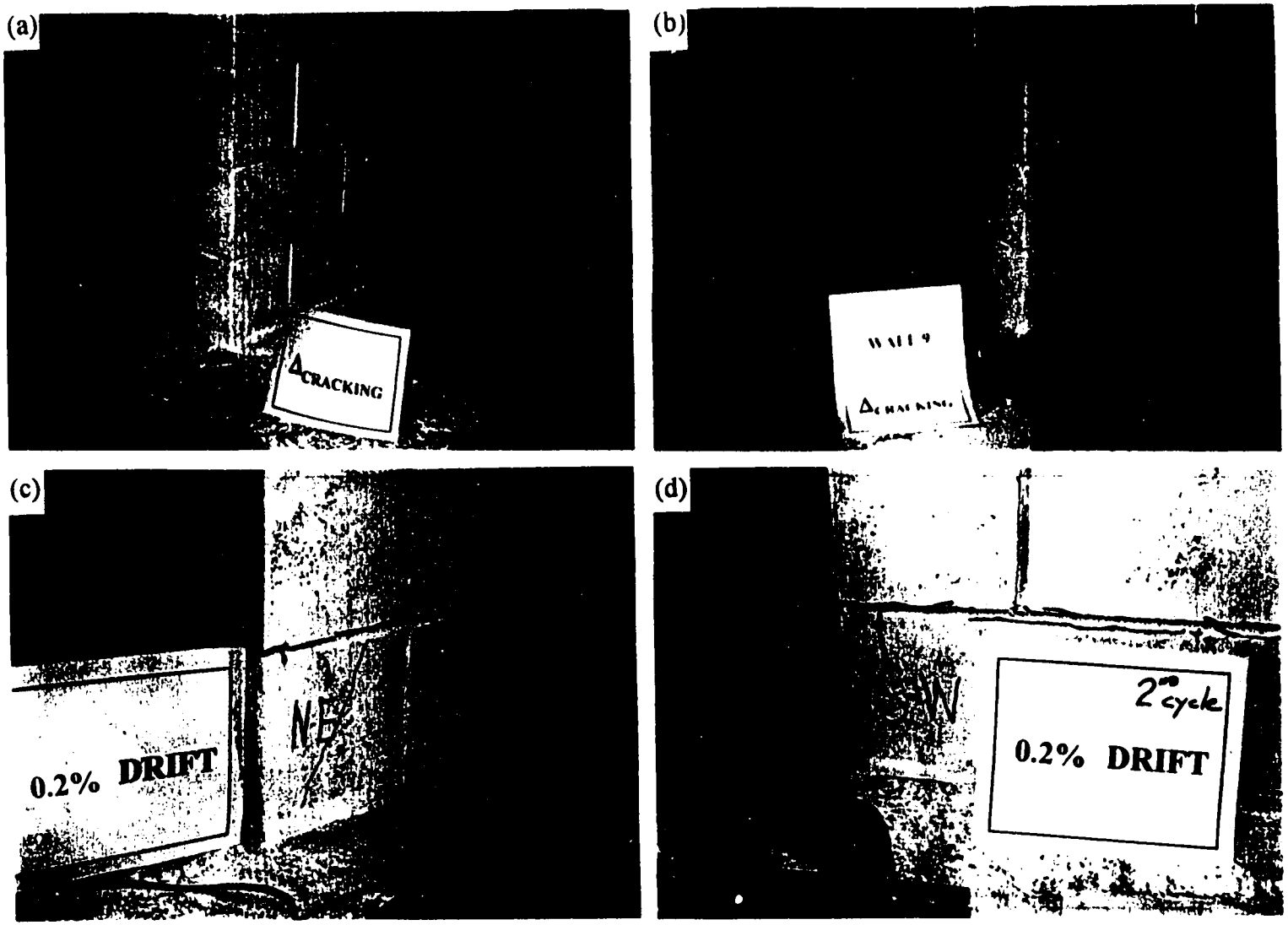

Figure 4.2 Wall 9 (URM) During testing: (a) First cracking at 57 kN (East End).(b) First cracking at -51 kN (west end). (c) Diagonal crack in corner block due to block compression during rocking about east end. (d)Vertical crack in corner block due to block compression at 0.2% drift (west end).

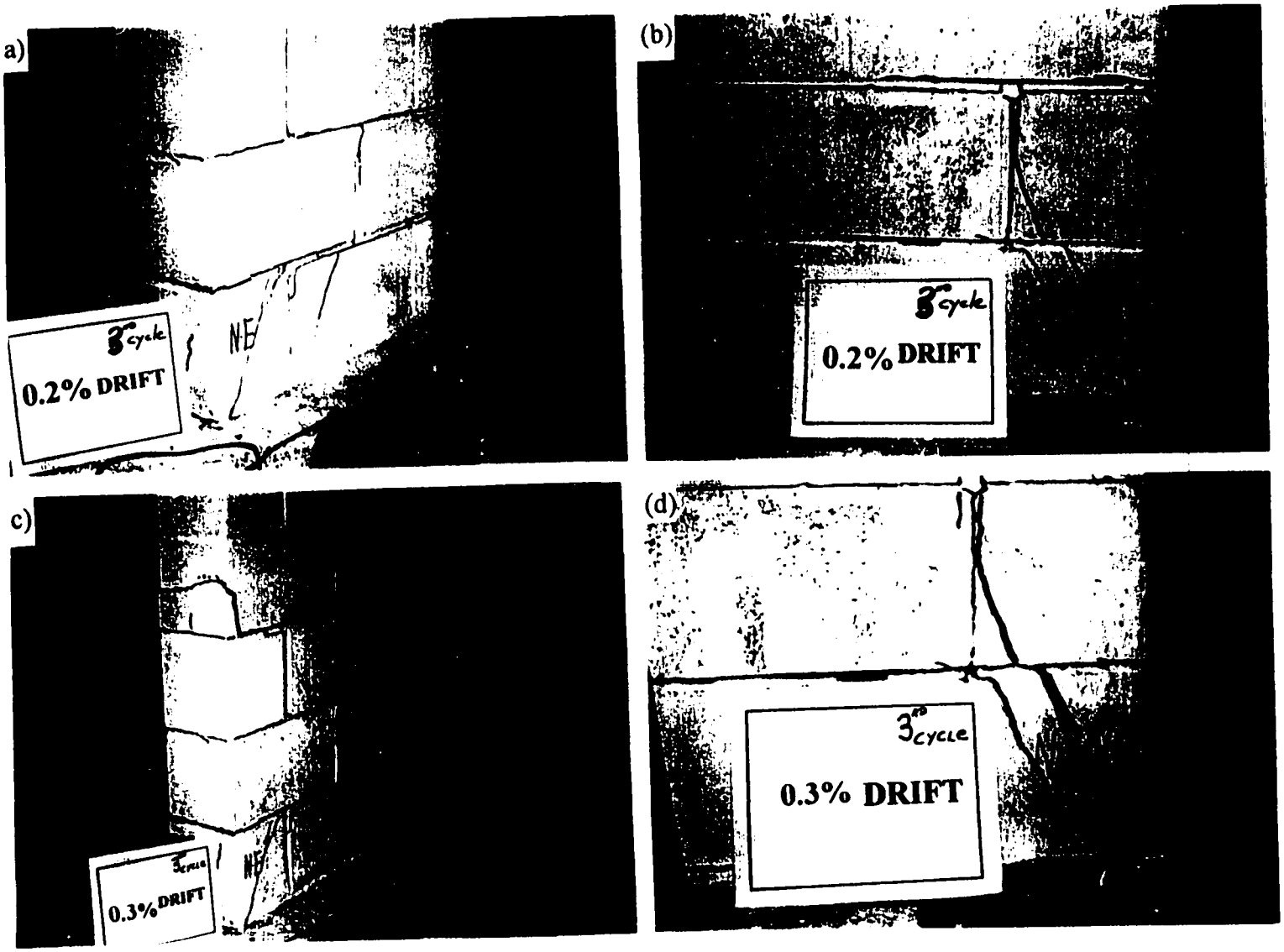

Figure 4.3 Wall 9 (URM) During testing: (a) Cracking propagation to the second and third level and some diagonal cracks at the 3rd cycle of 0.2% drift (east end). (b) Diagonal cracking of corner block at the west end. (c) Cracking propagation to the fourth bed joint at the 3rd cycle of 0.3% drift (east end). (d) Severe diagonal cracks at 0.3% (west end).

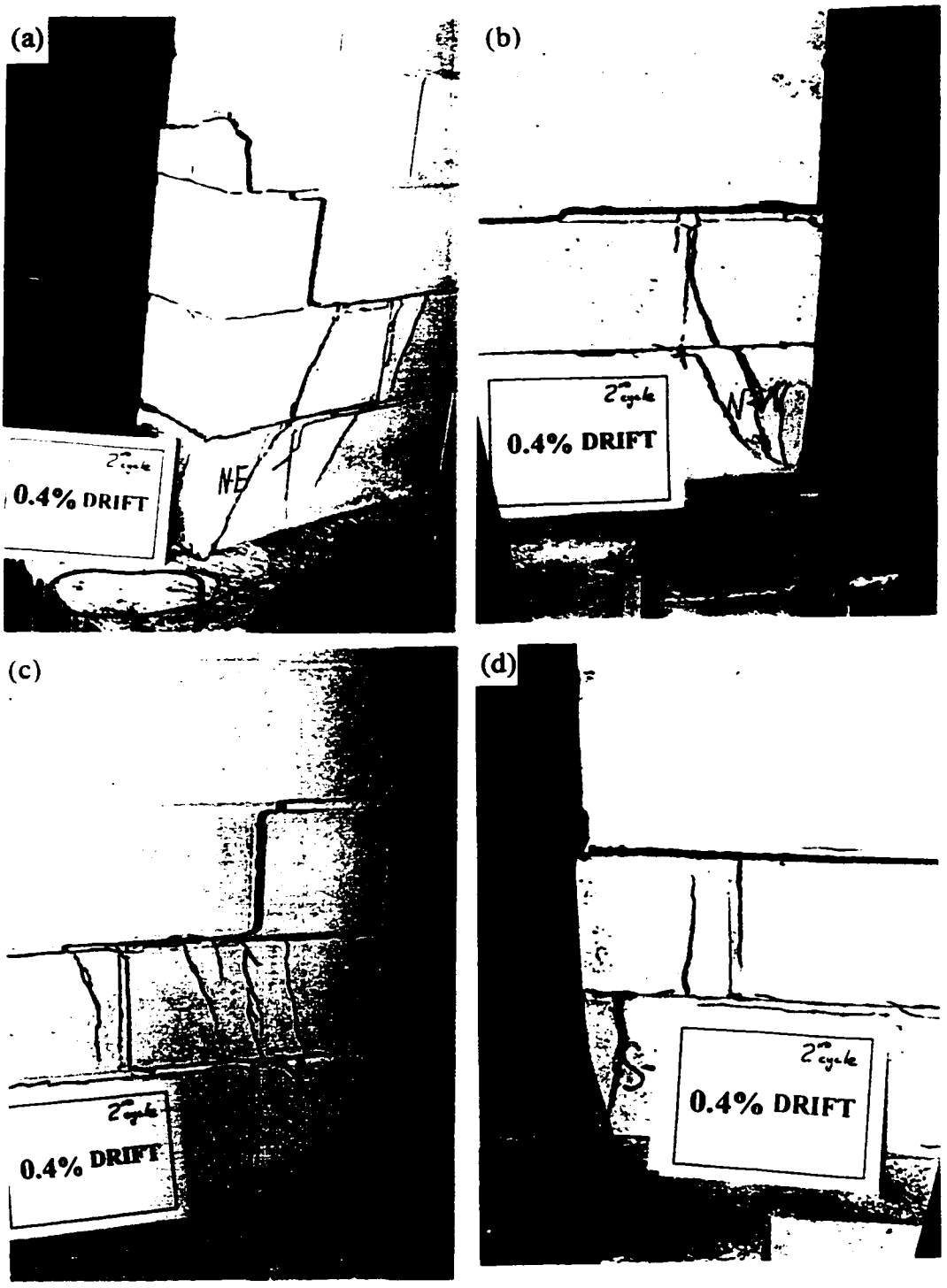

Figure 4.4 Wall 9 (URM) At 0.4% Drift: (a) N-E side. (b) N-W side. (c) S-E side. (d) S-W side.

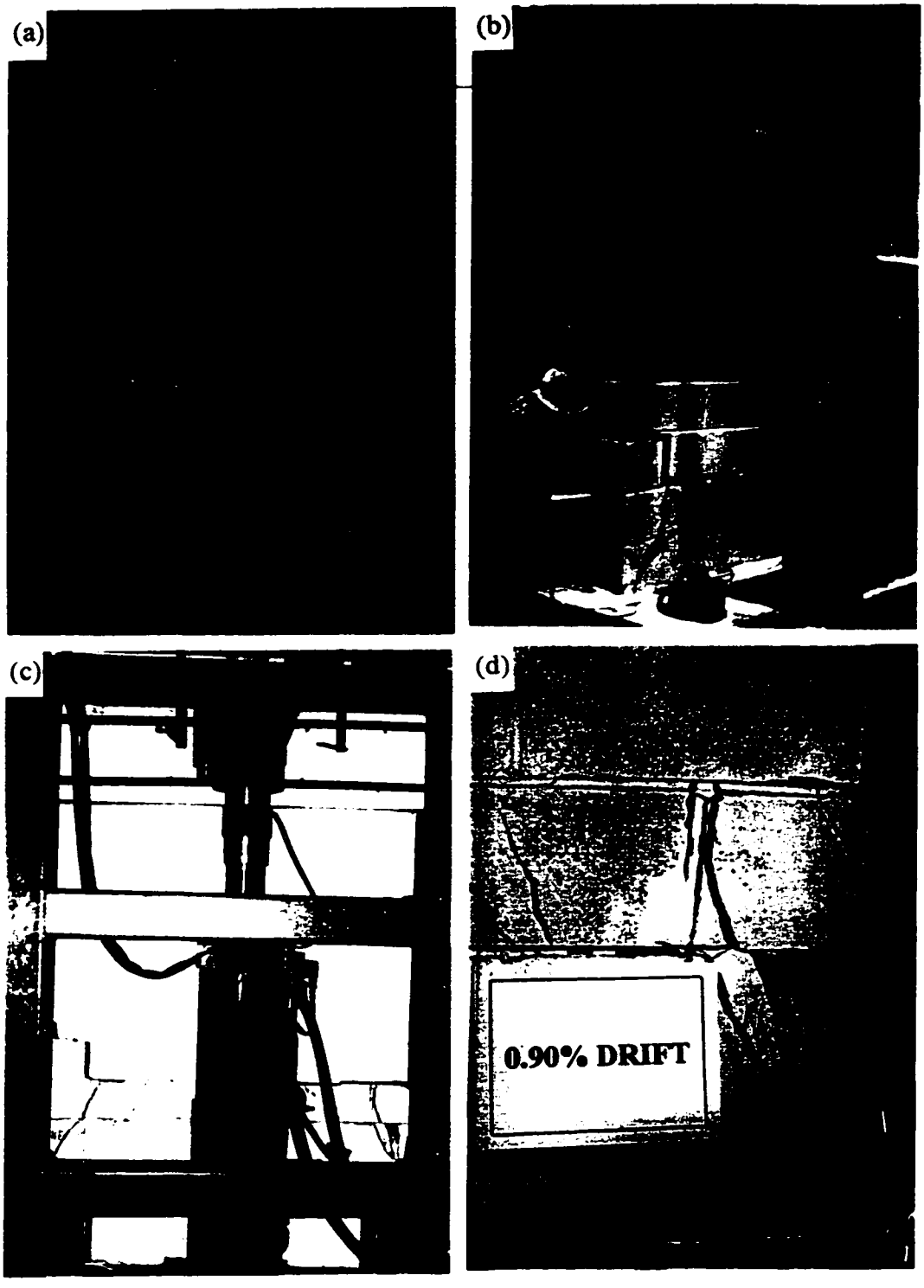

Figure 4.5 Wall 9 At higher drifts. (a) Large vertical crack due to sliding, and diagonal cracks at 0.8% drift. (b) Global view; Wall started to spall. (c) Unsymmetrical behaviour of URM; sliding westward and rocking in eastward. (d) Close-up view of crushing of blocks due to rocking.

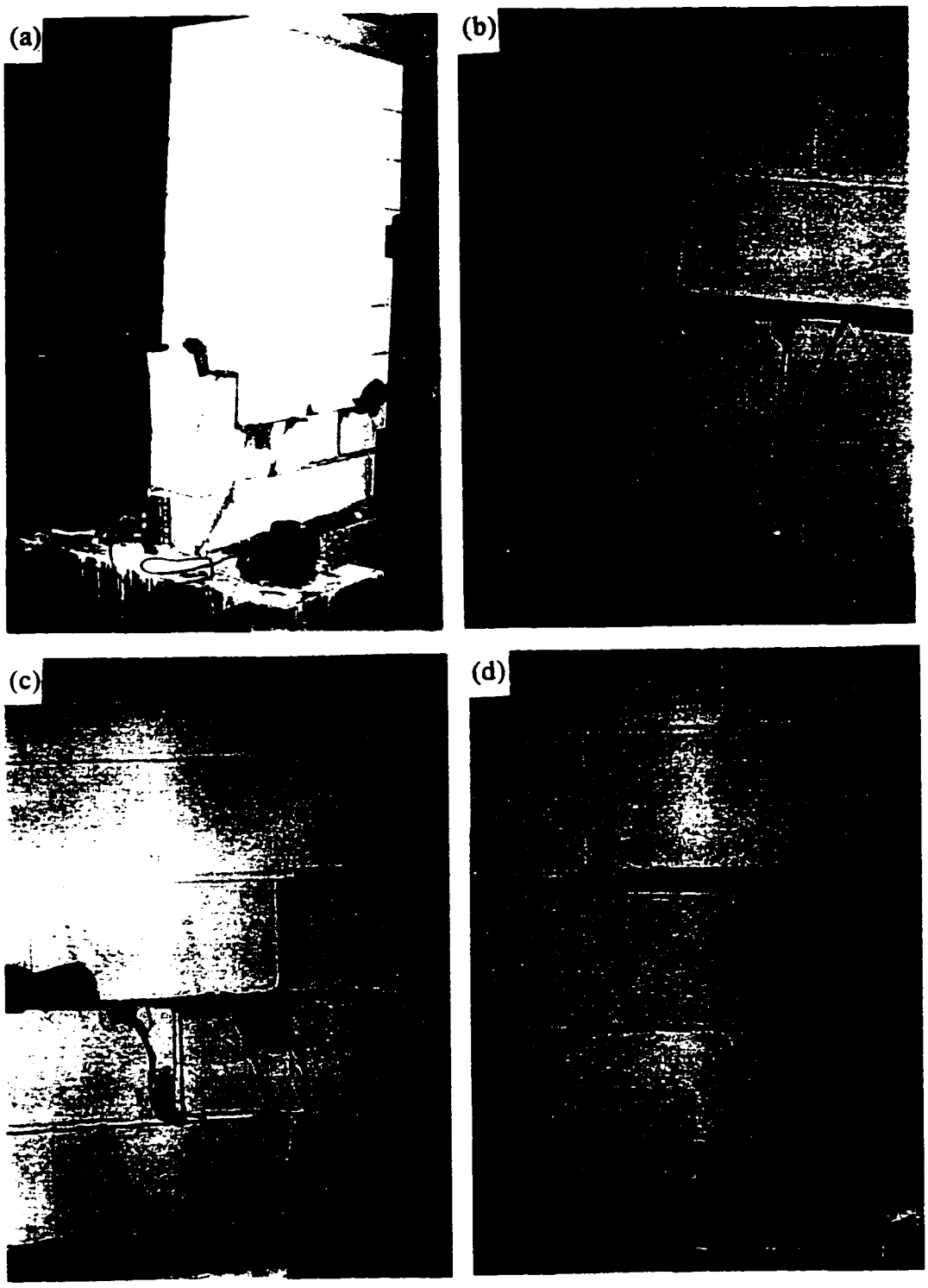

Figure 4.6 Severe damage to Wall 9: (a) Destroyed horizontal bed joint above the second row of blocks. (b) North east corner at 2.0% Drift. (c) Rocking at 2.0% drift. (d) Rocking behaviour near the end of the test, at 2.0% drift.

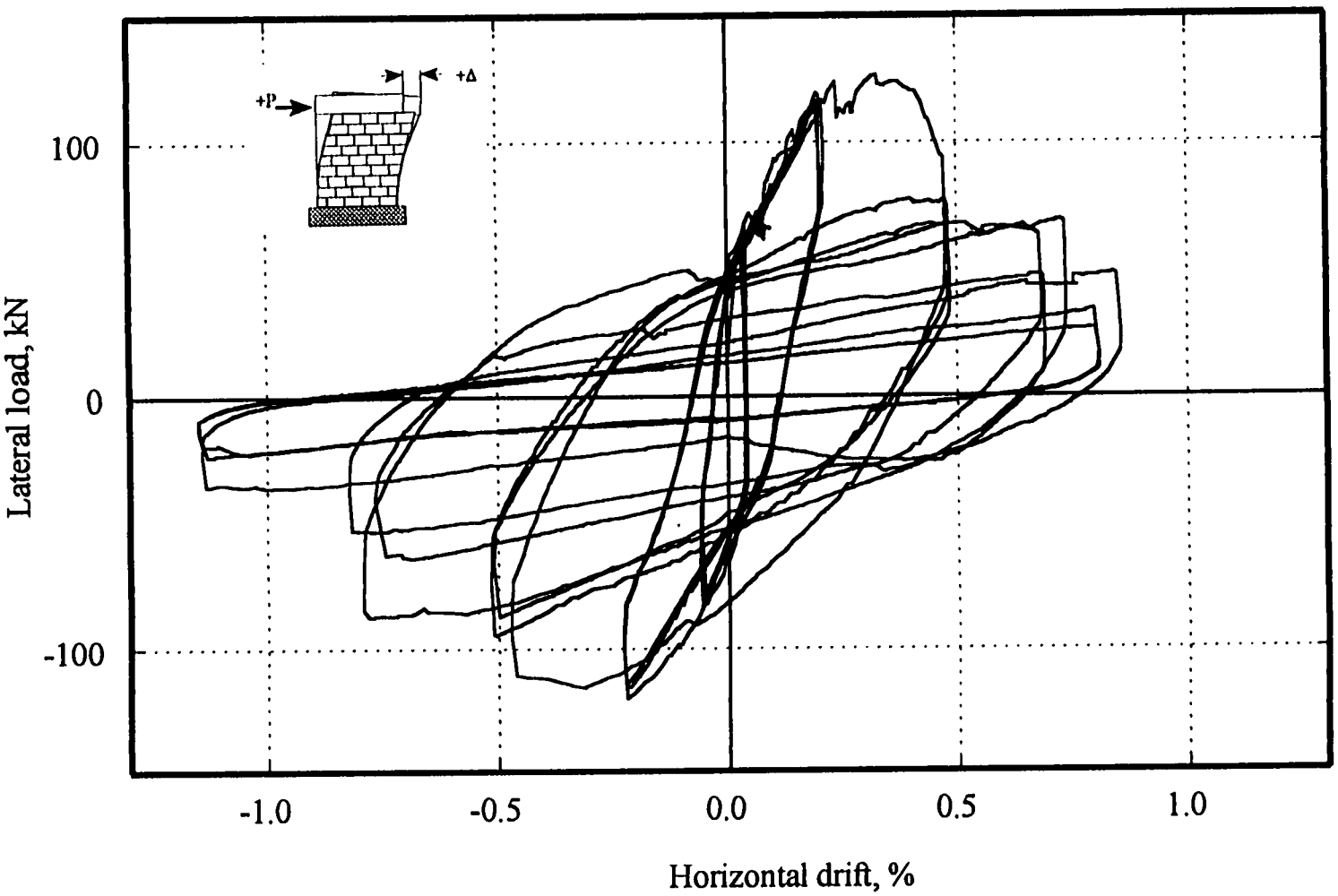

Figure 4.7 Hysteretic lateral load-displacement of Wall 10

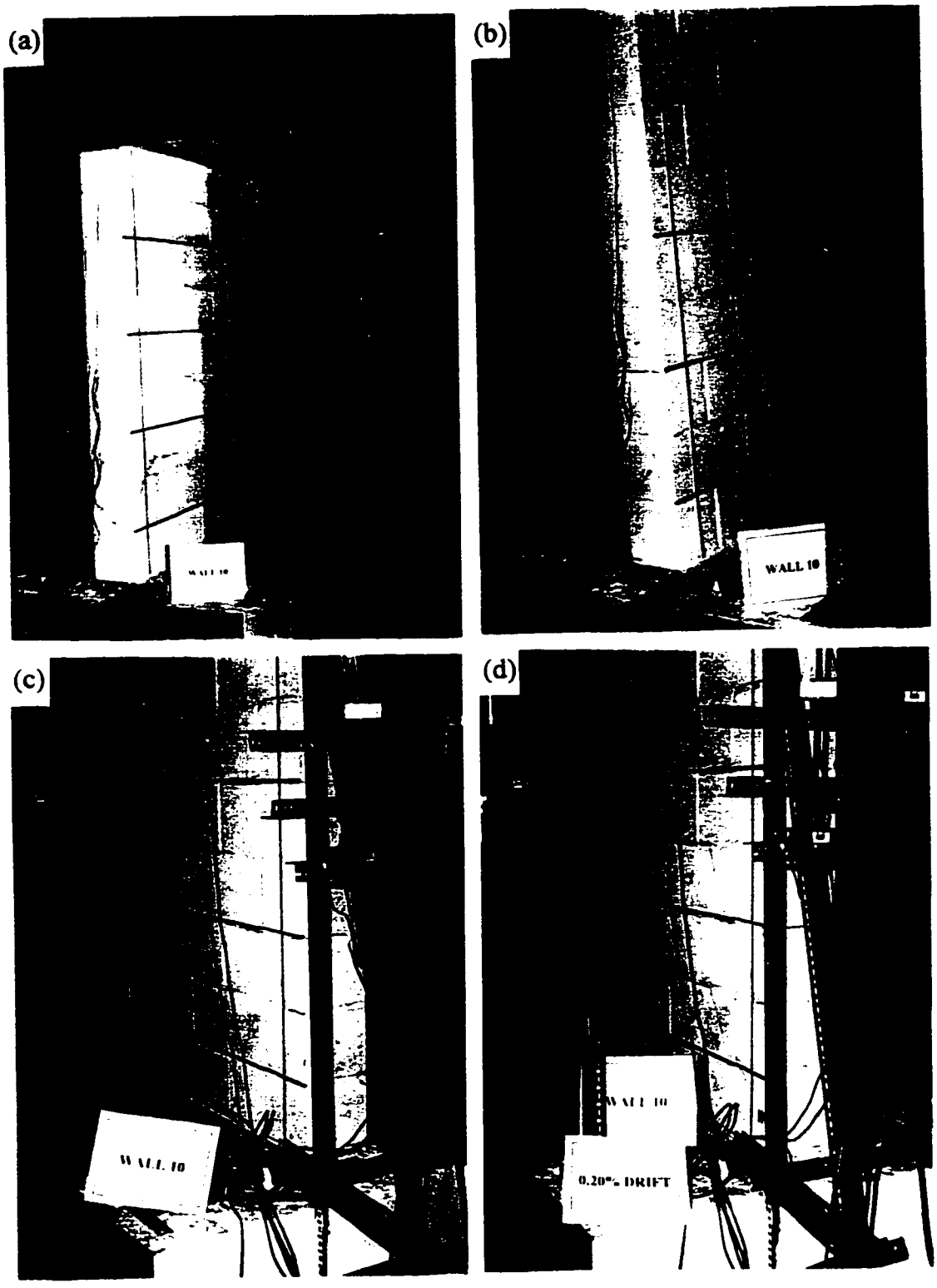

Figure 4.8 Wall 10 PRM: (a) At beginning of the test. (b) First diagonal tension crack east end. (c) First diagonal tension crack west end. (d) Shear cracking at 0.2% drift (west view).

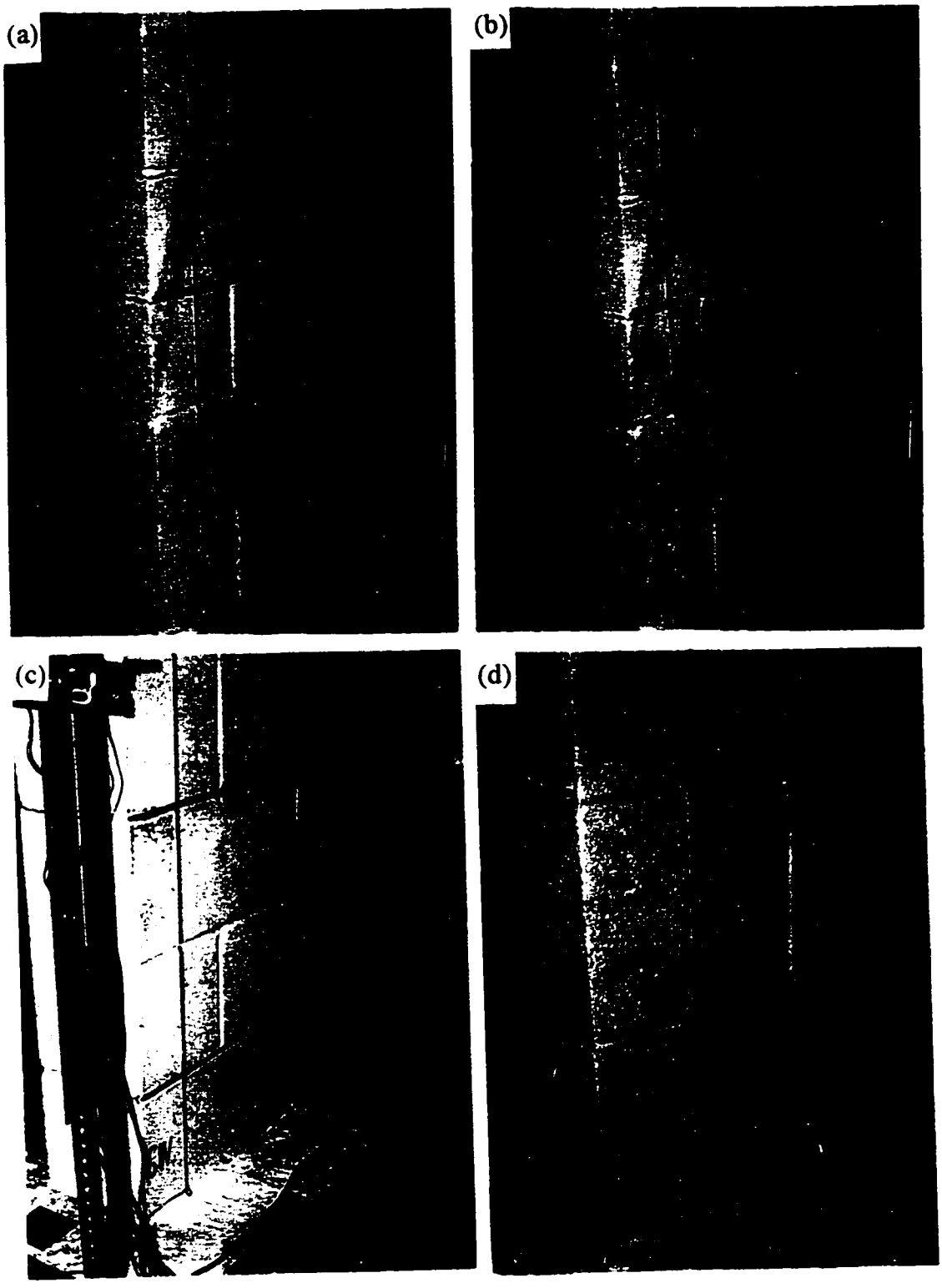

Figure 4.9 Wall 10 PRM: (a) Stair-step cracking and first diagonal through block cracking (east end). (b) Propagation of diagonal cracks through block (east end). (c) Diagonal cracks at west end. (d) Initial crushing of the west end.

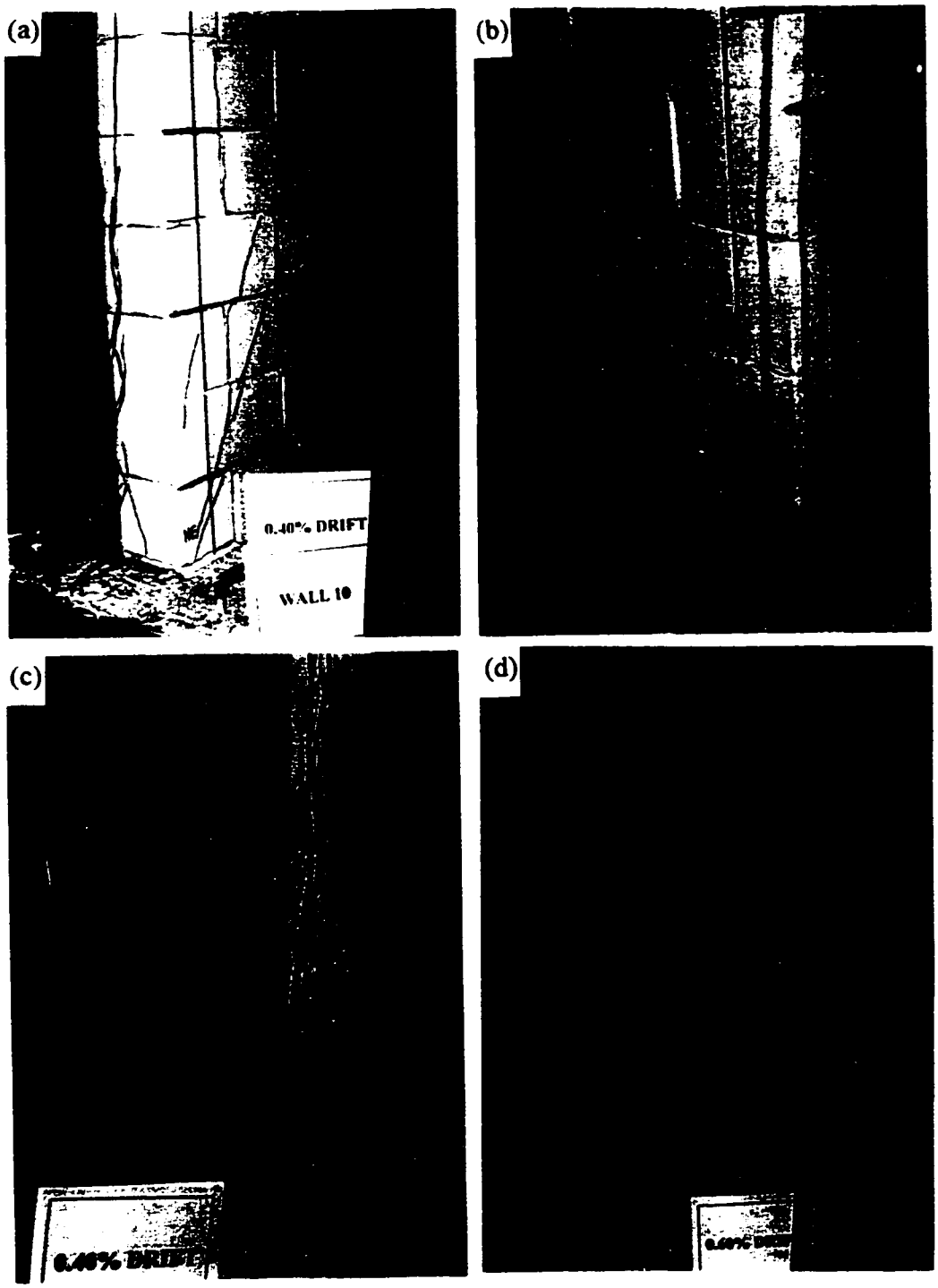

Figure 4.10 Wall 10 PRM: (a) At 0.4% drift (east end). (b) At 0.4% drift (west end), crushed mortar and masonry at the first and second level of blocks. (c) At 0.4% drift (S-E view). (d) At 0.6% drift (west end), crushing between third and fourth rows of blocks.

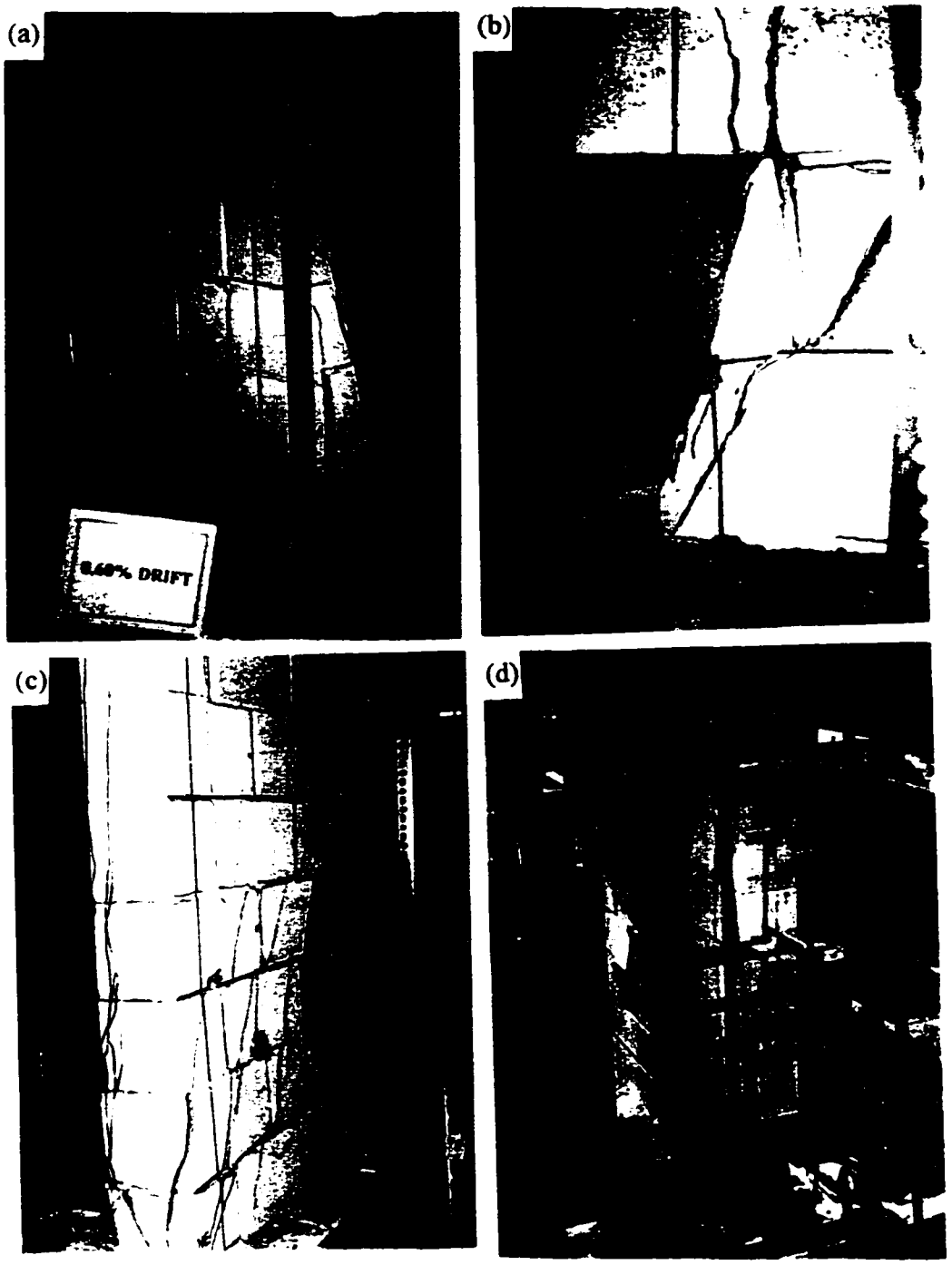

Figure 4.11 Wall 10 PRM: (a) Severe crushing at 0.8% drift. (west end). (b) Crushed mortar and re-bar buckling, on west side. (c) Crushing along third and fourth courses and vertical splitting of infilled cells on east side. (d) Global view near the end of the test.

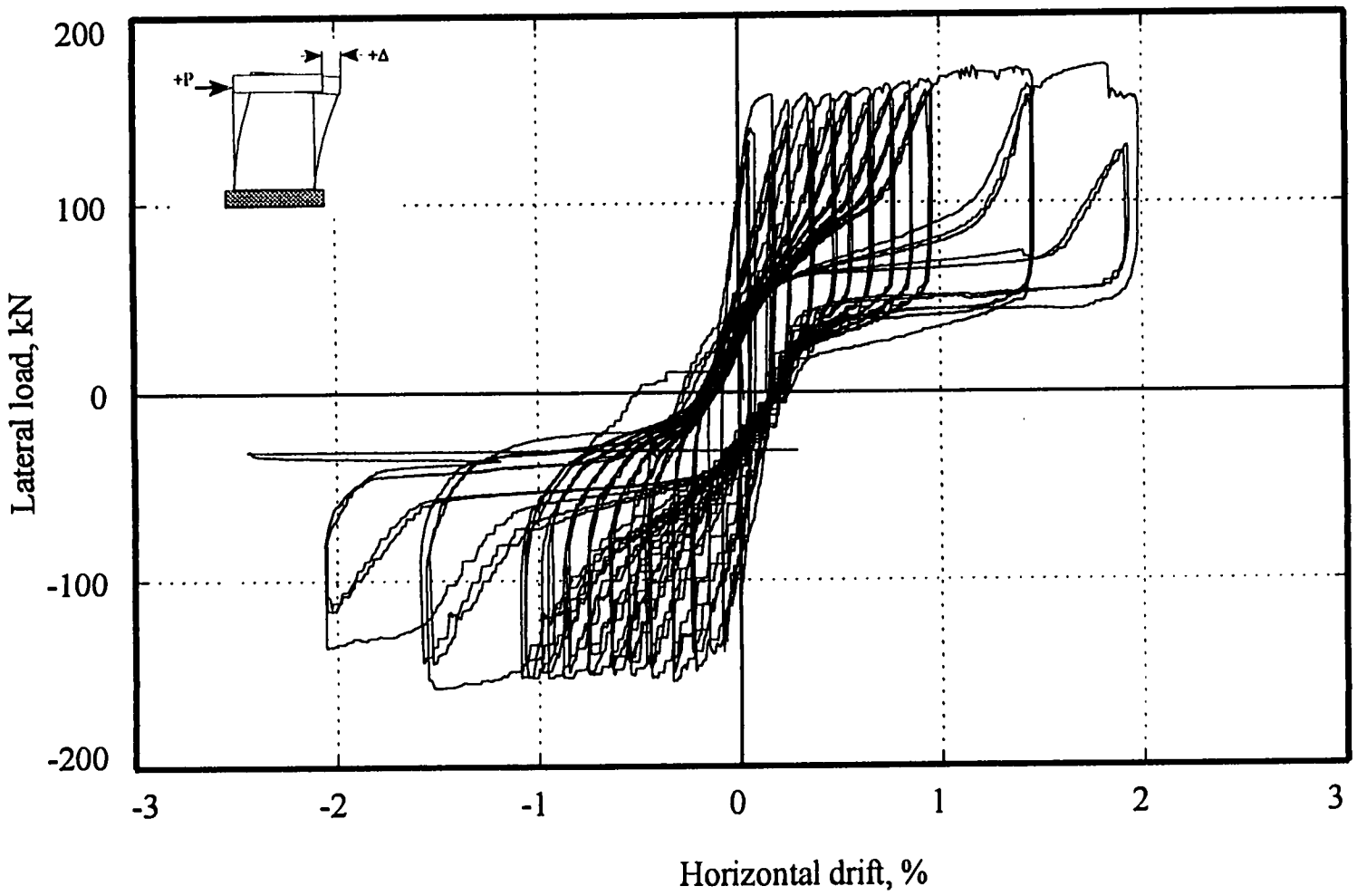

Figure 4.12 Hysteretic lateral load-displacement of Wall 11

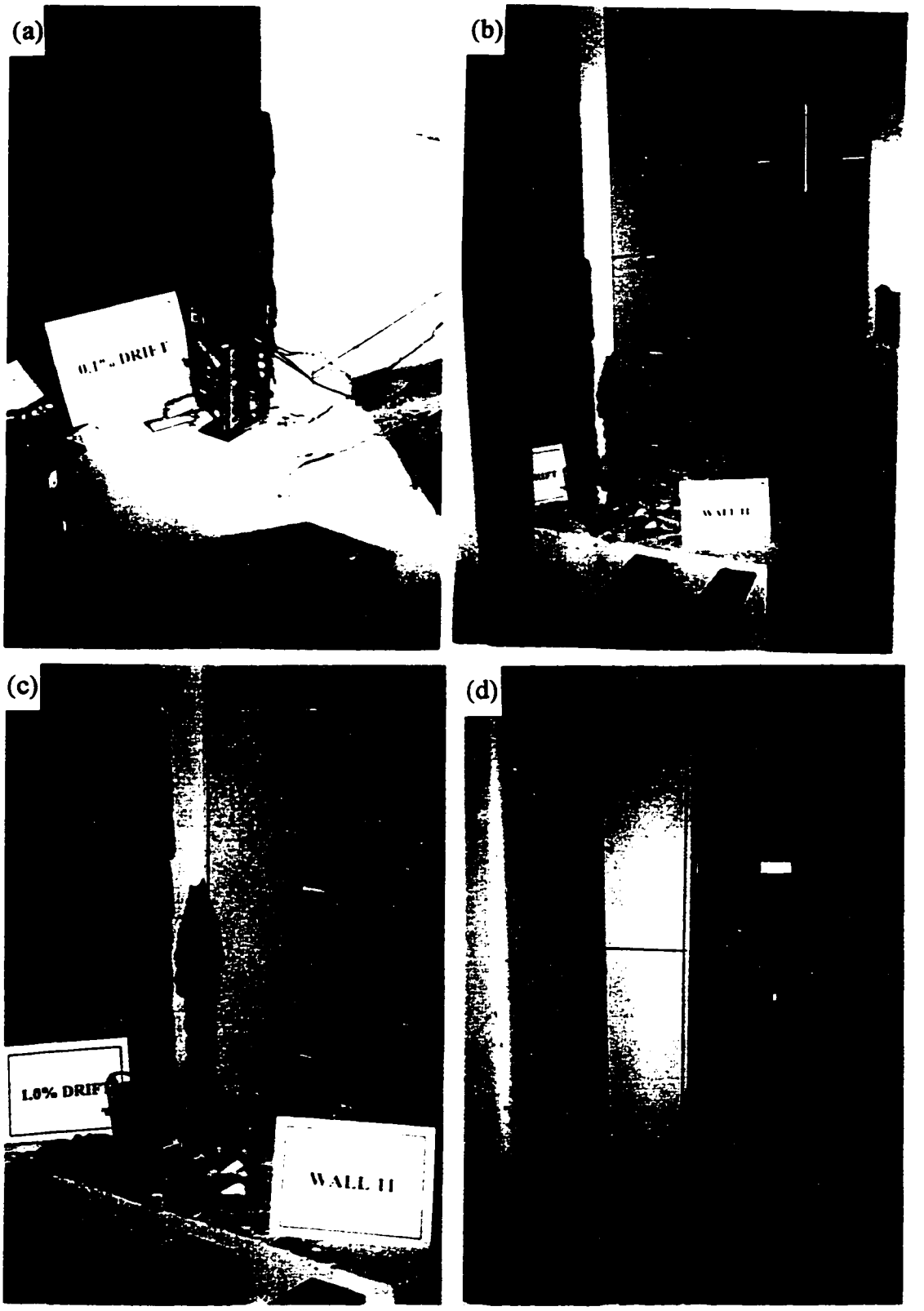

Figure 4.13 Wall 11 RC: (a) Horizontal flexural crack along wall length and buckling of end re-bar at east end, at 0.1% drift. (b) Spalled cover concrete and re-bar buckling, east corner at 0.8% drift. (c) At 1.0% drift (east view). (d) Buckled bars at west end at 1.0% drift.

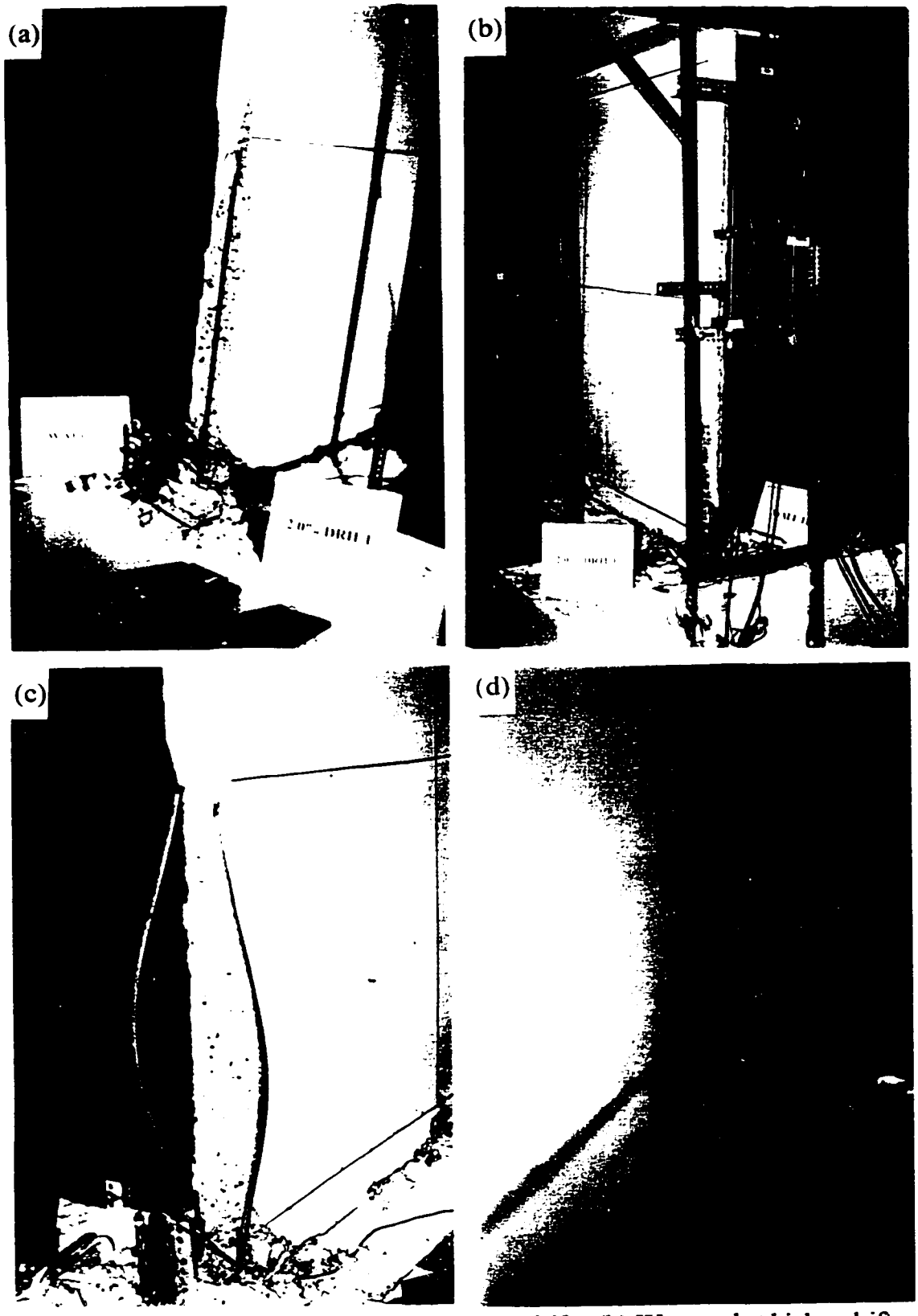

Figure 4.14 Wall 11 (a) East end at higher drifts. (b) West end at higher drifts. (c) Severe elastic buckling of end re-bars. (d) Rupture of vertical re-bars at the wall center.

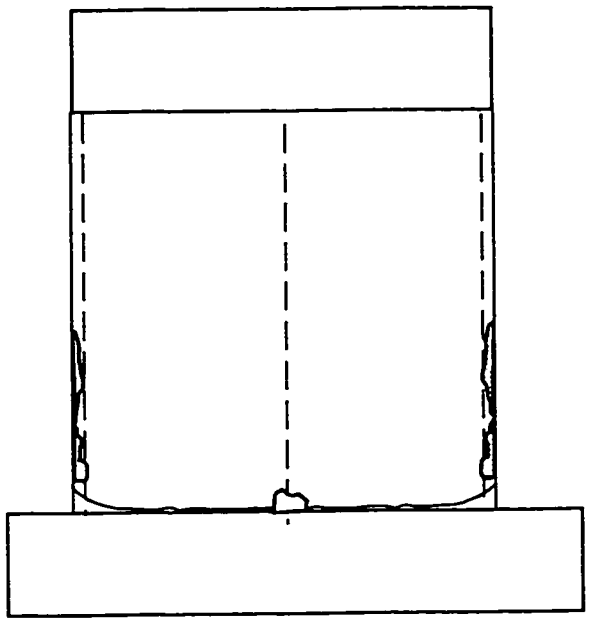

Figure 4.15 Schematic of cracking in Wall 11 (rocking path)

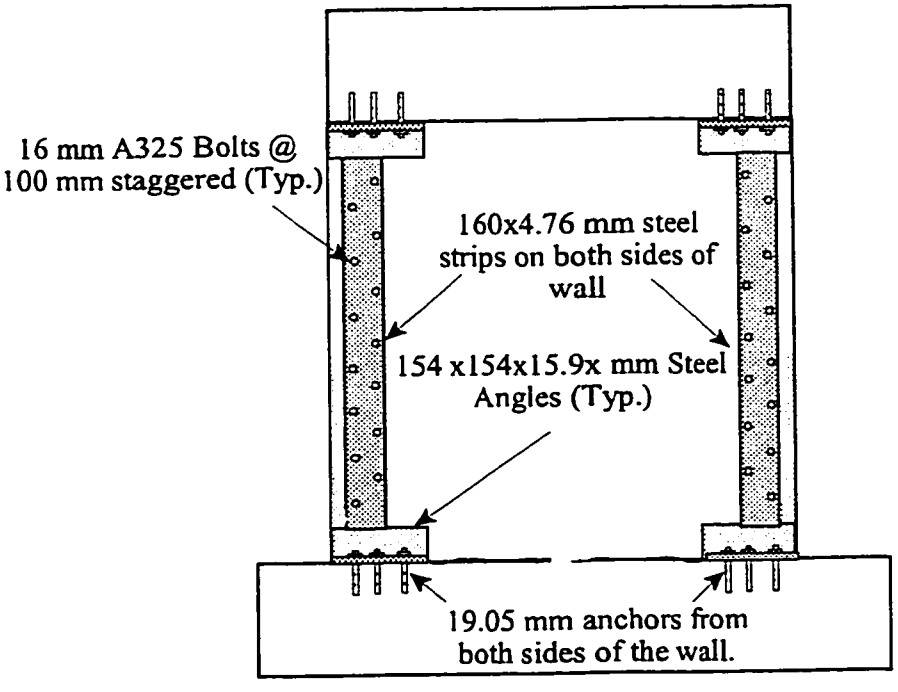

Figure 4.16 Layout of Wall 11RP

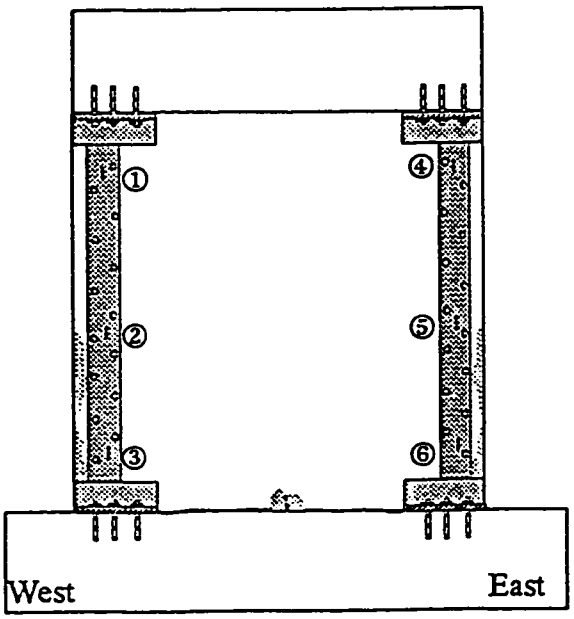

Figure 4.17 Strain gauge locations on steel strips of repaired wall (Wall 11RP)

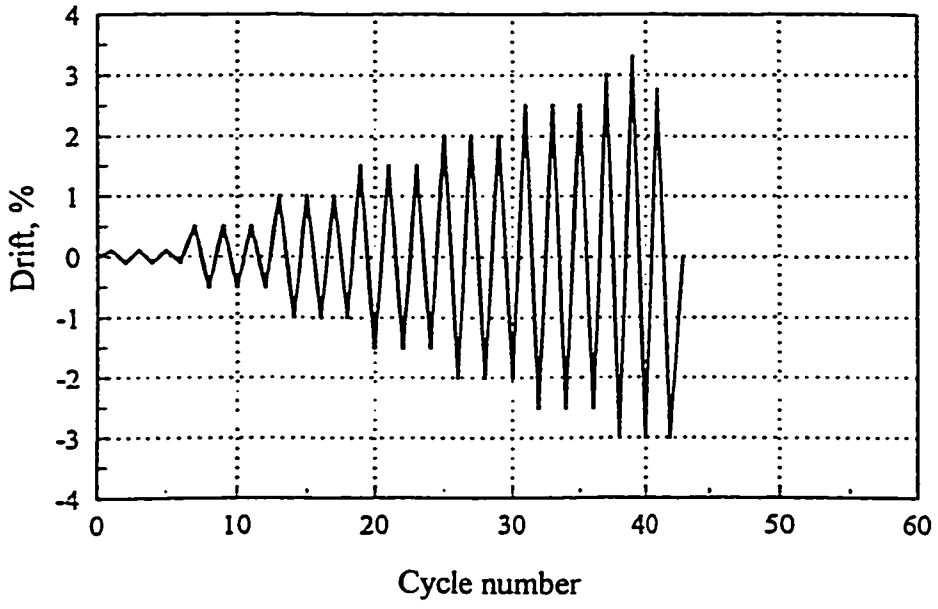

Figure 4.18 Displacement history of Wall 11RP

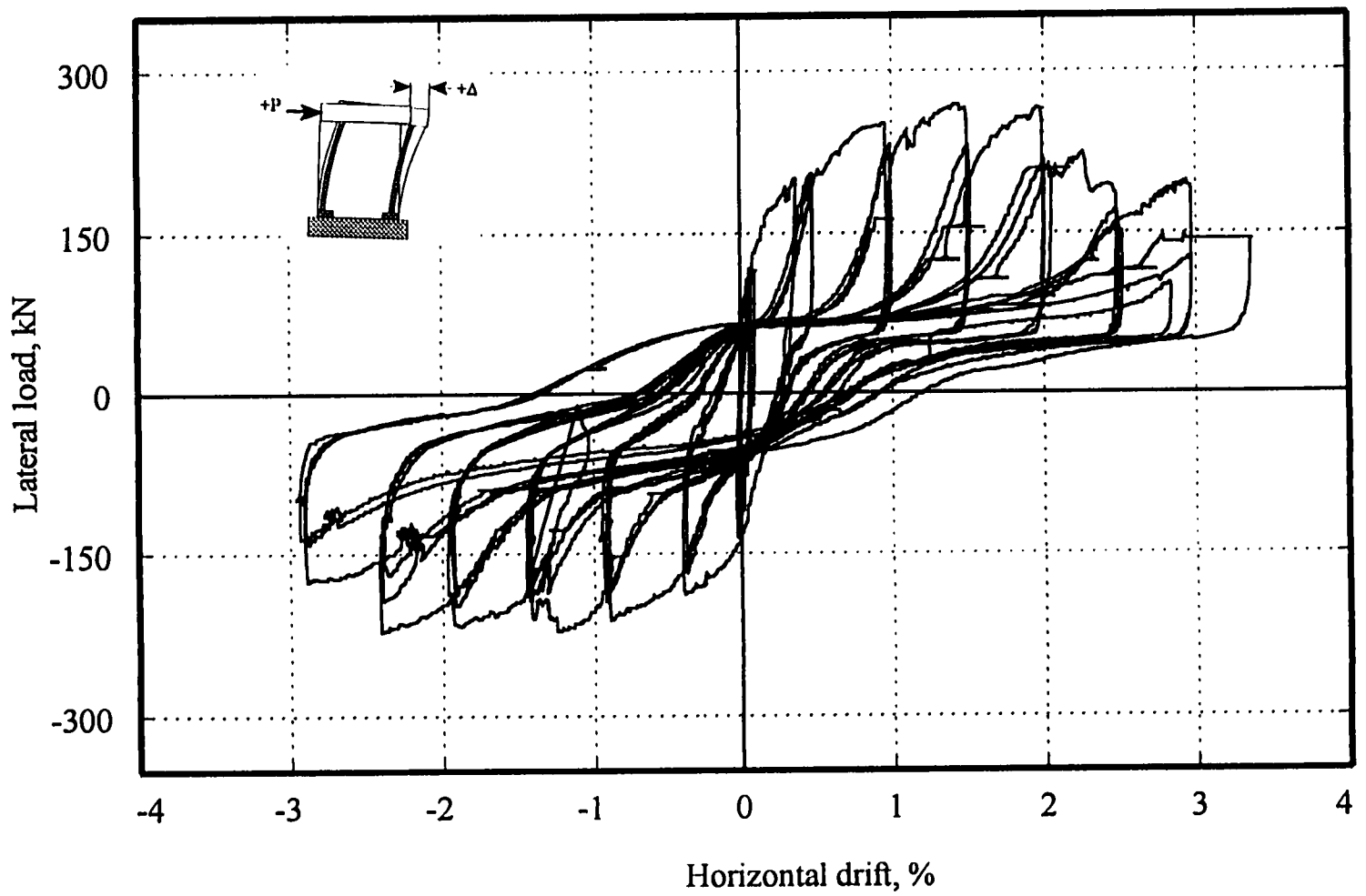

Figure 4.19 Hysteretic lateral load-displacement of Wall 11RP

Figure 4.20 Wall 11RP at 0.5% drift: (a) Rocking of angles at wall base and vertical cracking along the narrow face. (b) Angle rocking at the top. (c) Global view, east side. (d) West side.

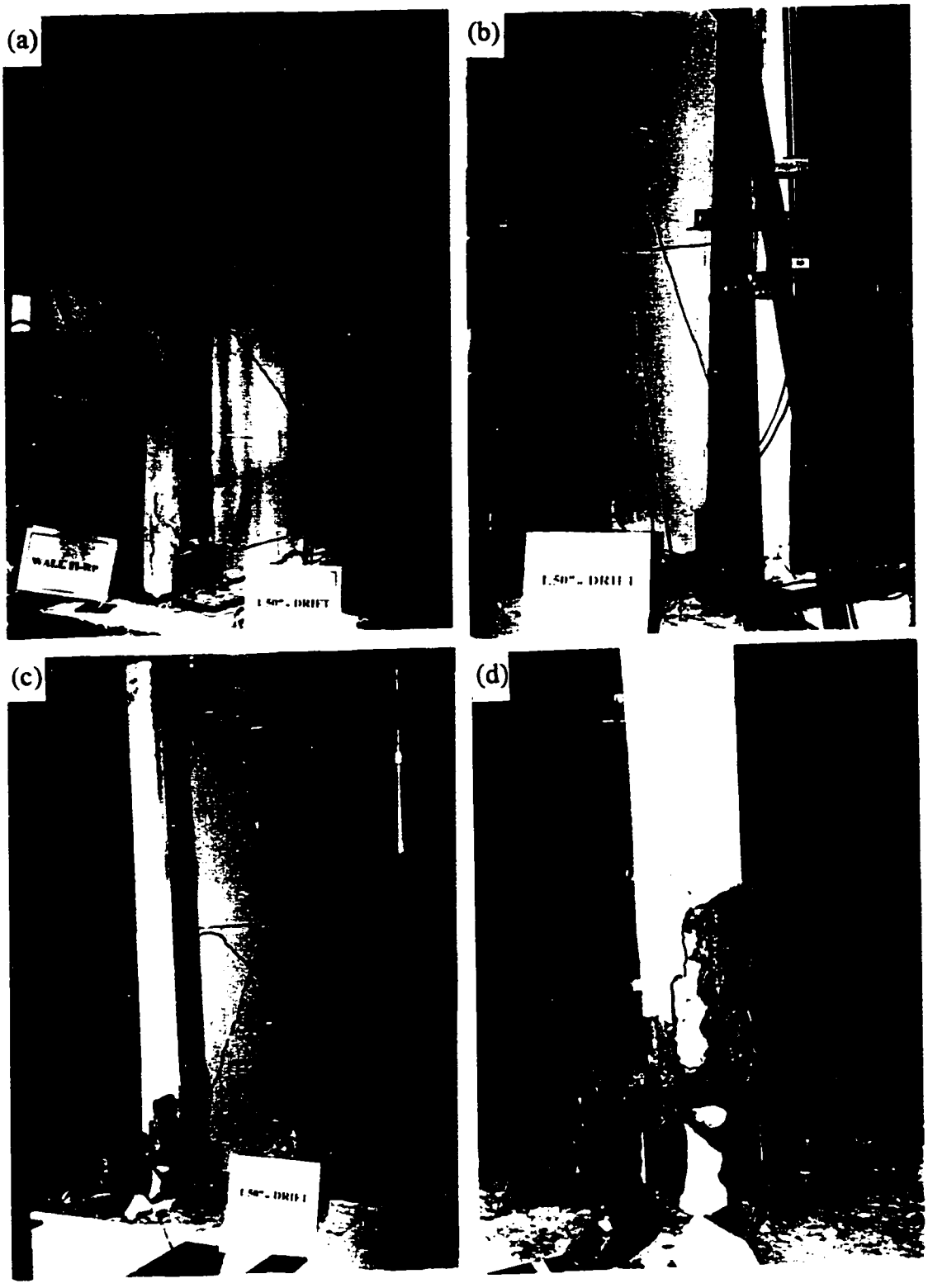

Figure 4.21 Wall 11RP: (a) First diagonal cracking at 1.5% drift. (east view). (b) First diagonal cracking at 1.5% drift (west view). (c) Diagonal tension cracks in both directions. (d) Buckling of steel strip at the NE side.

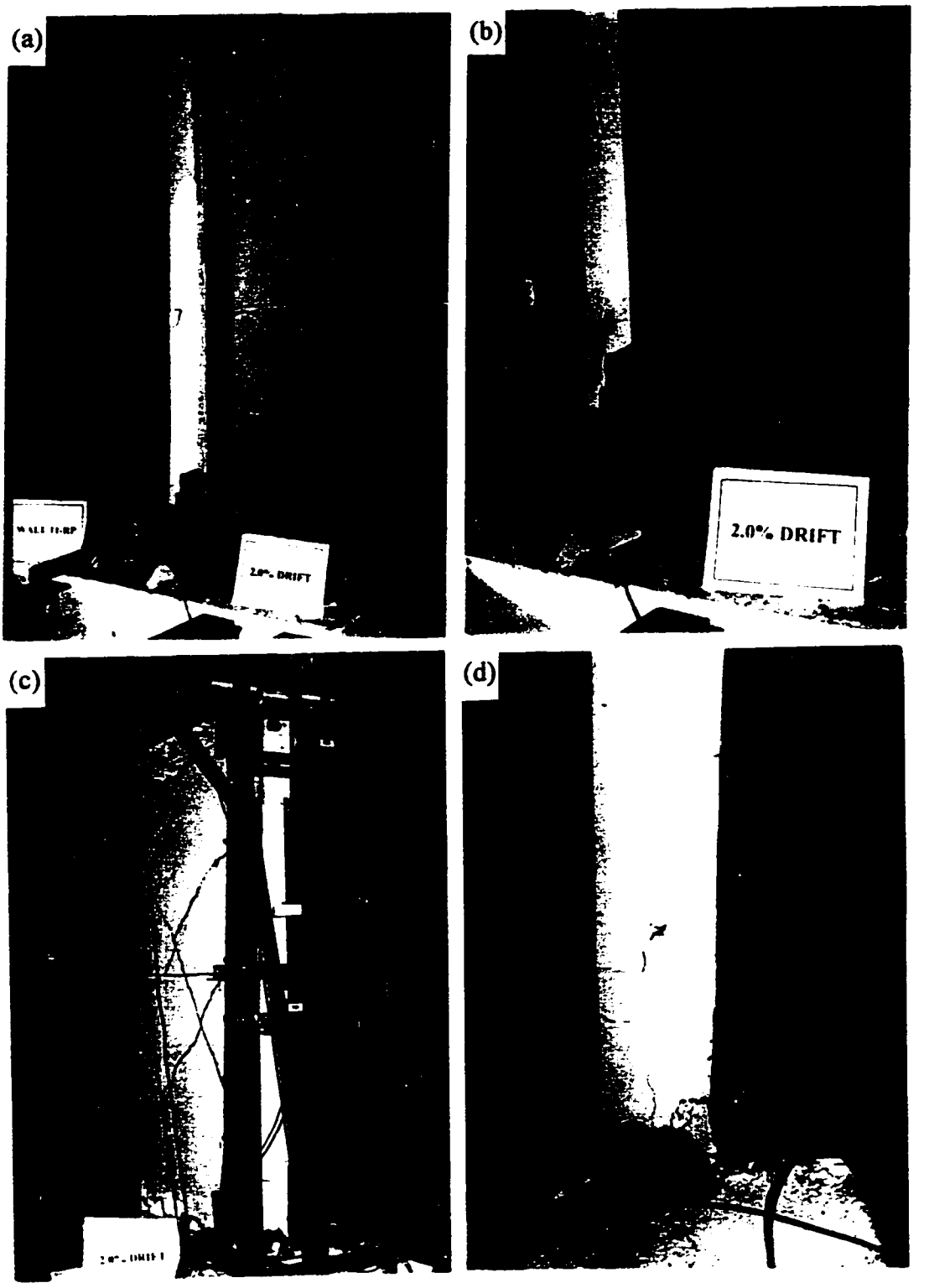

Figure 4.22 Wall 11RP at 2.0% drift: (a) Global view. (b) Close-up view of the NE corner (c) West view. (d) Buckling of steel strip.

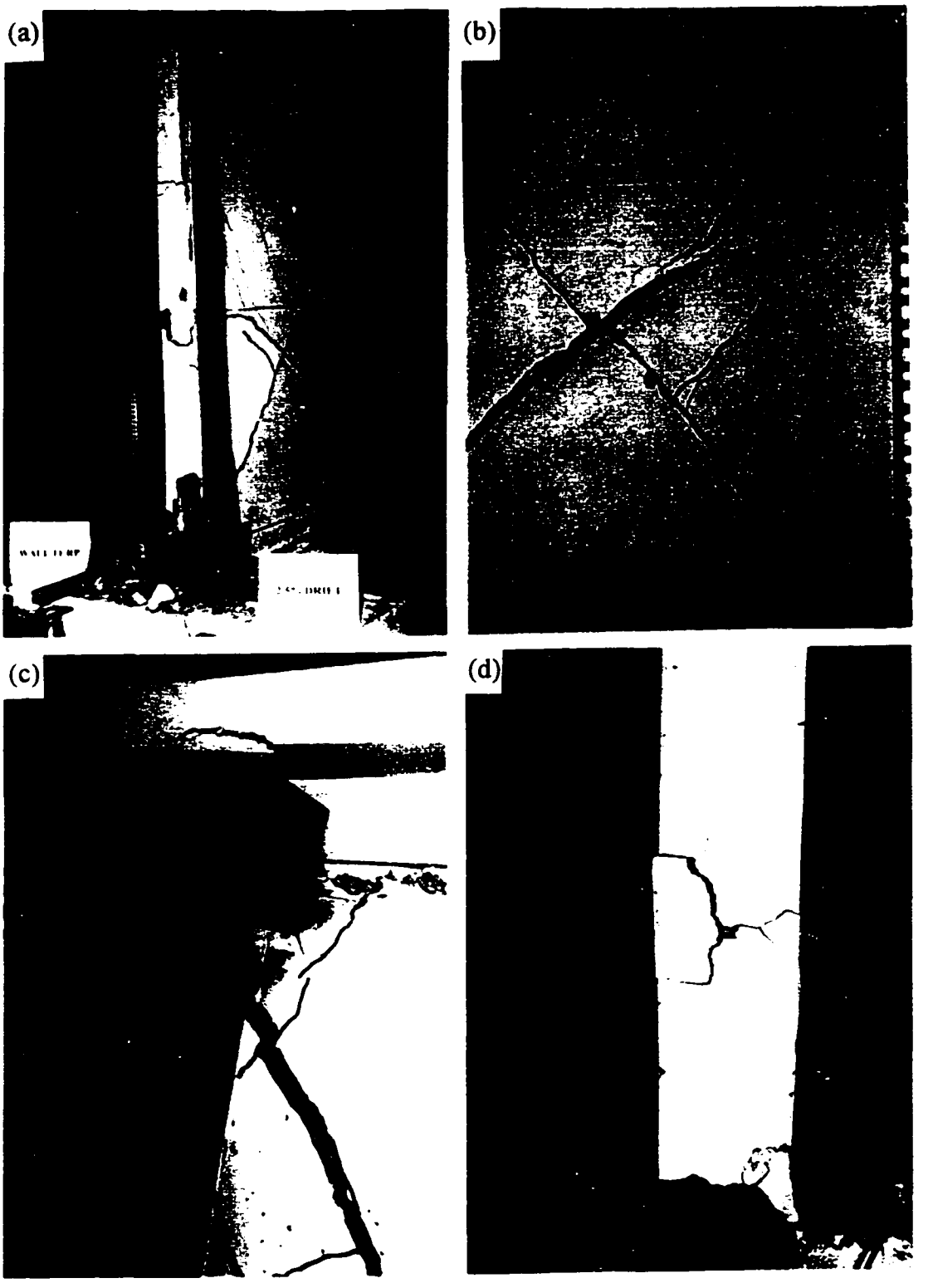

Figure 4.23 Wall 11RP at 2.5% drift: (a) More than 12 mm wide diagonal crack (east view). (b) Close-up view of large diagonal crack. (c) Concrete damage due to anchor pullout. (d) Severe buckling of steel strip.

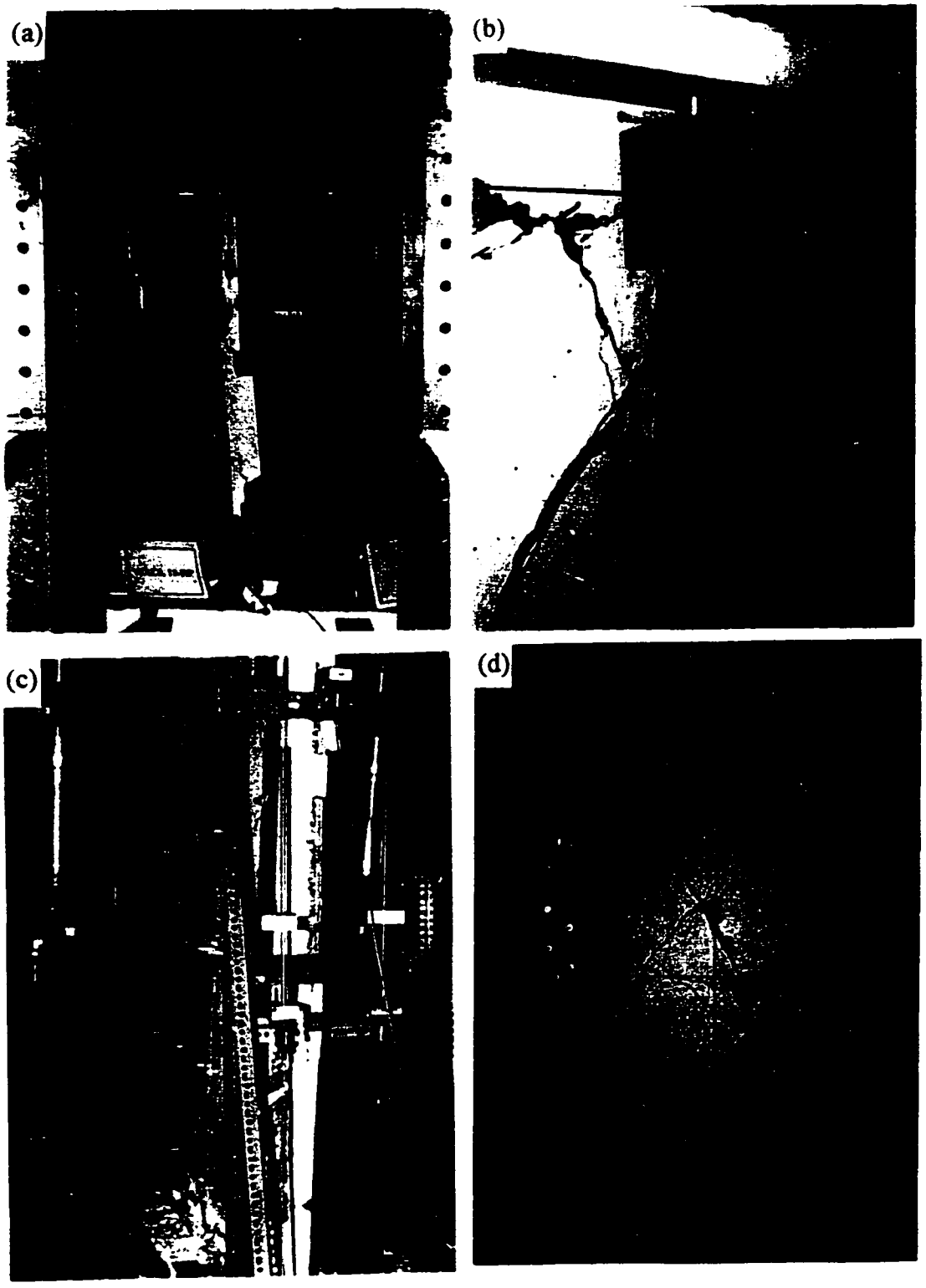

Figure 4.24 Wall 11RP: (a) Twisting of the wall at 3% drift. (b) Severe anchor pullout from the top beam. (c) Twisted wall near the end of the test (west view). (d) Damaged wall after testing.

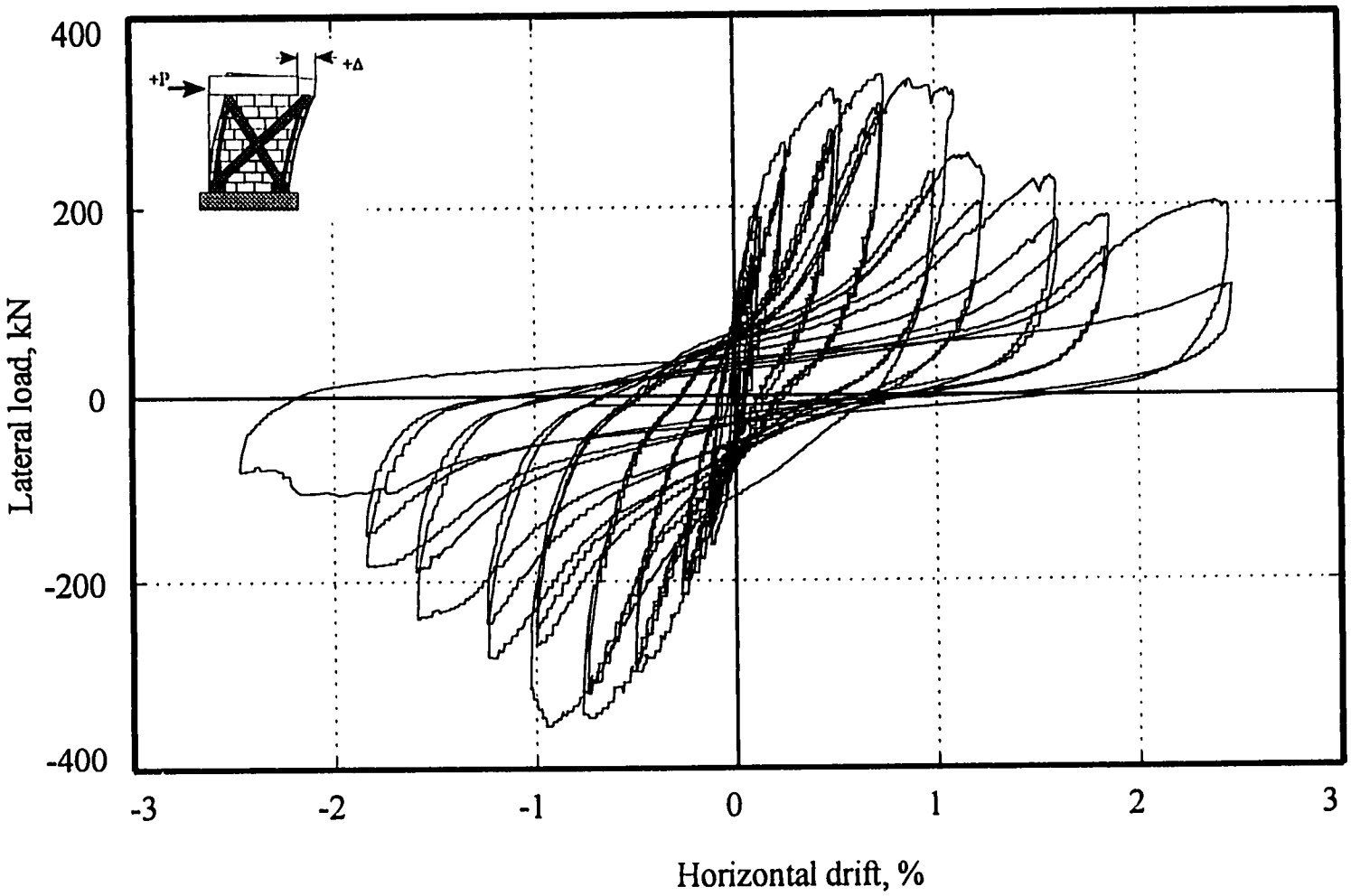

Figure 4.25 Hysteretic lateral load-displacement of Wall 9R

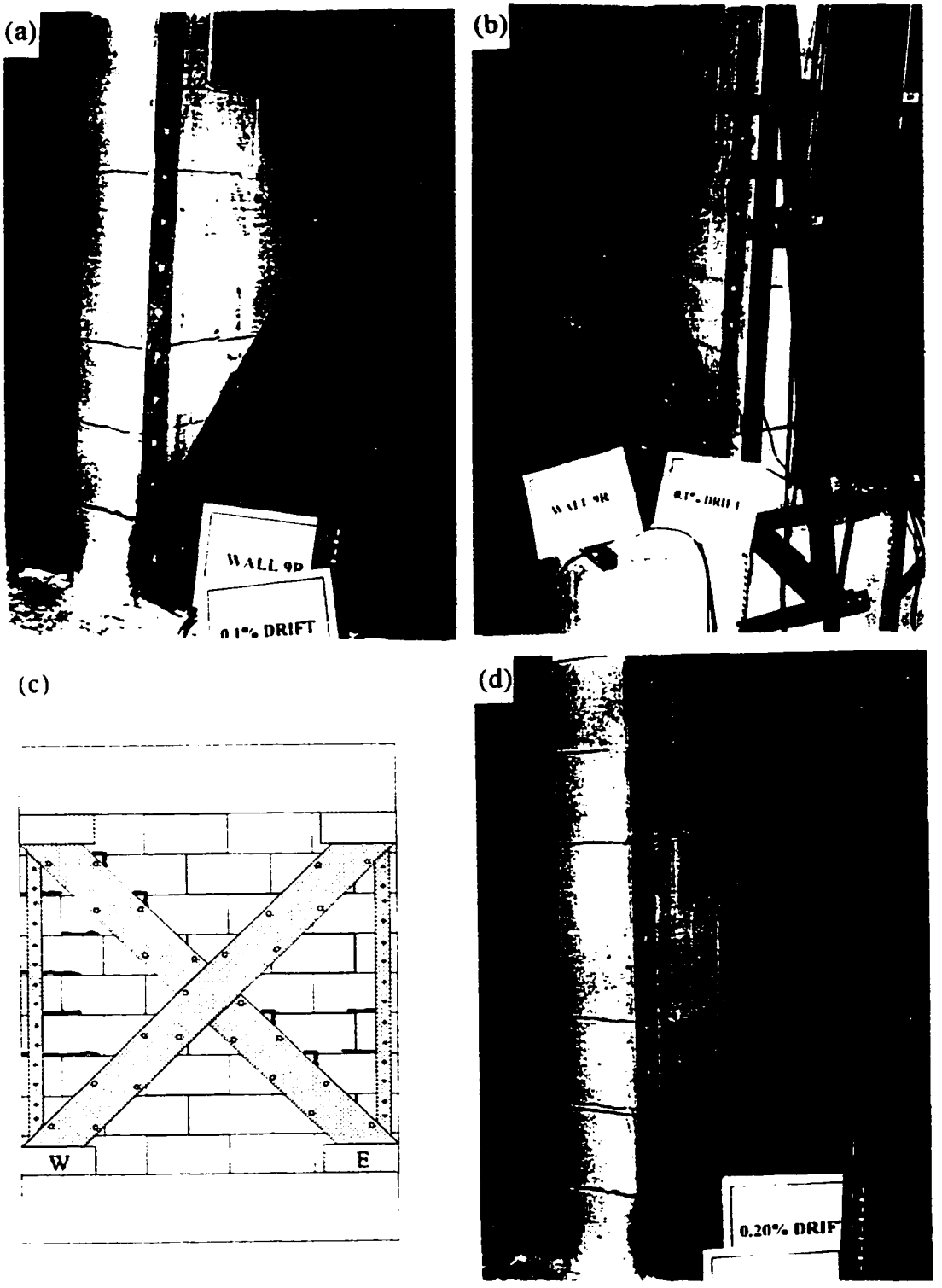

Figure 4.26 Wall 9R retrofitted URM: (a) First flexural cracks at 0.1% drift at the east end. (b) First flexural cracks at 0.1% drift at the west end. (c) Crack pattern at the end of 0.1% drift. (d) First diagonal crack at 0.2% drift.

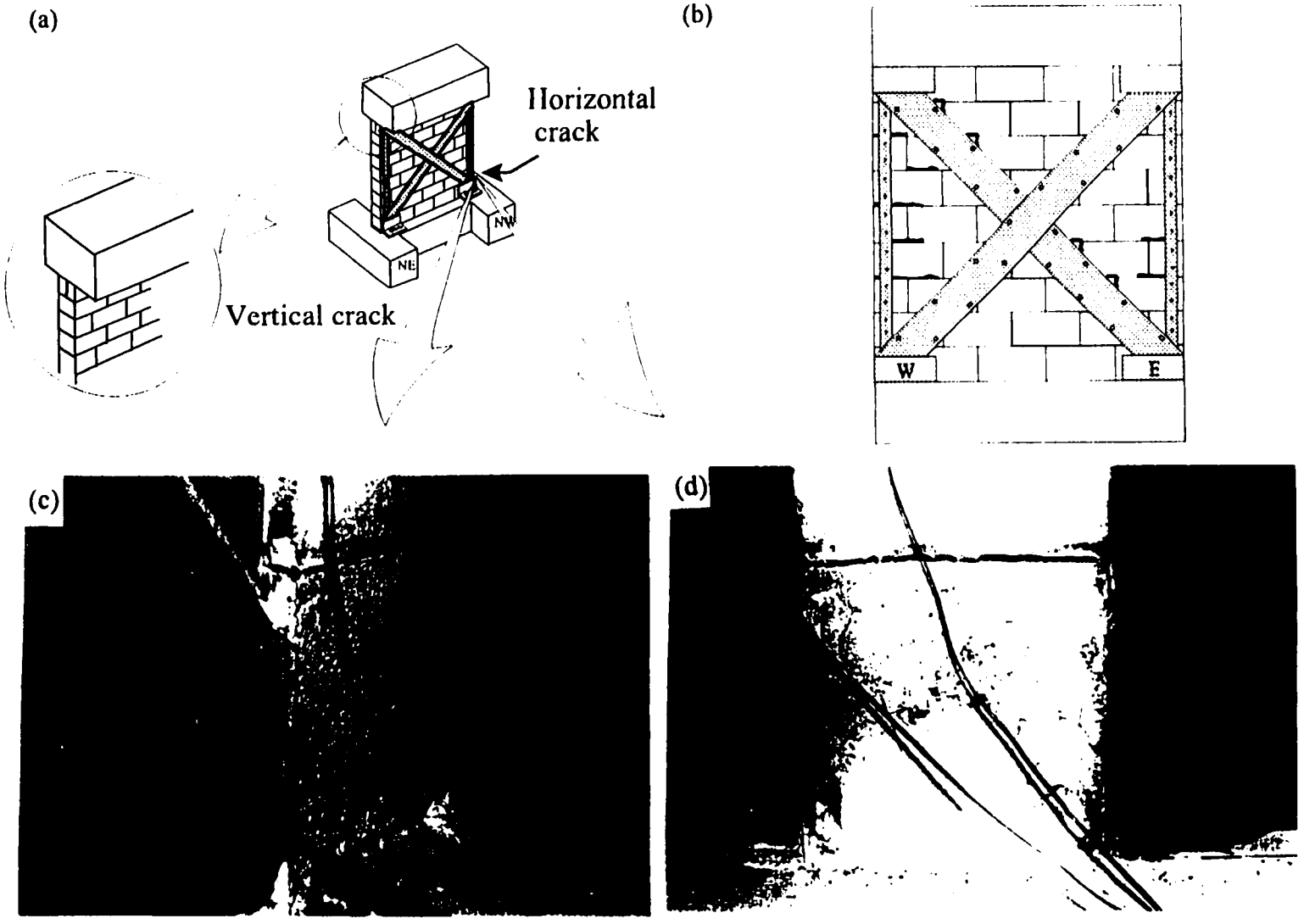

Figure 4.27 Wall 9R: (a) Vertical and horizontal cracks on the narrow wall faces. (b) Crack pattern at the end of 0.2% drift. (c) Close-up view of crushing at the bottom west side end of the wall. (d) Close-up view of the crushing at the bottom west side end of the wall.

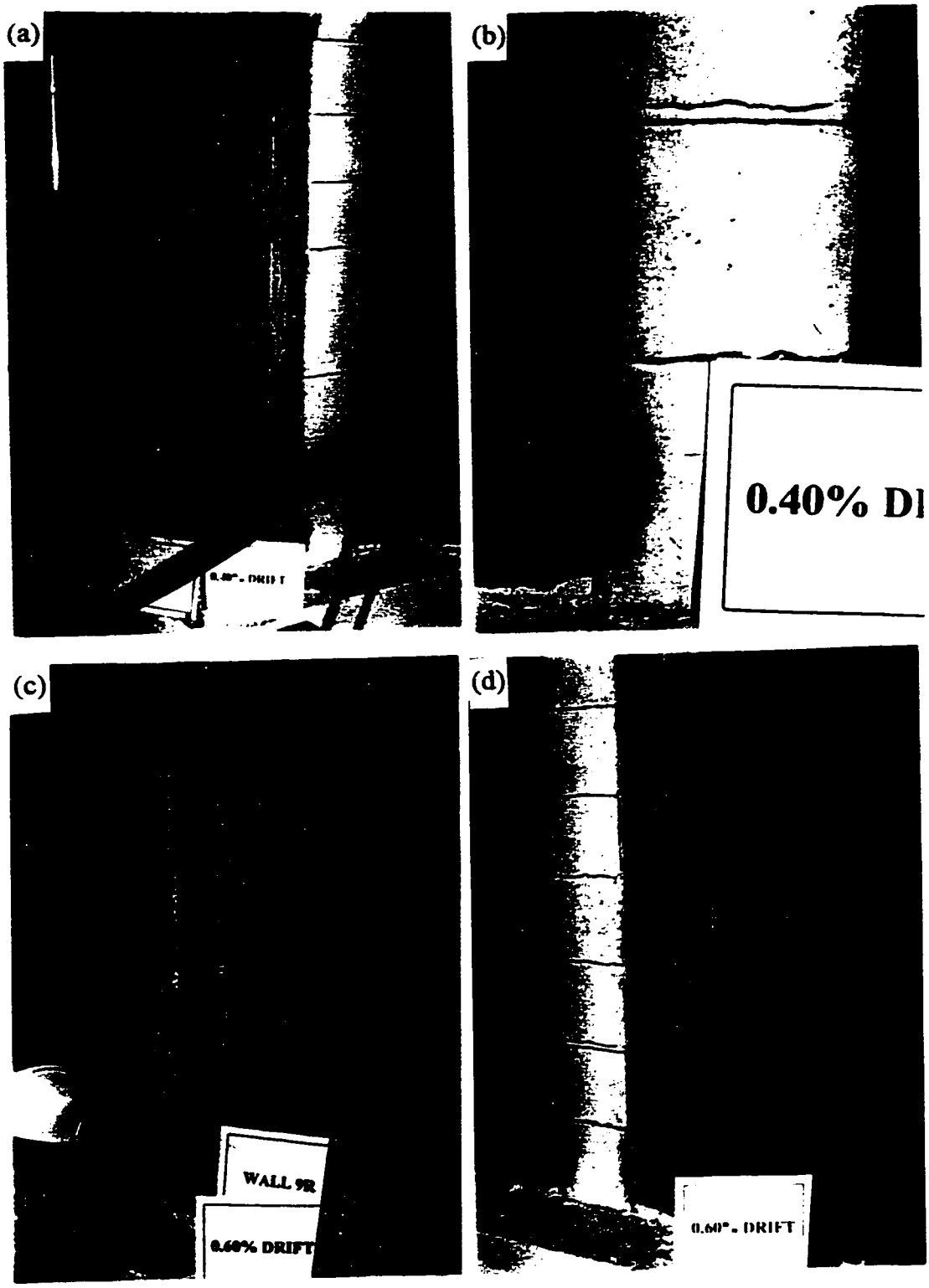

Figure 4.28 Wall 9R: (a) Cracking at 0.4% drift (east end). (b) Buckling of vertical steel strips. (c) Cracking during first cycle at 0.6% drift (east end). (d) Cracking during last cycle at 0.6% drift (east end).

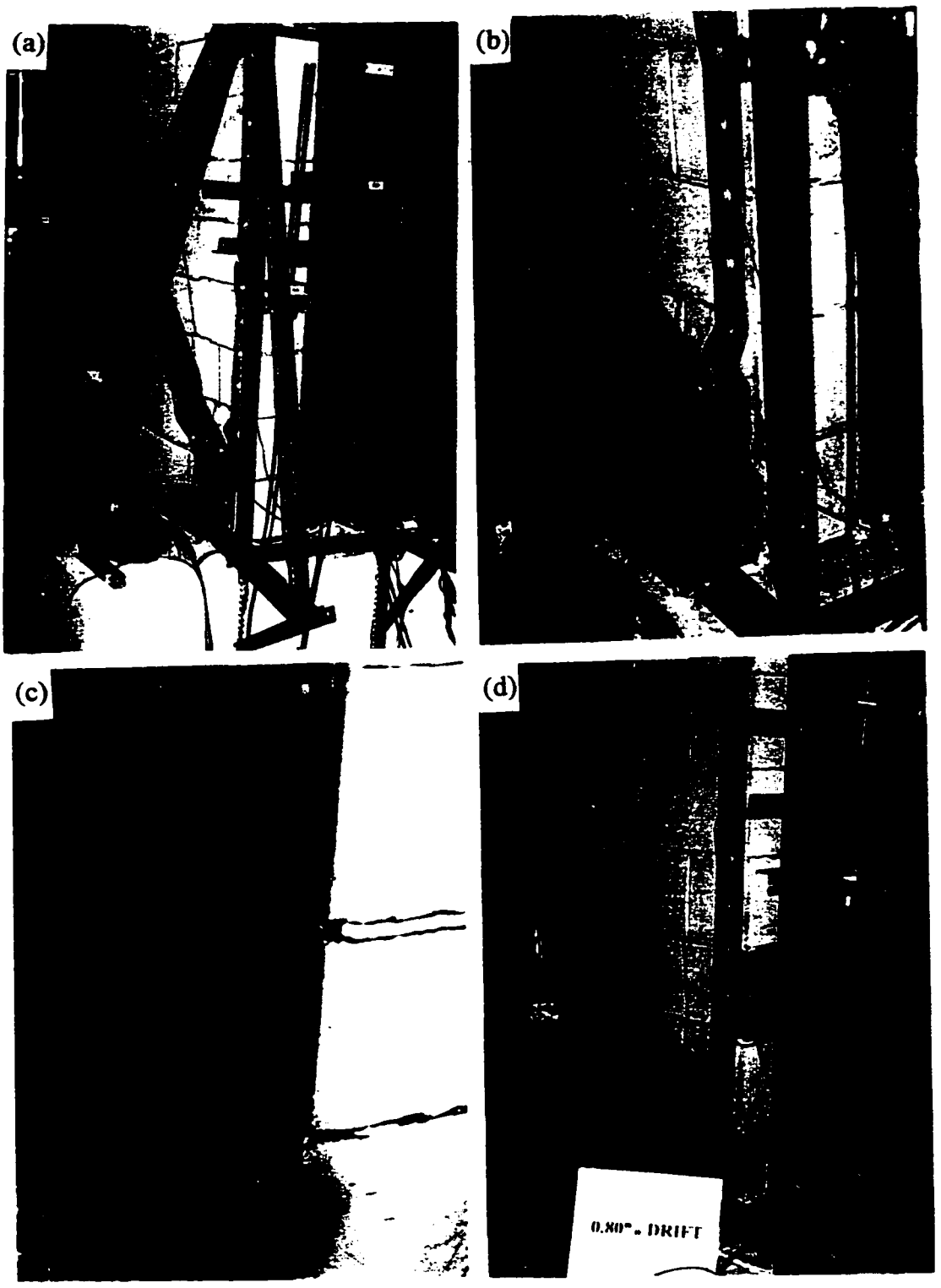

Figure 4.29 Wall 9R: (a) Cracking at 0.6% drift (west end). (b) Buckling of vertical and diagonal strips. (c) Close-up view of buckled steel strips at NW corner. (d) West end at 0.8% drift.

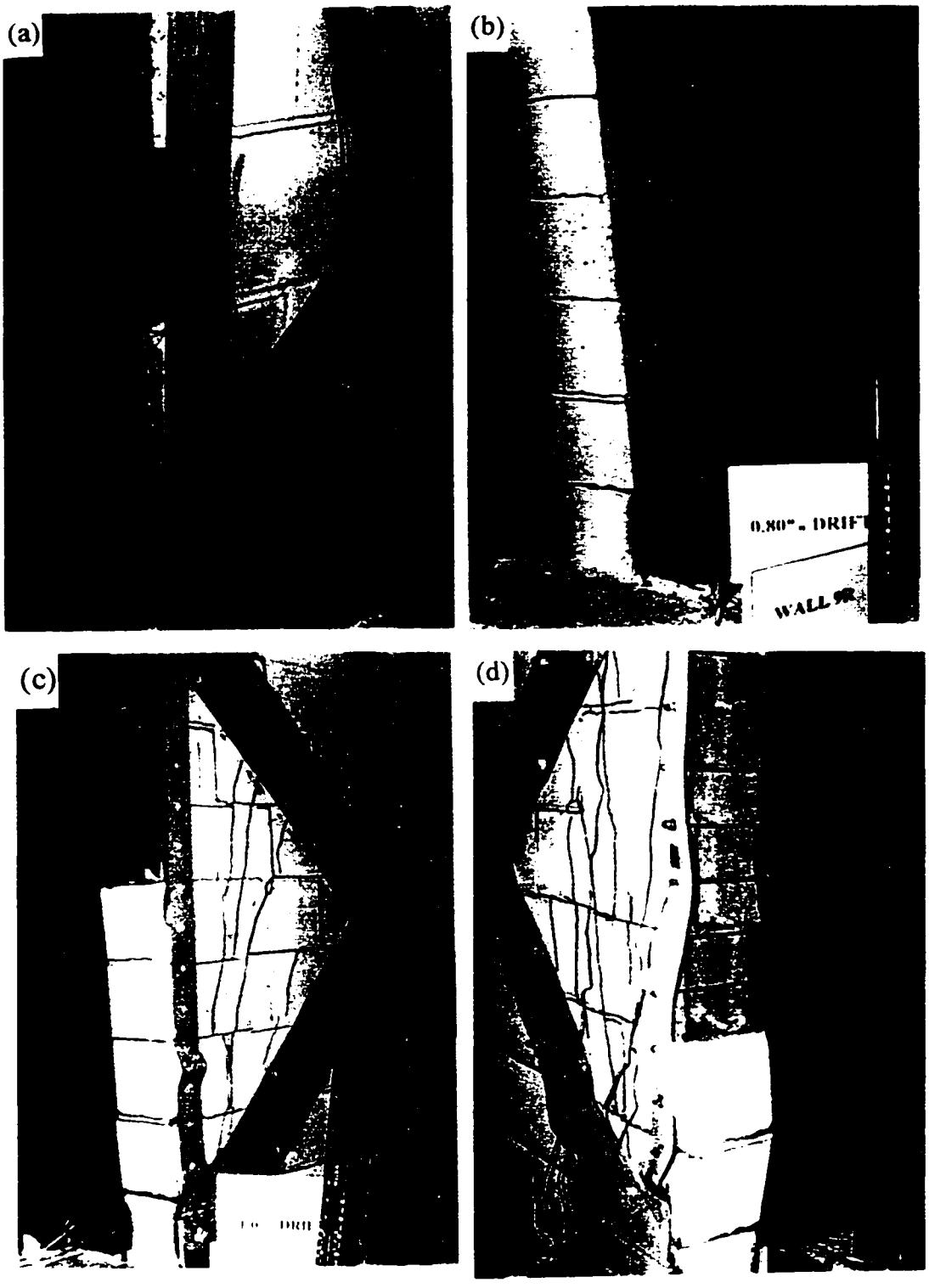

Figure 4.30 Wall 9R: (a) Close-up view of the west end at 0.8% drift. (b) Buckling of vertical steel strips at 0.8% drift (NE side). (c) Global view at 1.0% drift (east end). (d) Global buckling of the east vertical steel strips.

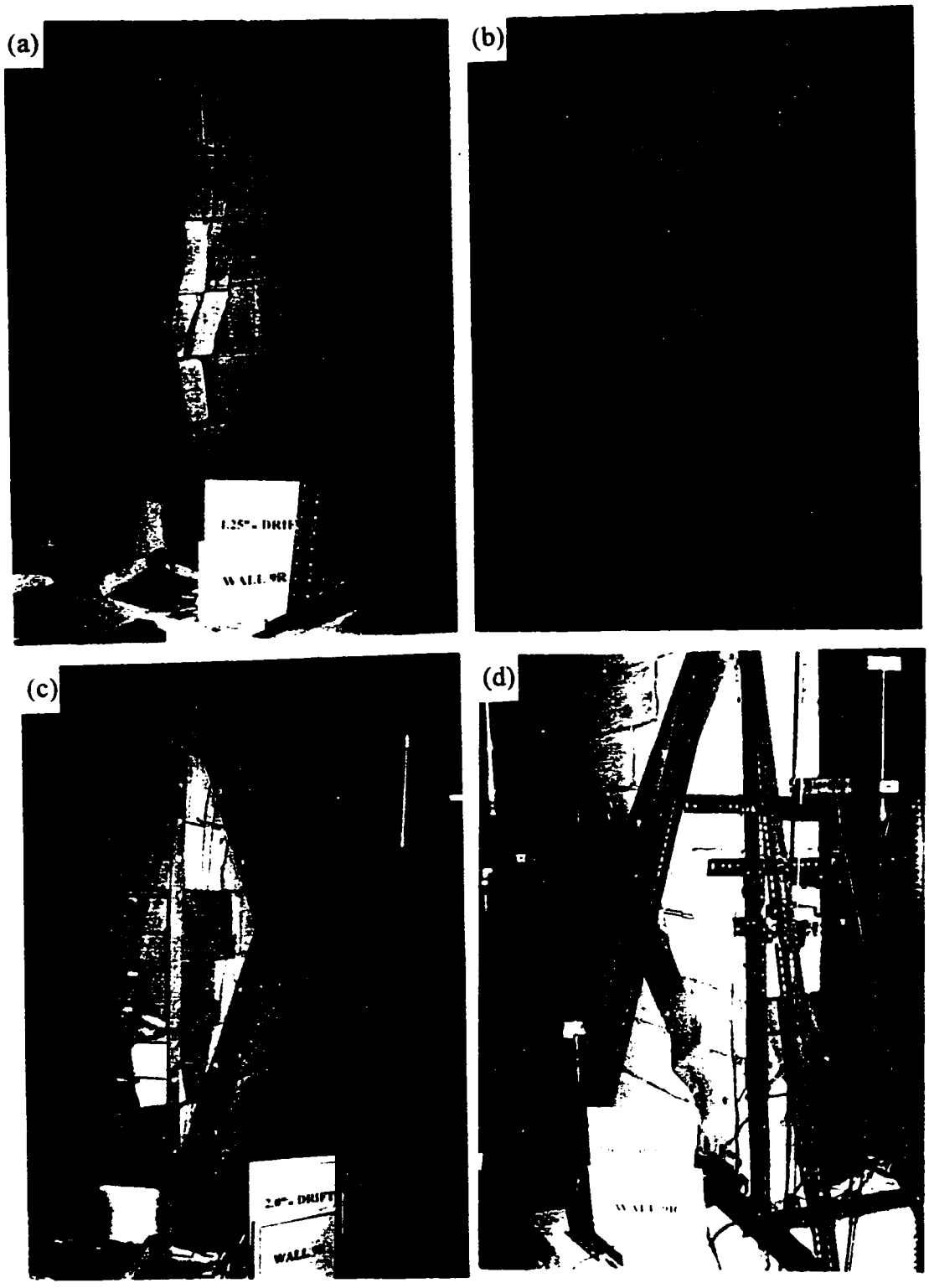

Figure 4.31 Wall 9R: (a) At 1.25% drift (east end). (b) Lateral displacement due to global buckling of vertical steel strips. (c) Lost masonry at the east end at 2.0% drift. (d) Severe global buckling of steel strips at 2.0% drift (west end).

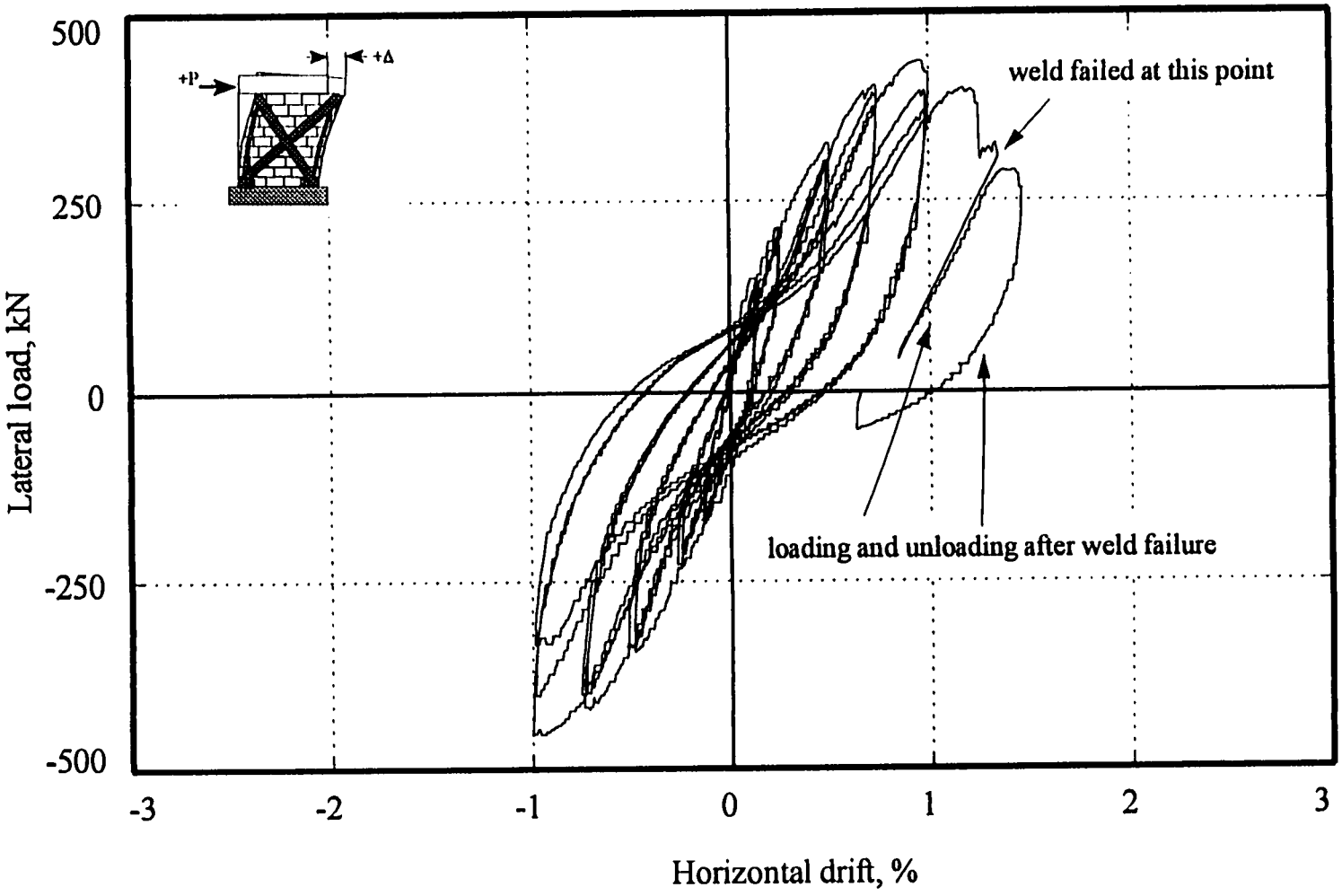

Figure 4.32 Hysteretic lateral load-displacement of Wall 10R before weld failure

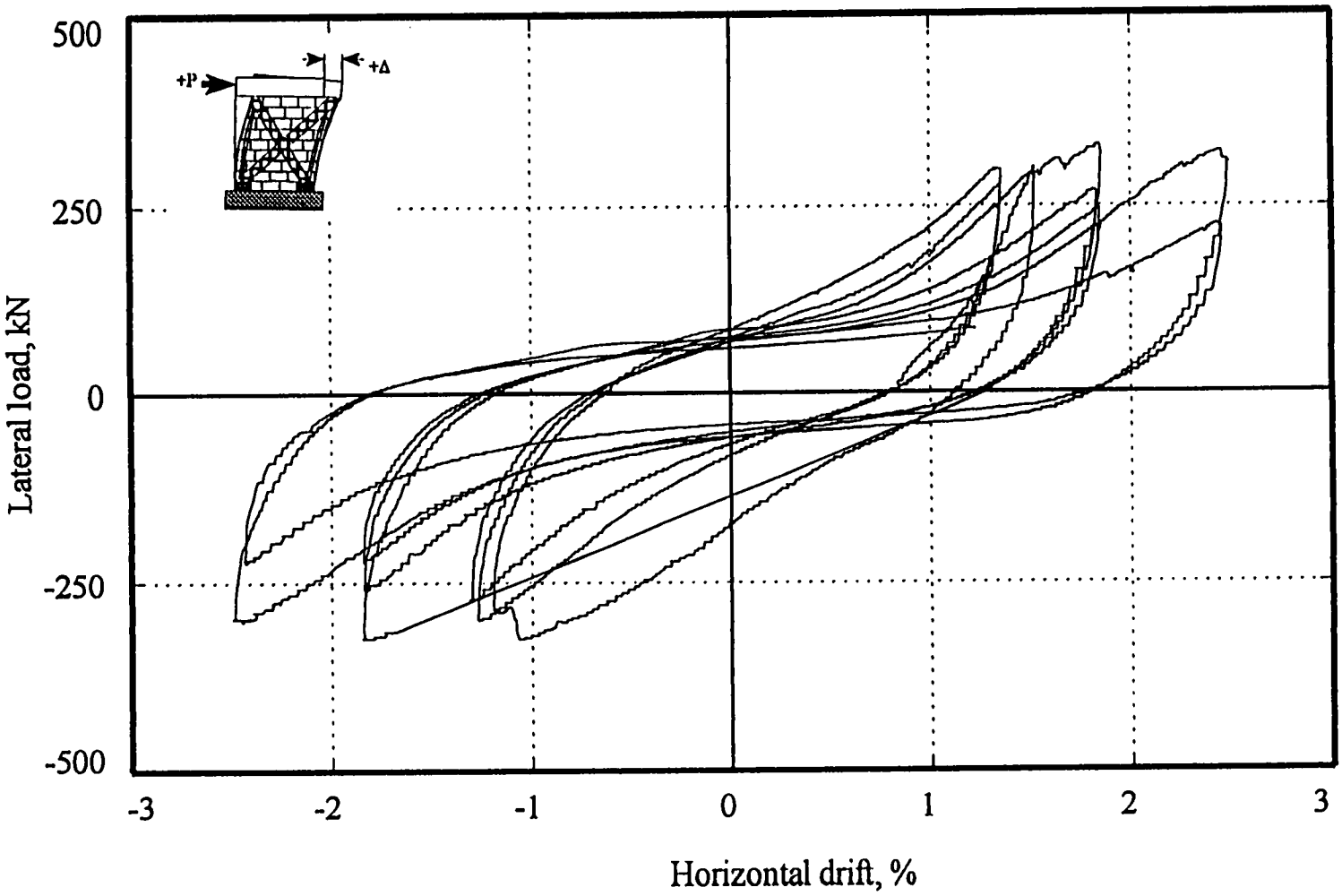

Figure 4.33 Hysteretic lateral load-displacement of Wall 10R after rewelding

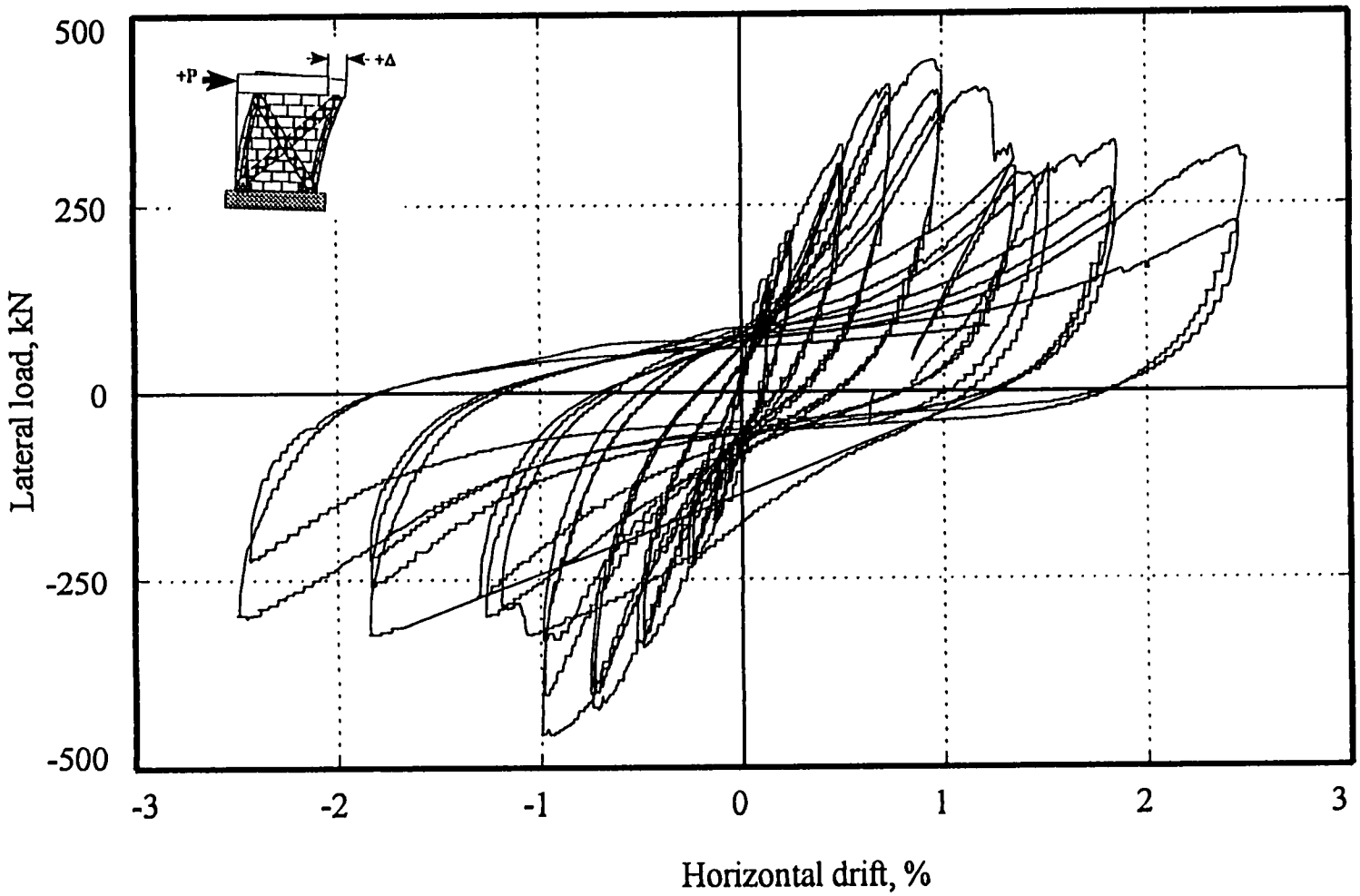

Figure 4.34 Hysteretic lateral load-displacement of Wall 10R

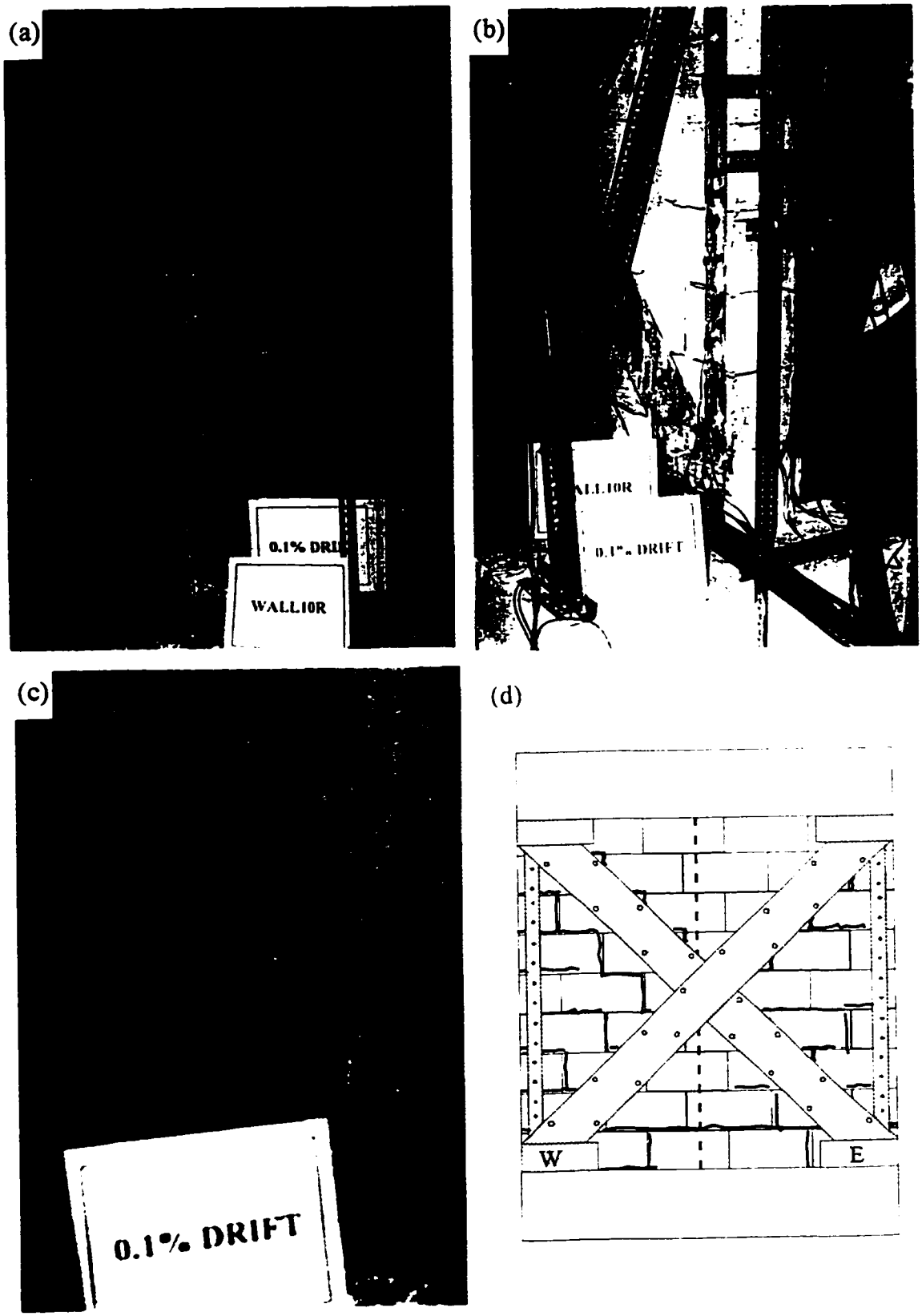

Figure 4.35 Wall 10R at 0.1% drift: (a) Horizontal cracking (east end). (b) Horizontal cracking (west end). (c) Horizontal cracking at the base (west end). (d) Crack pattern at the end of cycles.

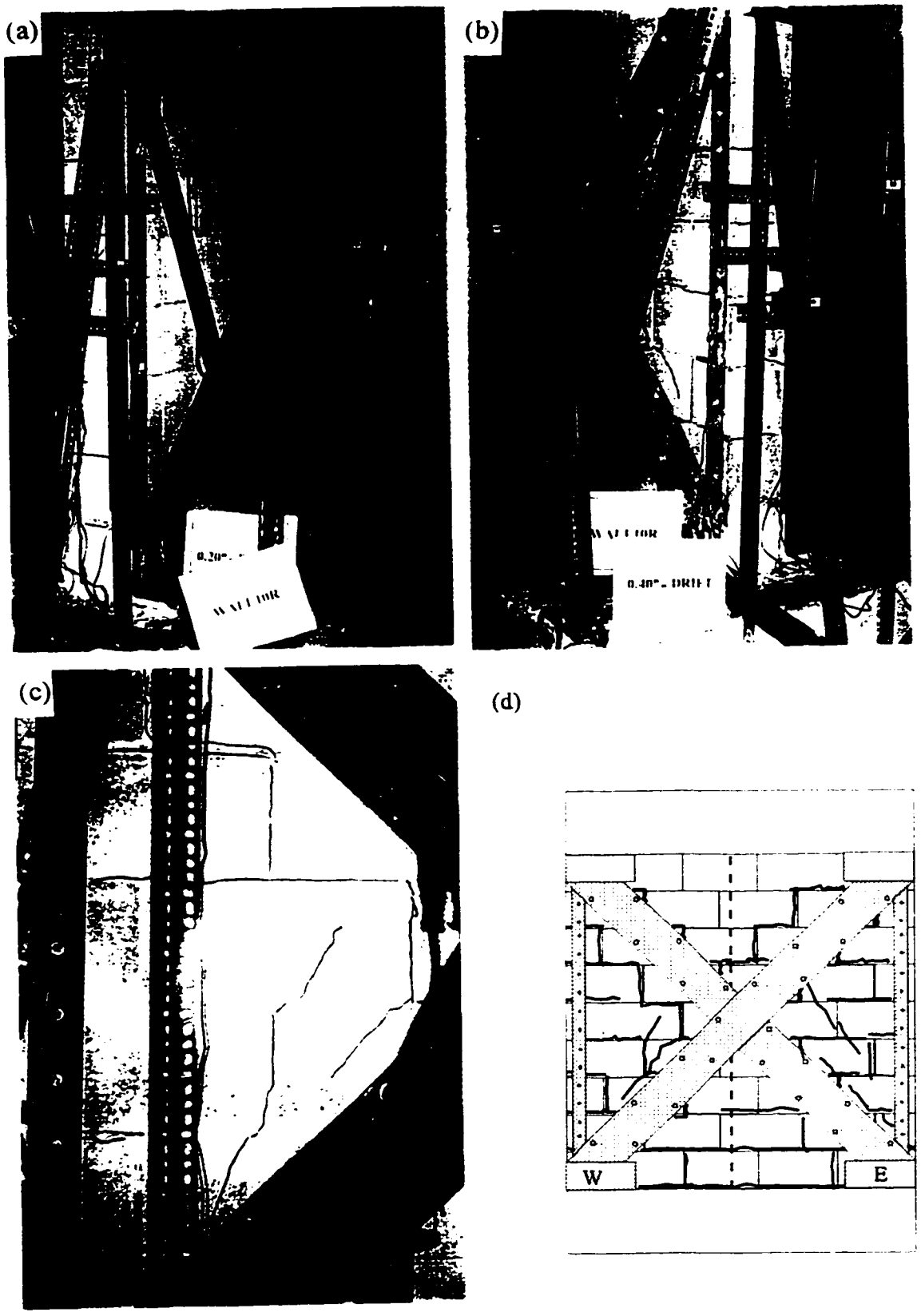

Figure 4.36 Wall 10R: (a) Stair-step cracking at 0.2% drift (west end). (b) Stair-step cracking at 0.4% drift (west end). (c) Crack pattern at the end of 0.4% drift. (d) First through blocks cracks at 0.6% drift.

Figure 4.37 Wall 10R: (a) At 0.6% drift (east end). (b) Mild buckling of diagonal steel strips on NE corner. (c) Buckling of diagonal strip on SW corner. (d) Buckling of diagonal strip on SE corner at 0.8% drift.

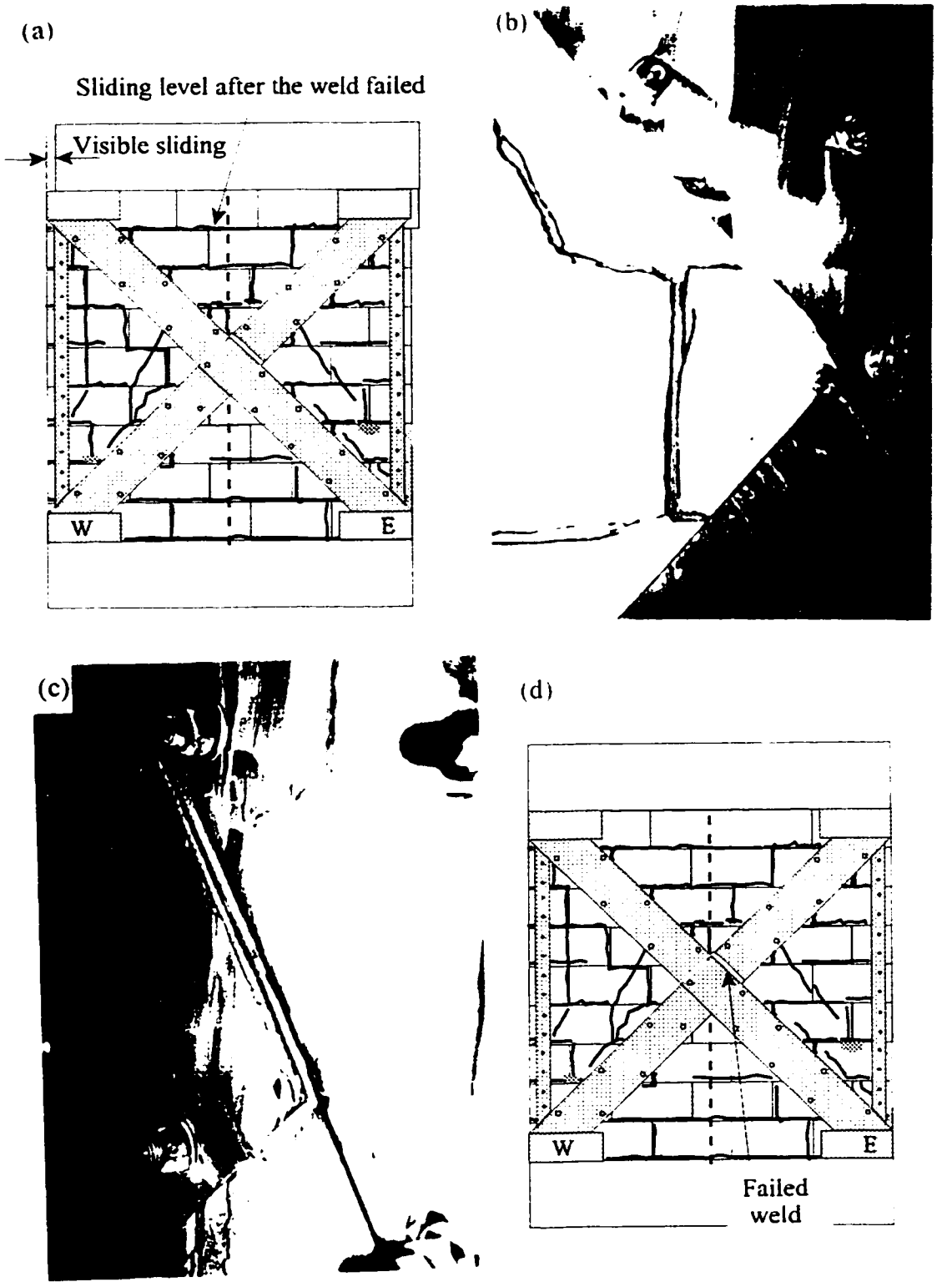

Figure 4.38 Wall 10R: (a) Sliding of top masonry blocks with the top beam after weld failure. (b) Fractured weld and wide vertical crack between blocks due to sliding. (c) Fractured joint. (d) Location of the first fractured joint.

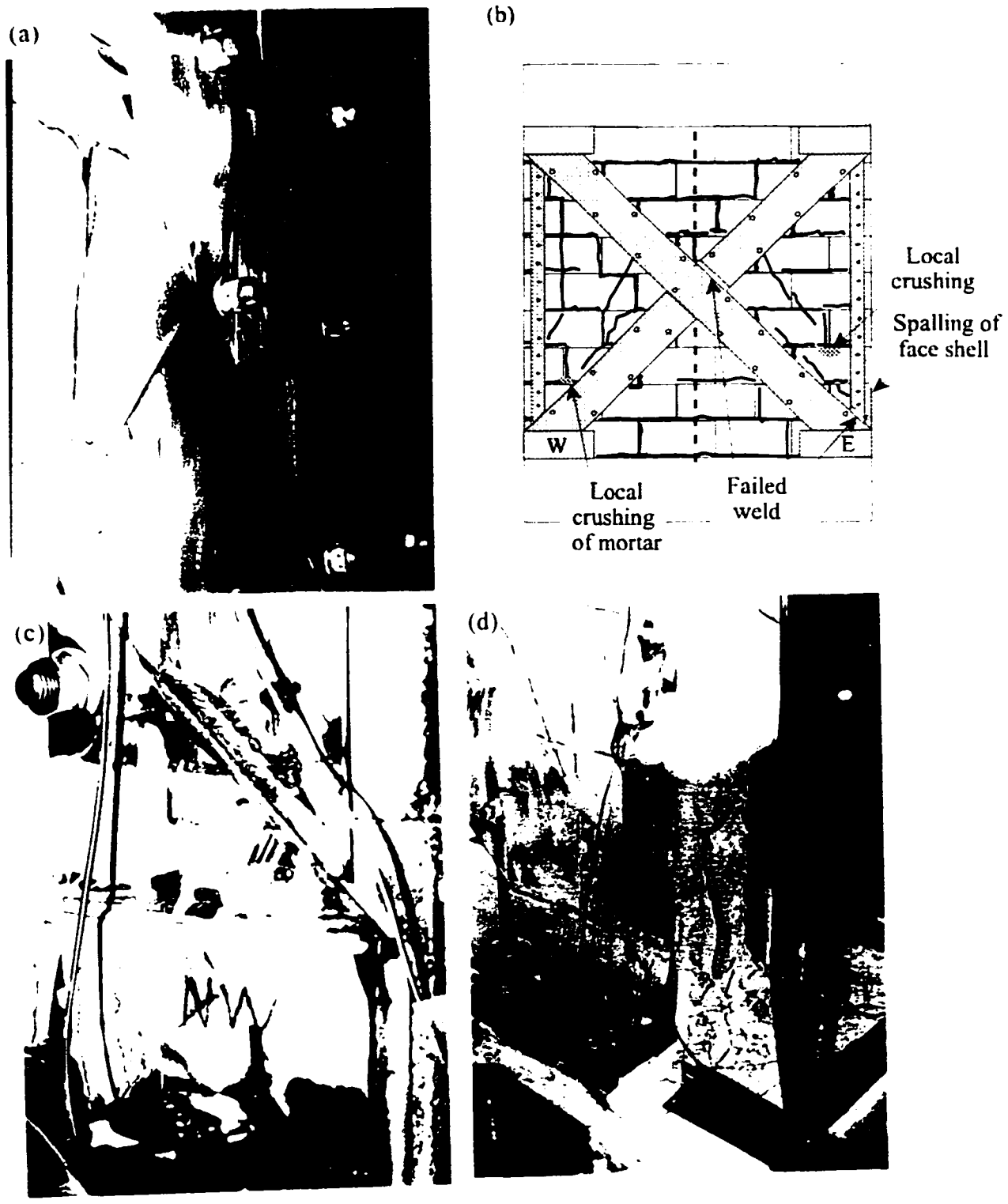

Figure 4.39 Wall 10R: (a) Failed joint after rewelding. (b) Location of the second fractured joint. (c) Close-up view of the second fracture joint between diagonal and vertical strips. (d) Buckling of vertical rebar at east end.

Figure 4.40 Wall 10R: (a) Details of the failed joint after reinforcing it. (b) East view of the wall after resuming the test at 1.5% drift. (c) Buckling of diagonal steel strips on NE corner at 1.5% drift. (d) Close-up view of vertical steel strips severe buckling.

Figure 4.41 Wall 10R at 2.0% drift: (a) Buckling of rebar, vertical and diagonal steel strips (east end). (b) Close-up view of fractured steel strip. (c) West view after damaged masonry fell-off the wall. (d) Global view at west end.

Figure 4.42 Wall 10R after testing.

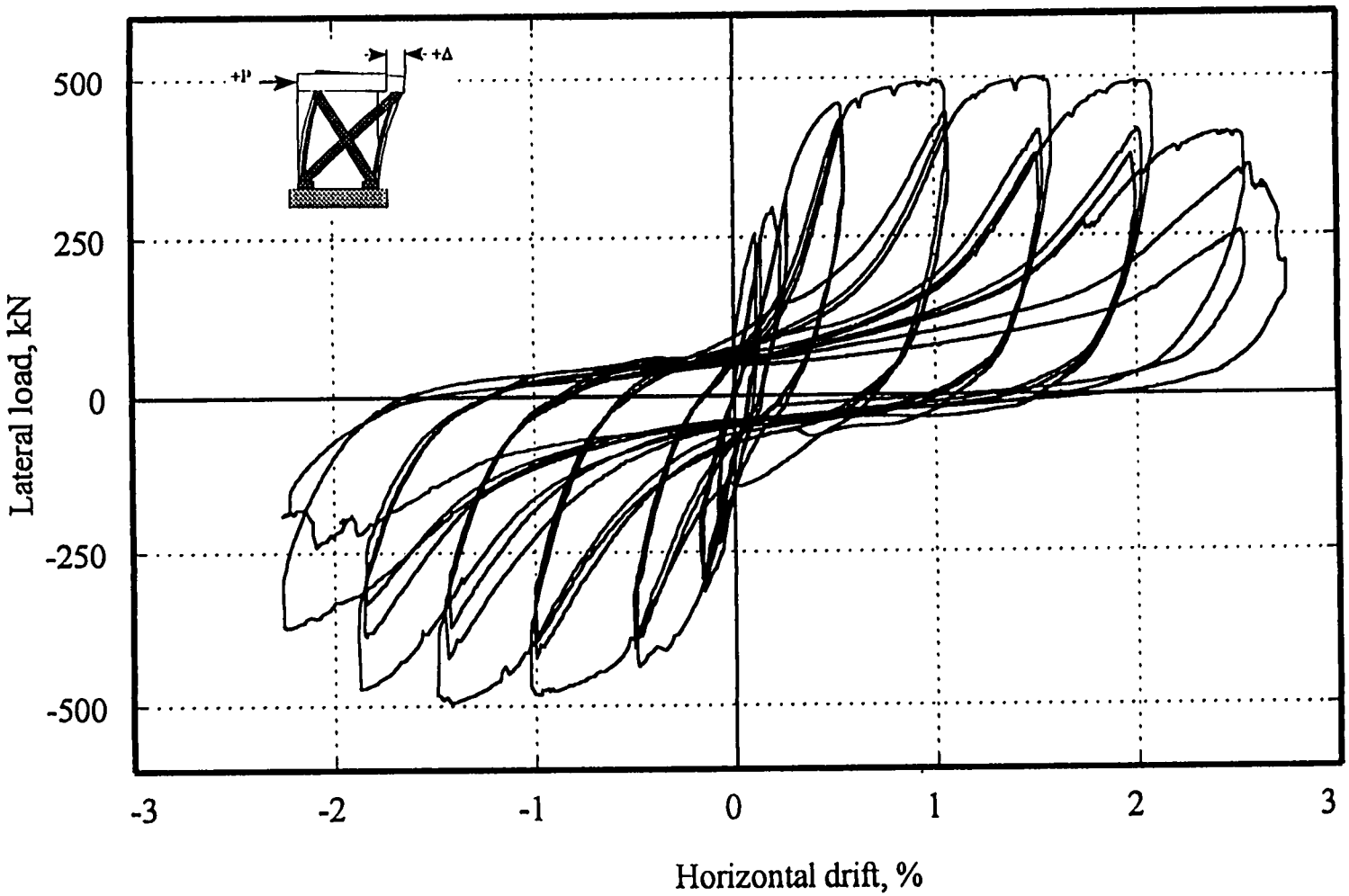

Figure 4.43 Hysteretic lateral load-displacement of Wall 11R

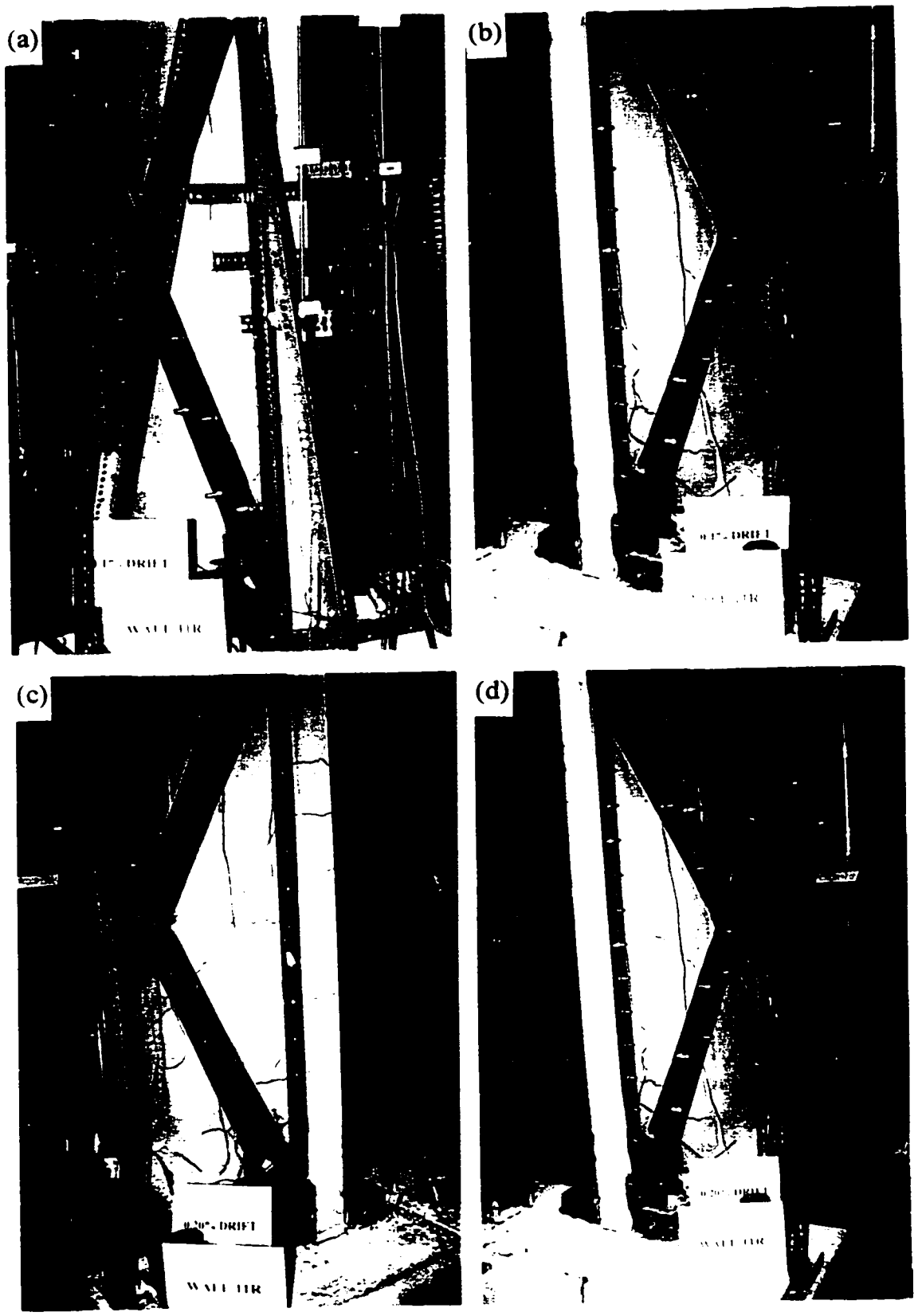

Figure 4.44 Wall 11R: (a) Cracking at 0.1% drift (west end). (b) Cracking at 0.1% drift (east end). (c) Inclined cracking starting at mid height at 0.2% drift (SE view). (d) Inclined cracking starting at mid height at 0.2% drift (NE view).

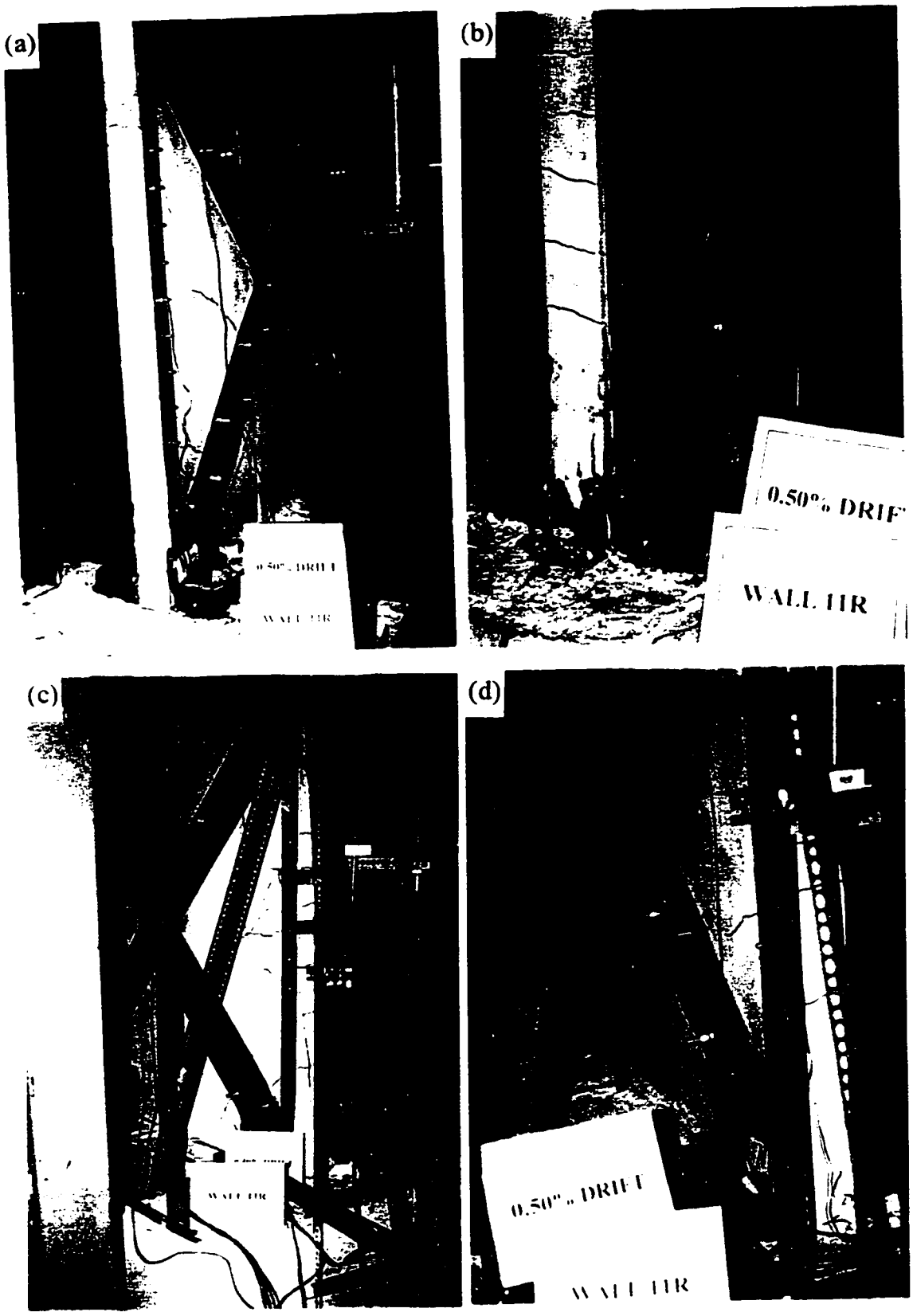

Figure 4.45 Wall 11R at 0.5% drift: (a) Extending of the diagonal cracks. (b) Spalling of the narrow face at the base. (c) More cracks in the narrow face and extending of the diagonal cracking (west end). (d) Horizontal and inclined cracks near the base.

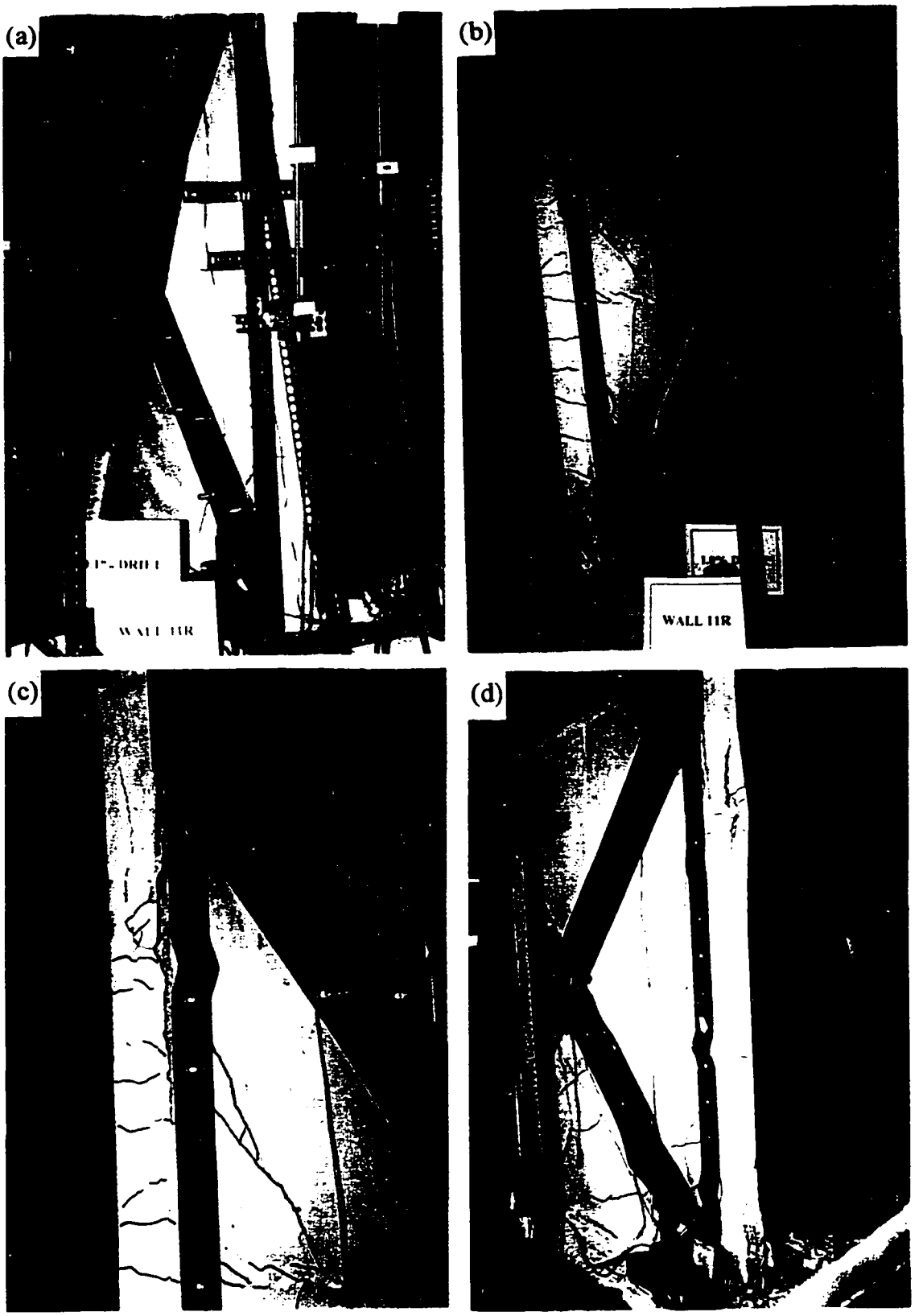

Figure 4.46 Wall 11R at drift of 1.0%: (a) East side view. (b) Buckling of NE vertical steel strips near the top. (c) Close-up view of the buckled vertical steel strip at 1.0% drift. (d) Buckling of the SE vertical steel strips.

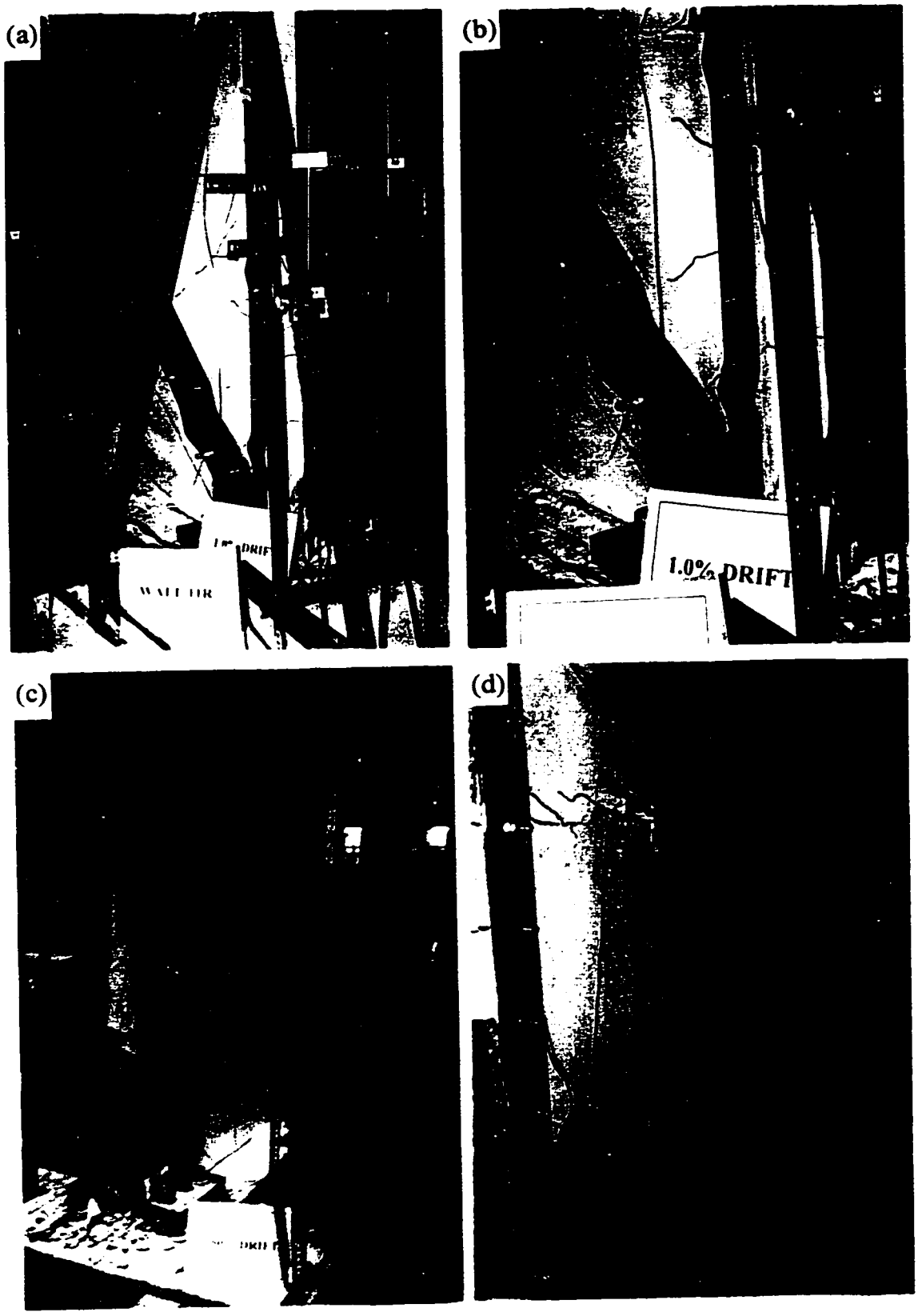

Figure 4.47 Wall 11R: (a) Buckling of NW vertical and diagonal steel strips at drift of 1.0%. (b) Close-up view to the buckled NW steel strips. (c) Global view of NW side at 1.5% drift. (d) Severe buckling of NE steel strips.

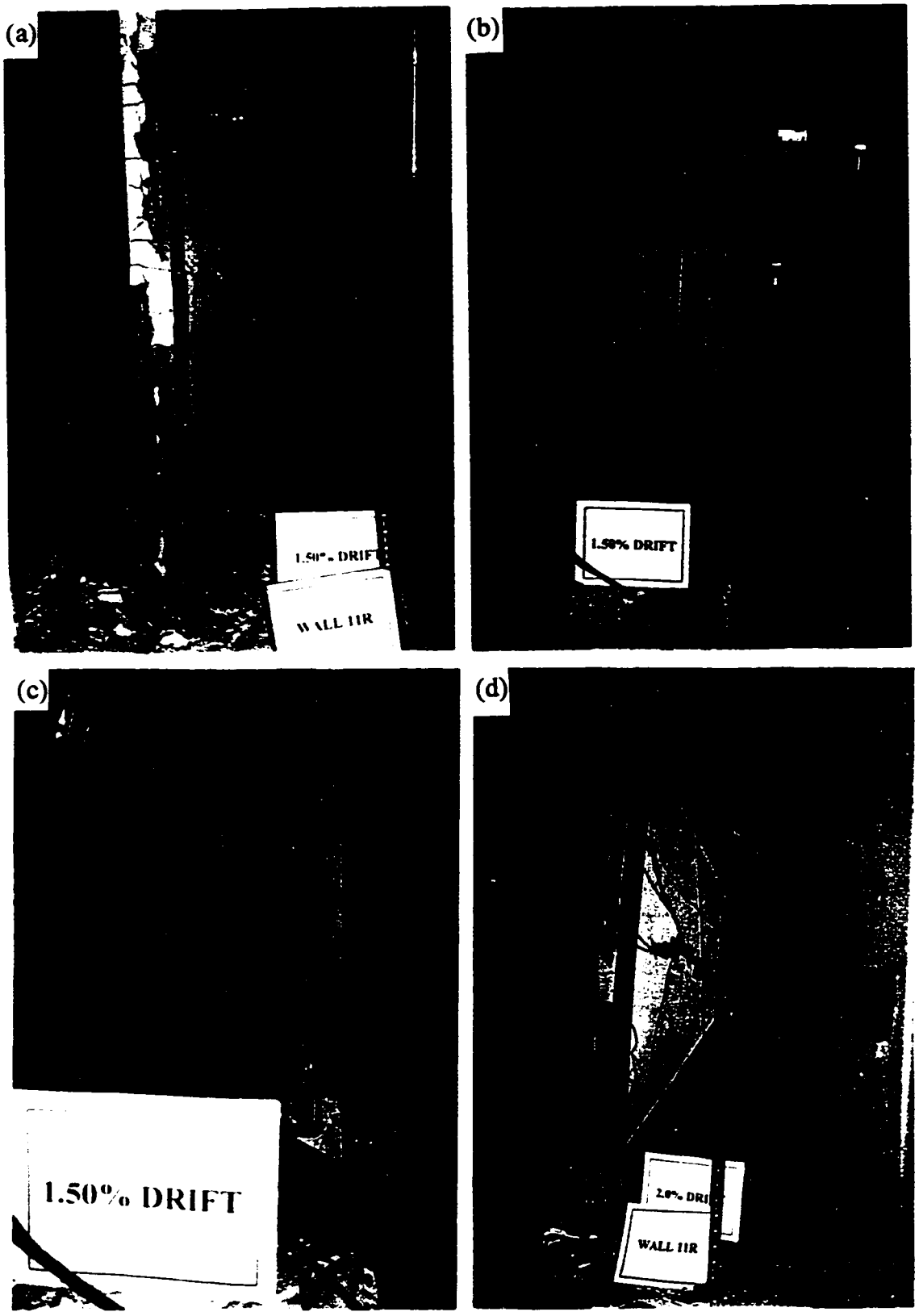

Figure 4.48 Wall 11R: (a) Buckling of steel strips and rebars at 1.5% drift on NE side. (b) Buckling of steel strips and rebars at 1.5% drift on NW side. (c) Close-up view to the buckled NW strips at 1.5% drift. (d) Global view at 2.0% drift (east side).

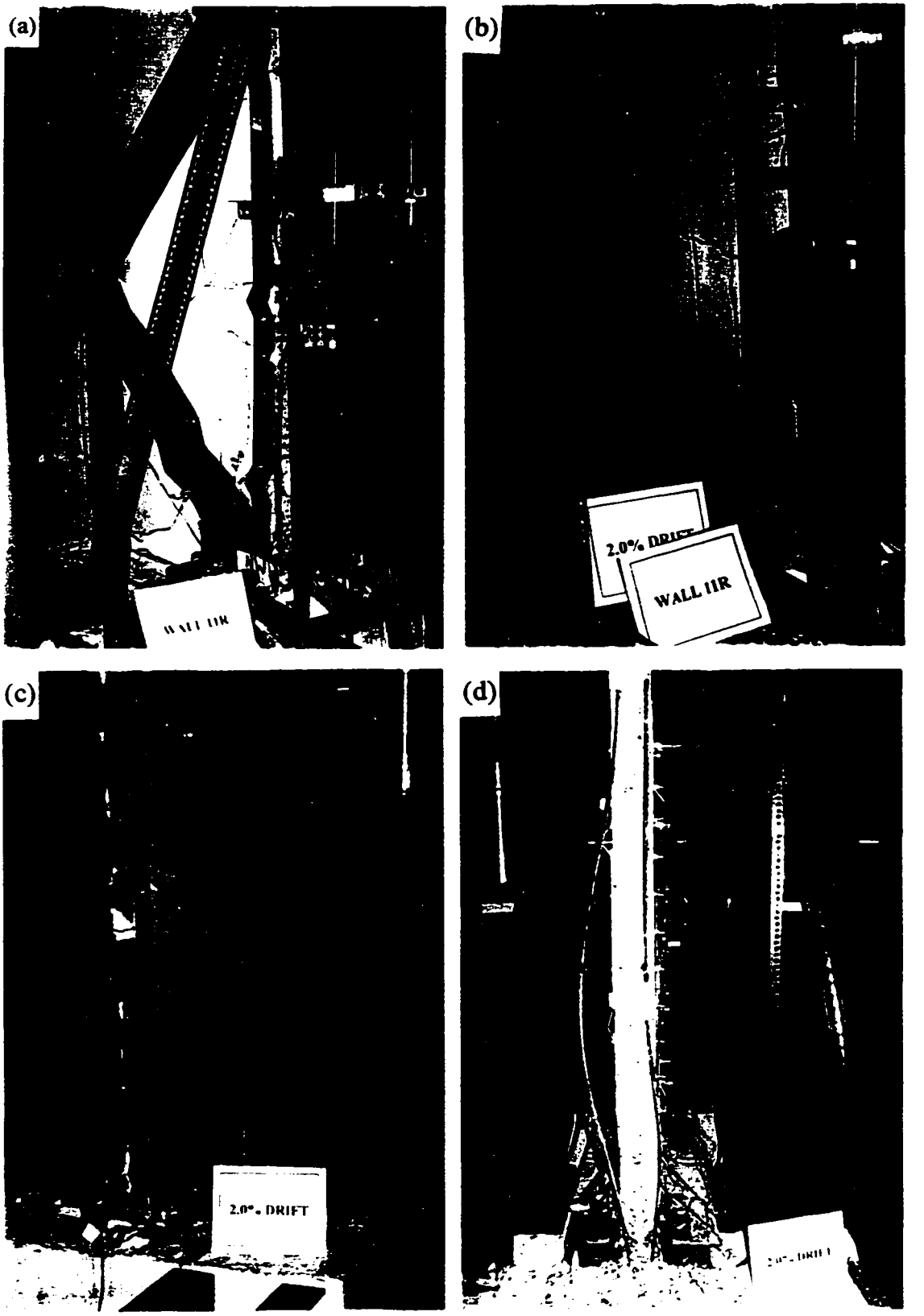

Figure 4.49 Wall 11R at drift of 2.0%: (a) Visible concrete crushing (west side). (b) Exposed vertical rebars. (c) Buckling of steel strips and rebars at east end. (d) complete crushing of the east narrow face.

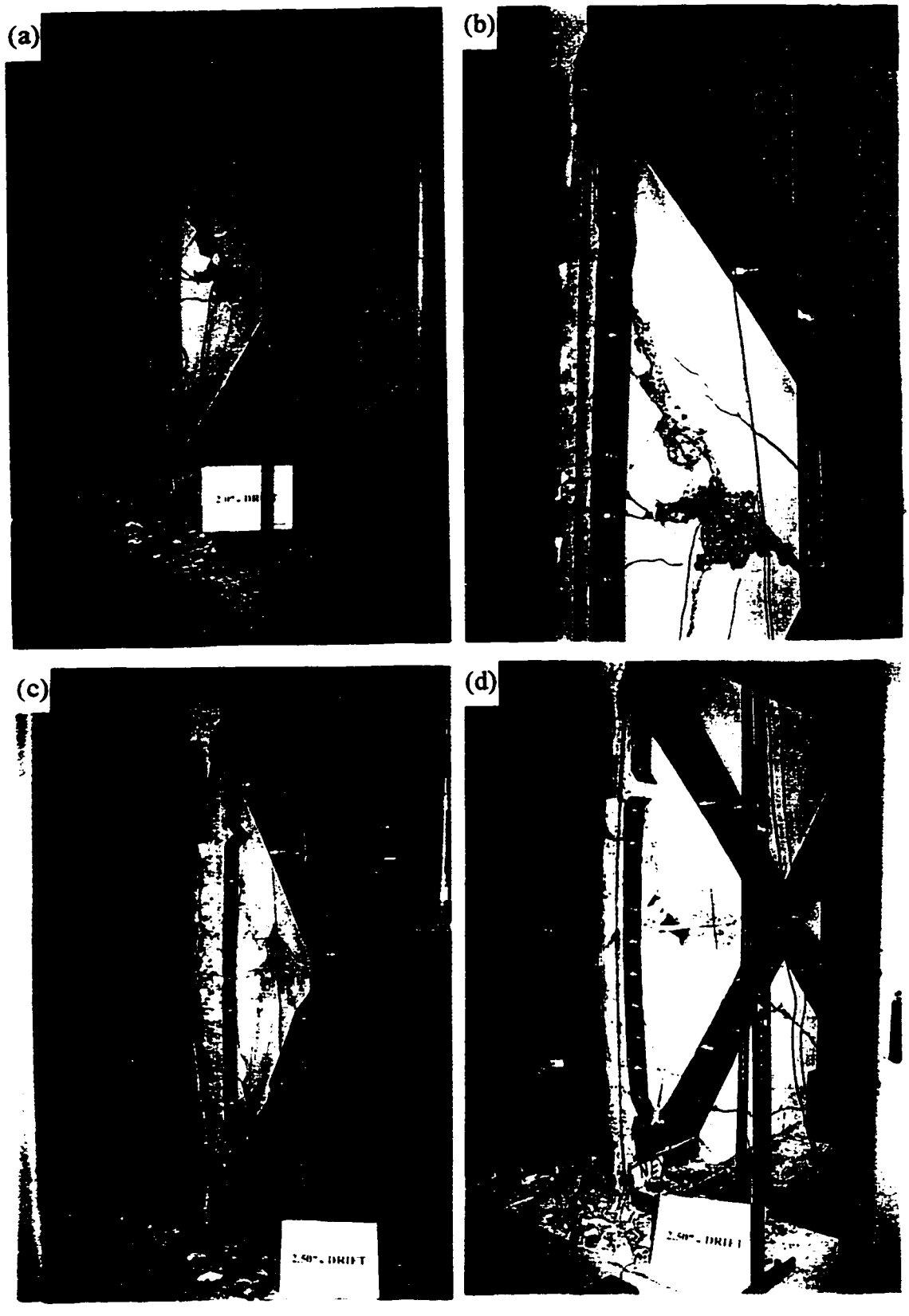

Figure 4.50 Wall 11R: (a) At 2.0% drift, rupture of the NE vertical steel strips. (b) Close-up view of vertical steel strip rupture and concrete crushing on NE side. (c) Global view at 2.5% drift. (d) Severe concrete damage between east vertical and diagonal steel strips.

Figure 4.51 Wall 11R at 2.5% drift: (a) Global view (west side). (b) Severe rebar buckling at west end. (c) Twisting of the wall due to rupture of the vertical steel strips. (d) Ruptured vertical steel strips at the east end.

Figure 4.52 Wall 11R: (a) Ruptured NW vertical steel strip. (b) Close-up view of ruptured NW vertical steel strip. (c) Crushing of concrete on the wall west side. (d) SE view of the wall after end of testing.

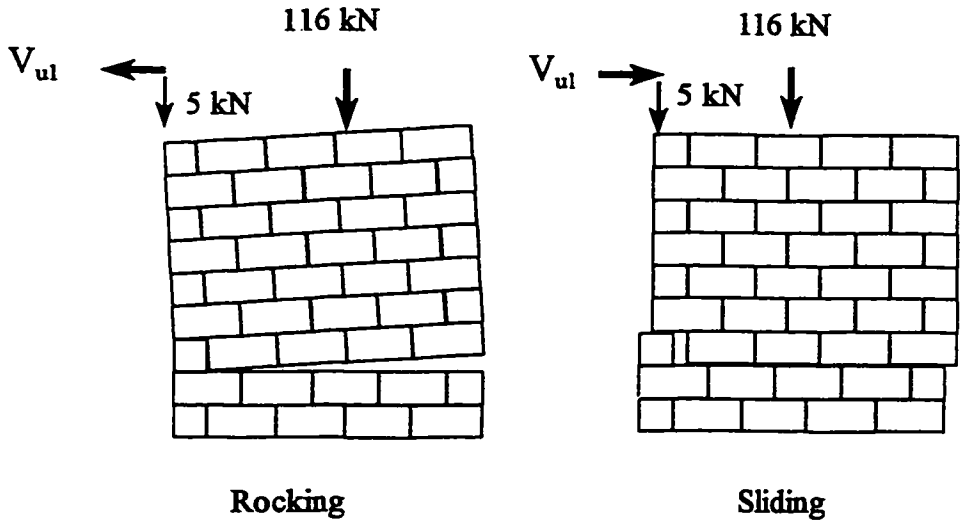

(a) Wall 9 at earlier stages

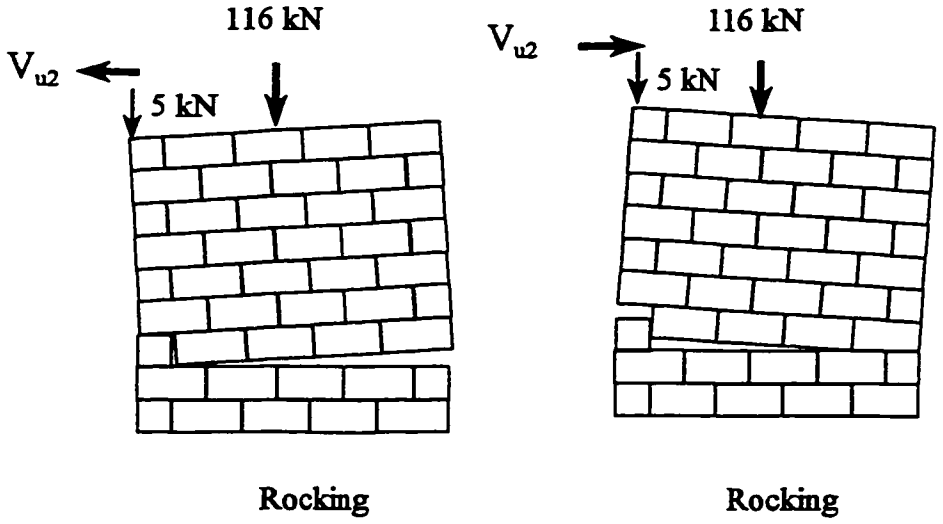

(b) Wall 9 at higher drifts

Figure 5.1 Behavior of Wall 9 under cyclic loading

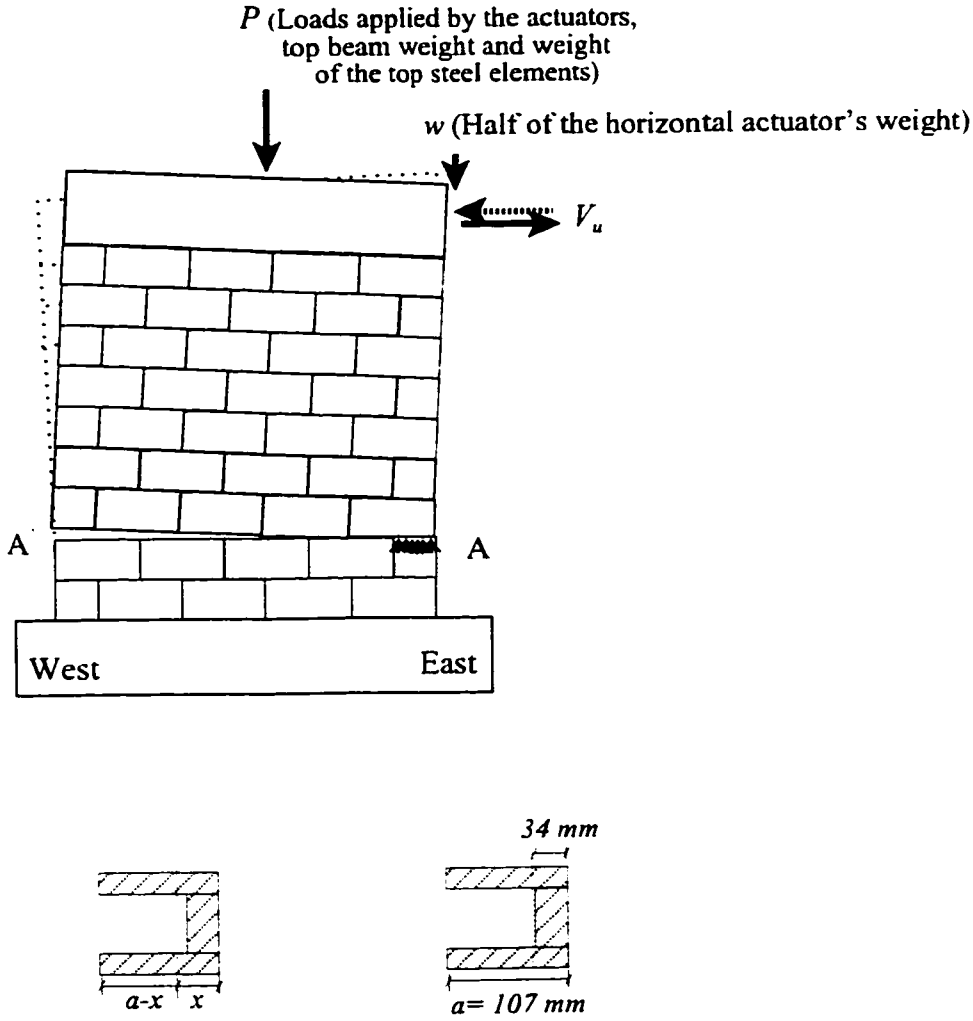

Figure 5.2 Freebody of Wall 9 under cyclic loading

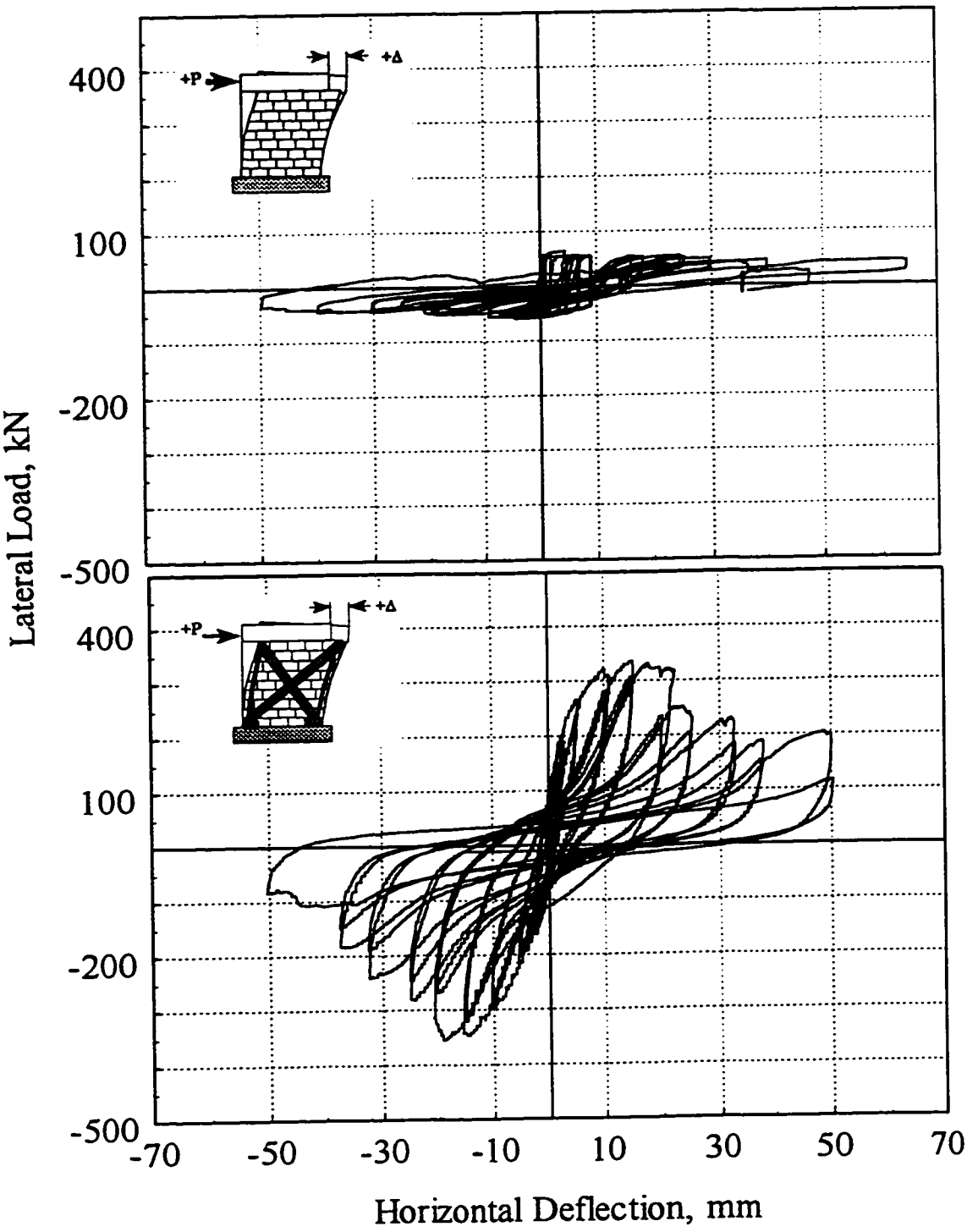

Figure 5.3 Hysteretic response of Wall 9 and Wall 9R

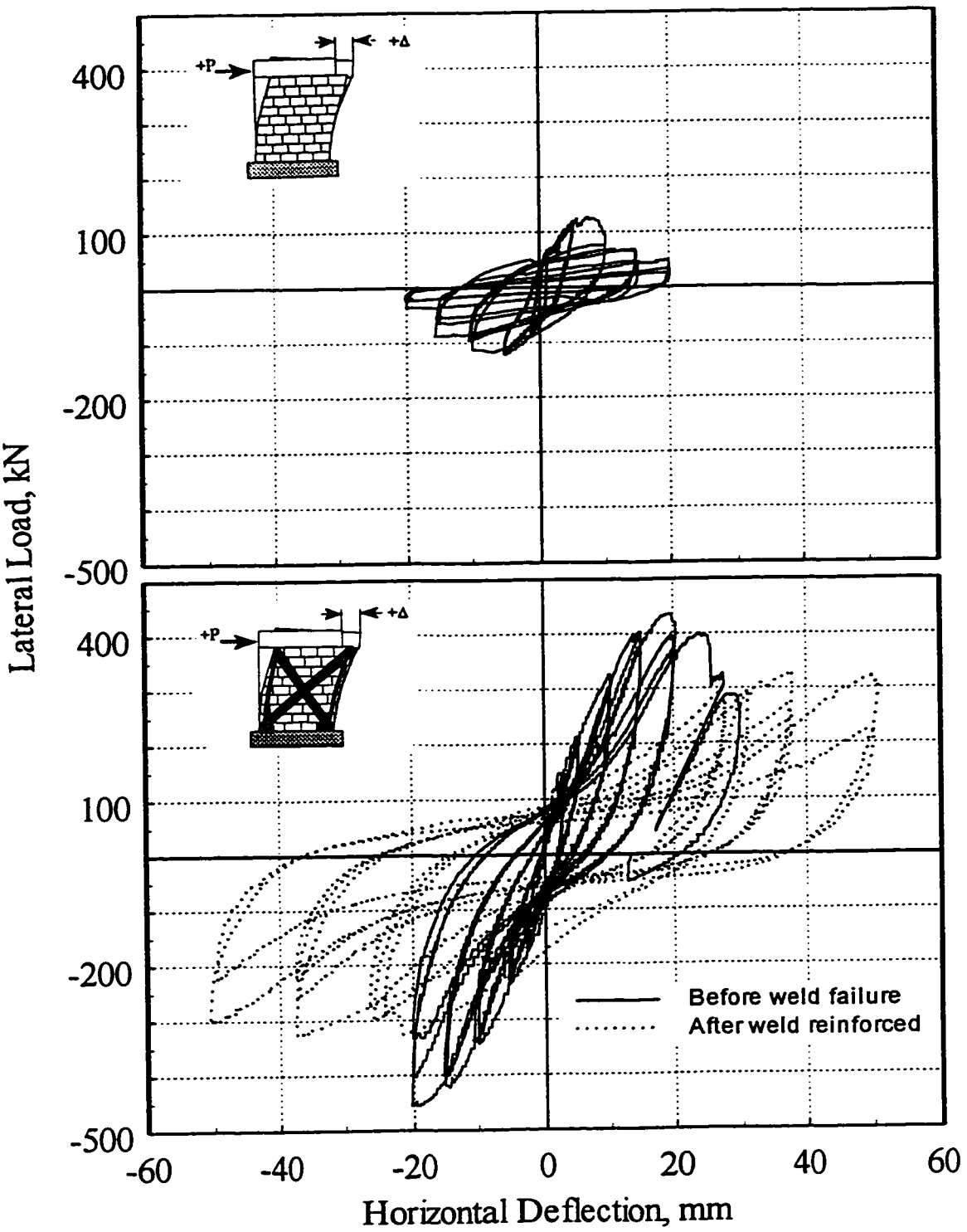

Figure 5.4 Hysteretic response of Wall 10 and Wall 10R

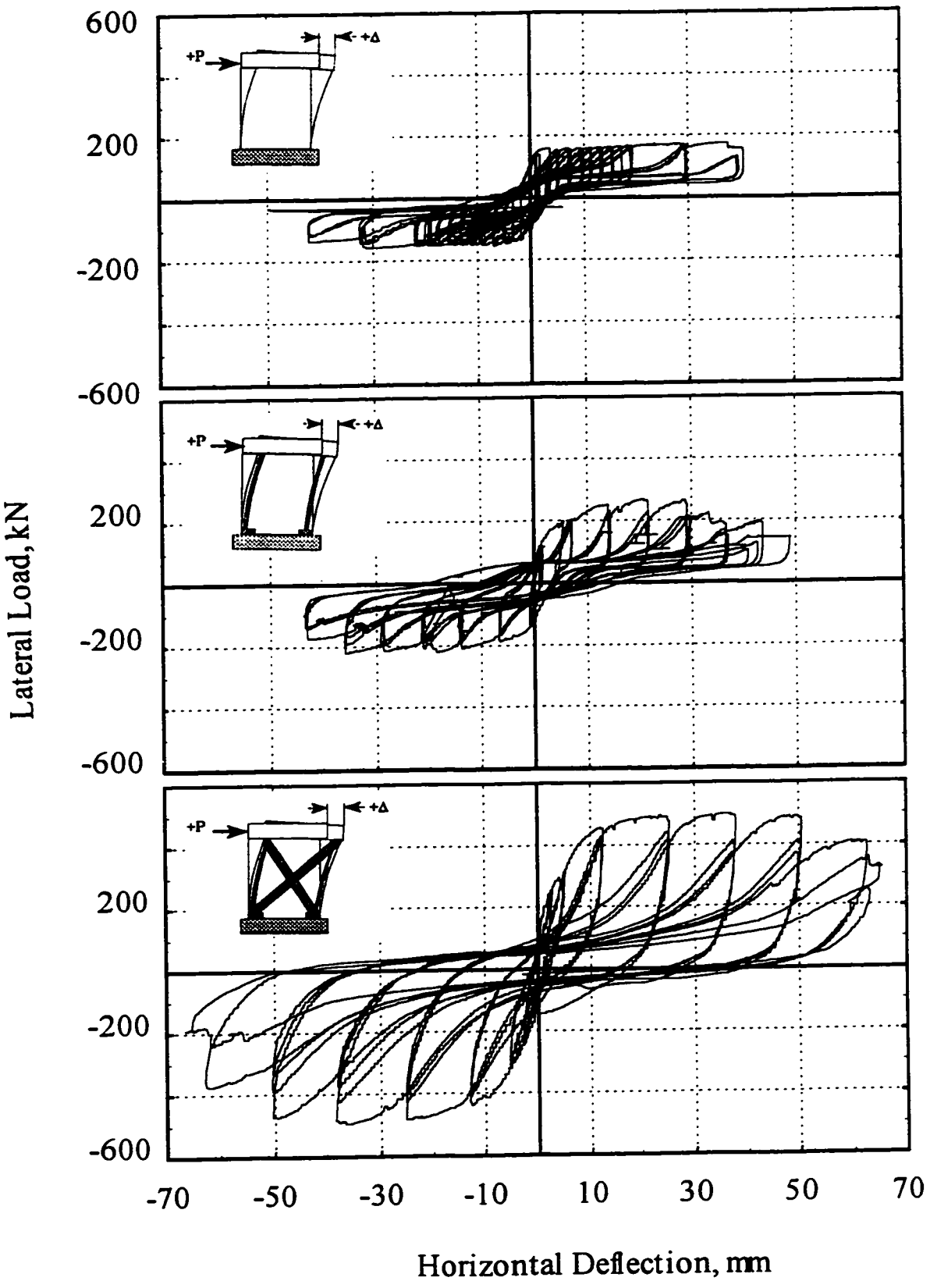

Figure 5.5 Hysteretic response of Wall 11, Wall 11RP and Wall 11R

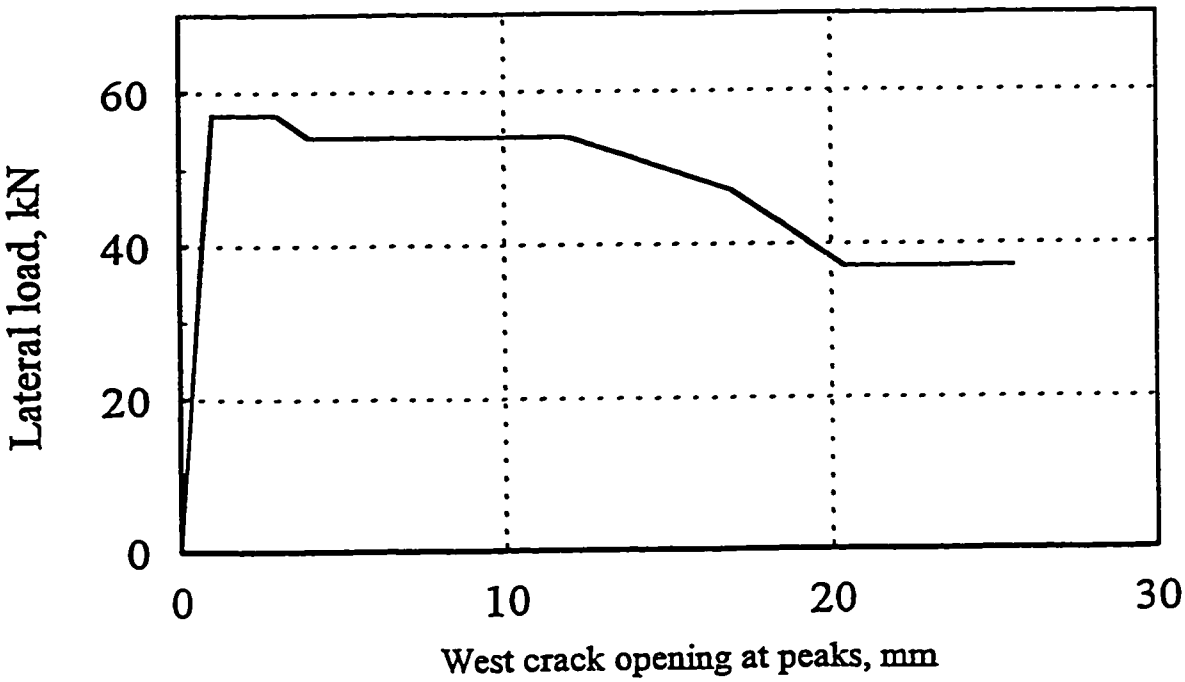

Figure 5.6 lateral load-crack width relationship (Wall 9)

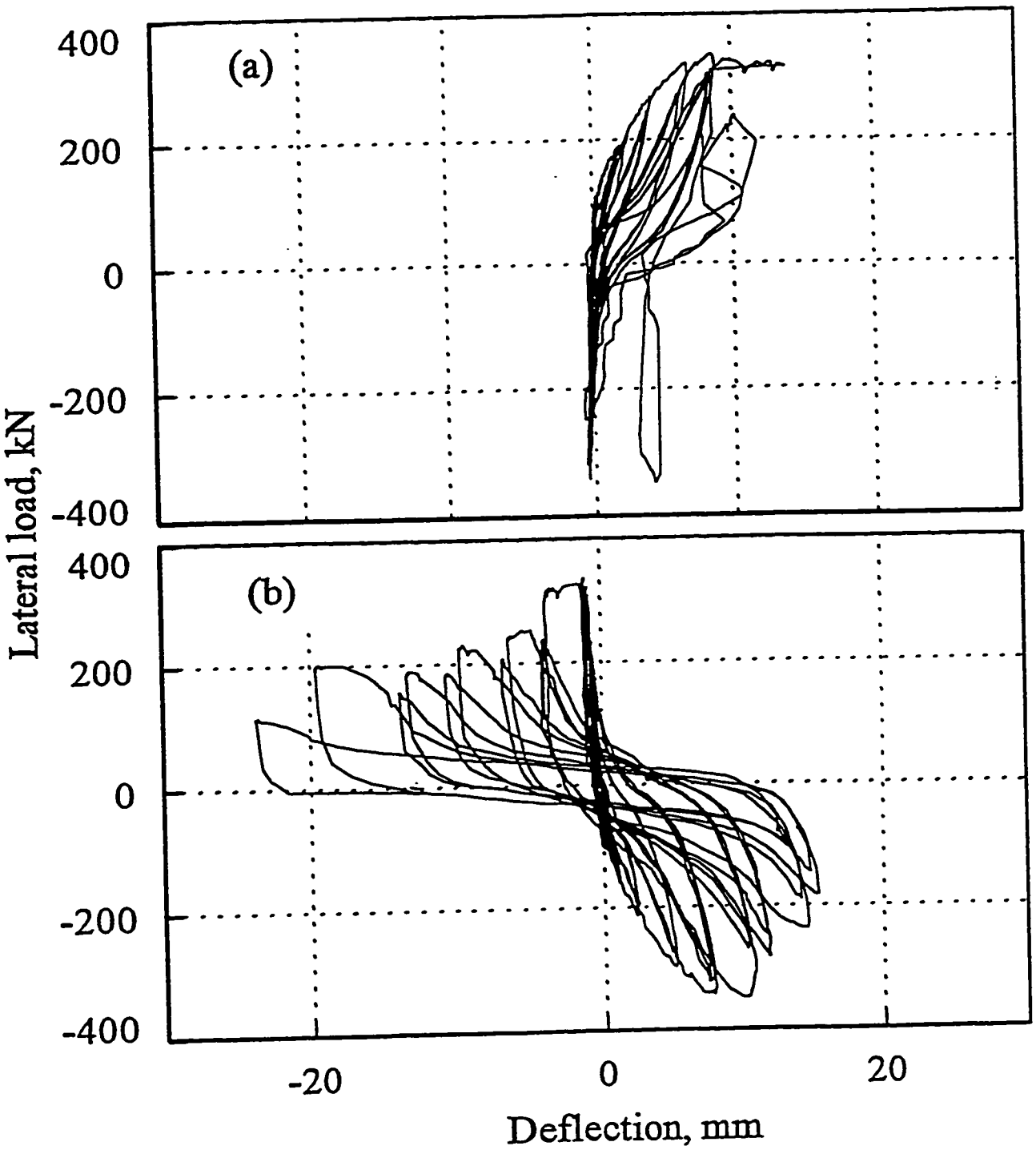

Figure 5.7 Wall 9R: (a) Lateral load-west top-deflection (b) Lateral load-east top-deflection

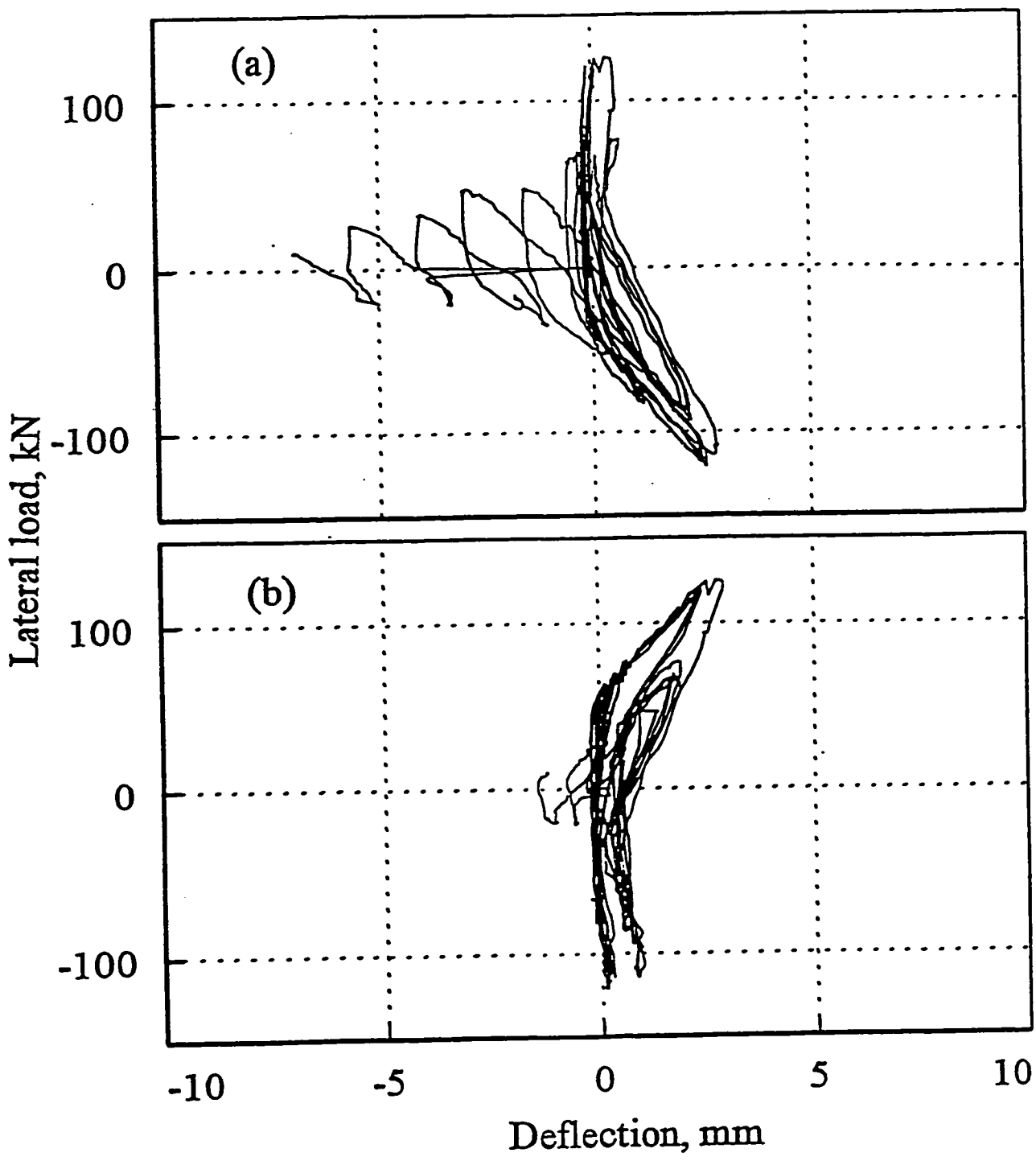

Figure 5.8 Wall 10: (a) Lateral load-west top-deflection (b) Lateral load-east top-deflection

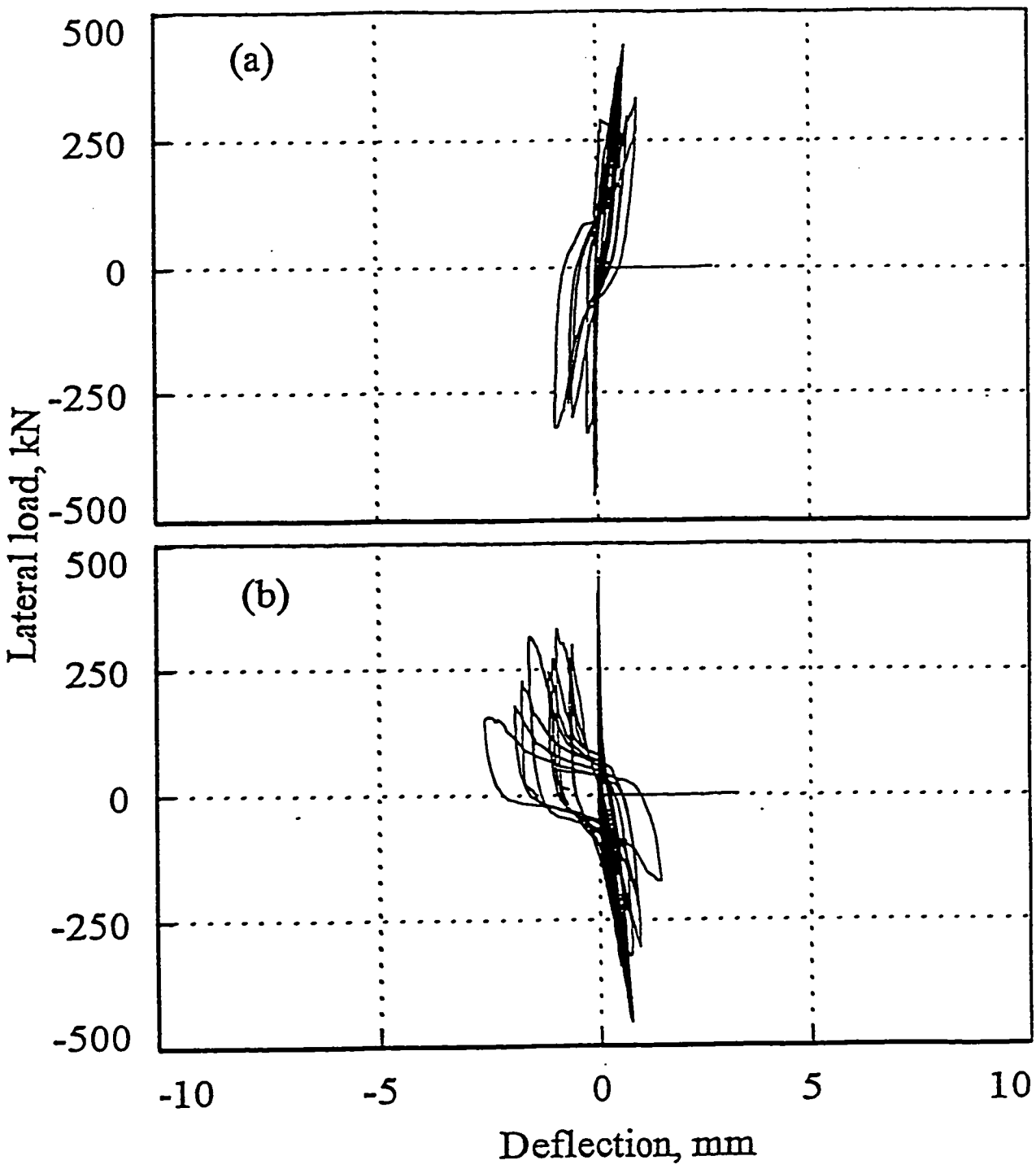

Figure 5.9 Wall 10R: (a) Lateral load-west top-deflection (b) Lateral load-east top-deflection

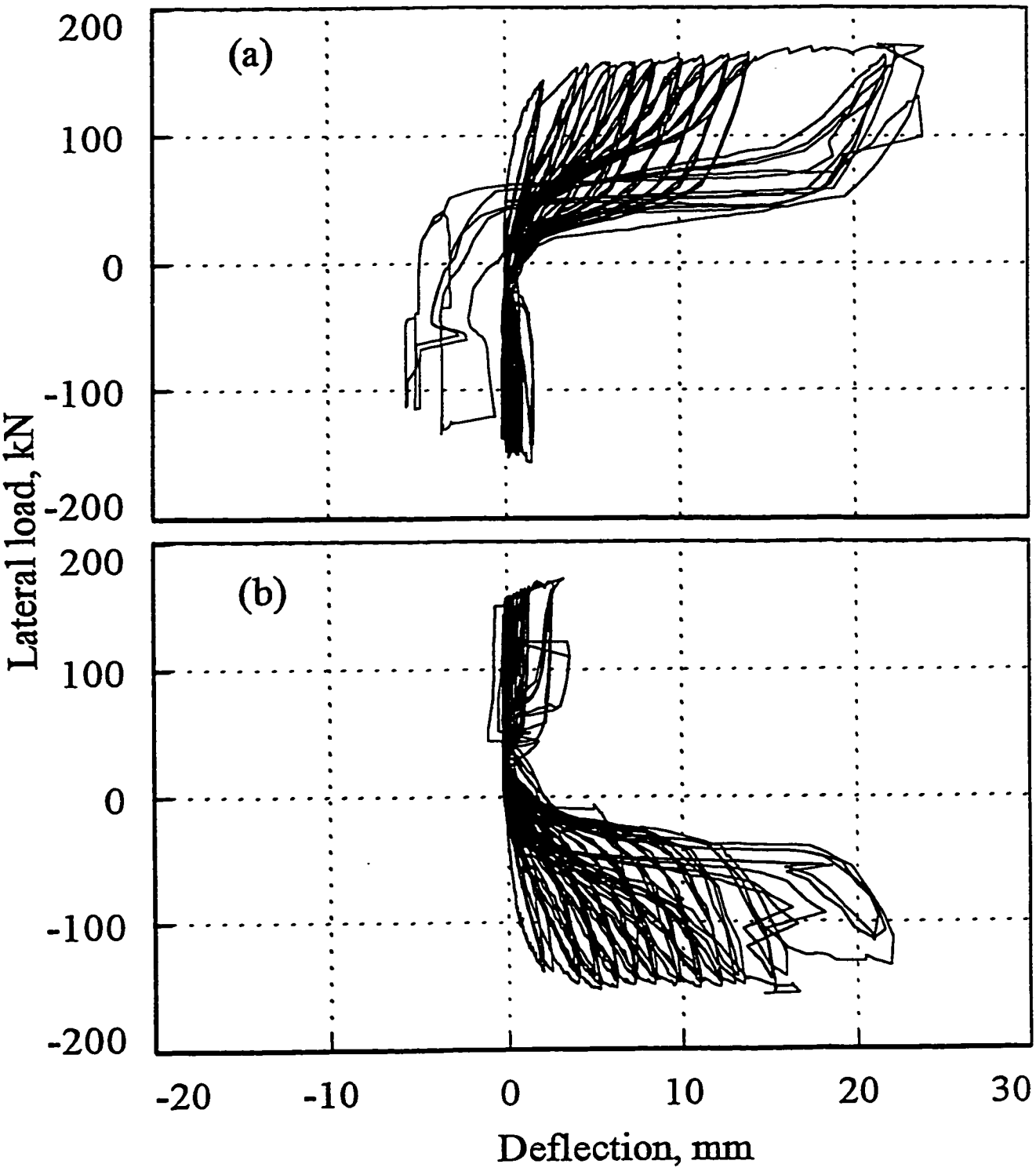

Figure 5.10 Wall 11: (a) Lateral load-west top-deflection (b) Lateral load-east top-deflection

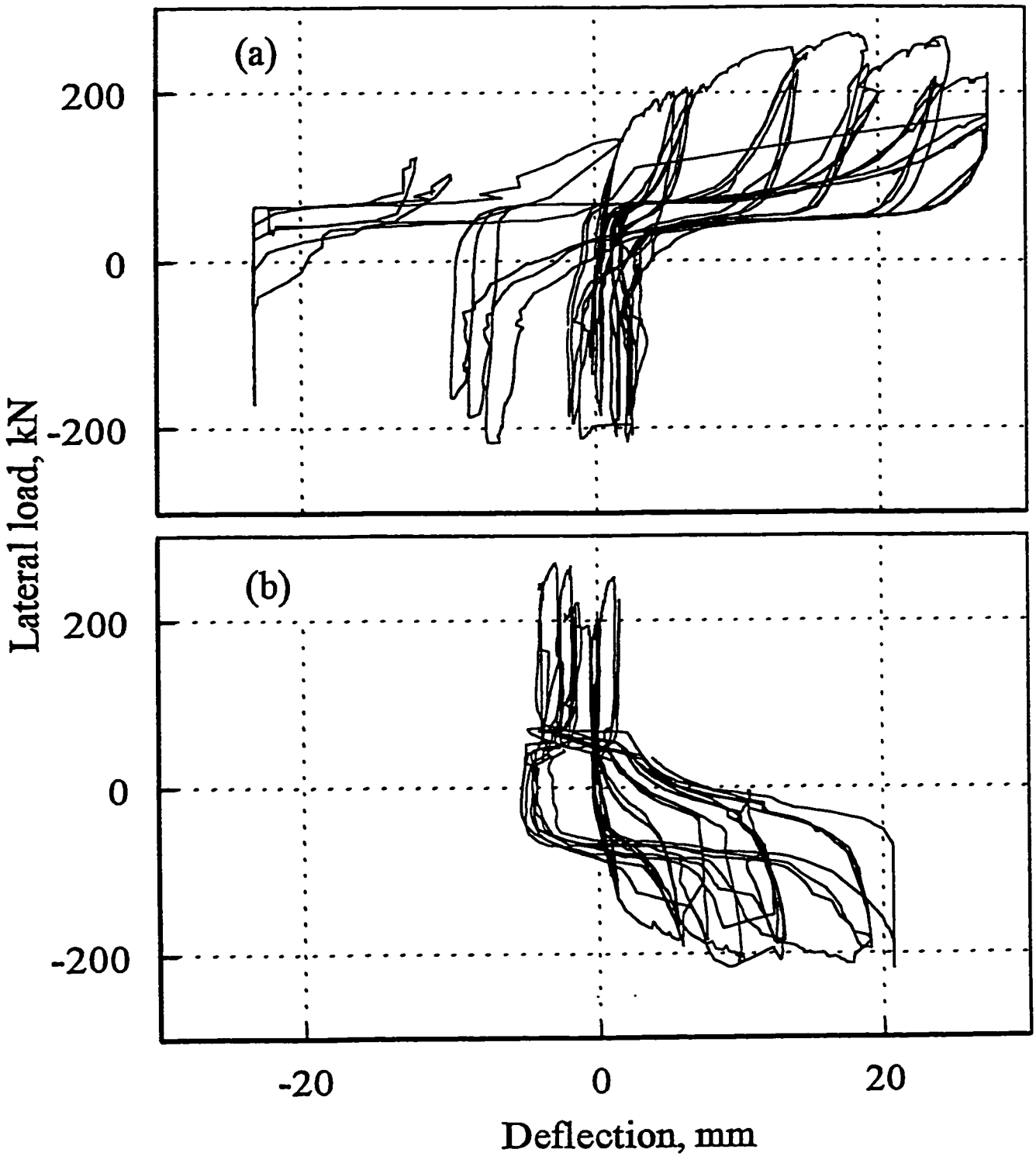

Figure 5.11 Wall 11RP: (a) Lateral load-west top-deflection (b) Lateral load-east top-deflection

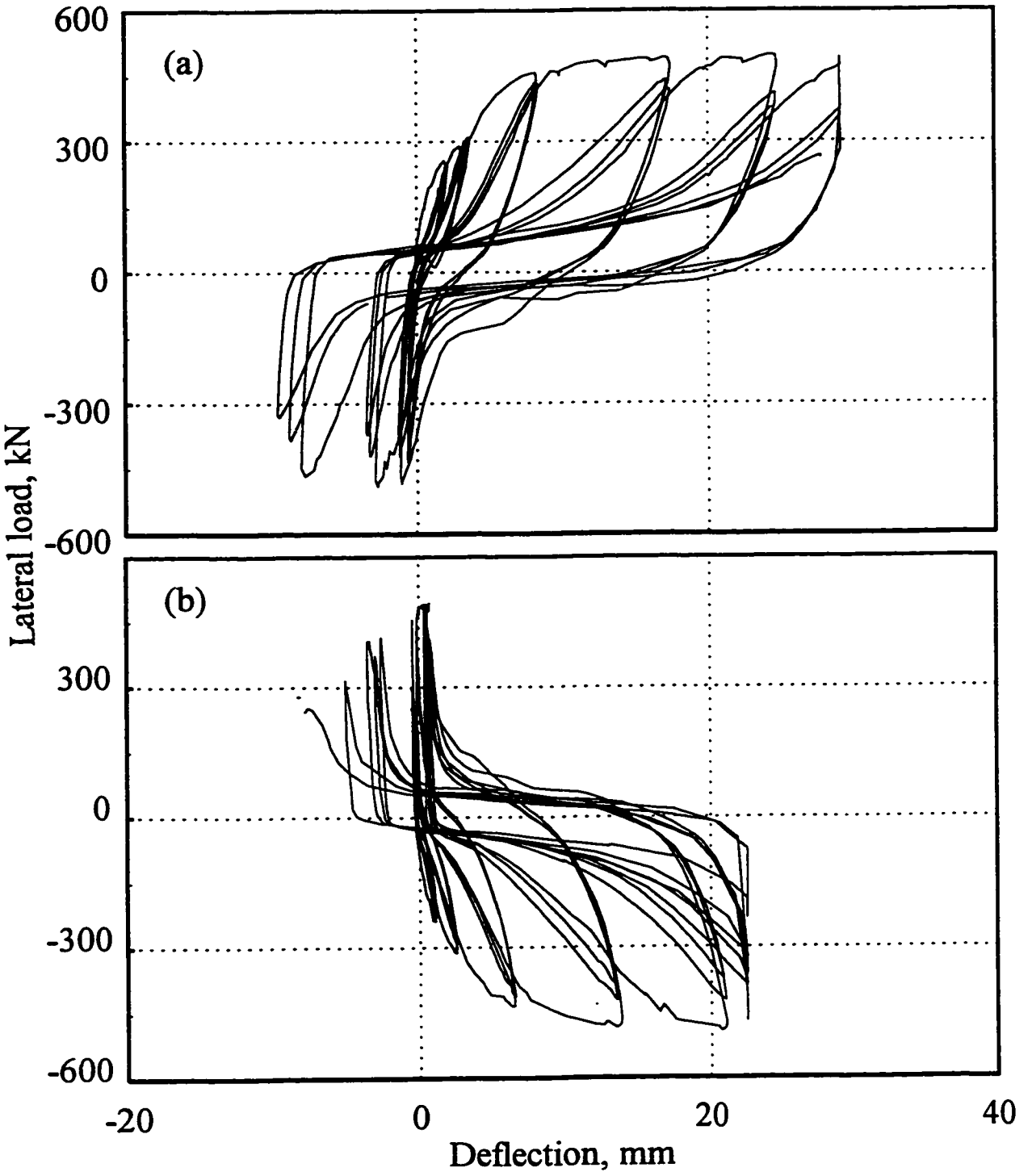

Figure 5.12 Wall 11R: (a) Lateral load-west top-deflection (b) Lateral load-east top-deflection

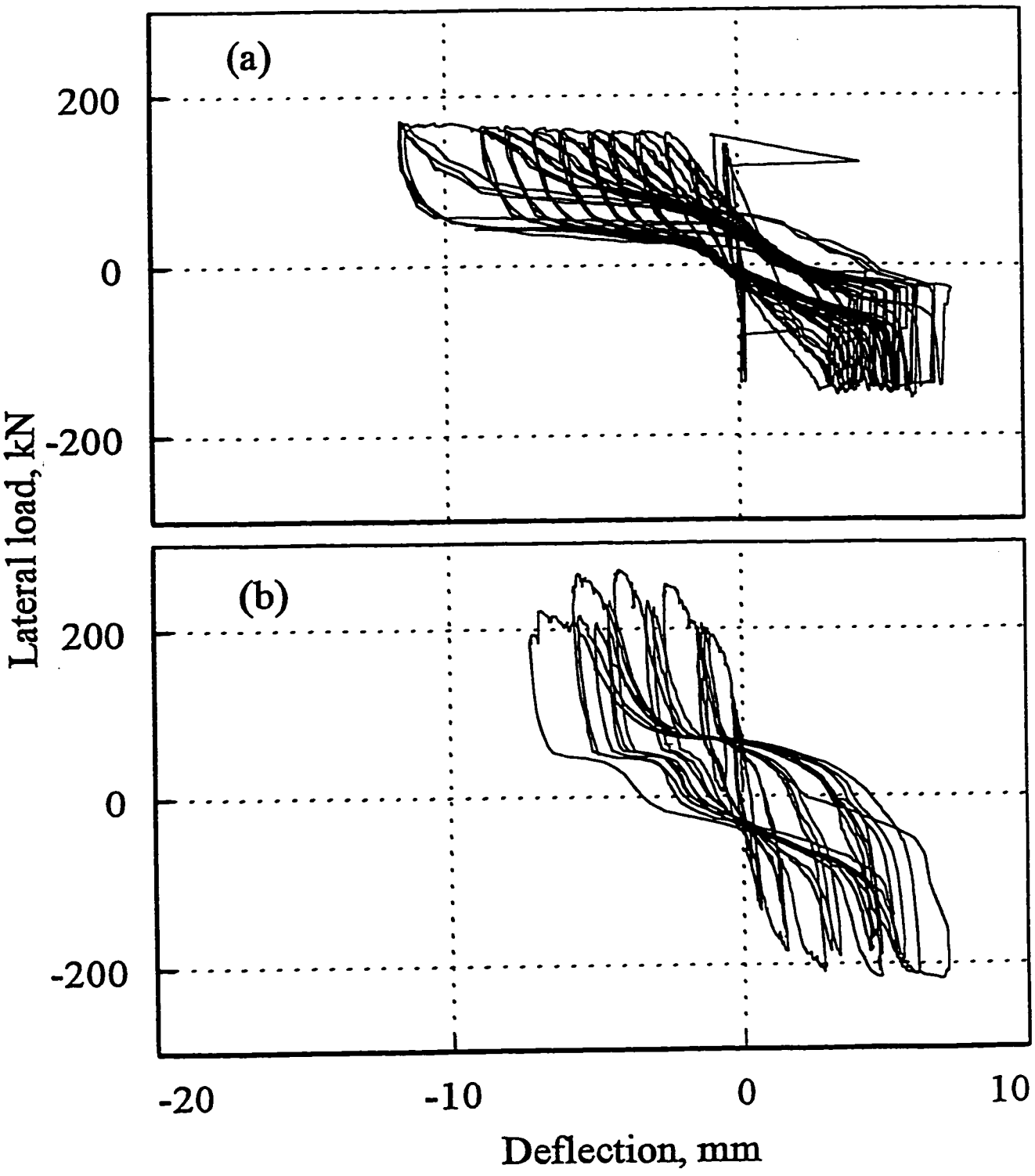

Figure 5.13 Lateral load-base shear sliding for (a) Wall 11 (b) Wall 11RP

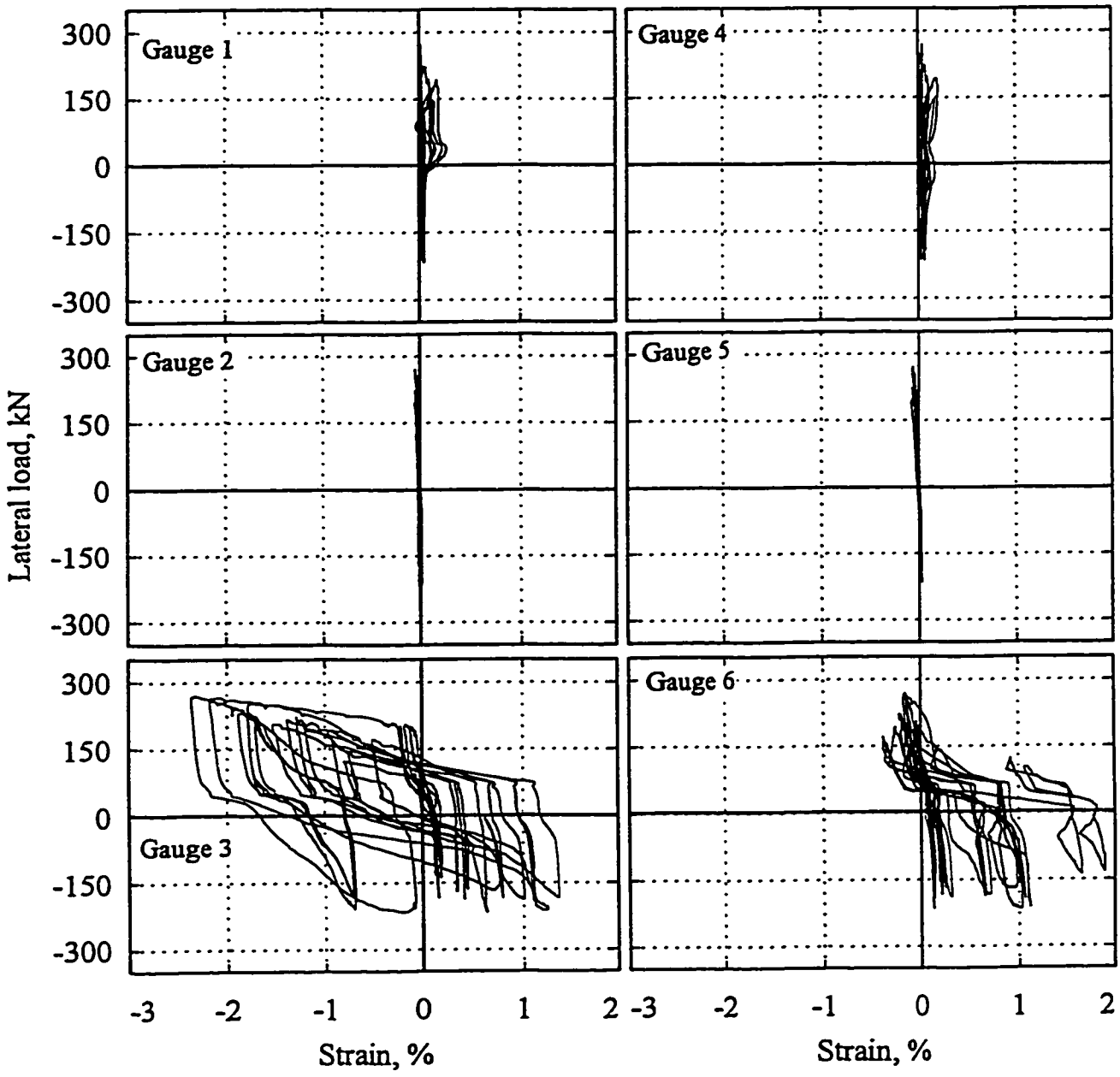

Figure 5.14 Lateral load-strain relationship for vertical steel strips of Wall 11RP

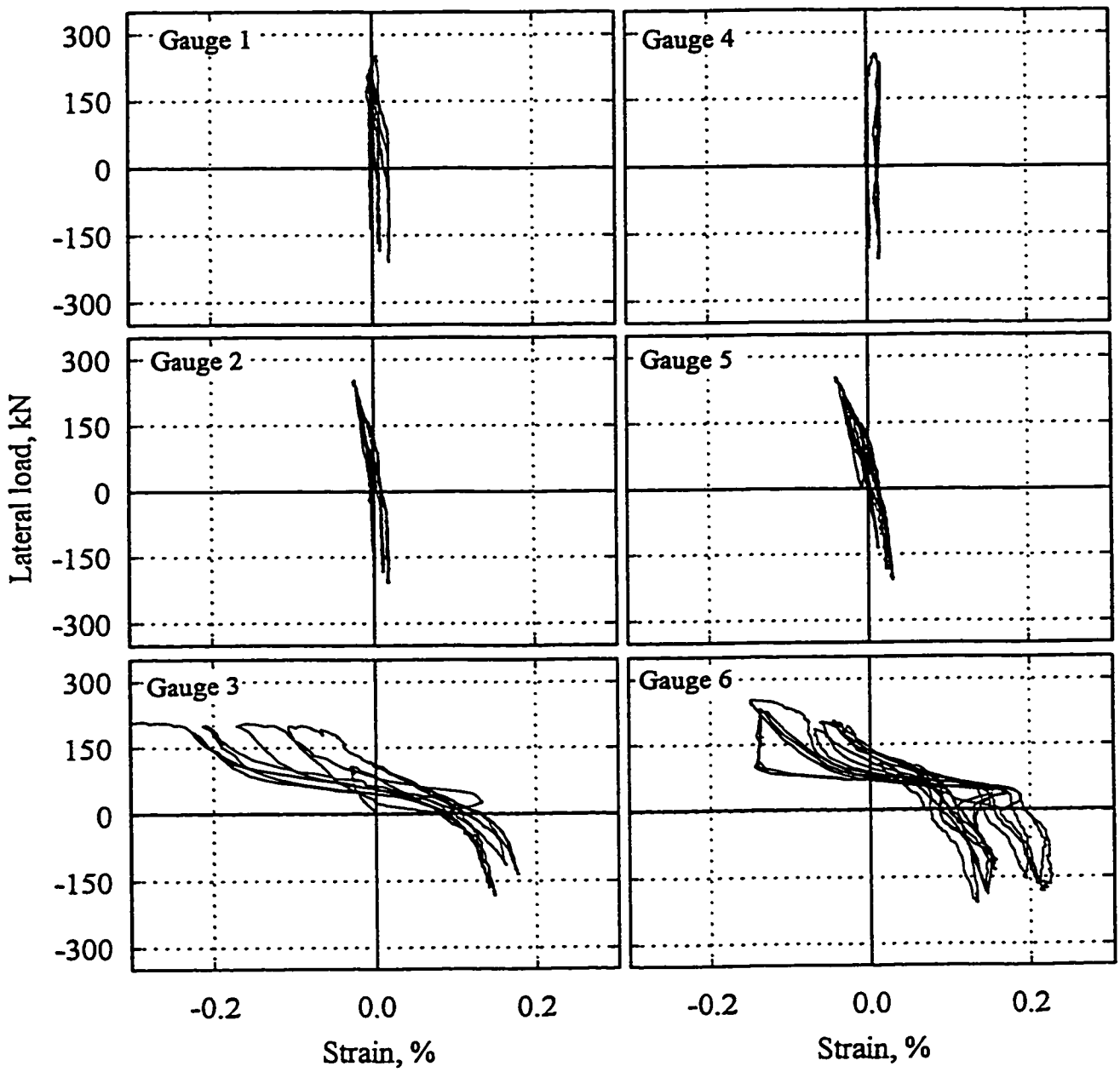

Figure 5.15 Load-strain relationship for vertical steel strips of Wall 11RP

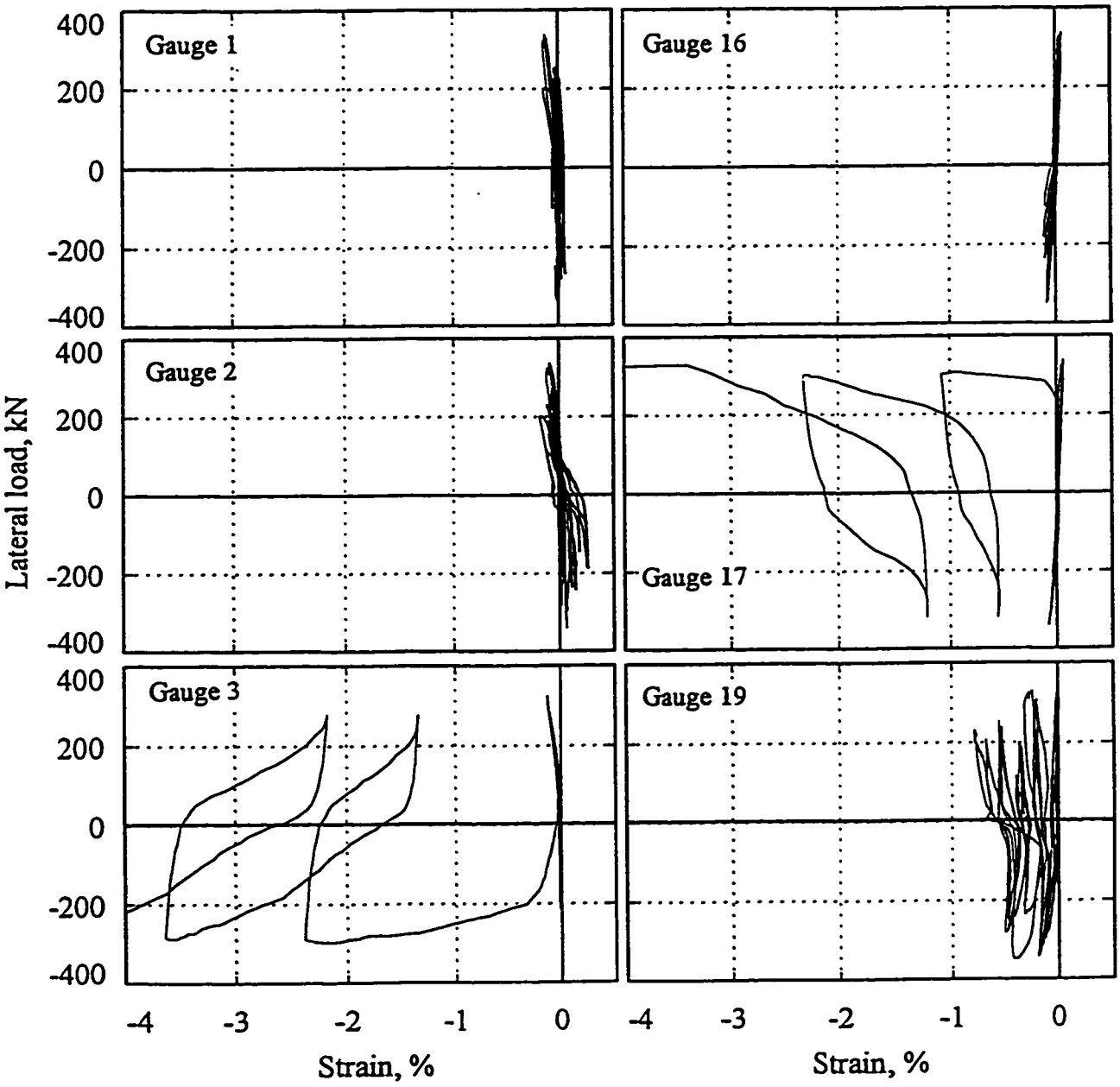

Figure 5.16 Load-strain relationship for vertical steel strips of Wall 9R

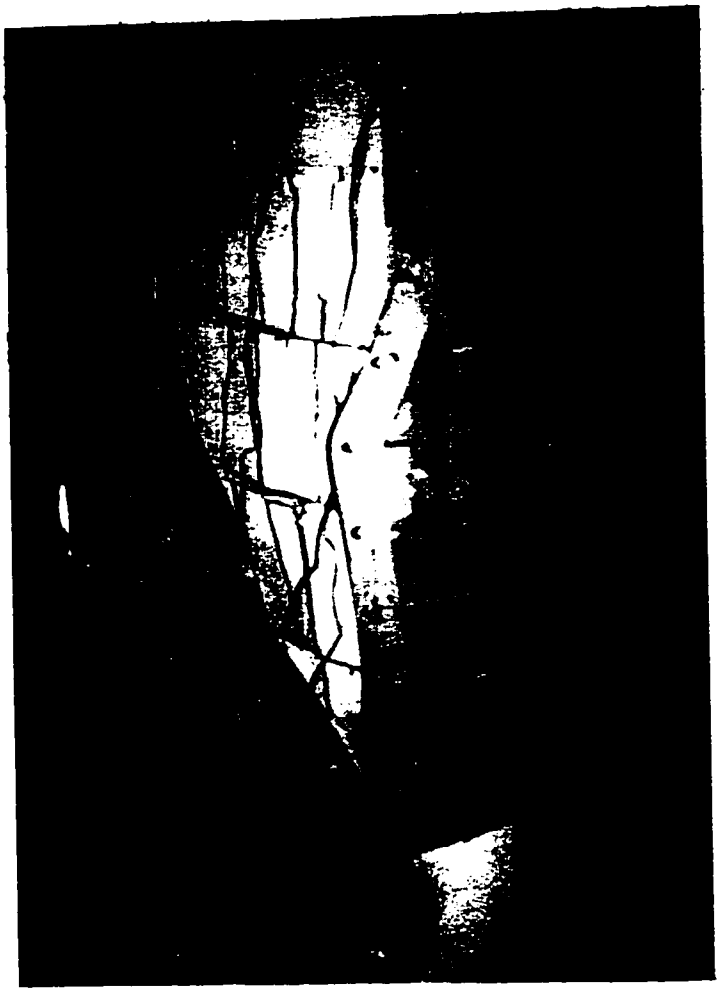

Figure 5.17 Strain gauge 3 glued on top of a plastic hinge due to buckling of vertical steel strip (Wall 9R)

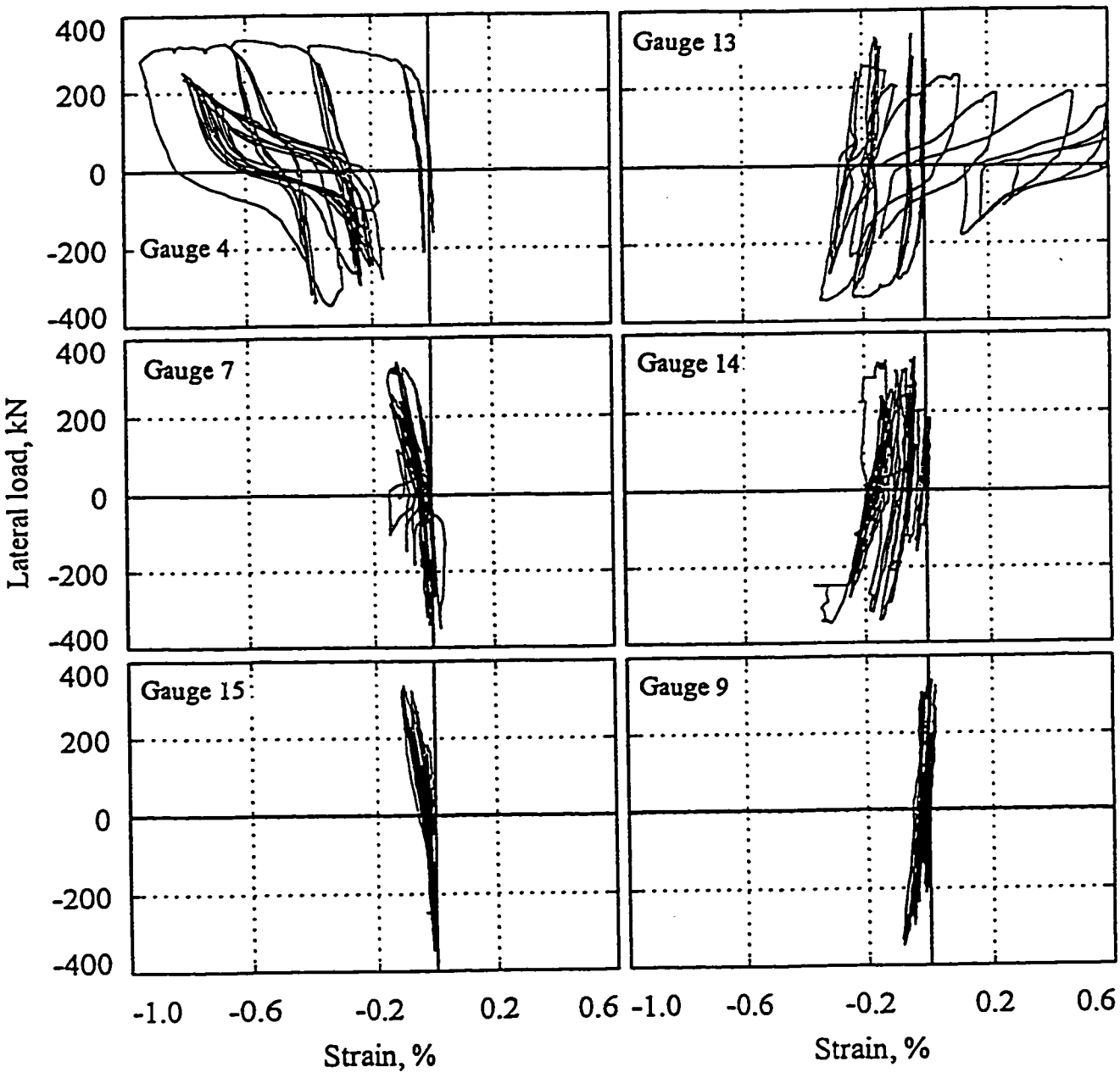

Figure 5.18 Lateral load-strain relationship for diagonal steel strips for Wall 9R

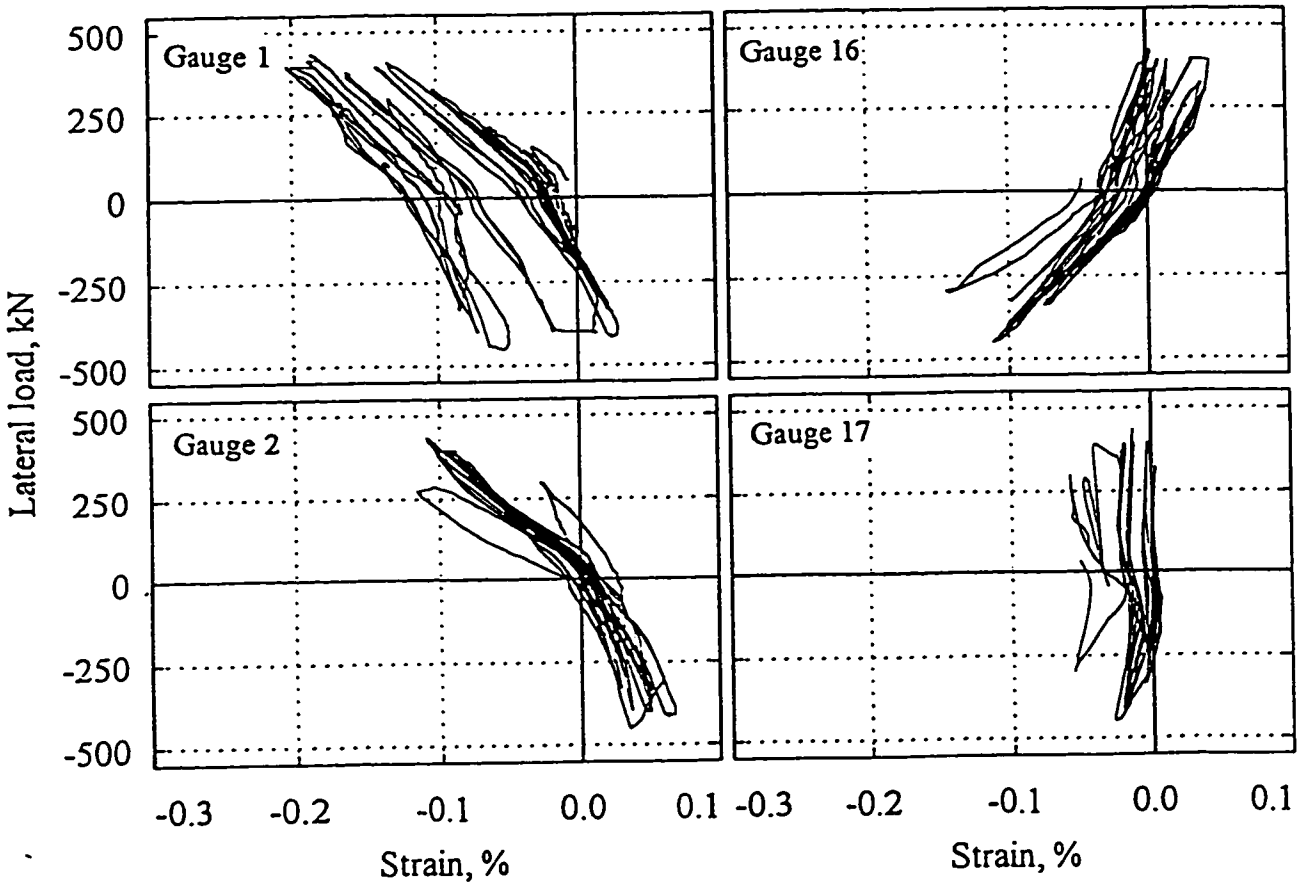

Figure 5.19 Load-strain relationship for vertical steel strips of Wall 10R

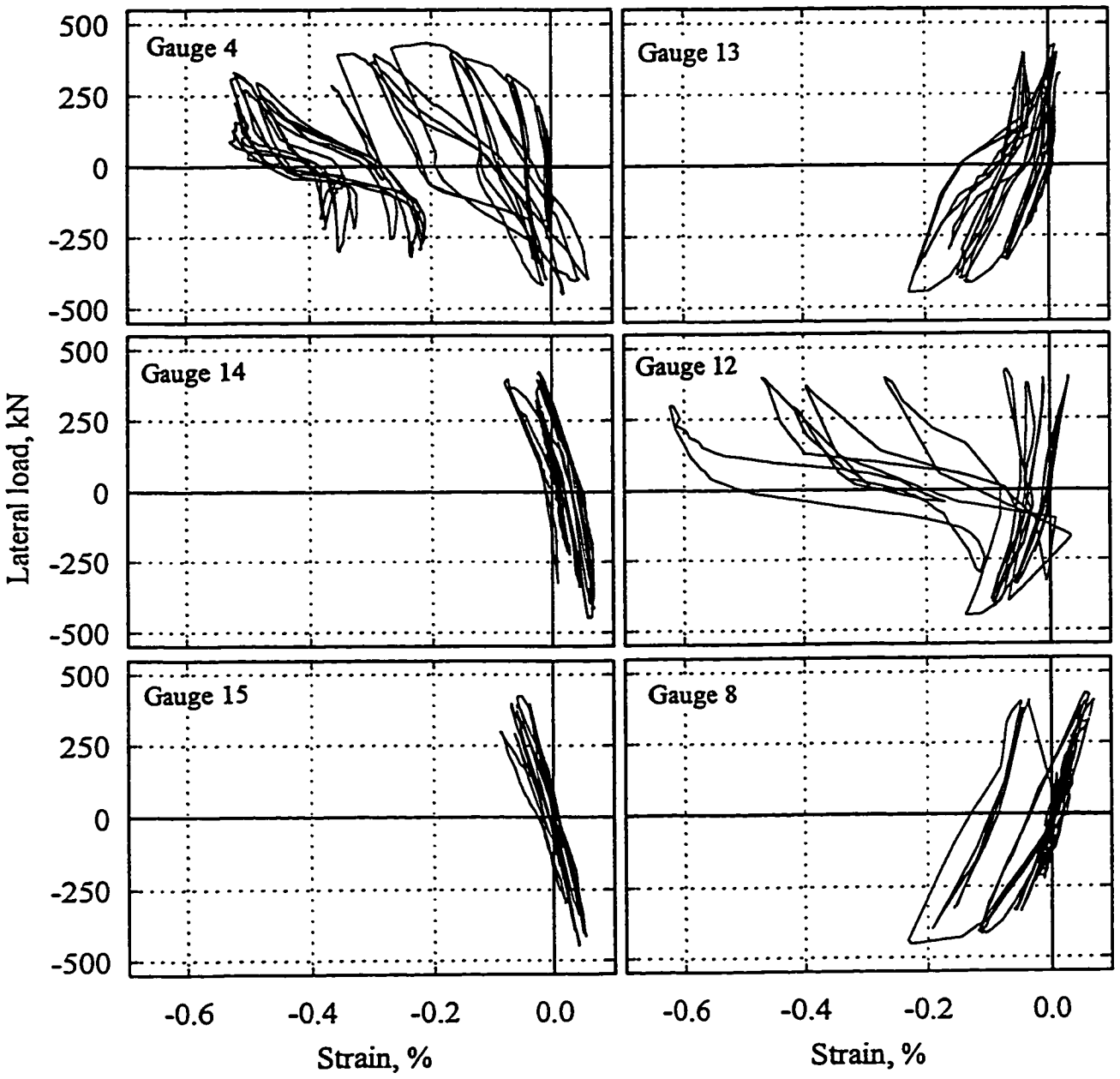

Figure 5.20 Load-strain relationship for diagonal steel strips for Wall 10R

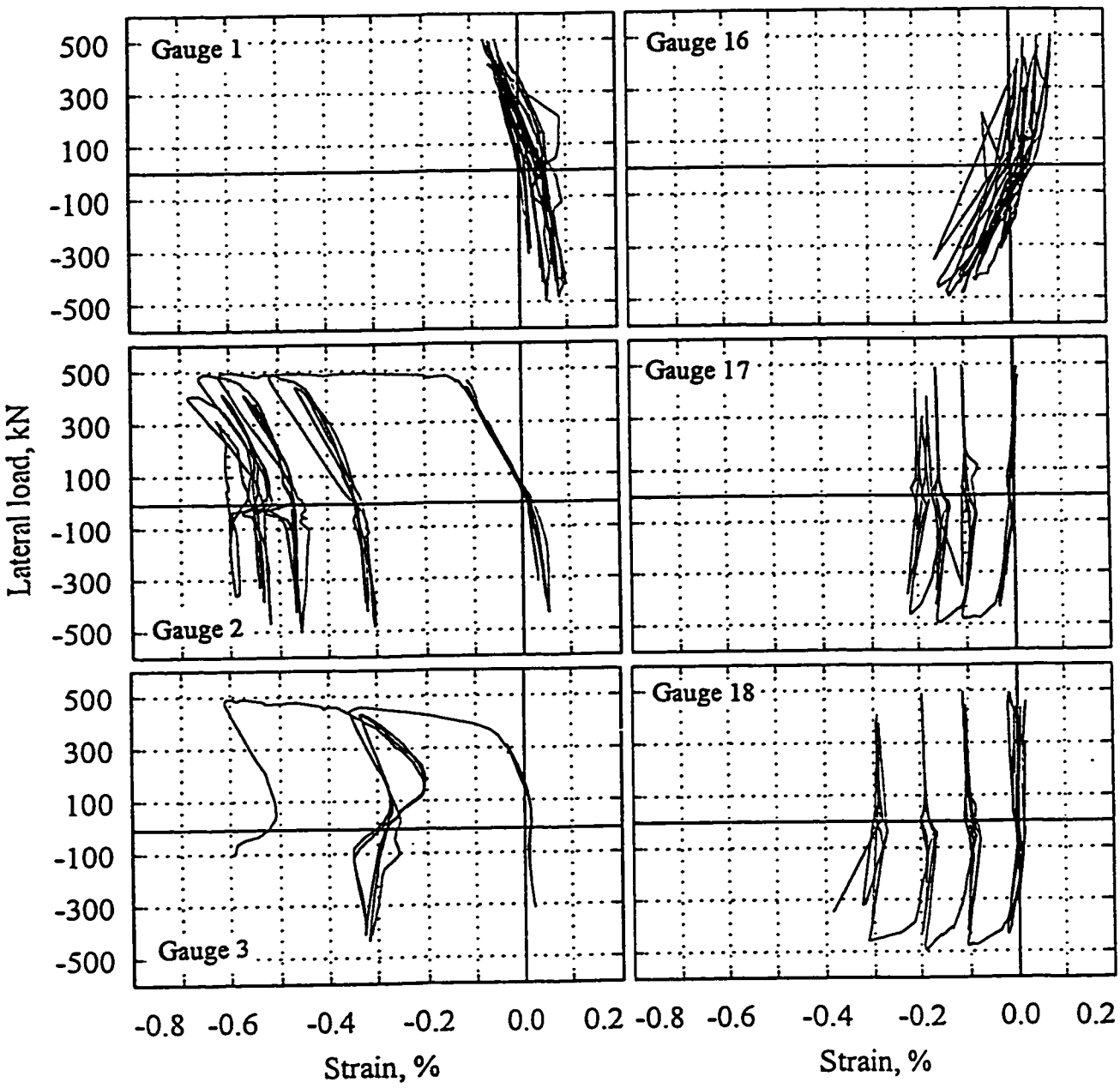

Figure 5.21 Load-strain relationship for vertical steel strips of Wall 11R (2713 point data)

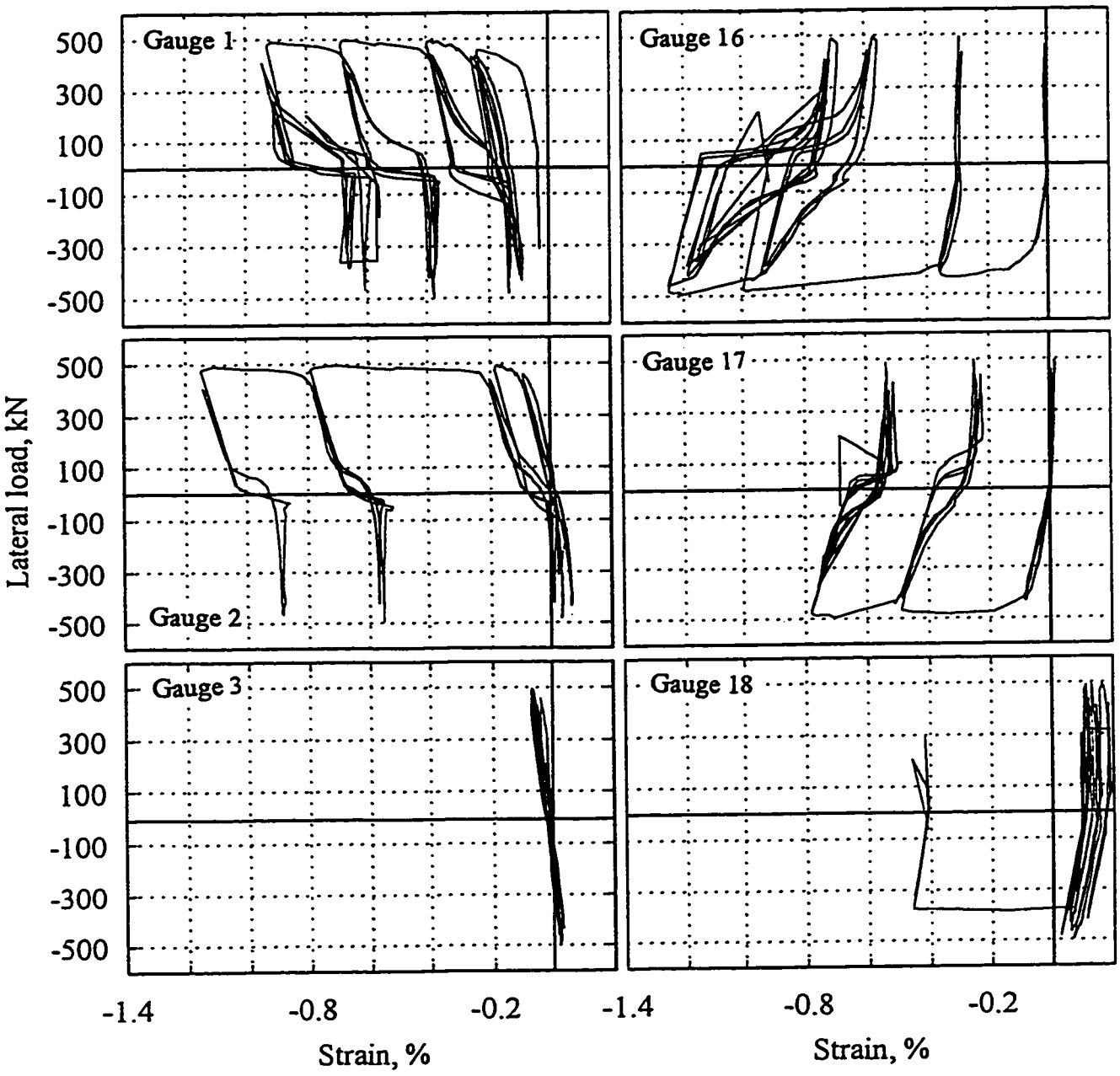

Figure 5.22 Load-strain relationship for diagonal steel strips of Wall 11R (2713 point data)

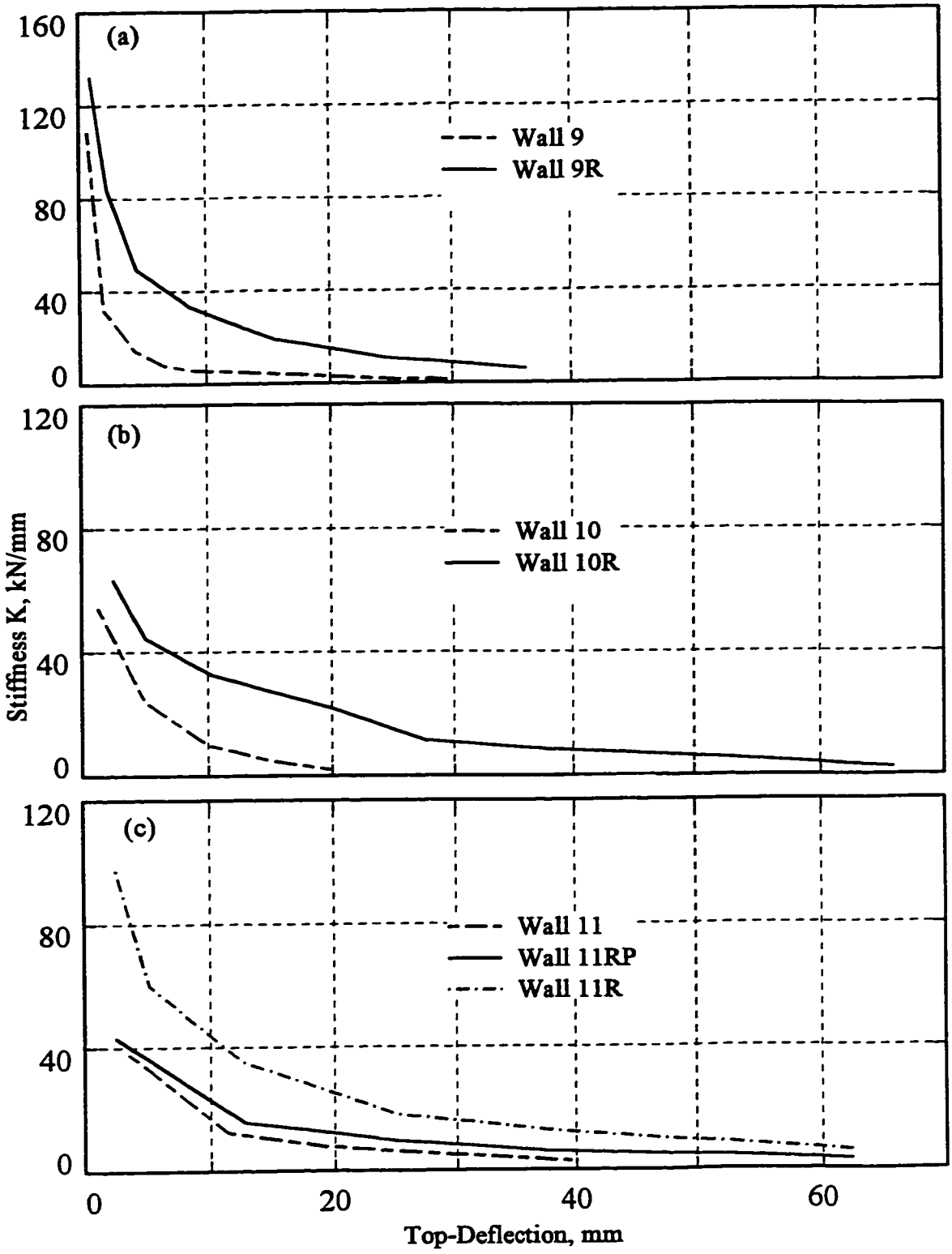

Figure 5.23 Variation in stiffness for (a) Wall 9R and Wall 9
(b) Wall 10R and Wall 10
(c) Wall 11R, Wall 11RP and Wall 11

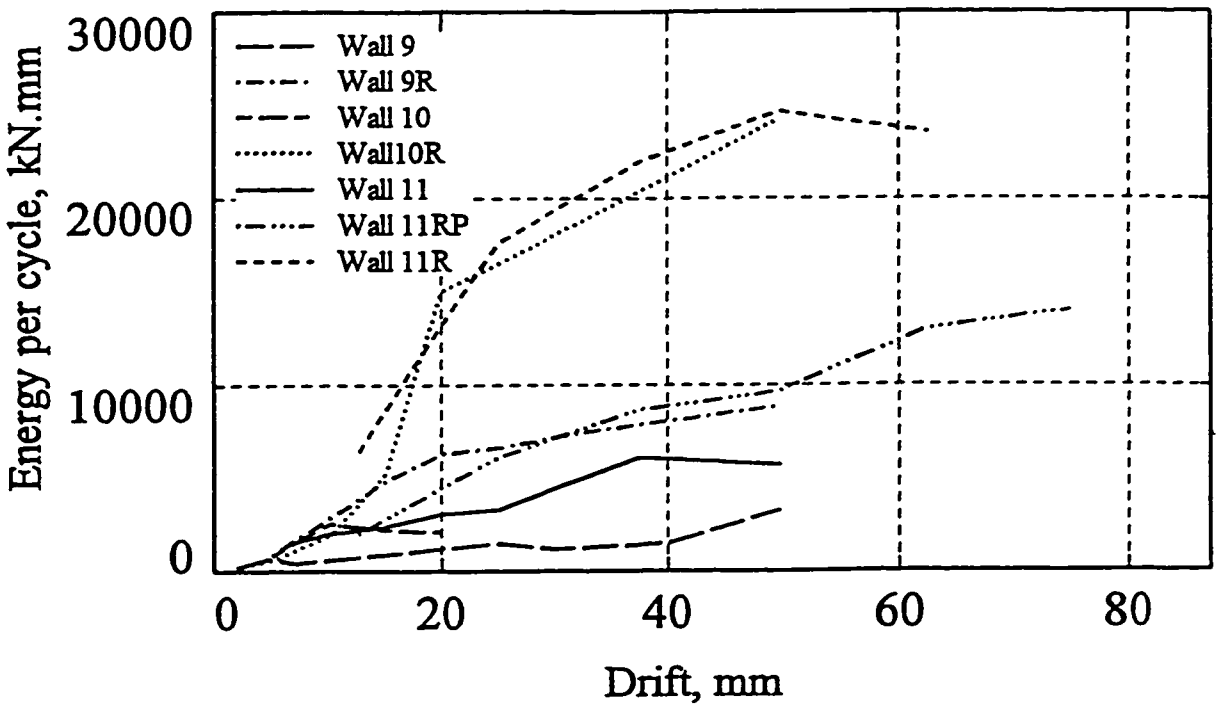

Figure 5.24 Energy dissipated at each hysterisis loop first cycle at each drift level

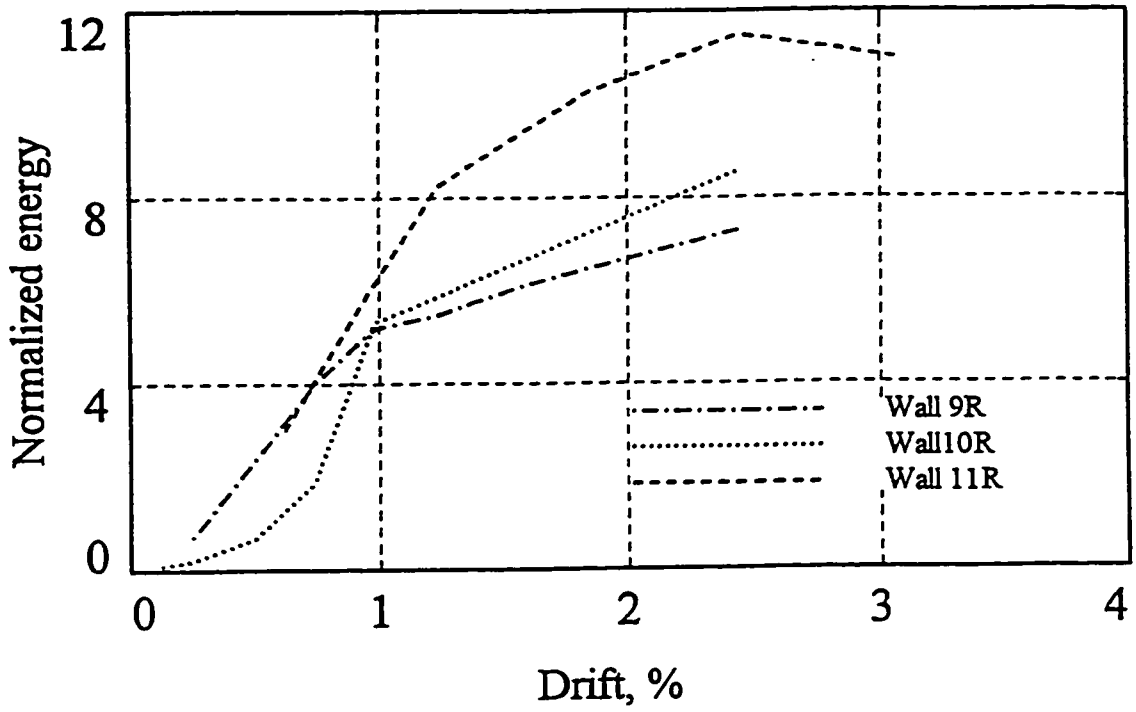

Figure 5.25 Normalized energy for retrofitted walls

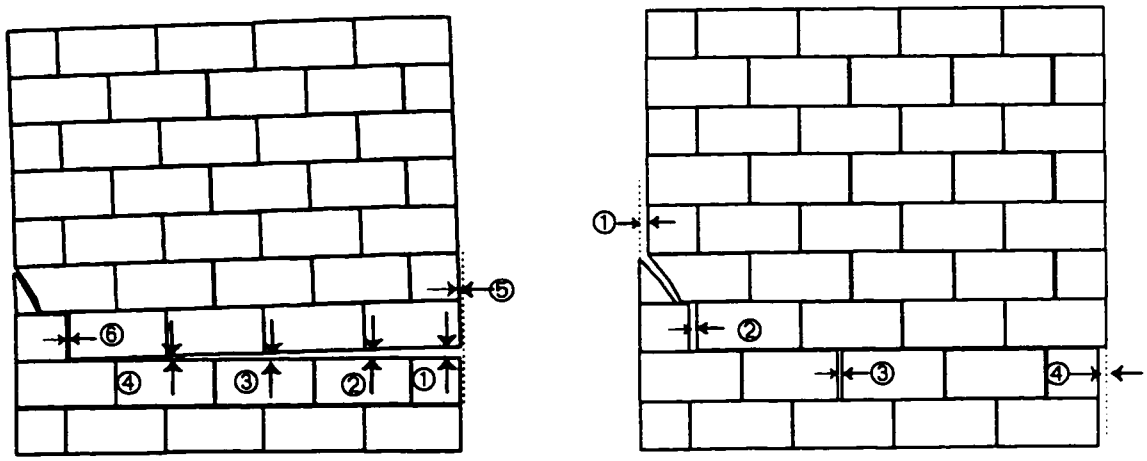

Figure 5.26 Cracking width for Wall 9 at lower drifts

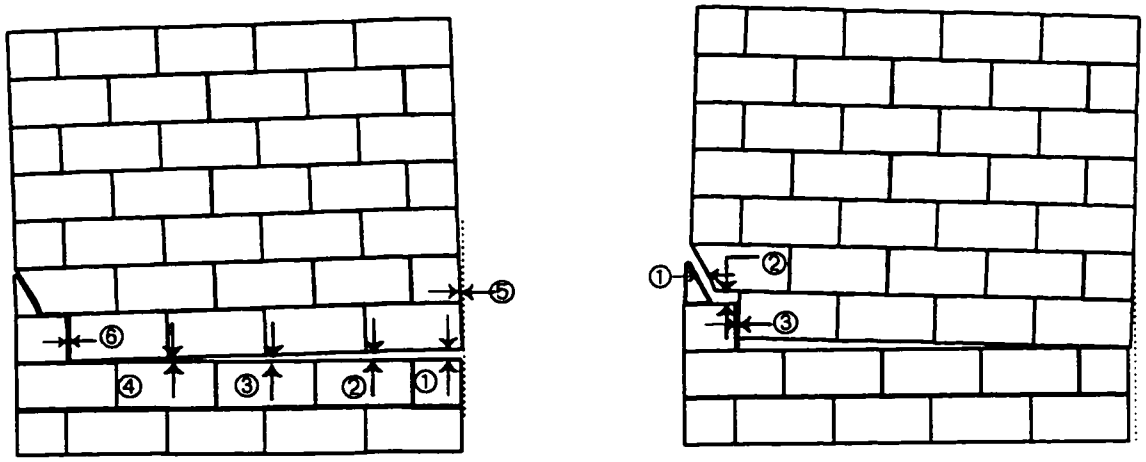

Figure 5.27 Cracking width for Wall 9 at higher drifts

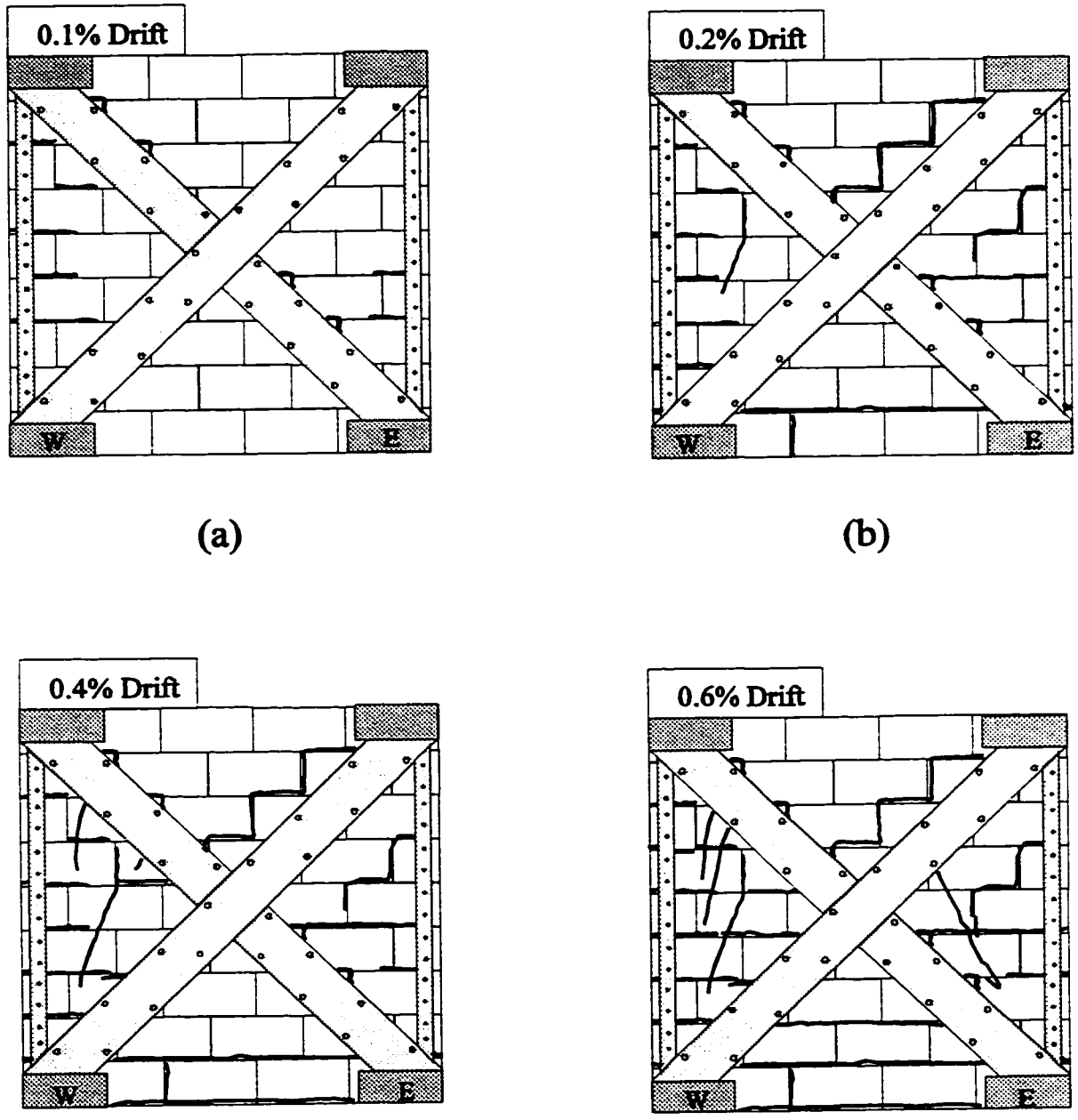

Figure 5.28 Cracking pattern for Wall 9R

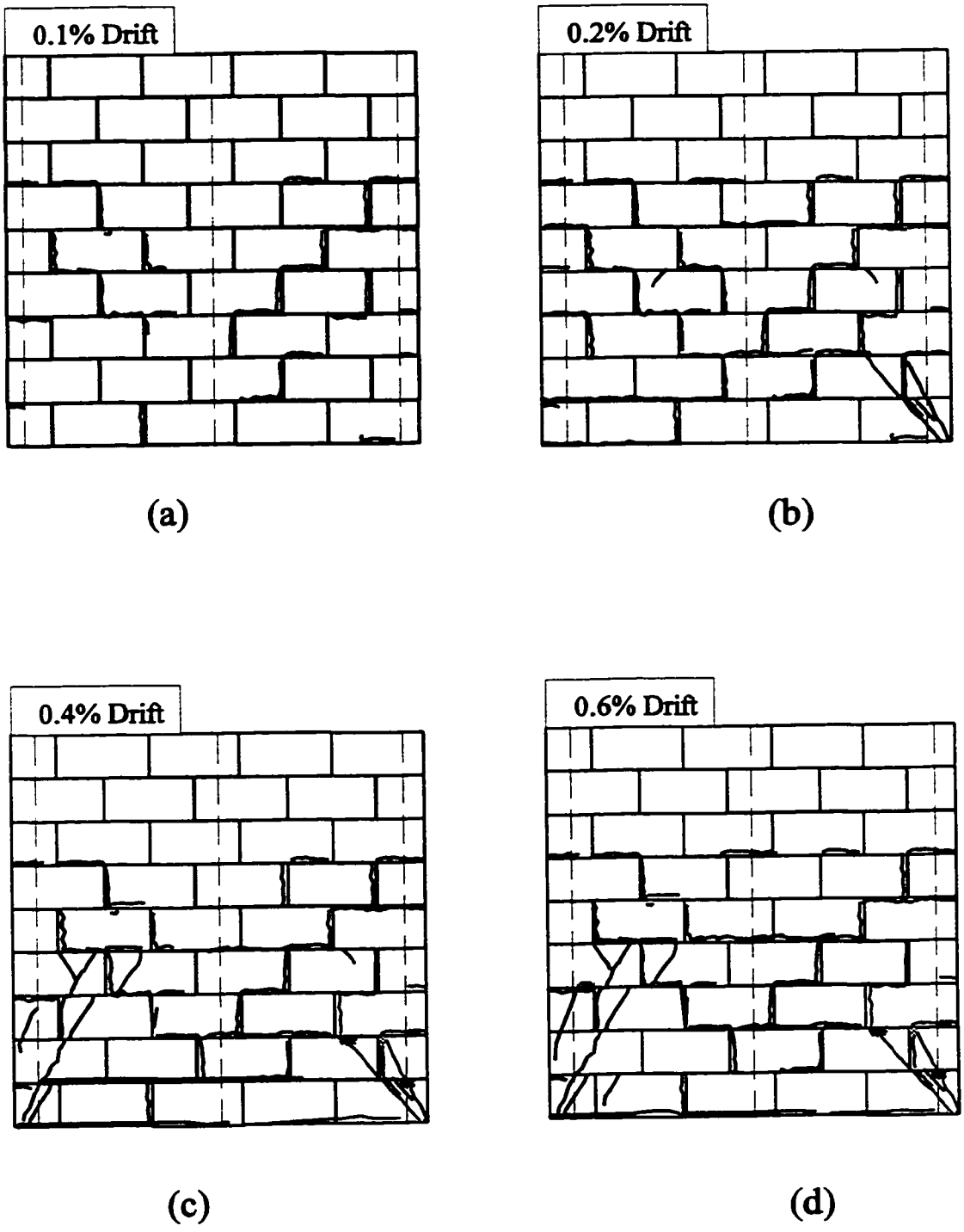

Figure 5.29 Cracking pattern for Wall 10

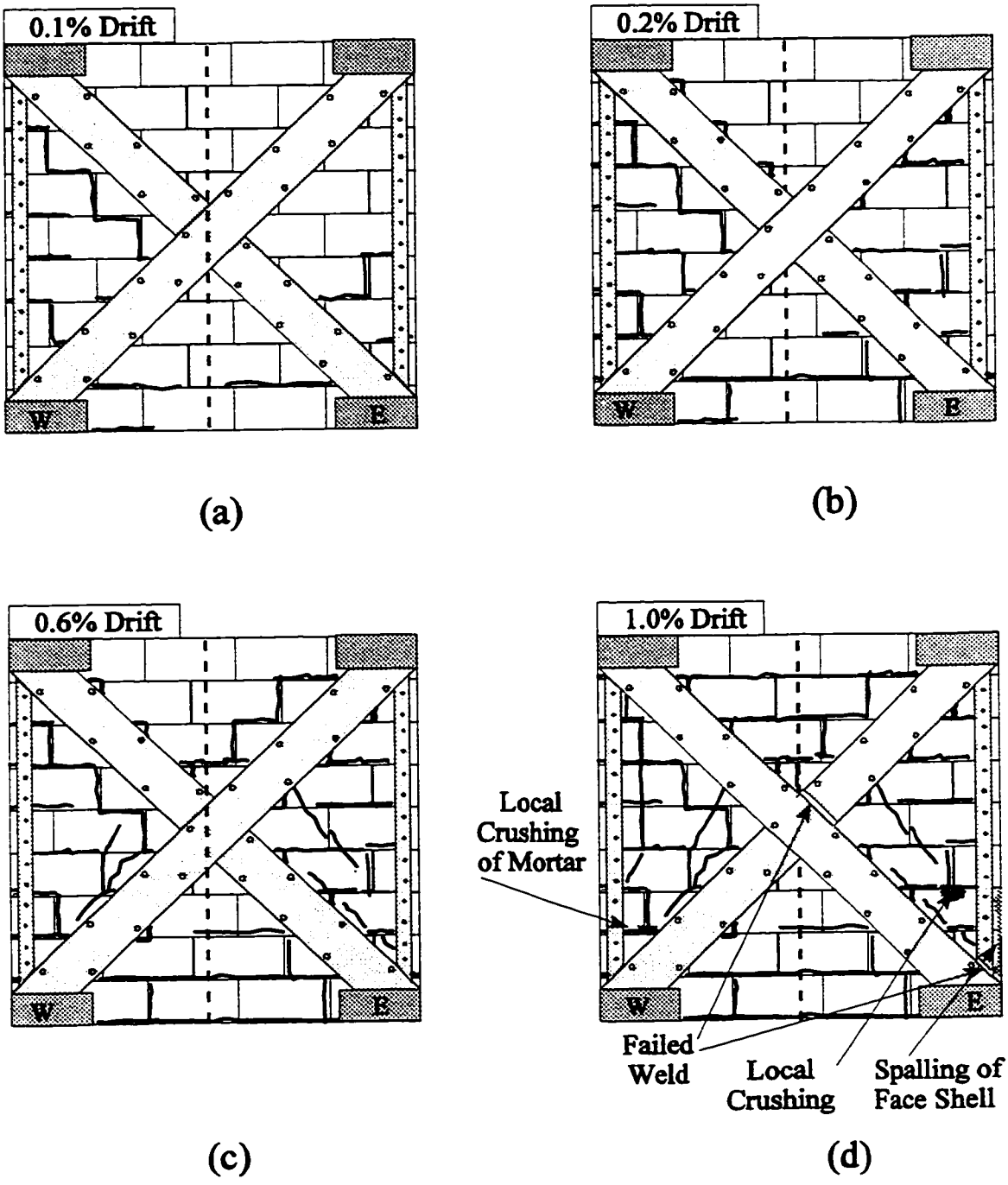

Figure 5.30 Cracking pattern for Wall 10R

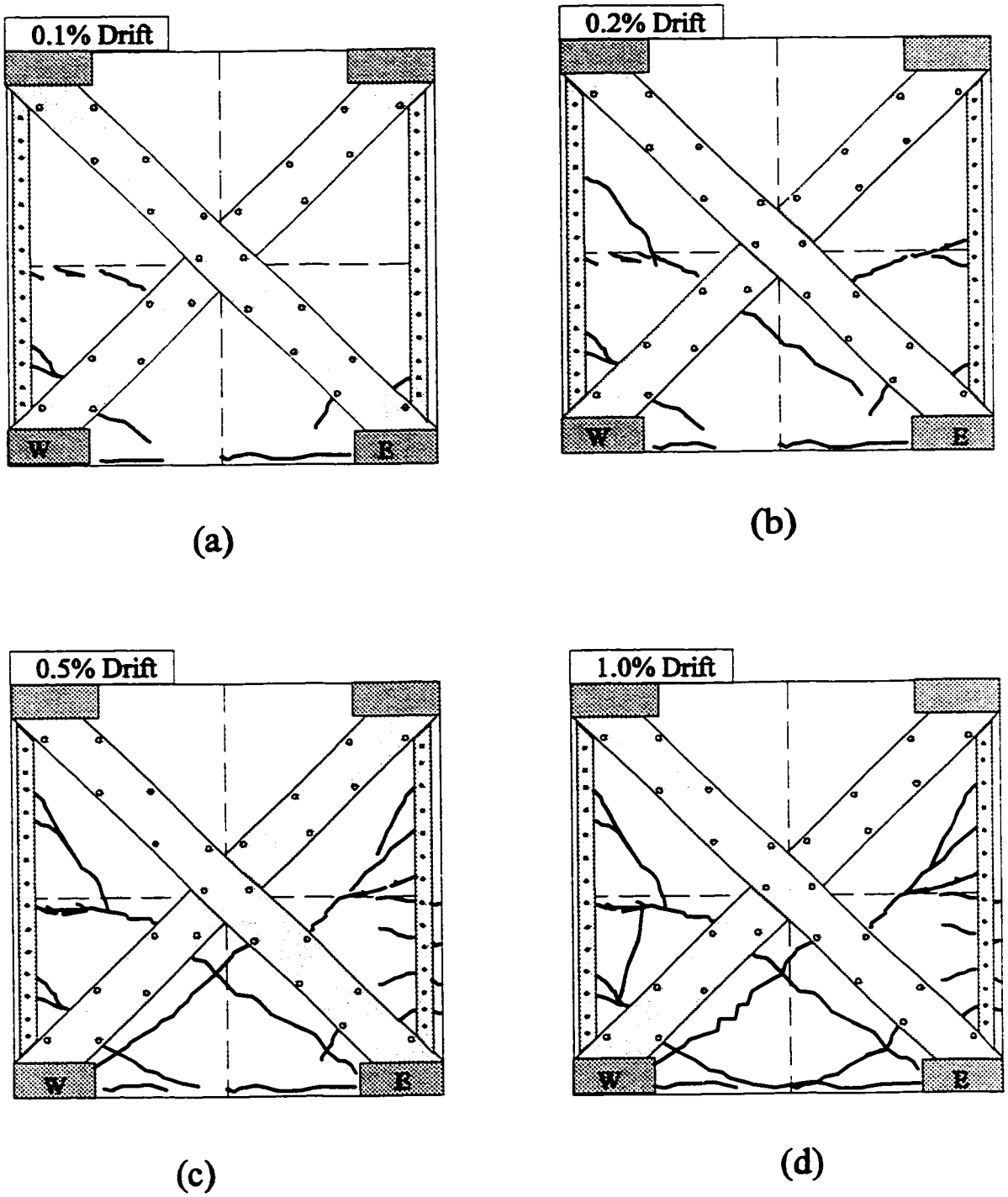

Figure 5.31 Cracking pattern for Wall 11R

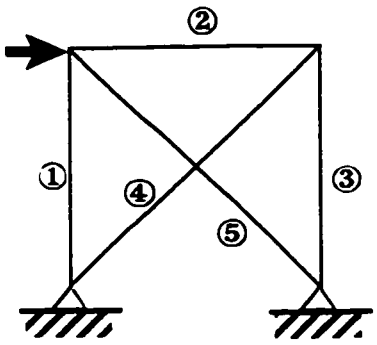

- 1 Vertical tension member
- 2 Rigid horizontal member
- 3 Vertical strut member
- 4 Diagonal tension member
- 5 Diagonal strut member

(a)

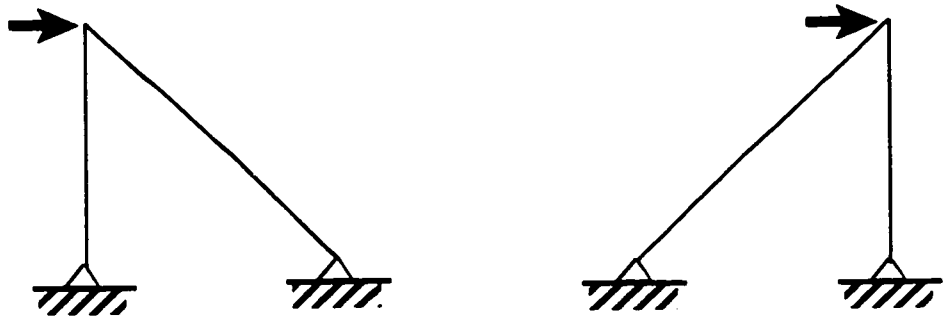

(b)

Figure 6.1 Simplified truss model

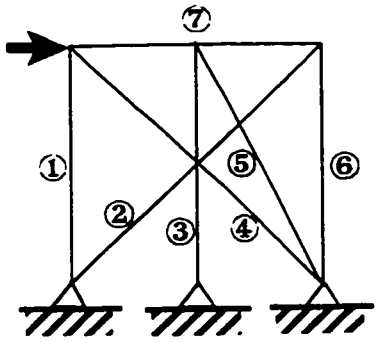

- 1 Vertical tension member
- 2 Diagonal tension member
- 3 Vertical tension member
- 4 Diagonal strut member
- 5 Diagonal strut member
- 6 Vertical strut member
- 7 Rigid horizontal member

Figure 6.2 Improved truss model

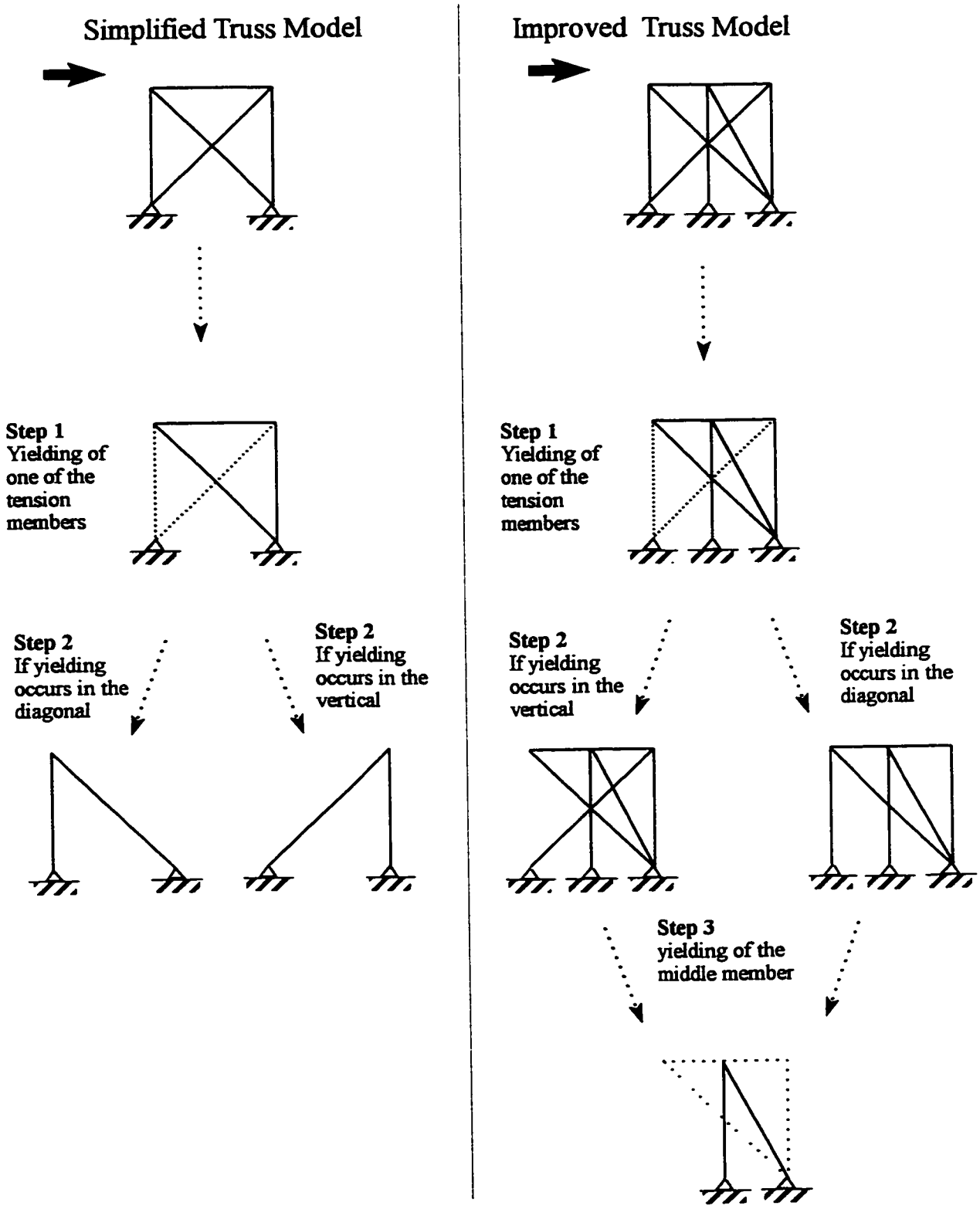

Figure 6.3 Yielding sequence of tension members in both truss model and improved truss model

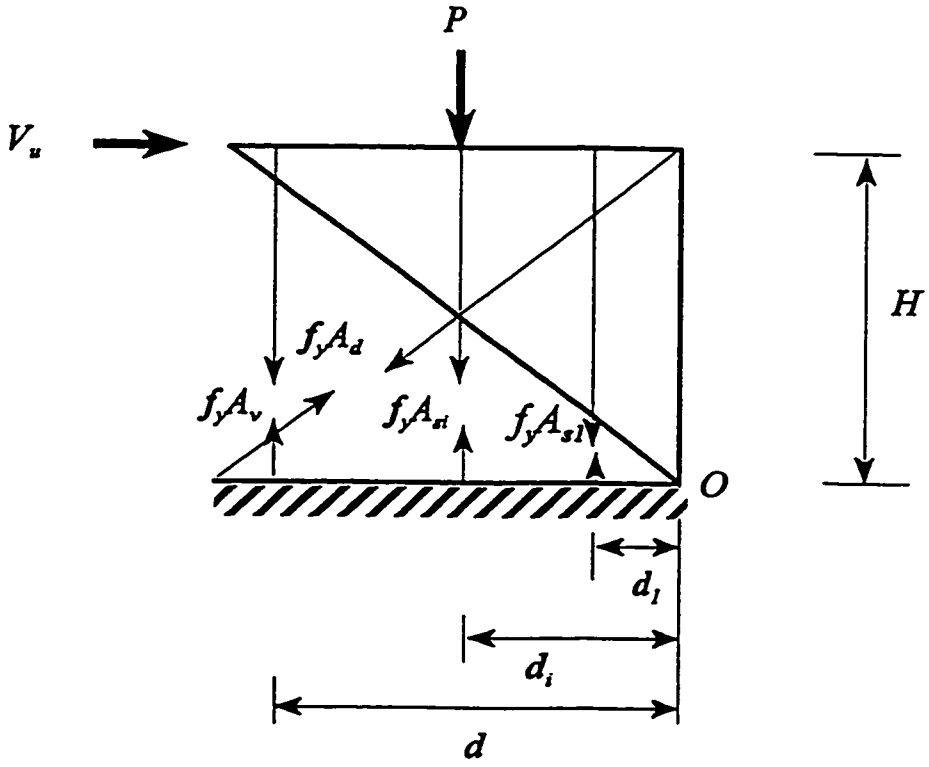

Figure 6.4 Assumed equilibrium for Lower Bound Method

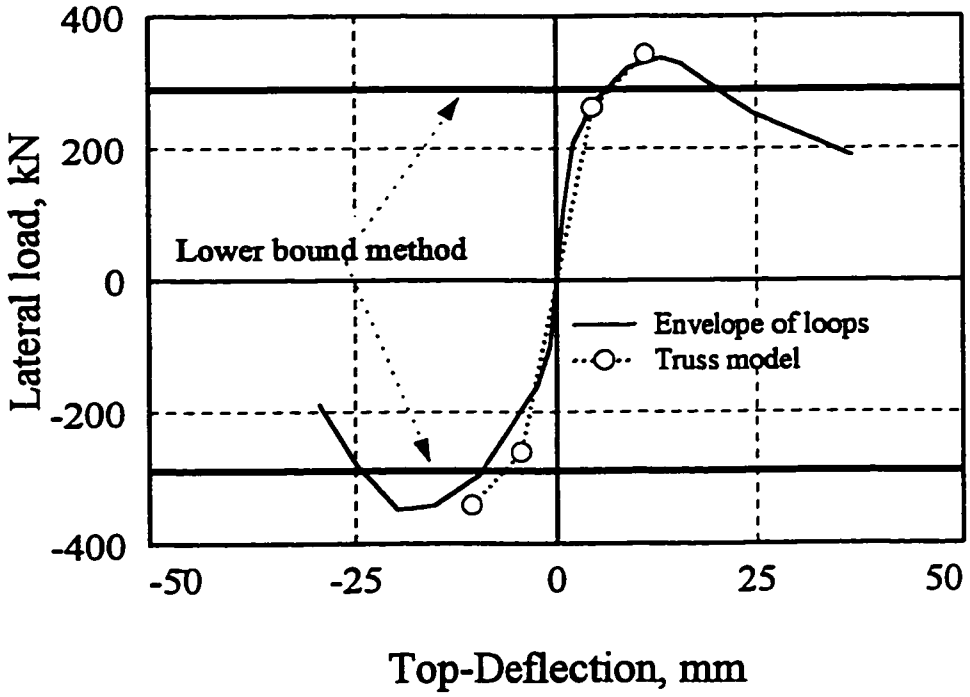

Figure 6.5 Comparison of test results with truss analysis for Wall 9R retrofitted URM

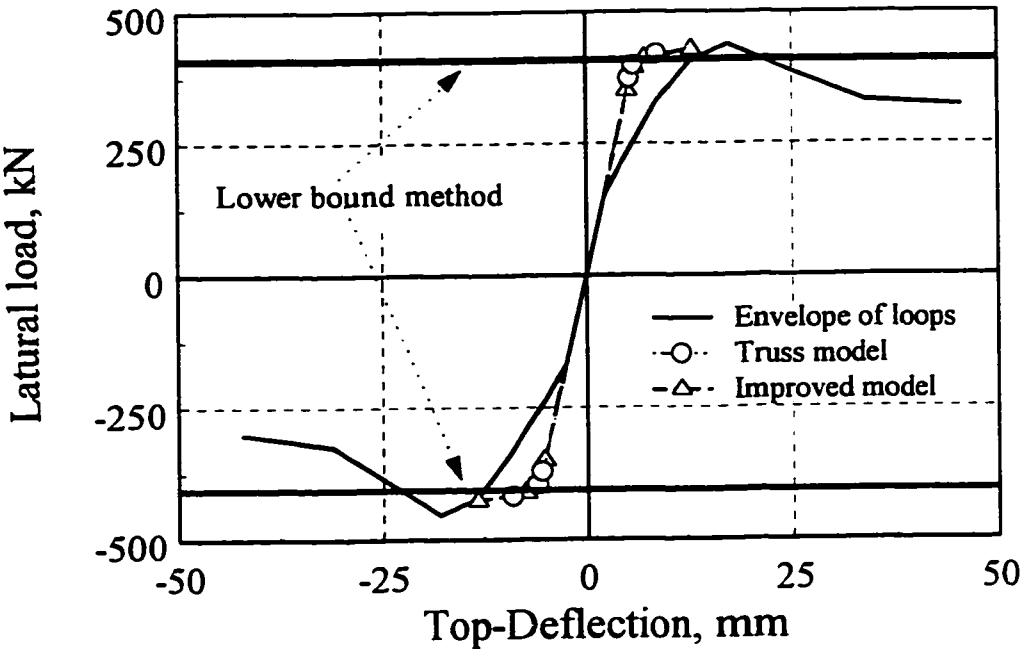

Figure 6.6 Comparison of test results with truss analysis for Wall 10R retrofitted PRM

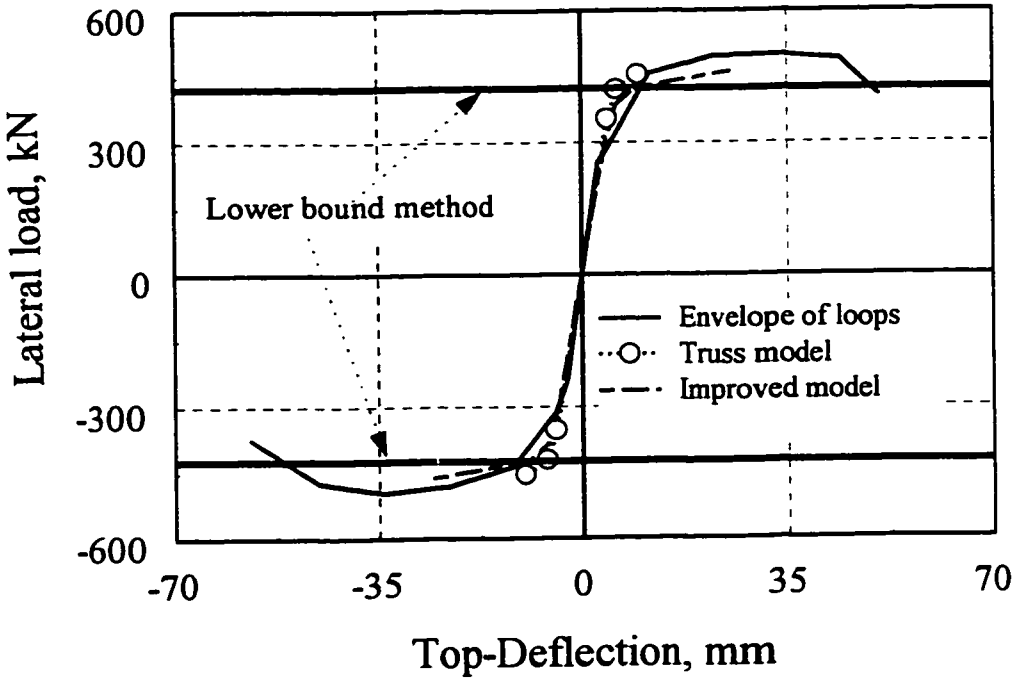

Figure 6.7 Comparison of test results with truss analysis for Wall 11R retrofitted RC

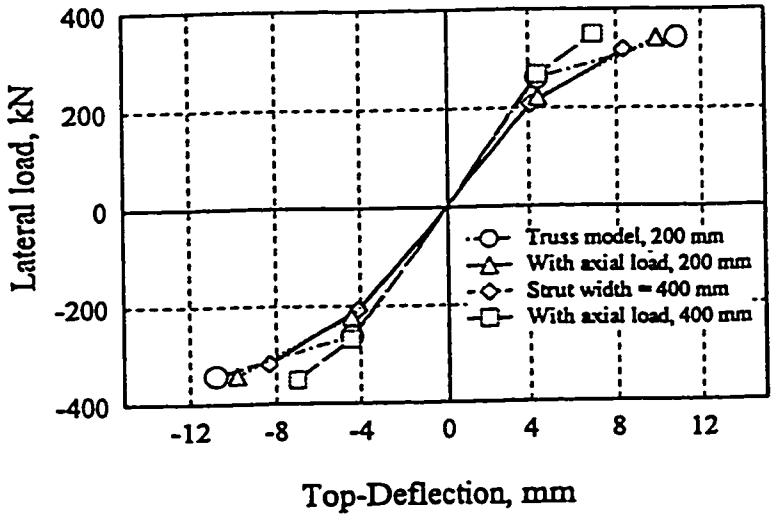

Figure 6.8a Comparison of truss analysis "different vertical strut width" for Wall 9R

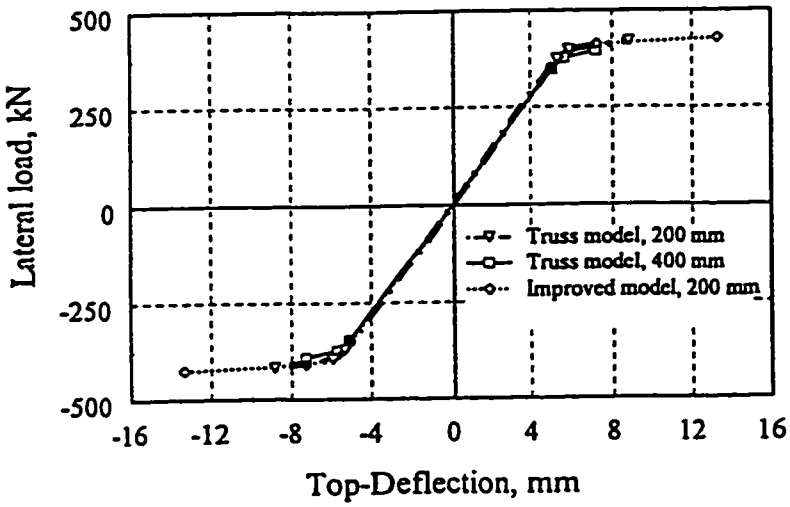

Figure 6.8b Comparison of truss analysis "different vertical strut width" for Wall 10R

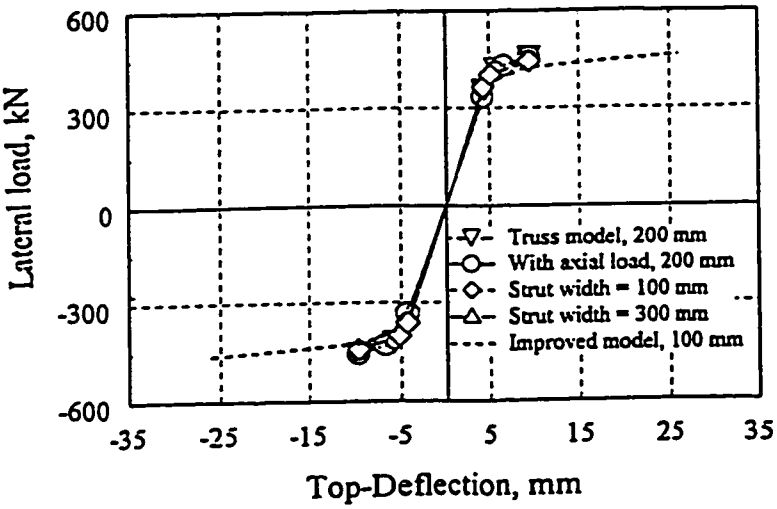

Figure 6.9 Comparison of truss analysis "different vertical strut width" for Wall 11R

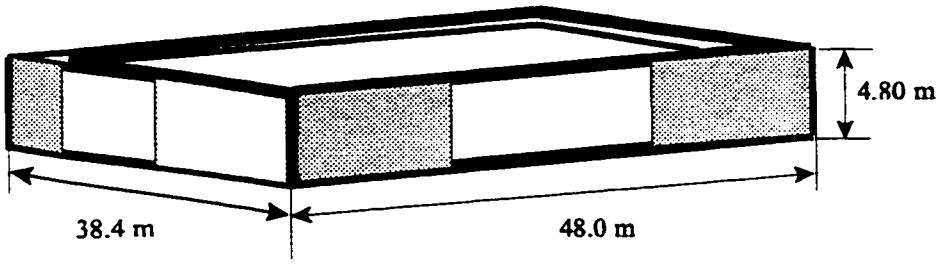

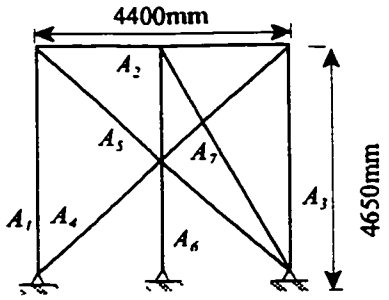

Four points model

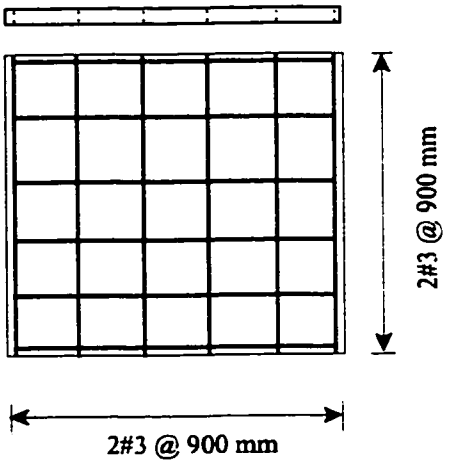

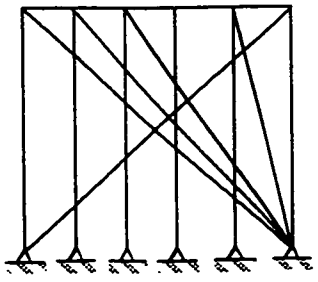

Seven points model

To transform the area of concrete members to equivalent area of steel, *the modular ratio n* must be calculated:

$E_s=200000\ MPa$

$E_c=27778\ MPa$

$n=200000/27778=7.2$

$A_1=914+2(142)=1198\ mm^2$

$A_2=(2000)(300/7.2)+0.0025\ (2000)(300)=84833\ mm^2$

$A_3=2(142)+914+(450)(100/7.2)=7448\ mm^2$

$A_4=3058 mm^2$

$A_5=3058+(470)(100/7.2)=9586\ mm^2$

$A_6=2(142)=284 mm^2$

$A_7=100(100/7.2)=1389 mm^2$

Figure 6.10 Illustrative design example; single-storey building

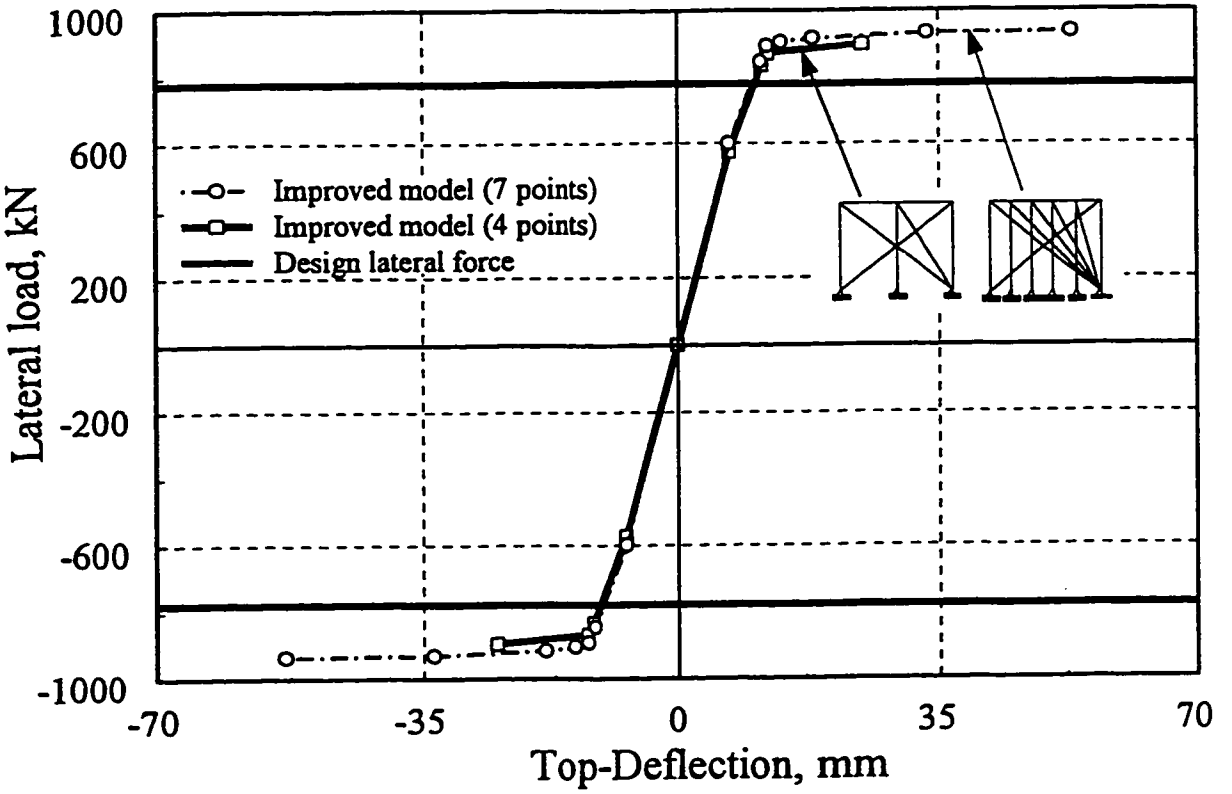

Truss analysis - example of retrofitting of RC wall

Figure 6.11 Retrofitting of single-storey building using steel strip system

Appendix A

Wall specimens design calculations

A.1 Unreinforced masonry (URM) wall specimens

A.1.1 Unretrofitted

The rocking capacity of the unretrofitted URM wall specimen was determined using simple static as shown in Fig. A.1:

$$V_r = 100\frac{(1800/2)}{2040} = 44kN$$

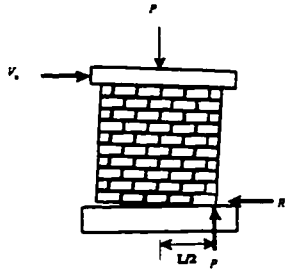

Figure A.1 Rocking of URM wall

The cracking shear capacity of the unretrofitted URM wall specimen was determined using CSA S304 clause 11.5.3.

$$V_m = 0.16\ (2-\frac{M}{Vd})\ \sqrt{f_m}\ bd\ \gamma_g + 0.25P \qquad \text{(A.1)}$$

where:

$$\gamma_g = \frac{A_e}{A_g}$$

The cracking shear capacity, V_m, can be calculated using equation A.1 as:

$$\gamma_g = \frac{2(33)(1800)}{(1800)(200)} = 0.33$$

$$\frac{M}{Vd} = \frac{2.04V}{1.8V} = 1.13$$

$f_m' = 15$ MPa See Fig. 3.2.

$$V_m = 0.16(2-1.13)\sqrt{15}\ (1800)(200)(0.33) + 0.25(100000) = 89kN$$

A.1.1 Retrofitted

Flexural capacity found using a small program, called Wall, that calculates moment-curvature relatiopnship. This program was original made for reinforced concrete sections and was modified to include inclined reinforcement as well as partial grouted masonry. Therefore flexural capacity for retrofitted URM wall specimen was found:

At 100 mm above specimen base:

M_u =765 kN.m

V_u =765/(1.8-0.1+.24)= 394 kN

At 900 mm above specimen base:

M_u =529 kN.m

V_u =529/(1.8-0.1+.24)= 464 kN

Shear capacity of the retrofitted wall specimen was found by adding the capacity of the unretrofitted URM wall specimen to the horizontal component of the yield strength of the steel strips in tension.

$$V_R = V_m + 2\,(A_n f_{yp})\,cos\,45$$
$$= 89 + 2\,(794.7)(450)\,cos\,45$$
$$= 600\ \text{kN}$$

A.2 Partially reinforced masonry (PRM) wall specimens

A.2.1 Unretrofitted

The flexural capacity of the unretrofitted PRM wall specimen was determined using Wall:

M_u =335 kN.m

V_u =335/(1.8-0.1+.24)= 164 kN

Similar to URM wall the cracking shear capacity was found as:

$$\gamma_g = \frac{2(33)(1800)+3(136)(126)}{(1800)(200)} = 0.47$$

$$V_m = 0.16(2-1.13)\sqrt{15}\,(1800)(200)(0.47) + 0.25(100000) = 106kN$$

A.2.1 Retrofitted

Flexural capacity for retrofitted PRM wall specimen was found:

At 100 mm above specimen base:

M_u =1045 kN.m

V_u =1045/(1.8-0.1+.24)= 539 kN

Shear capacity of the rertofitted PRM wall specimen is:

V_R = 106 + 2 (794.7)(450) *cos* 45

= 617 kN

A.2 Reinforced concrete (RC) wall specimens

A.2.1 Unretrofitted

The capacity of the unretrofitted RC wall specimen was determined using Doostdar's program to be:

V_u = 139 kN

A.2.1 Retrofitted

Flexural capacity for retrofitted RC wall specimen was found:

At 100 mm above specimen base:

M_u =964 kN.m

V_u =964/(1.8-0.1+.24)= 497 kN

Shear capacity of the retrofitted PRM wall specimen is:

V_R = 139 + 2 (794.7)(450) *cos* 45

= 645 kN

```
'*****************************************
'*       MOMENT - CURVATURE              *
'*         WALL PROGRAM                  *
'*                                       *
'*****************************************
  INPUT "PLEASE ENTER INPUT FILE NAME :"; IFN$
  INPUT "PLEASE ENTER OUTPUT FILE NAME :"; OFN$
  GFN$ = LEFT$(OFN$, (INSTR(OFN$, ".") - 1)) + ".DAT"
 OPEN "I", #1, IFN$
 OPEN "O", #2, OFN$
 OPEN "O", #3, GFN$
INPUT #1,GR
INPUT #1, EINI, EFIN, ESTP
INPUT #1, FCK, FCK1, FCT, FCT1
INPUT #1, EC1, EC2, EC3, ECT1, ECT2
INPUT #1, N, BE,B, H, XP, S, ACC,HH,YE
INPUT #1, NSL,AEB,BEB,CEB
'PRINT #3, EINI, EFIN, ESTP
PRINT #3, FCK, FCK1, FCT, FCT1
PRINT #3, EC1, EC2, EC3, ECT1, ECT2
PRINT #3, N, BE,B, H, XP, S, ACC,HH
'PRINT #3, NSL
DIM TP(NSL),BP(NSL),L(NSL),XS(NSL), SN(NSL), FS(NSL),TATH(NSL),CR(NSL),ESB(NSL)
DIM FYK(NSL),FYKH(NSL),ESY(NSL),ESH(NSL),ESR(NSL),PO(NSL),A(NSL),MO(NSL)
FOR I = 1 TO NSL
INPUT #1, TP(I),BP(I),L(I),XS(I), TATH(I),FYK(I),FYKH(I),ESY(I),ESH(I),ESR(I)
PRINT #3, TP(I),BP(I),L(I),XS(I), TATH(I),FYK(I),FYKH(I),ESY(I),ESH(I),ESR(I)
A(I)=2*TP(I)*BP(I):PO(I)=A(I)*FYKH(I)
MO(I)=PO(I)*TP(I)^2/4
NEXT I
' GR : 1 FOR GROUTED
'EINI : Initiatel strain value for the generation of M-K relationship
'EFIN : Final strain value for the generation of M-K relationship
'ESTP : Strain value increment
'FCK  : Peak value of parabolic portion of conc. comp. stress block
'FCK1 : End value of the decreasing linear portion of conc. comp stress block
'EC1  : Strain value corresponding to FCK
'EC2  : Strain value corresponding to FCK1
'EC3  : Strain value beyond EC2
'FCT  : Peak value of parabolic portion of conc. tens. stress block
'FCT1 : End value of the decreasing linear portion of conc. tens. stress block
'ECT1 : Strain value corresponding to FCT
'ECT2 : Strain value corresponding to FCT1
'FYK  : Yield stress of steel
'FYKH : Max. stress at strain hardening
'ESY  : Strain value at yield
'ESH  : Strain value at the start of strain hardening
'ESR  : Strain at rupture
'AST(): Area of steel layer
'XS() : Distance of steel relative to geometric center (negative below XP)

'N    : Axial force for wihch M-K relation to be obtained
'B    : Width of rectangular section
'H    : Depth of rectangular section
'XP   : Geometric center of the x-section
'S    : Thickness of concrete layers to calculate concrete stress
'ACC  : Accuracy required
C = .5 * H
' FOR J = 1 TO NSL: CR(J)=0
'NEXT J
C1 = 0: C2 = H: COLD = 0
AC = S * B
   PRINT #3, "   STRAIN  C (mm)  K (1/mm)xE-6  M (KN.m)   CRACK DEPTH "
   PRINT #3, " ├──────┼──────┼──────────┼──────────┼──────────┤"
   PRINT #2, "0.000000,0.000000"
 FOR EEF = EINI TO EFIN STEP ESTP
RESTART:

 FSTOT = 0: MSTOT = 0: FSC = 0

 FOR I = 1 TO NSL
 ASS=2*BP(I)*TP(I): XSS = XS(I) :SI=SIN(TATH(I)):L=L(I):MO=MO(I) :PO=PO(I)
```

```
FYK1=FYK(I):FYKH1=FYKH(I):ESY1=ESY(I):ESH1=ESH(I):ESR1=ESR(I)

CALL STEEL(AEB,BEB,CEB,PO,MO,L,YE,SI,FYK1, FYKH1, ESY1, ESH1, ESR1, EEF, C, XP, ASS,ES, XSS, FST,CR, MS, D,SIGNN)
' IF (FST < 0) THEN FSC = FSC + FST
FS(I) = FST
' IF FST<0 THEN go to cr2
ESB(I)=ES
cr2:   SN(I) = SIGNN
FSTOT = FSTOT + FST
MSTOT = MSTOT + MS
NEXT I
CALL FCOMPR(FCK, FCK1, EC1, EC2, EC3, EEF, C, H, XP, S, AC, FCOMP, MCOMP,BE,B,GR)
CALL FTENSILE(FCT, FCT1, ECT1, ECT2, EEF, C, H, XP, S, AC, FTEN, MTEN, CD)
DIFF = FCOMP + FTEN + FSTOT - N
IF ABS(DIFF) <= ACC THEN GOTO CONTI
IF DIFF >= 0 THEN C2 = C ELSE C1 = C
C = (C1 + C2) / 2
IF ABS(C - COLD) <= S THEN GOTO CONTI
COLD = C
GOTO RESTART
CONTI:

FOR I = 1 TO NSL
IF SN(I) = -1 THEN STOP
NEXT I

K = EEF * 1000000 / C
MOM = (MSTOT + MCOMP + MTEN) / 1000000
'if fst<0 then print #2, using "#####.#######,#######.##";es;fst
' if (fst>0) then goto pr1
ESB(1),FS(1) print #2, using "#####.#######,#######.##";k;mom
   print #2, using "#####.#######,#######.##";K,MOM

   pr1: PRINT #3, USING " |#.#####|####.##|####.###  |######.## | #####.## | #####.## | #####.## | #####.## |"; EEF; C; K;
MOM; fstot/1000;fcomp/1000
PRINT "*";
IF MOM < 0 THEN STOP

C1 = 0: C2 = H
C = COLD
NEXT EEF
'&&&&&&&&&&&&&&&&&&&&&&&&&&&&&&&&&&&&&&&&&&&&&&&&&&&&&&&&&&&&&&&&&
'&&&&&&&&&&&&&&&&&&&&&&&&&&&&&&&&&&&&&&&&&&&&&&&&&&&&&&&&&&&&&&&&&&
SUB FCOMPR (FCK, FCK1, EC1, EC2, EC3, EEF, C, H, XP, S, AC, FCOMP, MCOMP,BE,B,GR) STATIC
MCOMP = 0!: MC = 0
FCOMP = 0!: FC = 0
X1 = S
X2 = C
IF C > H THEN X1 = C - H + S: X2 = C
FOR XC = X1 TO X2 STEP S
XC1 = XC - S / 2
EC = EEF* XC1/C
XB = (XP - C) + XC1
IF GR=1 GO TO GR1
AC=S*BE
GOTO GR2
GR1:
AC=S*BE
IF(C-XC1<182)THEN AC=S*B
GR2:
' IF(C-XC1<46) THEN AC=S*B
 IF EC > EC1 THEN GOTO GD1
FC = AC * FCK * (2 * EC / EC1 - (EC / EC1) ^ 2)
MC = FC * XB
GOTO SUM
GD1:
IF EC > EC2 THEN GOTO GD2
 FC = AC * (FCK - (FCK - FCK1) * (EC - EC1) / (EC2 - EC1))
MC = FC * XB
GOTO SUM
GD2:
```

```
FC = AC * FCK1
MC = FC * XB
SUM:
FCOMP = FCOMP + FC
MCOMP = MCOMP + MC
NEXT XC
END SUB

SUB FTENSILE (FCT, FCT1, ECT1, ECT2, EEF, C, H, XP, S, AC, FTEN, MTEN, CD) STATIC
FTEN = 0: MTEN = 0: CD = 0
FT = 0: MT = 0
IF C >= H THEN GOTO EXITTT
ELF = EEF * (H / C - 1)
X1 = S
IF ELF > ECT2 THEN X2 = ECT2 * (H - C) / ELF: ETF = ECT2 ELSE X2 = H - C: ETF = ELF
FOR XT = X1 TO X2 STEP S
XT1 = XT - S / 2
ET = ETF * XT1 / X2
XB = XP - C - XT1
IF ET > ECT1 THEN GOTO GDE1
FT = -AC * FCT * ET / ECT1
MT = FT * XB
GOTO SUMT
GDE1:
FT = -AC * (FCT - (FCT - FCT1) * (ET - ECT1) / (ECT2 - ECT1))
MT = FT * XB
SUMT:
CD = H - C - X2
FTEN = FTEN + FT
MTEN = MTEN + MT
NEXT XT
EXITTT:
END SUB
'&&&&&&&&&&&&&&&&&&&&&&&&&&&&&&&&&&&&&&&&&&&&&&&&&&&&&&&&&&&&&&&&&&&&&&&&&&
SUB STEEL (AEB,BEB,CEB,PO,MO,L,YE,SI,FYK1, FYKH1, ESY1, ESH1, ESR1, EEF, C, XP, ASS,ES, XSS, FST,CR, MS, D,SIGNN)
STATIC
SIGNN = 1
E = FYK1 / ESY1
ES = EEF * (1 - (XP - XSS) / C)*SI^2
IF XSS>0 AND SI<>1 THEN GOTO BUKL
IF ABS(ES) >= ESR1 THEN SIGNN = -1
' IF ABS(ES)>=ESR1 THEN GOTO EXIT1
IF ABS(ES) > ESY1 THEN GOTO PLSTC
FST = ES * ASS * E *SI
GOTO CALCM
PLSTC:
IF ABS(ES) > ESH1 THEN GOTO STHRD
FST = SGN(ES) * FYK1 * ASS *SI
GOTO CALCM
STHRD:

FST = SGN(ES) * ASS * (FYK1 + (FYKH1 - FYK1) / (ESR1 - ESH1) * (ABS(ES) - ESH1)) *SI
IF ABS(ES) > .1 THEN FST = ASS * FYKH1 *SI
go to calcm
BUKL:
PRINT XSS ,SI
' ESB=-ES
IF (ES > ESY1) THEN GOTO PLSTB
FST = ES * ASS *E *SI
GOTO CALCM
PLSTB:
IF(ES > ESH1) THEN GOTO STHRB
FST = FYK1 * ASS *SI
GOTO CALCM
STHRB:
fst=AEB*(es^(BEB+CEB*log(es)))*ass*SI
' IF ABS(ES) > .1 THEN FST = ASS * FYKH1 *SI

CALCM:
MS = FST * XSS
EXIT1:
END SUB
```

Appendix B

Additional load-strain diagrams for reinforcing bars

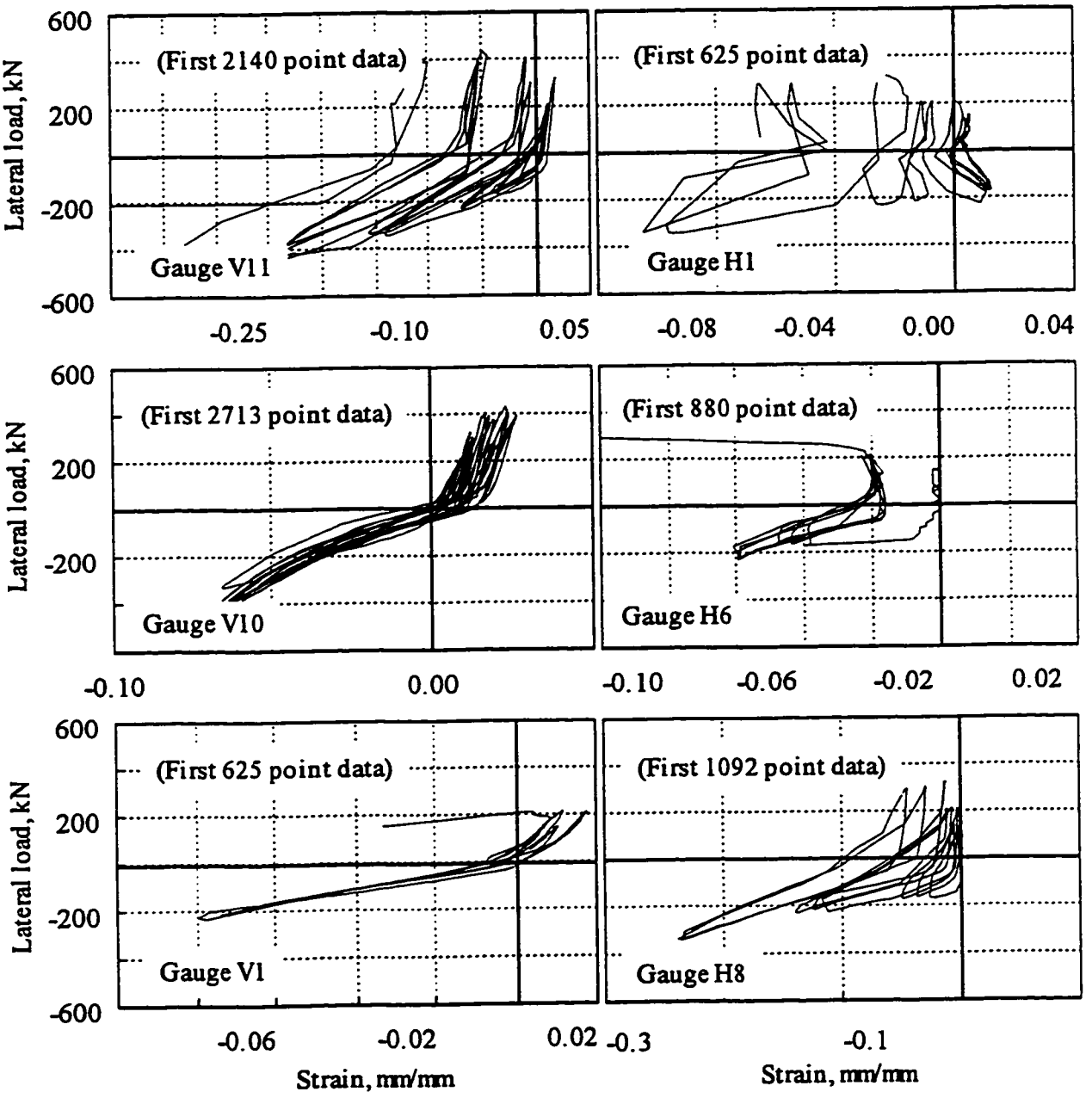

Figure B.1 Lateral load-strain relationship for vertical and horizontal bars of Wall 10R

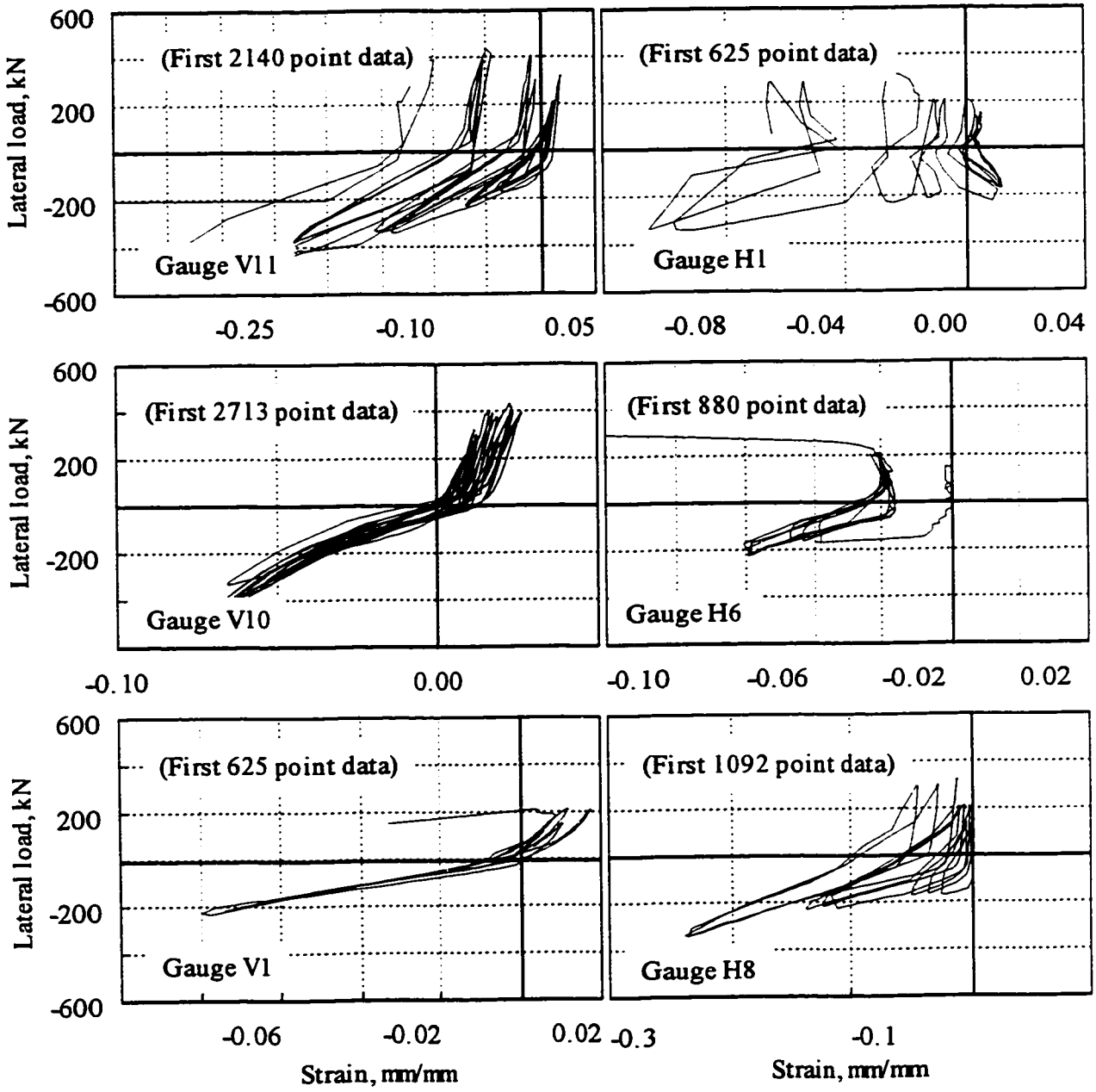

Figure B.2 Lateral load-strain relationship for vertical and horizontal bars of Wall 10R

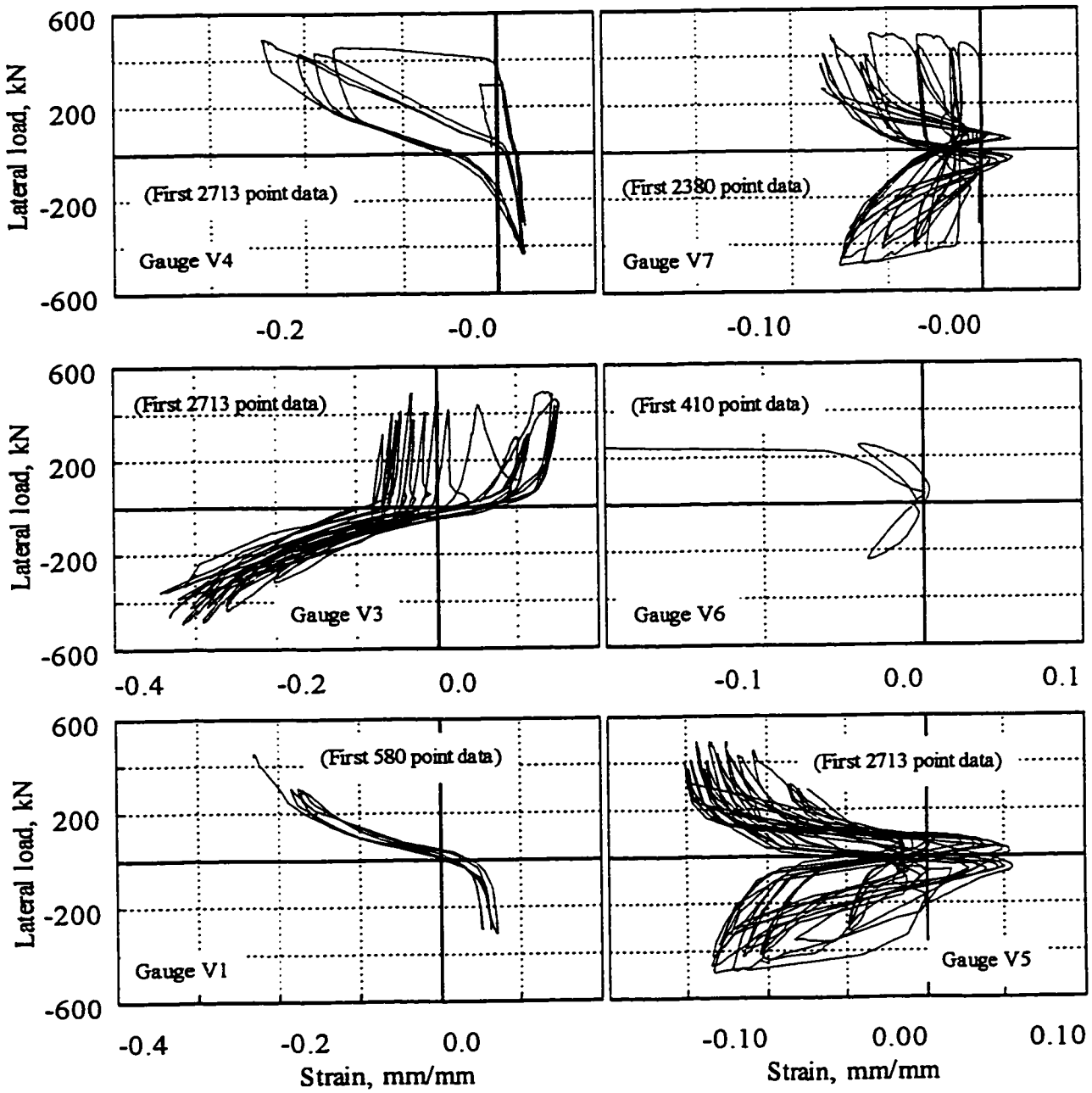

Figure B.3 Lateral load-strain relationship for vertical reinforcement of Wall 11R

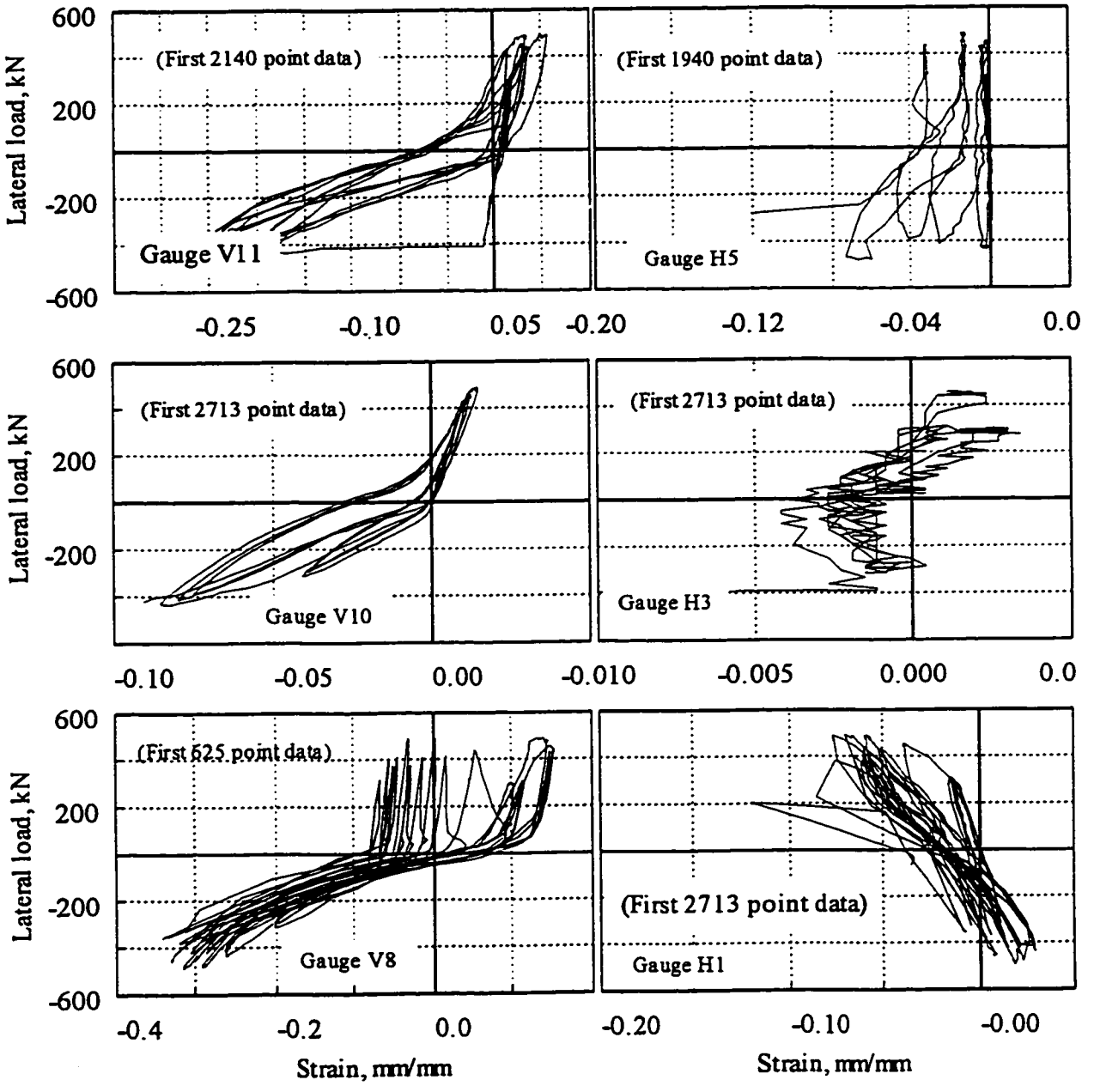

Figure B.4 Lateral load-strain relationship for vertical and horizontal bars of Wall 11R

IMAGE EVALUATION
TEST TARGET (QA-3)

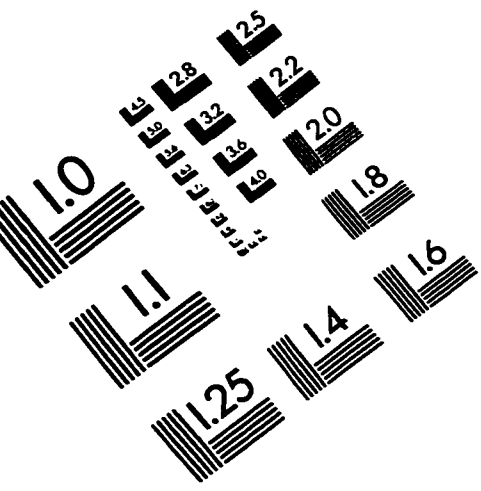

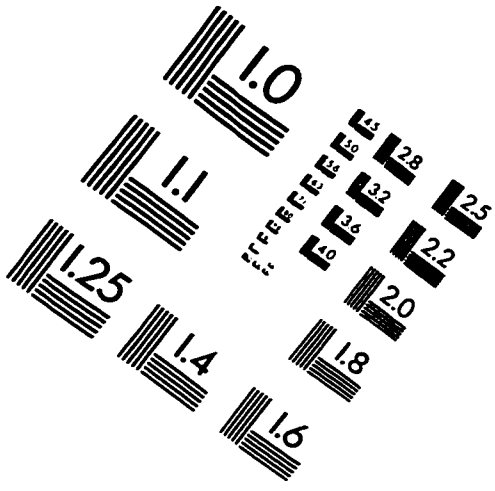

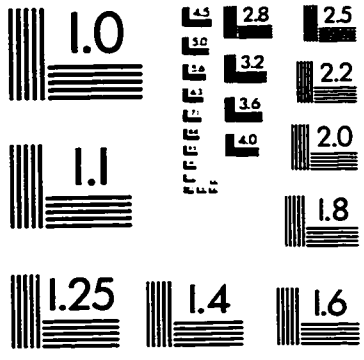

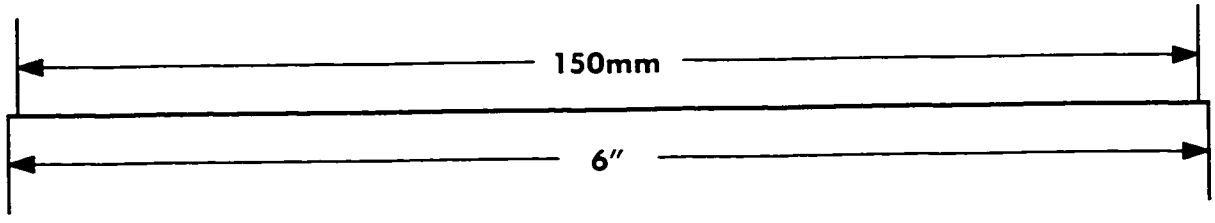

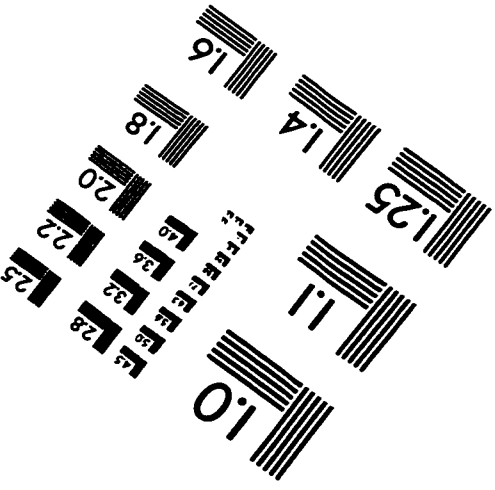

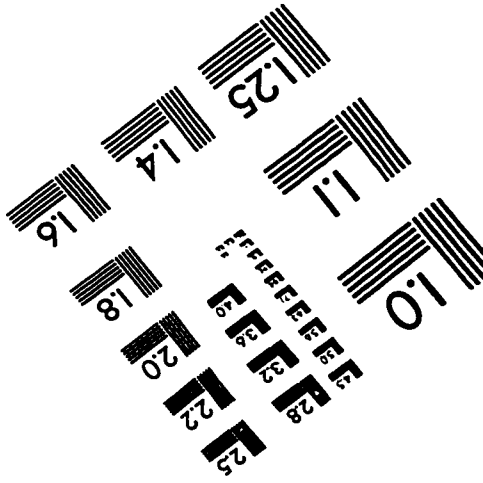

APPLIED IMAGE, Inc
1653 East Main Street
Rochester, NY 14609 USA
Phone: 716/482-0300
Fax: 716/288-5989